Department of Civil Engineering

Behaviour of Railway Track Subgrade under Cyclic Loading

Beng Heng Loh

This thesis is presented for the Degree of
Doctor of Philosophy
of
Curtin University

November 2011

Declaration

To the best of my knowledge and belief this thesis contains no material previously published by any other person except where due acknowledgment has been made. This thesis contains no material which has been accepted for the award of any other degree or diploma in any university

Signature: _____

Date: _____

Abstract

The railway track foundation of fine-grained soil subgrade, under repeated loading of cyclic nature, can gradually build up excess pore pressure and result in progressive shear failure at a stress level much lower than the monotonic loading strength of the soil. It is widely accepted that a threshold stress exists, above which, the induced stress generates large shear deformation and; below which, the soil deformation become stabilized irrespective of the number of loading applications. Previous studies into the behaviour of fine-grained subgrade under cyclic loading had mainly involved slow loading rate. The advance in transportation technology and the required efficiency of transporting goods and commuting passengers demands higher train speed and heavier loads. Consequently, better understanding on the behaviour of fine-grained subgrade under higher rate of loading (i.e. cyclic frequency) will be necessary as it influences the build-up of excess pore water pressure and strain accumulation of subgrade soil, hence the stability of the railway track. In addition, current design approaches to the railway tracks foundation of fine-grained subgrade have largely been empirical or semi-empirical unique to a range of geological characteristic, operating and traffic condition. The rationalization and reformulation of design approach may be required if general design means will to be devised.

In this research, an in-depth study of undrained triaxial testing on the behaviour of a typical fine-grained reconstituted kaolinite clay soil, simulating the characteristic subgrade responses exhibit under the passing axles / wheel load of the contemporary train speed was performed and discussed. Four series of both static and cyclic undrained triaxial test were conducted. The static undrained triaxial test provides the behavioural benchmark and a prior indication on the maximum stress level from which the cyclic stress level can be apportioned. The cyclic undrained triaxial test simulates the behaviour of clay subgrade under a large number of passing axles/wheel load. The results of the testing described and characterized the stress / strain behaviour for saturated kaolinite clay of various consolidated state and stress history. In particular, it described the general concept of cyclic stress equilibrium state and resilient state, and detailed the characteristic pattern of the line of cyclic stress equilibrium state which dictates the way in identifying the threshold stress (or critical level of cyclic stress). The study demonstrated that, using effective stress

analysis, the threshold stress can be obtained for clay under high cyclic loading rate. In conjunction with the stress response, the deformation and resilient characteristics of various series of cyclic undrained triaxial tests carried out on the saturated clay was described. Apart from highlighting and confirming the influence of consolidated state and stress history on the threshold stress and deformation characteristics, influence of the cyclic loading frequency simulating higher train travelling speed was also investigated and examined.

Using the framework of critical state soil mechanics, the study described the existence of cyclic stress equilibrium state surface CSESS within the stress state boundary surface SSBS for saturated clay under cyclic undrained compression. A form of analytical / theoretical model was established which enables threshold stress to be ascertained without resort to lengthy laboratory testing at the preliminary design stage of railway track foundation design. Developed from the "original Cam-clay" model and validated by the cyclic triaxial test data on reconstituted kaolin clay, the theoretical model which described the CSESS enables the prediction of threshold stress (or critical level of cyclic stress) of general saturated clay soil under undrained cyclic compression to be made from the fundamental properties of the soil, based on the designed consolidated state and the stress history of subgrade soil.

In addition, this study proposed a new approach which rationalized and reformulated the current state of design and management process of railway track substructure involved clay subgrade. The rational approach was developed based on the comprehension of "lower-bound threshold stress" and potential strengthening and densification of fine-grained subgrade soil through progressive and deliberate incremental loading of the track foundation. Concept of "Managing current lower-bound threshold stress" for clay subgrade was elaborated. The readily use of the developed theoretical model and design charts for predicting the threshold stress could offer a key advantage for the new approach over current practices.

Acknowledgement

I wish to express my grateful appreciation to members of the thesis committee headed by Professor David Scott (chairperson), for the administration and support during my doctoral research study at the Curtin University of Technology in Western Australia.

In Particular, I wish to express my deep sense of gratefulness towards Professor Hamid R. Nikraz, my main supervisor, for his enormous generosity and great capacity that provided me with support, guidance, encouragement and empowerment towards the completion of the thesis.

Acknowledgment and thank is expressed for the initial assistance and suggestion from Dr. M. Shahin. I also like to express my appreciation to the valuable assistance and advice from Dr. Peerapong Jitsangiam and Dr K. Siripun. Of the many fellow graduates, the brief but precious acquaintances and their contributions will sure to be cherished someday.

Appreciation is expressed towards the administrative staff including Liz. Field, Diane Garth and Kate White, whose assistance and support seem unbounded. To the laboratory staff, I expressed my thanks to John Murray, Mark Whittaker, Ashley Hughes and many others for their dedicated and extra support I was given in various ways.

Finally, I thank my family for their unconditional support and understanding in walking with me the pursuit of higher academic degree.

Publications Related to Thesis

Loh, R. B. H., and Nikraz, H. R. (2011). "Effective stress method on threshold stress of clay under high rate cyclic loading." 5th Asia-Pacific conference on unsaturated soils Geotechnical Engineering Research and Development Center (GERD); Kasetsart University, Thailand; Thai Geotechnical Society and Engineering Institue of Thailand, Pattaya - Thailand.

Loh, R. B. H., and Nikraz, H. R. (2011). "Critical state modeling of lower-bound threshold stress for clay subgrade." 5th Asia-Pacific Conference on Unsaturated Soils (AP-UNSAT 2011), Geotechnical Engineering Research and Development Center (GERD); Kasetsart University, Thailand; Thai Geotechnical Society and Engineering Institite of Thailand, Pattaya, Thailand.

Loh, R. B. H., and Nikraz, H. R. (2011). "Threshold stress and deformation characteristics of clay subgrade for railway tracks." 5th International Symposium on Deformation Characteristics of Geomaterials (IS-Seoul 2011), International Society for Soil Mechanics and Geotechnical Engineering (TC101); Korean Geotechnical Society, Seoul - Korea.

Loh, R. B. H., and Nikraz, H. R. (2011). "A rational approach to railway track foundation design with clay subgrade." The 14th Asian Regional Conference on Soil Mechanics and Geotechnical Engineering, Hong Kong Geotechnical Society; Hong Kong Polytechnic University, Hong Kong, China.

Shahin, M. A., Loh, R. B. H., and Nikraz, H. R. (2011). "Some Obsevations on the behaviour of soft clay under undrained cyclic loading." *Journal of GeoEngineering, TGS*, 6(No.2).

Publications under Review

Loh, R. B. H., and Nikraz, H. R. (2011). "Compressibility and strength of clay subgrade of railroad foundation in highly saturated condition." Journal of GeoEngineering, TGS. (Under Review)

Loh, R. B. H., and Nikraz, H. R. (2011). "State of stress equilibrium and threshold stress of saturated clay in undrained cyclic compression." Geomechanics and Geoengineering: An International Journal. (Under Review)

Table of Contents

List of Figures

List of Tables

Notation

B	Skempton pore pressure parameter, where $\Delta u = B \cdot \Delta\sigma_3$
c_v	Coefficient of consolidation
e	void ratio
e^1	Exponential function of 1
exp ( ) or $e^{( )}$	Exponential function of …..
G_s	Specific gravity of soil
E_r	Resilient Modulus, in kPa
M	The value of the stress ratio q/p' at the critical state condition
N	Specific volume of soil under isotropic normal consolidation at p'=1 kPa
PI	Plasticity index
p'	Mean effective stress
p_{cr}'	Mean effective stress at the intersection of the CSL and the yield curve
p_e'	Equivalent isotropic pre-consolidation pressure, in kPa
p_i'	Initial mean effective stress
p_o'	Isotropic pre-consolidation pressure, in kPa
p_t'	Mean effective stress correspond to the stress state on a $p'-q$ plane at which threshold stress is identified
$p'_{w/d}$	Mean effective stress at the wet / dry division of critical state line under cyclic undrained compression
q	Deviator stress or cyclic deviator stress
q_{cyc}	Cyclic deviator stress
q_t	Threshold stress of soil or critical level of cyclic deviator stress, in kPa
$\left(q/p'\right)_{equi}$	Stress obliquity at equilibrium
u	Pore water pressure
v	Specific volume of soil (v = 1 + e)

w_L	Liquid Limit of soil
w_P	Plastic limit of soil

Greek Symbols

Δ	Increment of …..
Δu	Excess pore water pressure
Δv	Increment of specific volume
ε_r	Resilient axial strain or elastic axial strain at resilient state
ϕ'	Coulomb effective friction angle
γ_{di}	In-situ dry density of soil, in kN/m^3
Γ	Specific volume of soil on critical state line when p'=1 kPa
η	Obliquity or stress ratio (q/p')
κ	Swelling/Recompression index – the average gradient of the swelling recompression line in $v - \ln p'$ plane
κ_1	The gradient of the swelling line in $v - \ln p'$ plane
κ_2	The gradient of the recompression line in $v - \ln p'$ plane
λ	Normal consolidation volumetric compression index – the gradient of normal consolidation line in $v - \ln p'$ plane
σ_1'	Major principal effective stress
σ_3'	Minor principal effective stress
σ_d	Deviator stress
$\sigma_{d(static-\max.)}$	Peak deviator stress under monotonic compression

---

Subscripts

cyc	Cyclic
e	Elastic component
equi	At stress equilibrium
p	Plastic component

Abbreviations

CSES	Cyclic stress equilibrium state
CSESS	Cyclic stress equilibrium state surface in the $p'-q-v$ space
CSL	Critical state line
CSR	Cyclic stress ratio
INCL	Isotropic normal-consolidation line
LCSES	Line of cyclic stress equilibrium state
LVDT	Liner variable differential transformer
NC	Normally-consolidated
OC	Over-consolidated
OCR	Over-consolidation ratio
SSBS	Stress state boundary surface

Chapter 1 Introduction

1.1 *Background*

One of the main criteria in the design of railway track foundation subgrade is to ensure that the subgrade do not fail progressively as a result of repeated loading. Research carried out by British Rail on the "London clay" (Heath et al. 1972; Waters 1968) served to enlighten the existence of threshold stress in the fine-grained subgrade. If the subgrade soil will to be stressed below its threshold, no progressive shear failure shall occur. To date, literatures do not provide sufficient data to aid the design of track foundation in fulfilling such criteria. In addition, the advance in train automobile technology and the required efficiency in railway transportation mean increasing train speed; and consequently cyclic loading of higher frequency is expected to exert at the track foundation subgrade.

This research is aiming to broaden the understanding of the behaviour, in terms of stress and strain response, of a fine grained soil under cyclic loading at loading frequency typical of that experienced by railway track foundation near its subgrade surface. The tests data and information gathered in this study will also be beneficial to other field in which geo-stress of cyclic nature are predominant.

1.2 *Objectives and Scopes*

This research investigated the behavioural characteristic of railway subgrade cohesive soil under repeated loading, at a cyclic loading frequency resembled that induced by the passing of train wheels / or axles during the travelling of contemporary train. The research aimed at improving the current state of knowledge on the behaviour of fine-grained subgrade soil i.e. clay soil in particular of railway track foundation under cyclic loading, focusing the effects of stress state and stress

history has on strain / deformation characteristics, pore pressure build-up and the "threshold stress" identification. It is believed that the knowledge gained from this study will aid the railway track engineer in the development of design guide for railway track foundation on fine-grained subgrade in general, and clay subgrade in particular.

Specifically, the research objectives are as follows:

a) A critical review of literature in the relevant field and a discussion of the findings.

b) Experimental investigation into the effects of parameters such as confining stress state and stress history, deviator stress magnitude, cyclic frequency, and number of loading cycles, on the behavioural characteristics of a fine-grained soil with regard to the pore water pressure build-up and its effective stress response and; the permanent and resilient deformation.

c) Evaluate and characterize both the effective stress response and deformation characteristic of a typical fine-grained soil of various consolidated state under both monotonic and cyclic undrained compression.

d) Identification of the "threshold stress" from experimental investigation for each test series of the same consolidated state with cyclic deviator stresses of varying cyclic stress ratio.

e) Identification of the effect of cyclic frequency as it influences the soil behaviour under cyclic loading.

f) Using the framework of critical state soil mechanics and in conjunction with the available critical state model, develop a theoretical relationship and method for predicting the "threshold stress" of a saturated fine-grained soil in undrained cyclic loading condition.

g) Explore a rational approach to the design of railway track foundation with a typical fine-grained subgrade based on lower-bound threshold stress, using the developed theoretical model.

1.3 *Thesis Structure*

There are eight chapters contained in this thesis. This Chapter 1 is an introductory chapter, which gives an introduction to the research study, it states the objective(s) and scopes of the study, and describes the structure of this thesis.

Chapter 2 began with a review on "Railway Track Substructure", focusing mainly on the role of subgrade and its relevant parameters in track foundation design. The general behaviour of fine-grained / clay soil under repeated or cyclic loading was given a critical review, followed by a review on the current approaches to the design of railway track foundation with fine-grained subgrade.

Chapter 3 described the relevant information on experimental set up and the testing procedure. The chapter first introduced the material soil used in the experimental testings, followed by the description of the triaxial testing facility used, the modification and instrumentation. Then, the method and technique of sample preparation and the testing procedure are illustrated. The chapter ended by outlining the details of the experimental programme of the laboratory works. The terminology used in the data analysis are also detailed and presented.

Chapter 4 presented the results and analysis of the tests carried out under both monotonic and cyclic undrained compression. The presentation of the results is in modular form, each representing a series of tests conducted on the soil specimen subjected to the same consolidation state and stress history prior to axial compression. The general and typical behaviour with respect to the build-up of excess pore water pressure and the development of axial strain are described for each test series. Analysis and illustration on the strength and the deformation characteristics are provided.

In Chapter 5, the experimental results of varies series of tests representing different stress history are further synthesized and discussed to give an overall picture of the characteristics and behaviour of the soil under undrained compression across wide-ranging degree of over-consolidation.

Chapter 6 described the development of a theoretical model for predicting the lower-bound threshold stress. Examination of the model is made by a comparison between the theoretical predictions and the results of experimental analysis.

Chapter 7 attempted and explored a rational approach to the design of railway track foundation design with clay as a typical fine-grained subgrade, in conjunction with practical application of the developed theoretical model.

Finally, Chapter 8 summarized the research study, the major findings, conclusion and contribution. Further improvement and future work in the same field is also recommended.

Chapter 2 Background and Literature Review

2.1 *Introduction*

Railway track is continually required to carry greater loading at higher speed. It becomes necessary that the behaviour of track foundation subgrade under cyclic and dynamic loading condition be fully apprehended, so that the effects of new traffic loading characteristics can be taken into consideration during the design phase and in-service.

This chapter began with a review on railway track structure, focusing on the substructure foundation with respect to the role of subgrade and its material parameters in track foundation design. Behaviour of fine-grained soil under repeated or cyclic loading in general and the response and performance models of fine-grained subgrade governing track foundation designs are reviewed. A review on the fundamental approaches to track foundation design was provided at the end of chapter.

2.2 *Railway Track Structure*

Conventional ballasted railway track is essentially a load distribution system in which the load arises from the passage of trains is transmitted through the rails to the sleepers (Figure 2-1). In turn, the load is spread onto the subgrade (or formation) through the ballast and sub-ballast layers. The magnitude of stress that may be applied to the subgrade is governed by the characteristics of the subgrade soil. Of all, cohesive soils have been most problematic.

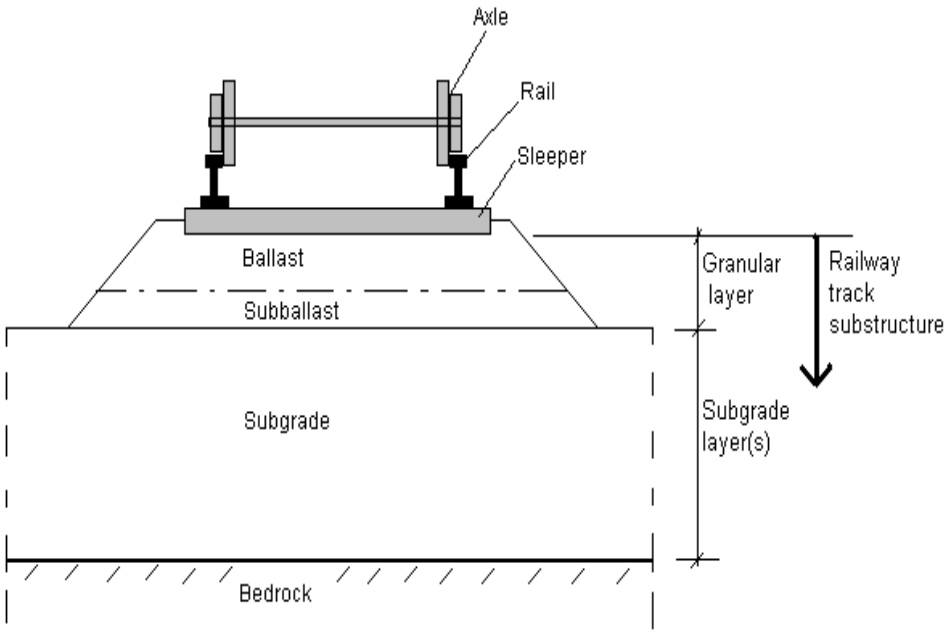

Figure 2-1 Conventional railway track structure components

The railway track structure may be grouped into a superstructure and a substructure. The superstructure consists of the rails, the fastening devices, and the sleepers (ties). Rails must have sufficient stiffness to serve as beams which transfer the concentrated wheel load to the evenly spaced sleepers. The vertical profile of the rail and the wheel surface defects can cause substantial dynamic loads which are detrimental to the track stability. Fastening devices secure the rails to the sleepers and provide vertical, lateral and longitudinal restraint. Sleepers (or ties) receive loads from the rail and distribute it over the ballast surface.

The substructure is separated from superstructure by the sleeper-ballast interface. It consists of the ballast/sub-ballast layer and the subgrade, as follows:

(1) Ballast and Sub-ballast

Ballast is a layer of selected, crushed, angular, hard stones and rocks, uniformly graded, free of dust and dirt. It serves to withstand/resist the lateral and longitudinal forces transmitted by the sleepers. More importantly, it protects the subgrade underneath by distributing the loads from above and limiting the stress at the subgrade to an acceptable level.

A layer of sub-ballast made up of broadly-graded naturally occurring or processed sand-gravel mixtures, or broadly-graded crushed natural aggregates or slags, between the ballast and subgrade is essential. It forms part of the granular layer. In addition, it acts an inverted filter which permits upward movement of water from subgrade, but prevents the downward movement of water from ballast into the subgrade. It prohibits subgrade attrition, which is the upward migration of subgrade particles in the presence of water.

(2) Subgrade

The subgrade is the foundation soil, either compacted natural ground or transported fill embankment, upon which the track structure is built. As much as it is protected by the granular layer, it is a load-bearing layer and it provides a platform for the laying of sub-ballast and ballast layers. The induced stresses of subgrade soil decreases with depth. As such, the critical subgrade stress normally occurs near its surface. The stiffness of subgrade soil is believed to influence ballast, rail and sleeper deterioration. It is a main source of rail differential settlement, particularly in the case of cohesive subgrade.

2.3 *Track Degradation and Subgrade Distress*

The development of irregularities at the surface of railway track in terms of vertical profile and longitudinal alignment causes track degradation. Various track components contributes towards such development. Of all, the track subgrade has a significant influence on track performance, though the rail surface permanent settlement due to ballast abrasion can sometime be a major factor with silty sand subgrade (Li 1994a).

Under various conditions, subgrade distress of different nature can develop (Selig and Waters 1994). There are:

(1) Massive shear failure

As shown in Figure 2-2, the possible driving forces of massive shear failure are the weights from the train, the track superstructure and the lateral force component of the cornering train. Typically, slip plane forms beneath the formation level of embankment, resulting in an abrupt loss of track surface.

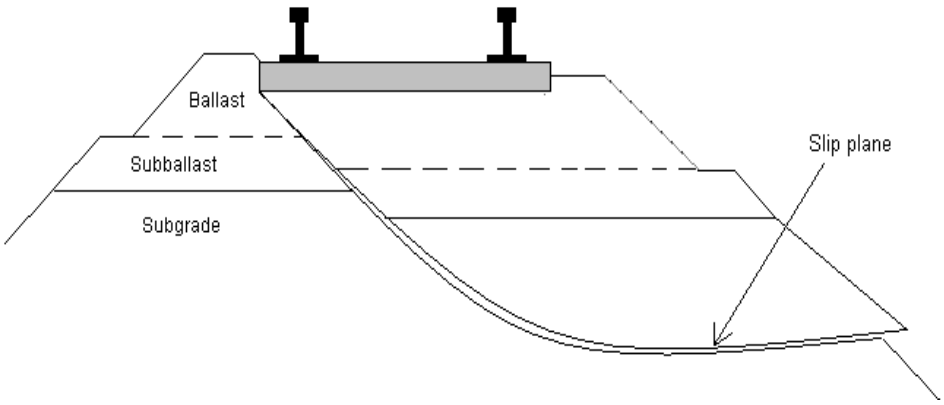

Figure 2-2 Massive shear failure

(2) Progressive shear failure

Progressive shear failure of subgrade is caused by the effect of cyclic loading. During repeated application of a shear stress, subgrade soil can fail at a shear stress less than the shear strength in monotonic loading. This occurs because the excess pore pressures do not return to zero after each unloading, rather accumulates during each cycle of loading, and thereby reduces the shear resistance of the soil. (Lambe and Whitman 1969). The localized shear failure produces plastic flow of subgrade soil near the subgrade surface, gradually pushing outward and upward toward the ground surface (see Figure 2-3). Progressive shear failure is accompanied by large progressive shear deformation. It deteriorates track's profile and renders the frequent raising of rails necessarily.

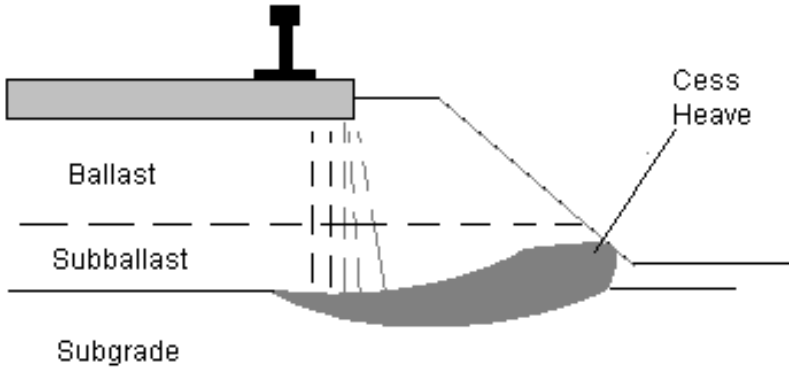

Figure 2-3 Forming of cess heave due to subgrade shear failure

(3) Long term consolidation settlement or swelling

Consolidation settlement due to the weight of added earth (in the case of embankment) or conversely swell from removal of earth as in the case of cut

construction, can produce substantial differential settlement, particularly at the transition where the fill/or cut meet the natural or existing ground. Nevertheless, soil consolidation problem can be readily analysed and solution obtained using well-established methods of geotechnical engineering.

(4) Excessive plastic settlement

Under repeated application of train loading, subgrade accumulates permanent (plastic) settlement. The development of cumulative plastic settlement can be attributed to:

(a) Progressive shear deformation due to repeated loading,

(b) Compaction effort due to the dynamic nature of loading, and

(c) Consolidation due to dissipation of excess pore water sets up by each load application.

Even without shear failure taking place, the magnitude of accumulated plastic settlement may reach a significant level (excessive) that can severely affect the riding quality and speed up the deterioration of the track, as increased irregularity in track profile causes higher dynamic wheel load that will induce higher stresses on track substructure.

Current practice to overcome the loss of track elevation due to excessive plastic deformation in the subgrade is to add more ballast to bring back its level. However, the topping up of ballast into the sunken subgrade surface developed ballast pocket in the subgrade (Figure 2-3). The ballast pocket traps water which in turn leads to weakening of the subgrade soil. This practice does not solve the problem completely (Selig and Waters 1994).

(5) Attrition

When ballast is placed directly on hard, fine-grained soil, without a layer of sub-ballast as an inverted filter, problem of soil attrition and mud pumping can occurs. In the presence of water and high saturation, water and fine-particles combined to form slurry on the subgrade surface. Under the compression of the passing trains, mud pumping occurs upward. The loss of subgrade soil due to migration of fine particles in the form of slurry will eventually contribute toward the settlement of rails and ballast layer. Moreover, the slurry can also accumulate and flow into the nearby drainage, thereby causing blockage.

(6) Frozen subgrade

In places where temperature could get below freezing point of water, subgrade especially those with frost-susceptible soil poses major concern. In saturated fine-grain soil, freezing of the pore water expanded its own volume which can cause the pore phase of the soil mass to increase by approximately 10 %, pushing the soil particles apart. This results in an increase in local soil volume. As soon as the ice begins to melt into water, it fills up the void left over by the contracting water phase. In the case of clayey soil, it goes through initial contraction, and then follows by swelling as the dissipating negative excess pore pressure draw in additional water nearby. The end result is thaw-softening which reduces the effective confining stress and the dry density of the subgrade with consequent reduction in its shear strength.

The problem of frozen subgrade can be overcome by providing a good drainage system to reduce saturation near the subgrade surface, and avoid feeding water to the subgrade when the frozen soil melts.

2.4 *Subgrade and Fine-grained Soil under Repeated Loading*

2.4.1 Subgrade Physical State

In general, the fine-grained formation soil beneath the future railroad may exist in its natural undisturbed state or a compacted state for 'fill' soil. Further compaction of specific compacting effort at optimum moisture content is usually provided as a method of improving the soil by densification. However, in the case of fine-grained soil i.e. clay material in particular, field control of moisture has never been easy. Not only is it difficult to attain homogeneous compaction within the soil mass in the field, there can be many changes to the soil physical state i.e. the moisture content and the dry density, that will affect the behaviour of a compacted soil after the compaction and during service. Consequently, the control of field compaction and the characterization of subgrade soil based on in-place engineering property i.e. in-situ dry density of the stabilized state has become necessary.

In the case of railway track constructed over lowland or those in the wet climate region, clay subgrade normally exists in a high saturation state despites the top compacted skin layer being prepared partially saturated initially. In general, track subgrade with compacted fine-grained subgrade though normally begins partially saturated can become highly-saturated when the wet weather / season sets in.

2.4.2 Stress and Strain during Unloading and reloading

By and large, soil particle in the subgrade experiences a large number of stress pulses, resemble stresses between that subjects to a confined compression and a constant stress confinement triaxial compression, each consisting of vertical, horizontal and shear stress components. Under confined compression, there is no lateral strain. The only vertical (axial) strain is equal to its volumetric strain. Given an application of vertical stress, the horizontal (lateral) stress ratio k_o, will be larger

during unloading than during the original loading. During the later stage of the unloading process, the horizontal stress may even exceed the vertical stress, causing constant alternation of the principle stress axis.

However, in the actual case, subgrade soil is allowed to bulge laterally due to slight absent of lateral restrain, thereby causing more vertical strain as compared to that of a confined compression (Lambe and Whitman 1969). In view of this, triaxial compression test is often preferred in the study of the performance of track subgrade soil, for it better simulates the actual phenomenon and its versatility.

2.4.3 Deformation Characteristic and Modelling

The strain response of soil under loading and unloading can be seen from Figure 2-4. Results of an oedometer test on a sample of "Cambridge clay" and on "Libyan sand" showed similar general stress-strain behaviour, except that the clay is much more compressible than the sand (Lambe and Whitman 1969).

Under the application of each wheel or group of wheels' loading, track subgrade seemingly behave elastically. However, soil being an elasto-plastic material can accumulate plastic (or permanent) deformation or settlement with each successive application of loading. Figure 2-5 showed an example of data plotted in a linear form for a Vicksburg Buckshort clay with water content = 28.7%, and dry density =1.44 Mg/m^3 (Li and Selig 1996; Townsend and Chisolm 1976), where a good correlation can be seen between the accumulation of axial strain and the number of repeated load (deviator stress) applications.

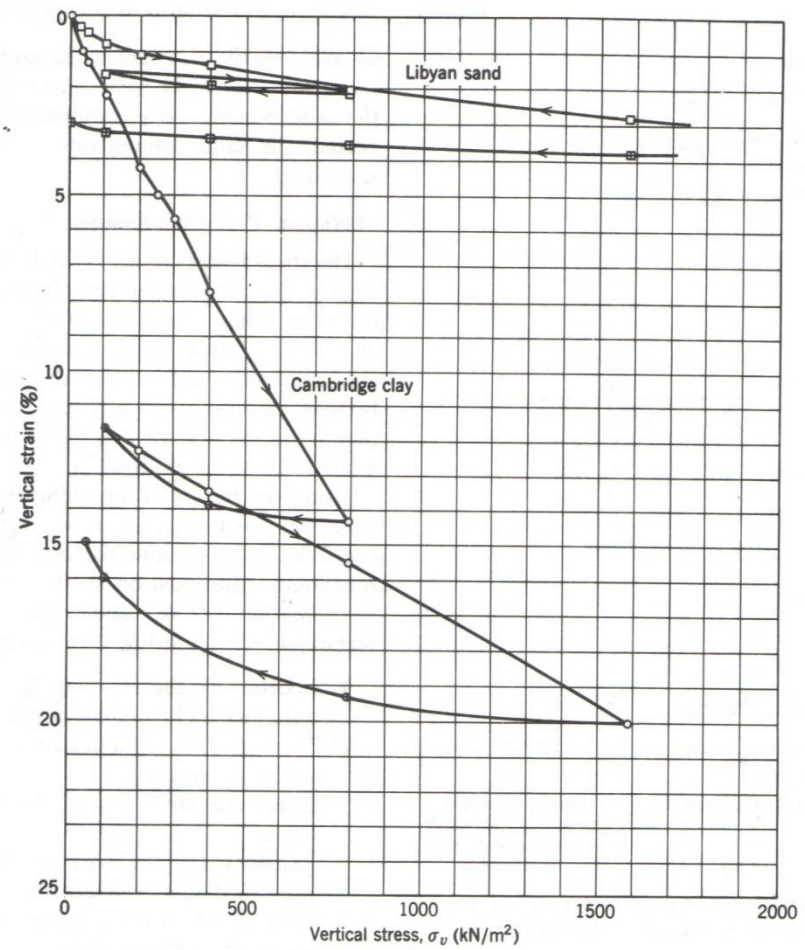

Figure 2-4 Results of Oedometer tests on Cambridge clay and Libyan sand (Lambe and Whitman 1969)

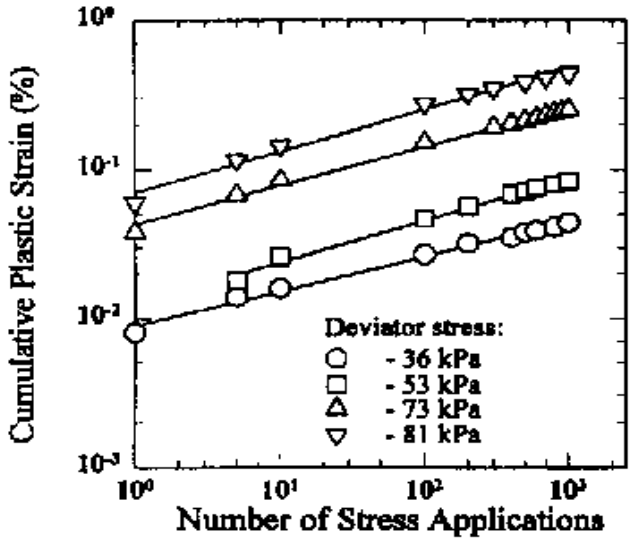

Figure 2-5 Development of plastic strain for a fine-grained soil: w=28.7%, γ_d =1.44 Mg/m^3 (Li and Selig 1996; Townsend and Chisolm 1976)

The developing mechanisms of permanent (plastic) deformation in a fine-grained soil subgrade under repeated loading can include some or all of the possible modes such as: (1) general plastic shear deformation, (2) progressive deformation as a result of consolidation due to dissipation of excess pore water pressure, (3) instant deformation and densification due to effect of compaction, and (4) deformation due to attrition as subgrade soil intermix with ballast. Current studies on permanent deformation of subgrade generally did not account for mechanism (4) as it only occurs when subgrade soil is overstressed, or/and drainage condition is poor.

There are several constitutive modelling equations available in the literatures which describe the relationship between the cumulative plastic strain and number of repeated load applications, as follows:

1. Monismith et al. (1975) discovered that the "Power" model (show below) represented the test results well for silty clay. The coefficient *b* is independent of

deviator stress and the coefficient A is a function of the stress level, previous stress history, and placement conditions.

$$\varepsilon_p = AN^b \tag{2-1}$$

where ε_p = cumulative plastic strain, and

N = number of repeated load applications

2. Puppala et al (1999) modified the model developed by Ullditz (1993) to accommodate the influence in confining pressure in the following expression:

$$\varepsilon_p = AN^{\alpha}\left[\frac{\sigma_{oct}}{\sigma_{atm}}\right]^{\beta} \tag{2-2}$$

where $\sigma_{oct} = \frac{\sigma_1 + \sigma_2 + \sigma_3}{3}$;

σ_{atm} = reference stress (atmospheric pressure of 100 kPa); and

A, α, β = constants

3. Li and Selig (1996) adopted the "Power" model and incorporated to it the effect of changing moisture content as it influence the static strength of soil, and suggested the following expression:

$$\varepsilon_p = a\left(\frac{\sigma_d}{\sigma_s}\right)^m N^b \tag{2-3}$$

where ε_p = cumulative plastic strain (%);

σ_d = deviator stress caused by train axle load;

σ_s = soil compressive strength; and

a, m, b = material parameter depending on soil type.

Of all the models presented above, Li's method (as in Equation (2-3)) allowed the changing physical state of the subgrade soil to be taken into consideration, and it appeared to be a more rational and favourable model. However, Equation (2-3) implied an ever increasing strain with respect to the number of load application (N), which contradicts the earlier report of the possible strain stabilization after certain load repetitions (Waters 1968). Another shortcoming in the model (Equation 2-3)) is the non-availability of conventional means to determine the material parameters a, m and b, to which a rough estimate of an average value had been suggested and back-calculated based on the limited tests data from literatures.

2.4.4 Strength of Soil in Cyclic Loading

Repeated (or cyclic) loadings can cause the shear strength of soil to change, depending on its physical state (void ratio and saturation). A loose soil can become compressed when dry, with resulting increase in its shear strength to a degree depending on its confining stress and applied loading. A dense soil can expand, with consequent strength reduction. On the other hand, a stress smaller than the static failure stress, when applied repeatedly can cause very large strain that will be defined as failure condition (Lambe and Whitman 1969; Sangrey 1969; Selig 1981). However, below the level of static strength of soil, there exists a maximum stress level below which deformation become stabilized.

In the real in-situ condition, though fine-grained subgrade under cyclic loading occurs in various degrees of 'partial-drained' condition (neither 'drained nor 'undrained' as in standard testing condition), the parametric study and characterization of the behaviour of soil under cyclic loading cannot be meaningfully studied in laboratory under 'partial-drained' or open-drainage condition. This is because the length of drainage path which influences the dissipation of excess pore water pressure for the small laboratory specimen will be very much shorter and by no means resembles that of the in-situ subgrade. Under possible quick successive cyclic loading, track subgrade with clay soil will have little time for dissipation of excess pore water pressure. Consequently, characterization of a clay subgrade soil of a non-transient state assuming saturated undrained condition has been adopted in this study.

2.4.4.1 Cyclic Undrained Application of Loading

During repeated undrained application of a shear stress, a soil may fail at a stress less than its monotonic shear strength. This occurs because the positive excess pore pressure do not return to zero after each cycle of loading, but rather accumulated and hence reduces the effective confining stress. The increase in pore pressure is caused by a progressive rearrangement of the soil particles during each successive unloading/reloading cycle. These rearrangements would have led to a decrease in volume, which, in the case of loose dry soil produced densification and increase in shear strength (Lambe and Whitman 1969).

In cyclic triaxial tests, failure of soil can be defined by a specified magnitude of strain occur in either of the two modes along axial axis. For tests with no shear reversal occurred (i.e. cyclic compression), the failure mode will be one in which the permanent axial strain reaches the specified value. When there is shear reversal (i.e. compression and tension), the magnitude of cyclic strain (or double-amplitude strain) will be the governing factor. (Selig 1981)

Sangrey et al (Sangrey 1969) conducted undrained triaxial tests on sample normally consolidated at confining pressure of 57 psi. Figure 2-6 shows the stress-strain-excess pore water pressure response of a specimen T1, taken to failure at an axial strain rate of 0.0002 % per minute in a single cycle and then unloaded. The peak stress of 54 psi was reached at about 6 % axial strain, while the maximum excess pore water pressure of 30 psi was attained at 2 % axial strain. Upon unloading, a residual axial strain of 5.8 % remained, while the pore water pressure increased further to 37 psi. In the subsequent tests on similarly consolidated specimen T2 and T3, loading cycles with peak stress of 47.1 psi and 26.2 psi respectively were repeatedly applied. In test T2 (Figure 2-7), residual axial strain increases after each additional cycle, while excess pore water pressure oscillates and increases at the same time. By the 10^{th} cycle, large axial strain occurred and the specimen failed. For test T3 (Figure 2-8), both the residual axial strain and excess pore pressure increases with loading cycle until the maximum were reached after the 6^{th} cycle. Further loading cycles produced no net changes to the stress-strain-pore water pressure responses, a state termed non-failure equilibrium (Sangrey 1969). The study by

Sangrey et al had provided an in-depth knowledge into the effective stress response of saturated clayey soil under repeated loading with very slow rate of loading i.e. ten hours per cycle, required for the equalization of pore water pressure within specimen. Contemporary train speed, however, produces cyclic stress near the surface of subgrade with considerably higher rate of loading i.e. in excess of 1 Hz (one second per cycle).

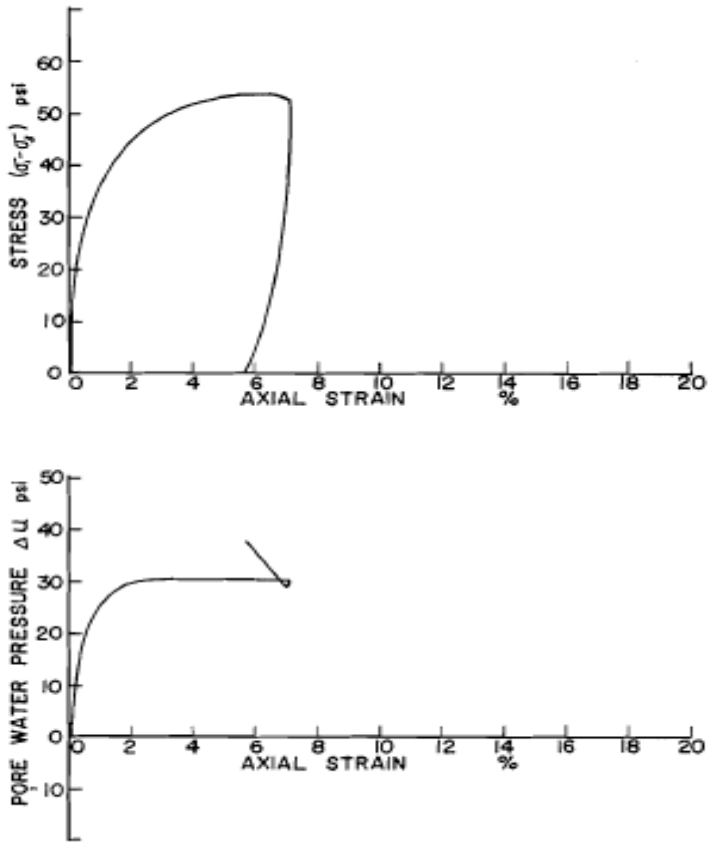

Figure 2-6 Stress-strain-pore water pressure response for test T1 (Sangrey 1969)

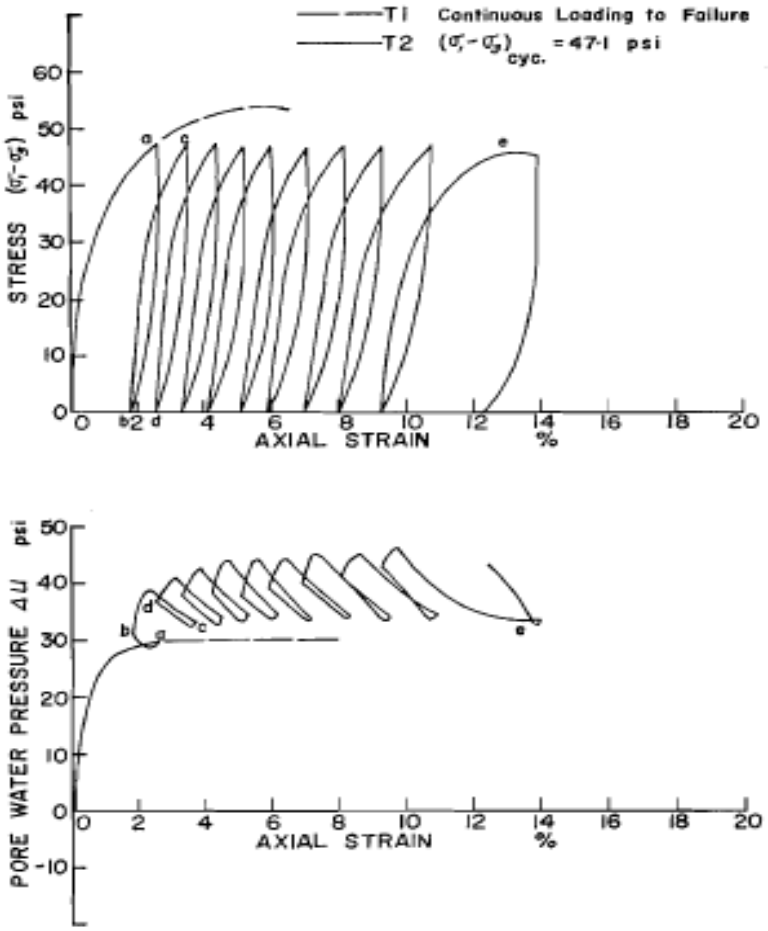

Figure 2-7 Stress-strain-pore water pressure response for test T2 (Sangrey 1969)

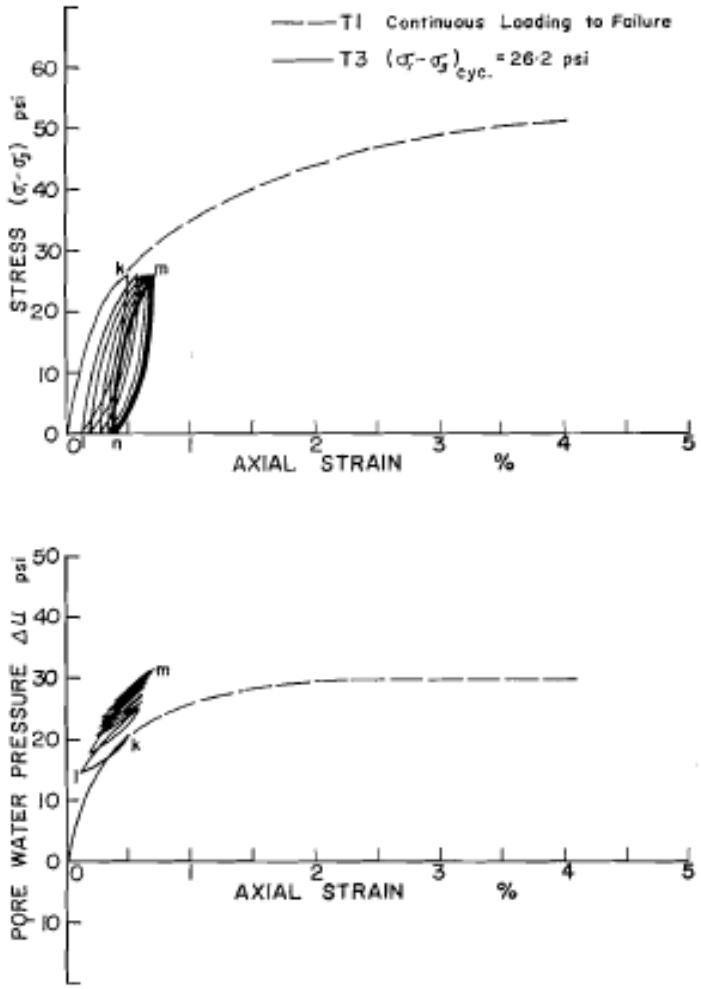

Figure 2-8 Stress-strain-pore water pressure response for test T3 (Sangrey 1969)

An experimental investigation was performed by Lefebvre (Lefebvre 1986) to study the response to cyclic loading of the highly sensitive Grande Baleine clay. Figure 2-9 and Figure 2-10 showed the stress-strain-pore pressure response of a structured (over-consolidated) and a normally consolidated clay, where the development of pore pressure and axial strain with the number of cycles for all tests was shown in a semi-logarithmic scale. For the failure test, axial strain developed progressively with each loading cycle, but increased suddenly on approaching failure, which pore pressure

increased without a sudden surge before failure. In the case of stabilized samples, axial strain curve remained practically horizontal with additional loading cycles, as did the development of pore pressure which remained constant after a large number of cycles.

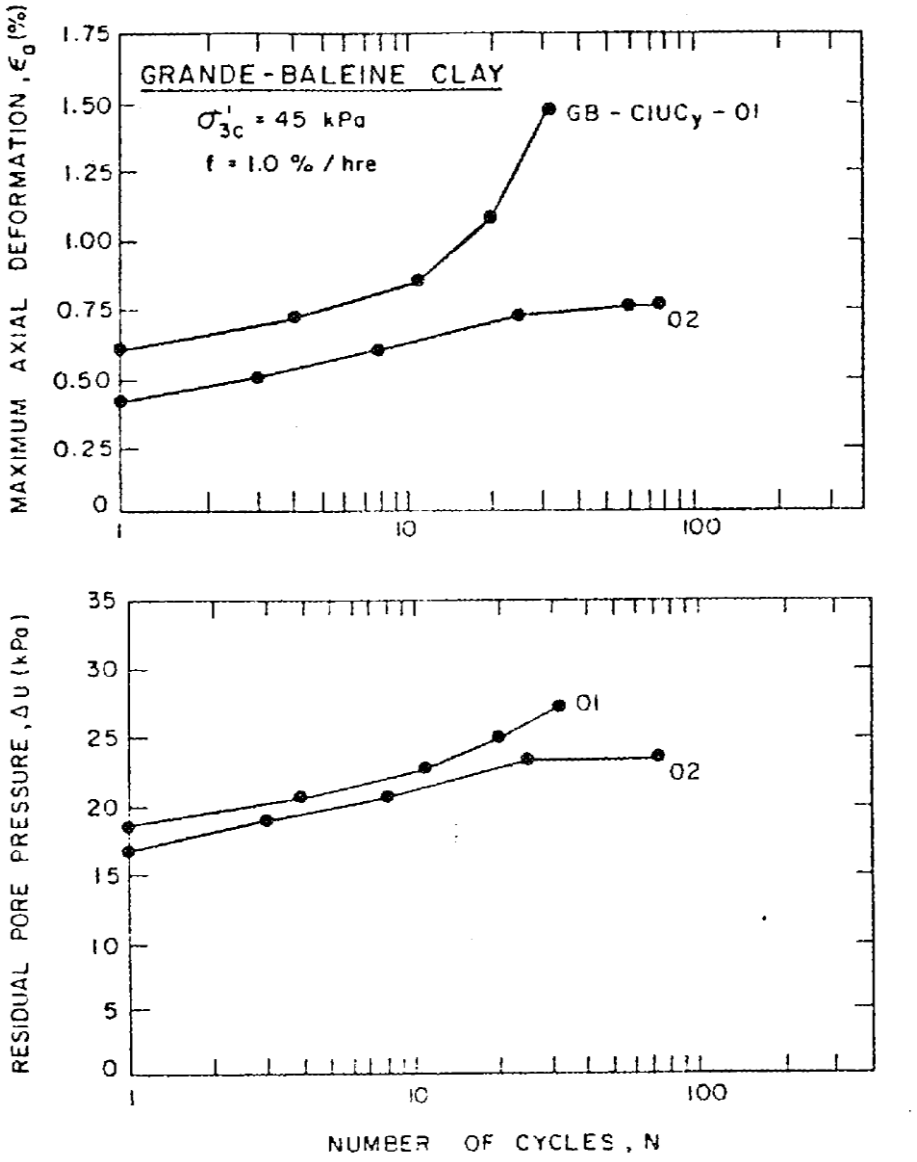

Figure 2-9 Typical stress-strain-pore pressure response of a structured clay under cyclic loading (Lefebvre 1986)

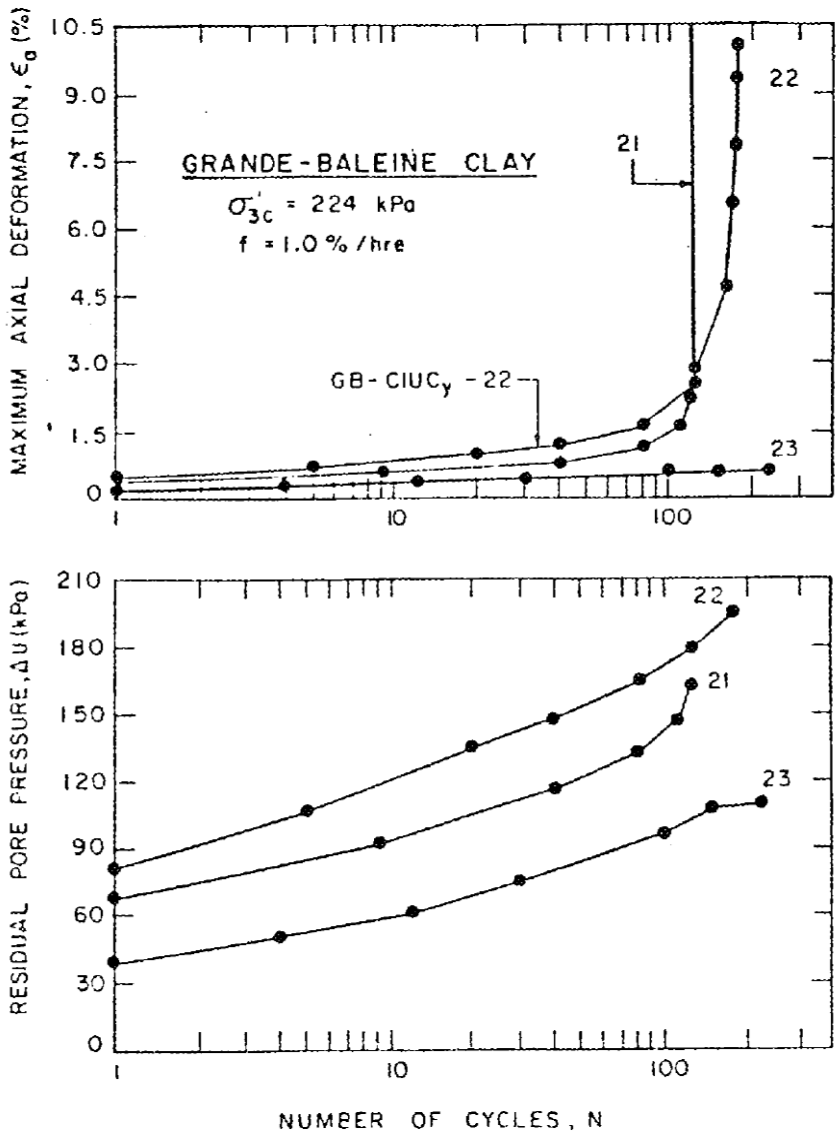

Figure 2-10 Typical stress-strain-pore pressure response of a structured clay under cyclic loading (Lefebvre 1986)

2.4.4.2 Cyclic Compression Strength and Threshold Stress

Under a single loading (or static compression), the strength of a soil is usually defined in terms of stresses developed at the peak of the stress-strain curve (called peak strength), and it corresponds to a certain amount of strain. When considerable straining of soil is expected on site, one speaks of the ultimate (or constant volume or critical) strength, which is the stress level sustained at large strain.

In the case of cyclic loading, given a predetermined number of loading cycles, the cyclic strength can be defined as the level of cyclic stress that will develop a preset amount of accumulated strain, in response to the number of loading cycles applied, though the number of loading cycles is usually difficult to be defined in practical sense. Alternatively, it is widely recognized that a critical level of stress exists (termed threshold stress) below the level of monotonic peak strength (Heath et al. 1972; Lefebvre 1986; Procter 1984; Sangrey 1969; Waters 1968), above which large shear deformation takes place, and below which soil strain stabilized irrespective of the number of loading cycles applied. In cases when large number of cyclic loads occurs in quick succession, the strength parameter of fine-grained soil can be characterized by the threshold stress instead (Lefebvre 1986).

In the tests for Grande Baleine sensitive clay, Lefebvre (1986) defined the cyclic stability threshold as the maximum cyclic stress level which the soil will not suffer failure regardless of the number of applied cycles. He reported the stability threshold for both structured or normally consolidated specimen under cyclic loading was about 60 – 65 % of the undrained shear strength measured at the same strain rate as used in the cyclic tests, and that the normalized stability threshold appeared independent of the consolidation pressure and structure effect. A simple approach had been used by Lefebvre (1986) in determine the stability threshold by ascertaining the level of cyclic stress which lies between the lowest stress ratio for a failed specimen and the highest stress ratio for a stabilized test.

2.4.4.3 Determination of Threshold Stress

The means and technique to determine the threshold stress of a fine-grained soil has been proposed and described by many different researchers. Generally, they fall under either the 'total stress' method with only measurement of strain development, or the 'effective stress' method with measurement of both pore pressure response and strain development. They include:

(a) Plastic Strain Development Observation Technique

British researcher (Waters 1968) developed the threshold test procedure to characterize the strength of 'London clay' subgrade and to correlate its resistance to permanent deformation of the in-situ subgrade. In ascertaining the threshold stress, axial deformation data obtained from tests of various principal stress differences (under the same confining pressure) are rearranged in the form of logarithm of number of loading cycles against principal stress difference (Figure 2-11). For any given percentage cumulative strain, a discontinuity in the curve is apparent. Stress immediately below such discontinuity is termed the threshold stress level. In the similar technique / method used by British researchers, Procter et al (Procter 1984) also presented a graph (Figure 2-12) showing the constant strain contours that were constructed based on strain data from series of tests conducted at various cyclic (shear) stress level. Each contour (or curve) represents combinations of shear stress and number of cycles needed to attain a specified double-amplitude cumulative strain. These curves gradually tend to a horizontal asymptote, with the value of its intercept on the axis of cyclic shear stress being the level of threshold stress (or threshold stress ratio as in Figure 2-12).

However, the value of asymptote (threshold stress) so obtained is very sensitive to the data readings, i.e. the value of strain and the associate number of cycles, and many test sets (minimum four) would be required to produce enough of the data points. Very often, one or two confirmation tests have to be conducted at cyclic deviator stress levels near the asymptote in order to identify the threshold stress.

Consequently, large numbers of tests are often needed. This technique mainly provides good illustration of the constant strain contour, and it offers a crude means of determining the threshold stress.

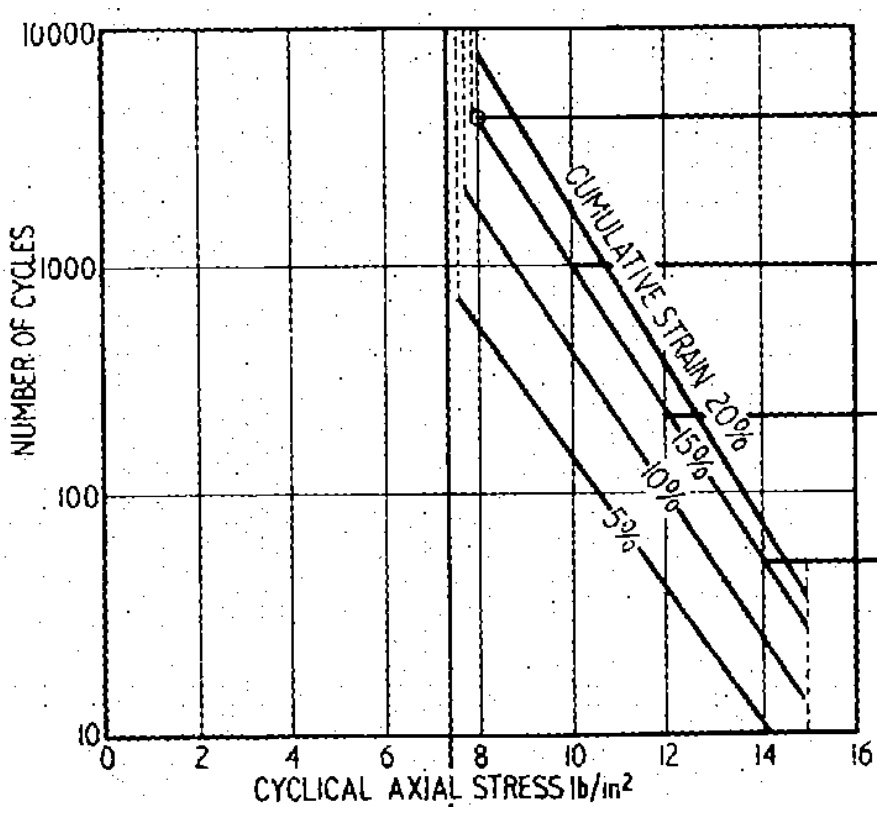

Figure 2-11 Constant cumulative strain contours for tests conducted on "London clay" (Water 1968)

(b) Fully Weakened Stress State Observation Technique

Procter (1984) further proposed that the fully weakened stress state of soil, which is the maximum stress level (minimum strength) below which cyclic action is assumed

to have negligible weakening effect to the soil, can be achieved and determined in any single displacement-control test. The test required that a constant average double-amplitude strain larger than 5 % and number of loading cycles *N* larger than 10,000 cycles is applied. A single curve (contour) relating shear stress to number of cycles needed to attain say, 5 % cumulative strain, similar to the constant strain curve in Figure 2-12 can be plotted and obtained in one single cyclic test (Dobry and Swiger 1979; Procter 1984). The procedure and technique offers a more efficient means as compared to that of the stress-control tests. However, more research will be required to substantiate its claim with respects to the pre-set strain magnitude and the minimum numbers of load cycles, when it applies to the general clay material.

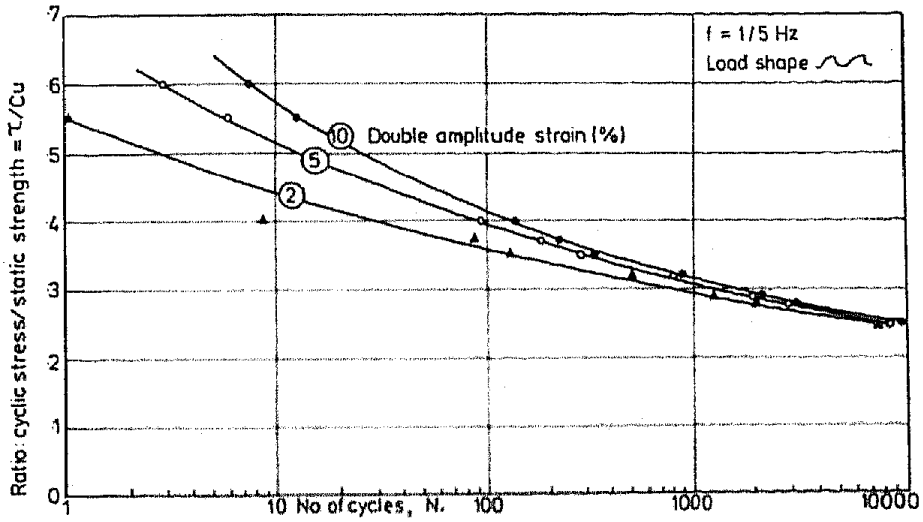

Figure 2-12 Constant strain contours for tests on Derwent clay (Proctor 1984)

(c) The Equilibrium Line method

Sangrey et al (Sangrey 1969) conducted a series of repeated loading undrained triaxial tests on an undisturbed clay soil obtained from the face of landslide scarp, to study the stress-strain behaviour of soil under repeated loading. Interpretation of the test results were made in terms of effective stress response in the 3-dimensional

principle stress space. He suggested and illustrated that a critical level of repeated stress (CLRS) exists, above which repeated application of loading continues to produce cumulative deformation. Below the critical level, a state of non-failure equilibrium will be arrived in which the stress-strain curves forms closed hysteresis loops. In the 3-D stress space, a straight line passing through the locus of the stress peaks of equilibrium hysteresis loops and the point at initial consolidated state is "the equilibrium line" (Figure 2-13). The equilibrium line intersects the failure line at a point "P" where the critical level of repeated stress can be derived.

The Equilibrium line method is essentially an effective stress analysis which depends upon accurate measurement of the response of excess pore water pressure. The slow process required for the equalization of excess pore water pressure within the specimen means that, this method have so far been used only for cyclic loading with very slow rate of loading.

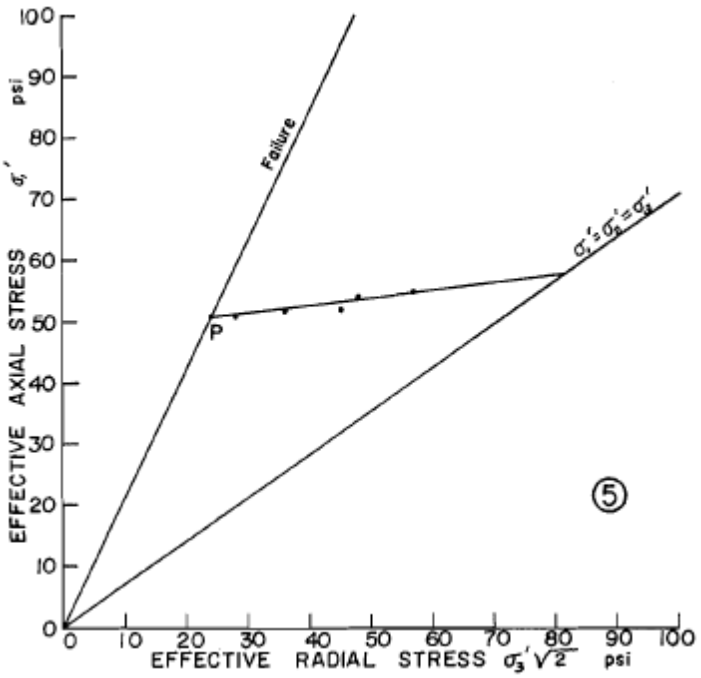

Figure 2-13 The equilibrium line (Sangrey 1969)

2.4.5 Resilient State Behaviour and Modelling

The characterization of subgrade soil by its resilient modulus has been widely practiced. In analysing the railway track support system, knowledge of the resilient modulus of subgrade is needed for calculating stresses, strains or deflection in conjunction with the use of computer modelling. At the beginning of the stress-strain curve (see Figure 2-14), soil is approximately elastic if both the loading and the corresponding strain is small. The linear elasticity in this small strain region is defined by its elastic modulus. Under moderate levels of repeated loading (Selig and Waters 1994), the elastic strain of a soil gradually reducing and become constant after large number of loading cycles. It is the elastic modulus at this point (termed resilient modulus) that is of interest for characterizing the soil as follows:

$$E_r = \frac{\sigma_d}{\varepsilon_r} \tag{2-4}$$

where E_r = resilient modulus;

σ_d = repeated deviator stress $(\sigma_1 - \sigma_3)$; and

ε_r = recoverable (or resilient) strain in the direction of σ_1.

Li et al (1994b) reported that the resilient modulus of fine-grained subgrade is strongly dependent upon many different factors such as stress state or moisture content. Consequently, variation of moisture content on site can potentially change the stiffness property of fine-grained soil.

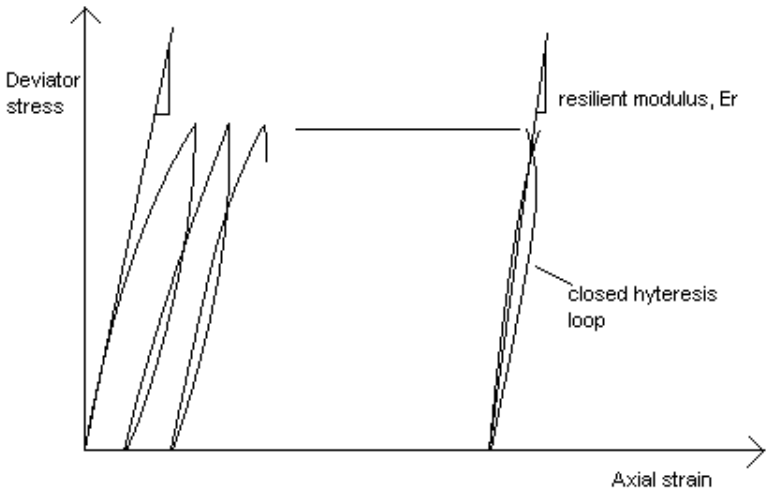

Figure 2-14 Typical stress-strain curve of a cyclic triaxial testing

Modelling the Resilient Modulus

The magnitude of the resilient modulus is very much depending on the state of stress. Studies (Hicks and Monismith 1971; Selig and Waters 1994) have shown that the resilient response of unbound granular materials increases as the confining pressure increases and is affected only to a smaller extent by its deviator stress. As such, the resilient modulus can be approximately related to the confining pressure σ_3, or to the sum of principal stresses according to,

$$E_r = K_1(\sigma_3)^{K_2} \tag{2-5}$$

and

$$E_r = K_1^{'}(\theta)^{K_2^{'}} \tag{2-6}$$

where, E_r = resilient modulus;

$K_1, K_2, K_1^{'}$ & $K_2^{'}$ = constants determined from tests; and

θ = first stress invariant ($\sigma_1^{'} + \sigma_2^{'} + \sigma_3^{'}$) or the sum of principal stress in the loaded state

Uzan et al. (Uzan 1985) observed that the $K-\theta$ model described above failed to match the measured triaxial data. He considered the effect of both the confining pressure and shear stress, and added the deviator stress as a parameter and proposed the following model:

$$E_r = K_1 P_a \left(\frac{\theta}{P_a} \right)^{K_2} \left(\frac{\sigma_d}{P_a} \right)^{K_3} \qquad (2\text{-}7)$$

where K_1, K_2, K_3, is the regression coefficients;

θ is the sum of principal stresses;

P_a is the reference atmospheric pressure 100 kPa ≈ 1 kgf/cm^2 ≈ 2000 psf ≈ 14.5 psi; and

σ_d is the deviator stress in the same unit as P_a.

In the case of fine-grained soil, Drumm et al. (1990) reported that the AASHTO design guide recommended the resilient modulus of fine-grained soils be estimated using the empirical correlation (proposed by Heukelom and Klomp (1962)) from the California Bearing Ratio (CBR) test as follows:

$$E_r = 1{,}500 CBR \quad \text{(psi)} \qquad (2\text{-}8)$$

Fine-grained soils typically display a decrease in moduli with increasing amplitude of cyclic loading or increasing deviator stress (Thompson and Robnett 1979). The behaviour is characterized by a bi-linear model as shown below. A “breakpoint”

resilient modulus, E_{ri} at which a significant change of gradient occurs, can be identified. The "breakpoint" resilient modulus, E_{ri} with respect to its deviator stress, σ_{di} was used by Thompson and Robnett (1979) to characterize the resilient response of a wide range of Illinois subgrade.

$$E_r = K_3 - K_1\sigma_d \qquad \text{for } \sigma_d \langle \sigma_{di} \tag{2-9}$$

and

$$E_r = K_4 - K_2\sigma_d \qquad \text{for } \sigma_d \rangle \sigma_{di} \tag{2-10}$$

where K_1, K_2, K_3 and K_4 is model parameter

A nonlinear relation in a form of "power model" that has been widely used to best represent the above bi-linear model (Moossazadeh and Witczak 1981) is,

$$E_r = K_1(\sigma_d)^n \tag{2-11}$$

where K_1 and n is material constant depending on soil type and physical state. This model is further proposed by Brown et al. (1975) to incorporate effective confining stress σ_3' to become,

$$E_r = K_1\left(\sigma_d / \sigma_3'\right)^n \tag{2-12}$$

While the bi-linear model represents a closer modelling of the resilient behaviour of fine-grained soil in response to cyclic load and had been popular in numerical analysis, Li and Selig (1994b) recommended the power model (Equation (2-12)) for it provided reasonable representation of the resilient behaviour of test data analysed and was simple in its use as only two parameters are involved (as compared to five

for the bi-linear model). In addition, they highlighted the resilient modulus of fine-grained subgrade soils is not a constant stiffness property, but strongly dependant upon the following factors:

(1) Loading condition or stress state, which includes the magnitude of deviator stress and confining stress, and the number of repetitive loadings;

(2) Soil type and structure, which depends on compaction method and effort for a new subgrade; and

(3) Soil physical state, which is represented by its changing moisture content and dry density as the environment changes.

A method was developed (Li 1994b; Selig and Waters 1994) for the estimation of resilient modulus of compacted fine-grained subgrade soils of any dry densities and moisture contents, from the following relations based on the known resilient modulus, $E_{r(opt)}$ from literature:

$$E_r = R_{m1} E_{r(opt)} \tag{2-13}$$

(For *w* variation with constant dry density); and

$$E_r = R_{m2} E_{r(opt)} \tag{2-14}$$

(For *w* variation with constant compactive effort)

With $$R_{m1} = f_1(w - w_{opt}) = 0.98 - 0.28(w - w_{opt}) + 0.029(w - w_{opt})^2 \tag{2-15}$$

$$R_{m2} = f_2(w - w_{opt}) = 0.96 - 0.18(w - w_{opt}) + 0.0067(w - w_{opt})^2 \tag{2-16}$$

where E_r is the resilient modulus of interest,

$E_{r(opt)}$ is the reference resilient modulus at maximum dry density at the optimum moisture content w_{opt} of a particular compaction effort; and

w being the in-situ moisture content of the soil.

2.4.6 Influence of Rate of Loading

One of the important aspects of cyclic loading is the rate-dependent response concerning how the rate of loading (cyclic frequency) influences the strength deterioration due to build-up of excess pore water pressure, and the strain development and effect of creep. The advance in train automobile technology and the required efficiency of transporting goods and commuting passengers mean higher train speed which induces higher cyclic loading frequency at track foundation subgrade. Better understanding on how the dynamic frequency of cyclic loading induced by the higher train speed influences behaviour of the subgrade soil and hence the stability of track, is required.

Procter et al. (1984) investigated the weakening of undrained saturated clays under cyclic loading concerning the problem of soil conditions affected by wave action beneath offshore gravity structures. A series of undrained stress-controlled reversed cyclic triaxial test were performed on saturated remoulded Derwent clay (Clay fraction = 45 %, Plasticity index = 26 %) at a frequency range of 0.008 to 1 Hz. Constant strain (double-amplitude) contours were plotted based on the tests data in order to establish the limiting cyclic strength (or minimum cyclic stress (τ) / undrained strength (Cu)) with respect to the number of cyclic load applications (Figure 2-15). From the plot, the effect of frequency on cyclic performance suggests that a frequency change from 0.008 Hz to 1 Hz causes approximately 30 % increase in the limiting cyclic strength for the range of 10 to 5000 cycle-applications. Final weakening of samples was thought possible after more than 100,000 cycles. However, when normalized by the modified undrained strength ($C\bar{u}$) which had been adjusted for the same cyclic loading rate effect, Procter (1984) concluded that

the final weakening of samples tested (limiting cyclic strength) was similar, i.e. independent of frequencies, at higher number of loading cycles as shown in Figure 2-16.

Lefebvre (1986) reported the one-way triaxial compression tests on Grande Baleine sensitive clay that, the effect of increasing the cyclic loading frequency from 0.01 Hz to 2 Hz did increase the stability threshold for both the structured (over-consolidated) and normally consolidated specimens by about 33 %.

Ansal et al. (1989) conducted series of undrained cyclic simple shear tests on the re-constituted one-dimensional-consolidated and the remoulded isotropic-consolidated kaolinite samples, with different shear stress amplitudes and cyclic loading frequencies. The effect of the rate of cyclic loading (at a frequency range of 0.01 to 1.0 Hz) was studied with respect to different shear stress amplitudes and the number of cycles. It was reported that the frequency effect diminishes with an increasing number of cycles and with decreasing shear stress amplitude. The influence of cyclic frequency appeared to be significant if relatively small numbers (up to 100 cycles) were used in evaluating the cyclic behaviour. For a large number of cycles, the frequency of the cyclic loading has no significant influence on the behaviour of normally-consolidated clays. Ansal (1989) further indicated that a critical shear stress amplitude exists below which the effect of frequency disappears all together.

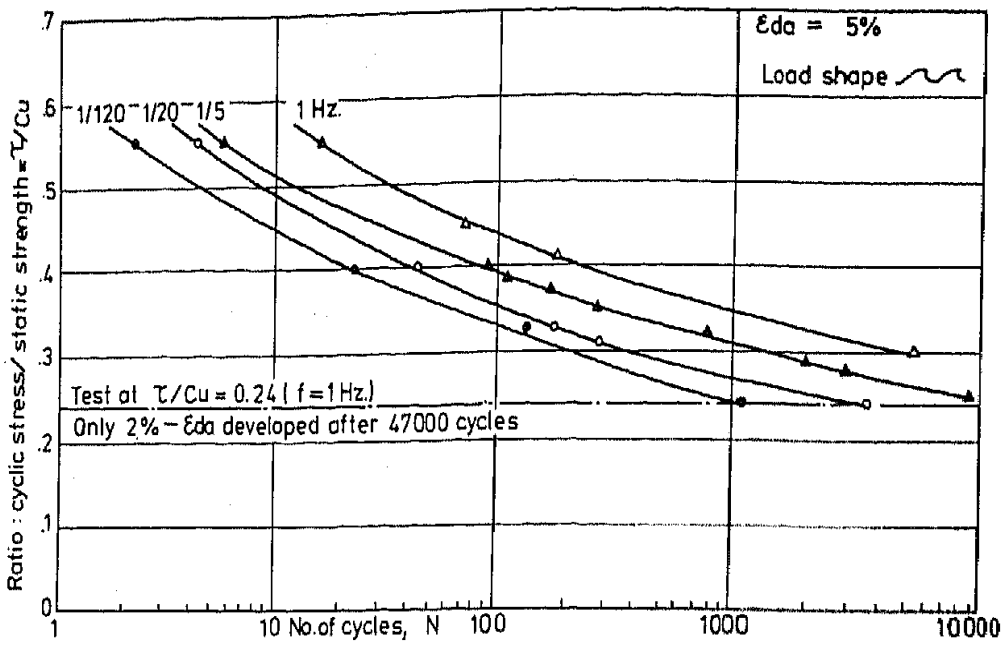

Figure 2-15 Frequency Response of Cyclic Stress Ratio causing 5% double-amplitude strain (Procter 1984)

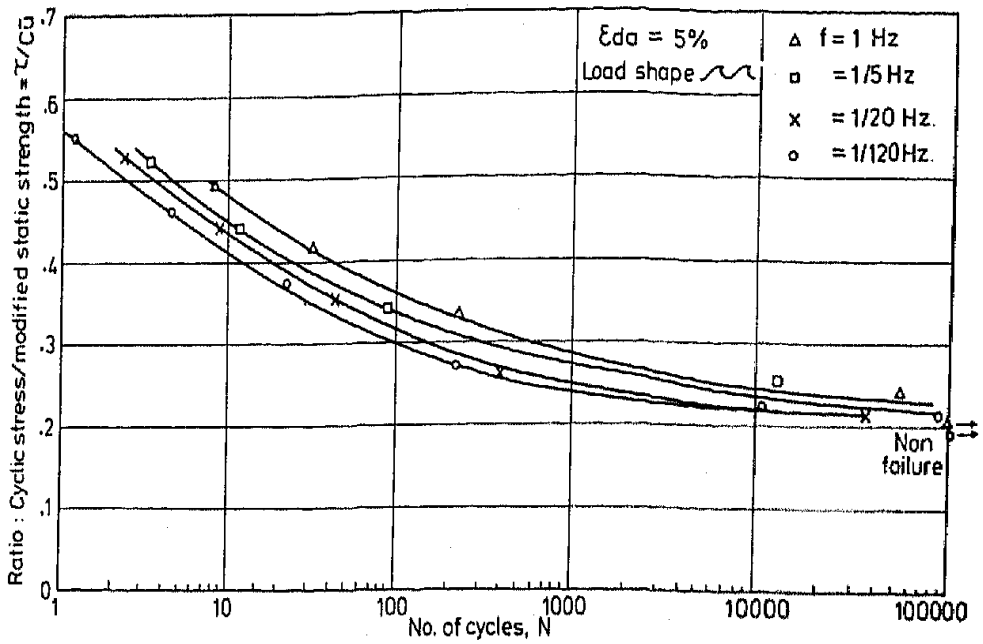

Figure 2-16 Frequency response of modified cyclic stress ratio causing 5% double-amplitude strain (Procter 1984)

2.5 *Current Railway Track Foundation Design Approach*

The design of railway track foundation has primarily been intended in limiting applied stress to subgrade such that it does not overwhelm the strength capacity of subgrade as to cause excessive deformation or failure. The current design methods are largely empirical or semi-empirical in its approach. With the advance in computational capability, use of finite element method can potentially provide added advantage for improved design, when the general soil behaviour and other relevant parameters can be properly accounted for. The followings are reviews of the prevalent approaches and methodologies for the design of railway track foundation, with particular reference to fine-grained subgrade.

2.5.1 Conventional North America Method

The North America practice has the design objective of limiting the applied stress P_c to the allowable bearing pressure (or design bearing pressure) σ_{des} (Selig and Waters 1994), such that,

$$P_c \leq \sigma_{des} \tag{2-17}$$

The American Railway Engineering association (AREA) manual lists four equations for calculating the applied stress P_c (in psi) as a function of the applied stress on ballast P_m and the ballast depth h.

$$\text{Talbot equation: } P_c = \frac{16.8P_m}{h^{1.25}} \tag{2-18}$$

$$\text{Japanese National Railways Equation: } P_c = \frac{50P_m}{10 + h^{1.35}} \tag{2-19}$$

Boussinesq equation: $P_c = \frac{6q_o}{2\pi h^2}$ (2-20)

Love's equation: $P_c = P_m \left[1 - \left(\frac{1}{1 + \left(r^2 / h^2 \right)} \right)^{3/2} \right]$ (2-21)

where P_m = the applied stress on ballast (psi);

h = ballast depth (in.);

q_o = the static rail seat load (lb); and

r = radius of circle with area equal the sleeper bearing area (in.).

In determine the required thickness of granular layer that will satisfy the condition required in Equation (2-17), AREA Manual recommends a universal allowable subgrade bearing pressure (σ_{des}) of 20 psi (135 kPa) for all soil conditions. Use of a common value for the allowable subgrade bearing pressure will most likely lead to over-estimate for soft soil subgrade. For this, Selig et al. (1994) had proposed the allowable bearing pressure be based on soil conditions i.e. soil classification, by adopting the empirical value of static bearing strength of subgrade from the US NAVFAC design manual (Navy 1962). A factor of 0.6 was applied to allow for variation in sleeper support condition (Dipilato et al. 1983).

Jeffs and Tew (1991) also suggested the allowable subgrade bearing pressure (σ_{des}) can be determined by modifying the safe average bearing pressure σ_{safe} by an additional safety factor X_s accounting for possible settlement, as follows:

$$\sigma_{des} = X_s \cdot \sigma_{safe} \quad (2\text{-}22)$$

where the determination of safe average bearing pressure σ_{safe} can be done

by conducting a static load test such as California Bearing Ratio (CBR) test, whereby an approximate correlation between the CBR value and the safe bearing pressure (σ_{safe}) for compacted subgrade is available in the empirical chart at reference (Research and Laboratory 1961); and X_s = 0.6 (Clarke 1957) or 0.5 (AREA 1973)

However, the allowable bearing pressure so determined may still be over-estimated as the allowable bearing strength under repeated or cyclic loading is much smaller than that in static condition as most of the empirical record had, especially for the soft cohesive soil.

2.5.2 British Rail Formation Design Method

Heath et al. (1972) reported a track foundation design method for British Rail Research which relates the subgrade performance to the cyclic stress cause by train axles loading. Triaxial compression test were carried out on samples of London clay for three different ambient pressures. Axial stresses simulating the field condition were cycled at 30 square wave pulses per minute (0.5 Hz), with open-drainage allowed. "Threshold stress" was thus established, above which deformation continues exponentially with further cyclic load applications; and below it, deformation ceased to a stabilized state. Based on these test results, the relationship for the increment of threshold stress with the depth of construction (distance between bottoms of sleepers to surface of subgrade) has become available. However, due to the open drainage allowed during the test, such relationship will not remain unchanged had the size of the specimen or the rate of loading cycle been different.

The design method pre-supposed that a balanced design will be achieved when induced stress due to the heaviest commonly occurring axle load is equal or smaller than the threshold stress at that depth in the subgrade. The induced stress at different depth, for a range of axle loads was derived using single layer simple elastic theory. Figure 2-17 showed a family of curves which depicts the variation of induced stress

(solid lines) with depth, superimposed by another family of dash lines for threshold stress derived from the standard tests. A summary chart (Figure 2-18), derived from Figure 2-17 which directly relates the required depth of granular layer construction to the threshold stress for a range of axle load, had been made available for design purposes. Field assessment of the validity of design method was conducted by British Rail and performance of track foundation was found optimum.

The rational approach of the BR design method aimed at limiting the induced stress to the threshold stress of subgrade by spreading the stress transmitted from the wheel through varying the thickness of the ballast / sub-ballast layer. However, the soil testing method with regards to specimen size, cyclic loading rate and drainage condition has been unique, as the level of "threshold stress" so obtained e.g. with open-drainage allowed will be peculiar to the soil type, the size of specimen and the cyclic loading rate. This means that British Rail (BR)'s method in the design of the granular layer is essentially based on the correlation between a unique characterization of subgrade strength and the local probabilistic traffic pattern and characteristics. As such, the BR design method is semi-empirical and the design chart which was field-validated is peculiar to its practical application for UK. The cyclic frequency employed in the soil test is considerably lower than that of the contemporary train speed is capable of producing near subgrade surface.

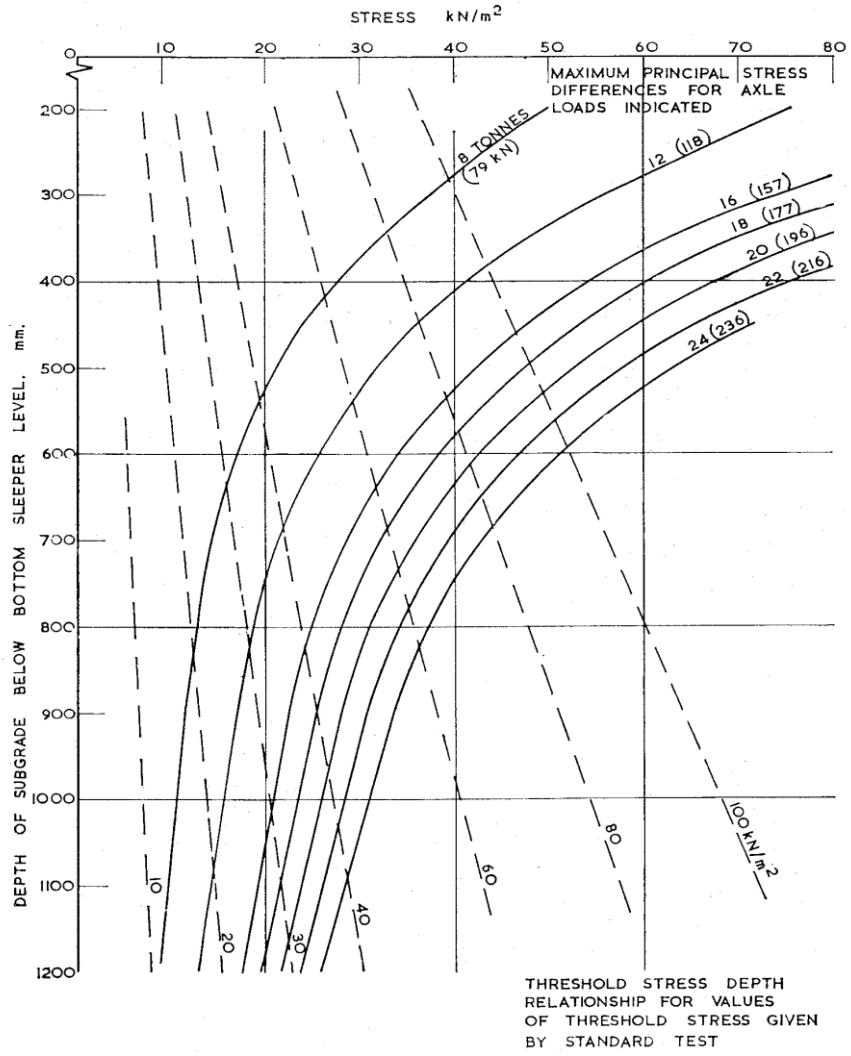

Figure 2-17 Relationship of the induced stress and the soil strength with depth (Heath 1972)

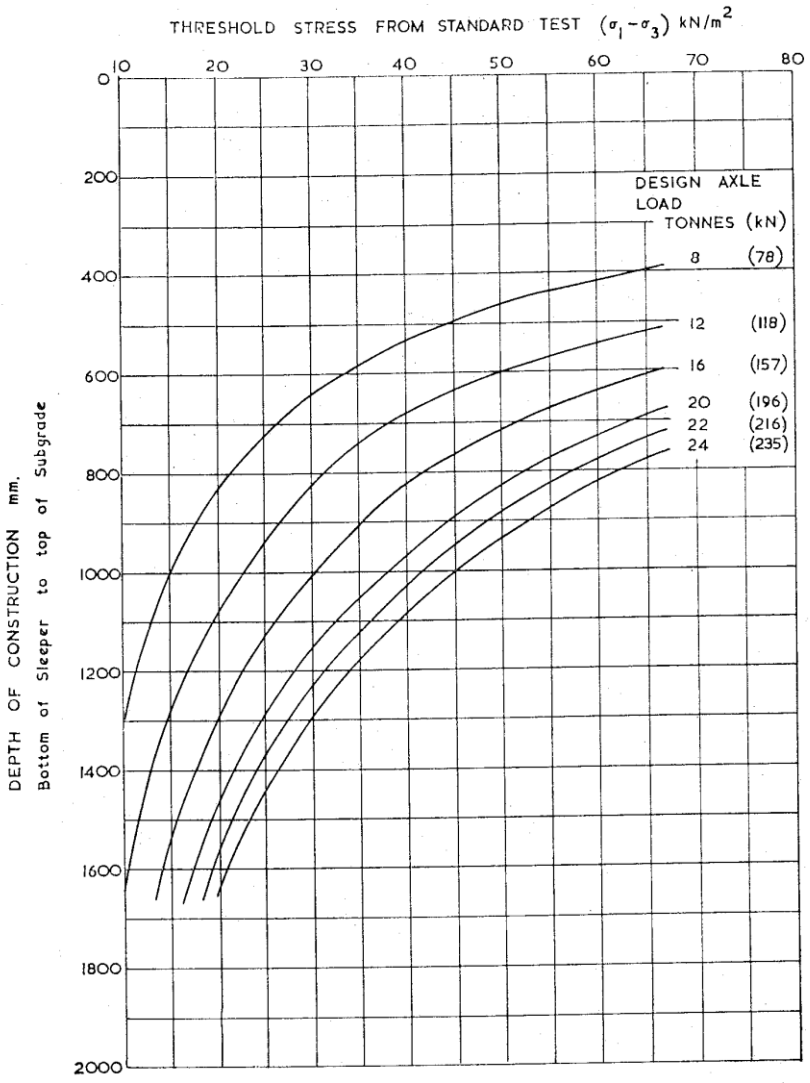

Figure 2-18 Design chart directly relates depth of construction to soil strength (Heath 1972)

2.5.3 Numerical Method

Primarily a strain-focus approach which aims to prevent progressive shear failure and excessive plastic deformation of subgrade, Li and Selig (Li 1994b; 1996; Li and Selig 1998a; Li and Selig 1998b) developed the mathematical models for predicting

the subgrade cumulative plastic strain (ε_p) in relation to the soil deviator stress (σ_d) and the number of stress applications (*N*), and the cumulative deformation (ρ) as follows:

$$\varepsilon_p = a\left(\frac{\sigma_d}{\sigma_s}\right)^m N^b \quad (\%) \tag{2-23}$$

And the cumulative deformation (ρ),

$$\rho = \int_0^t \varepsilon_p dt \tag{2-24}$$

where σ_s is the compressive strength of the soil, a, b, m are the parameters depend on the soil type, and t being the depth of subgrade layer.

The design objective is achieved by limiting the total cumulative plastic strain at subgrade surface and the total cumulative plastic deformation of subgrade layer to an allowable level, given the number of repeated axle's loads.

A three-dimensional, multi-layered elastic model known as GEOTRACK was used to analyse and compute the subgrade stress distribution under a combination of traffic loading condition. Together with the above Equation (2-23) and (2-24), and the data base of material parameters back-calculated from available test data of cumulative plastic strain in the literature, two sets of design graphs were produced for the various relative stiffness of ballast and subgrade layers. One set of the design graphs (as typically shown in Figure 2-19) gives the minimum thickness of granular (ballast / sub-ballast) layer that limit total plastic strain at subgrade surface in order to prevent progressive shear failure. The graphs relate the design strain influence factor I_ε (Equation (2-25)) to the thickness of granular layer and is normalized by an arbitrary length factor (L) that has a value equal to 0.152m (6 in.)

The other set of graphs (as typically shown in Figure 2-20) gives the minimum thickness of granular layer to prevent excessive plastic deformation. The graph relates the deformation influence factor I_ρ (Equation (2-26)) to the thickness of granular layer as follows:

$$I_\varepsilon = \frac{\sigma_d A}{P_d} \tag{2-25}$$

$$I_\rho = \frac{\rho_a / L}{a\left(\frac{P_d}{\sigma_s A}\right)^m N^b} \times 100 \tag{2-26}$$

where σ_d = deviator stress at subgrade surface;

P_d = design dynamic wheel load;

A = an arbitrary area factor that has value of 0.645 m^2 (1,000 $in.^2$);

and

ρ_a = allowable total subgrade plastic deformation for the design period

Li et al's method has been analytical and rigorous in its approach to track foundation design. However, no indication on what constitute an allowable level of strain at subgrade surface and an allowable total deformation were made available pending future study. The model (Equation (2-23)), though take into account the effect of soil physical states (moisture content; dry density) on its strength and stiffness, will have some difficulties to put into practice since the physical state of soil is unlikely to remain constant and it also varies along the track. In addition, the model presupposed the incessant accumulation of strain and deformation with respect to the number of

load applications, which ignores possible strain stabilization and rendering the model over-conservative for large number of loading repetition.

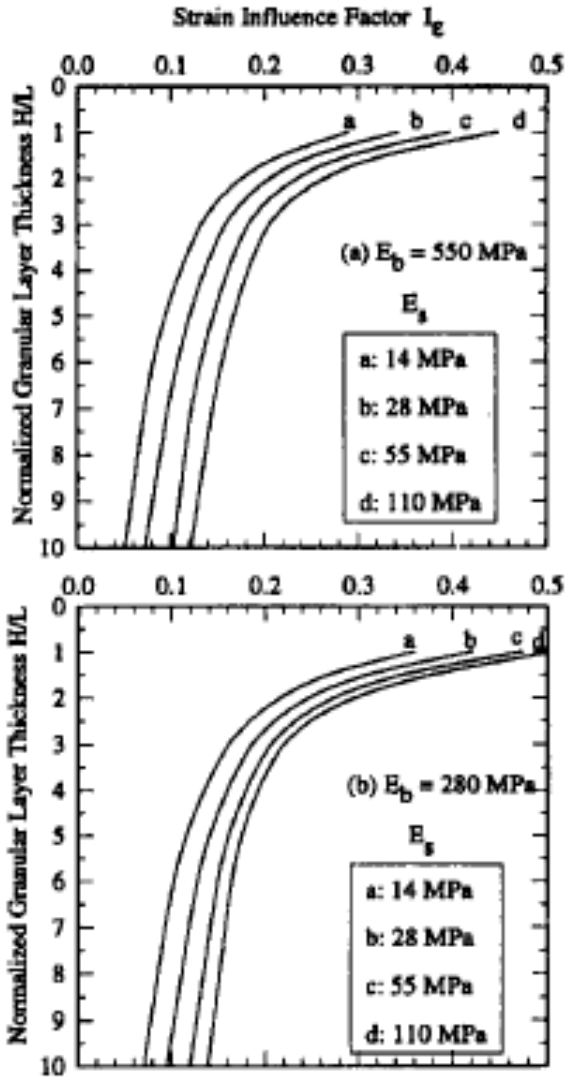

Figure 2-19 Granular layer thickness design graph for preventing progressive shear failure (Li 1988)

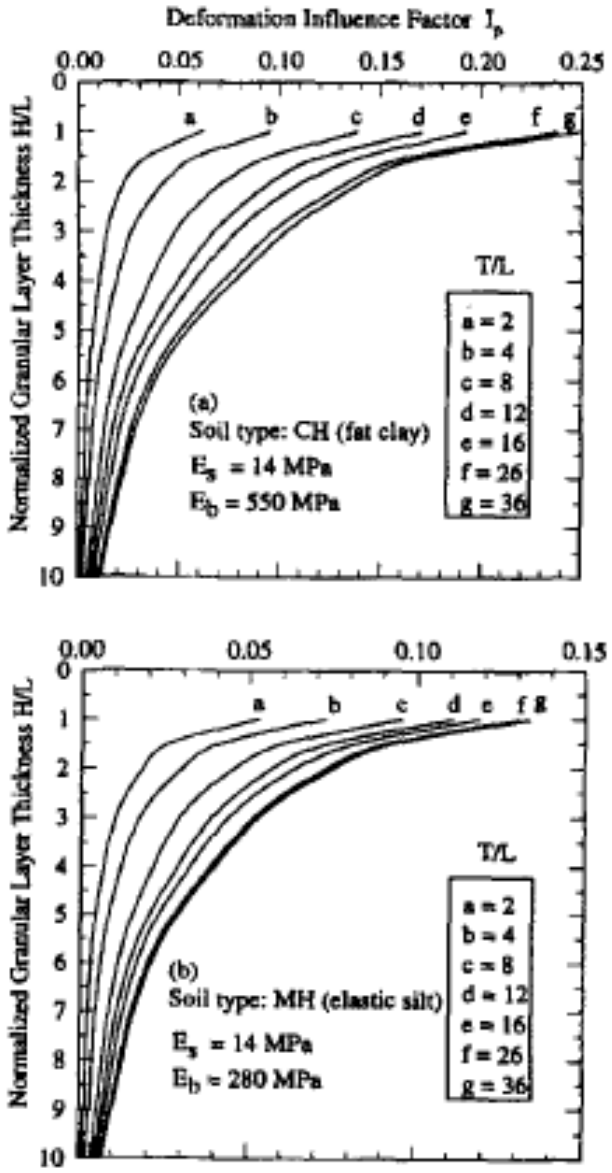

Figure 2-20 Granular thickness design graph for preventing excessive total deformation (Li 1998)

2.6 *Summary*

A general perspective on the various components of railway track structure, in particular the substructure which forms the geo-foundation, was described. The subgrade of railway track has a significant influence on the overall track performance. Of the various nature of subgrade distress for fine-grained subgrade i.e. clay material in particular, progressive shear failure near the subgrade surface caused by the effect of cyclic loading is one of the most important failure modes.

The physical state (i.e. moisture content and dry density) of subgrade soil can change considerably during service. As such, characterisation of subgrade soil based on the in-place engineering property is necessary. In studying the behaviour of track subgrade soil, triaxial compression test is preferred for its better simulation of actual stress condition. In general, clay subgrade over lowland or in wet climate region though begins partially saturated can become highly saturated subsequently. In addition, under the cyclic loading due to quick succession of passing trains, clay subgrade will have little time for dissipation of excess pore water pressure. Therefore, characterisation of clay subgrade assuming a non-transient state in saturated undrained condition will be adopted in this study.

A review was provided on the behaviour and deformation characteristic of the fine-grained subgrade and fine-grained soil in general under cyclic loading. Under undrained cyclic application of shear stress, fine-grained soil which develops strain and accumulate positive excess pore pressure may fails at a stress level less than its monotonic strength. The strength of soil can be defined as the level of cyclic stress that will develop a preset amount of accumulated strain, in response to the number of loading cycles applied. However, in the real context, the magnitude of allowable strain is often controversial and the number of loading cycles is difficult to be defined. Instead, the strength parameter of fine-grained soil can be characterized by the "threshold stress" - a level of stress lower than its monotonic peak strength, above which large shear deformation takes place, and below which soil strain stabilized irrespective of the number of loading cycles applied. The means and technique in the determination of threshold stress has been described and their relative merits discussed. The 'effective stress' method with measurement of both

pore pressure response and strain development is preferred as it offers fundamental understanding.

The strain response of soil under loading and unloading was given a review. Several constitutive modelling equations available in the literatures which describe the relationship between the cumulative plastic strain and number of repeated load applications for fine-grained soil were described. The models are semi-empirical and soil parametric data has been limited.

The characterization of subgrade soil by its resilient modulus is needed for calculating stresses, strains or deflection in conjunction with the use of conventional track modelling. Common modelling equations of the resilient modulus for fine-grained subgrade were described. These models are largely empirical and overlooked the changing nature of soil physical state in the case of fined-grained soil.

Influence of the rate of loading on fined-grained soil was reviewed. In general, they were parametric studies which provide the observation(s) from different perspectives on how the rate of loading affects the stress / strain relationship. This study will seek to provide some new perspective.

Current design principle of railway track foundation is primarily intended in limiting applied stress to subgrade such that it does not overwhelm the strength capacity of subgrade or cause excessive deformation. Reviews of the prevalent approaches and methodologies for the design of railway track foundation are provided. There are generally empirical or semi-empirical in its approach unique to a range of geological characteristic, operating and traffic condition. This study sought to devise a design means suitable for general contexts.

Chapter 3 Laboratory Experiment: Soil, Apparatus and Testing Procedure

3.1 *Introduction*

This chapter presents information on the experimental set up and procedure carried out in this study. The chapter first described the soil used in the laboratory experiment. This is followed by the description of the triaxial testing facility used in the research, their modification and instrumentation will be the next focus. Then, the sample preparation technique and testing procedure are described. Finally, an overall program of the laboratory experiment and the terminology used in the data analysis are detailed and presented.

3.2 *Type and Characteristics of Soil Used*

In any parametric study involved the investigation into fundamental behaviours of soil, repeatability of tests with reasonably high degree of consistency in test results is a pre-requisite. The triaxial testing of the soil in this program uses fully saturated *reconstituted kaolin clay*, in favour of the undisturbed sample of natural soil. Kaolinite is a clay mineral with chemical composition as hydrated aluminium silicate, $AI_2\ Si_2\ O_5\ (OH)_4$. It is a layered silicate mineral, with one tetrahedral sheet linked through oxygen atoms to one octahedral sheet of alumina octahedral. Soil or rocks that are rich in kaolinite are commonly known as kaolin. It is the most important industrial clay in terms of both consumption and value.

The reconstituted kaolin clay produced from the industrial grade kaolinite powder used in this experimental study has the basic characteristics as follows:

- Plastic Limit (%): 26
- Liquid Limit (%): 53
- Plasticity Index: 27
- Specific Gravity: 2.65

Consolidation and Compressibility of Kaolin clay

The compressibility of the kaolin clay was obtained by carrying out an isotropic consolidation test in triaxial cell. The test specimen was prepared in the same way as described later in paragraph 3.4.1. With the specimen mounted on triaxial pedestal, isotropic consolidation was given to the specimen, and drainage was allowed at both top and bottom of the specimen. The consolidation was carried out on a step increment, with the consolidation time for each step taken up to 24 hours (beyond its 100 % theoretical consolidation time). Upon reaching the maximum effective consolidation pressure of 1000 kPa, the specimen was allowed to swell in steps under a smaller consolidation pressure, until it reached 50 kPa. Finally, the specimen was recompressed to 1000 kPa in two steps.

The coefficient of consolidation (c_v) for the isotropic normal-consolidation process, the swelling and the recompression was analysed and plotted as shown in Figure 3-1. It can be observed that the coefficient of consolidation generally increases with higher consolidation pressure. Under same consolidation pressure, the process of swelling and recompression has a higher coefficient of consolidation than the normal-consolidation process, with the coefficient of consolidation for the swelling being the highest.

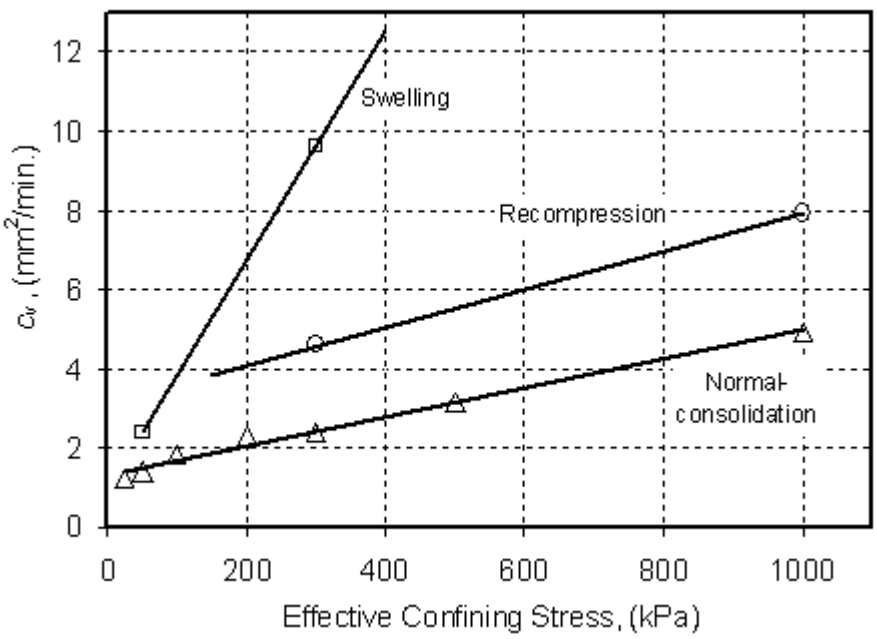

Figure 3-1 Coefficient of consolidation (c_v) for kaolin clay

Using critical state soil mechanics framework, the compressibility of kaolin clay determined from the consolidation test is illustrated in Figure 3-2. It can be represented by the various volumetric compressibility parameters as follows:

Gradient of isotropic normal-consolidation line, $\lambda = 0.18$

Gradient of swelling / recompression line, $\kappa = 0.06$

Specific volume for $p' = 1$ kPa
(of isotropic normal-consolidation line), $N = 2.94$

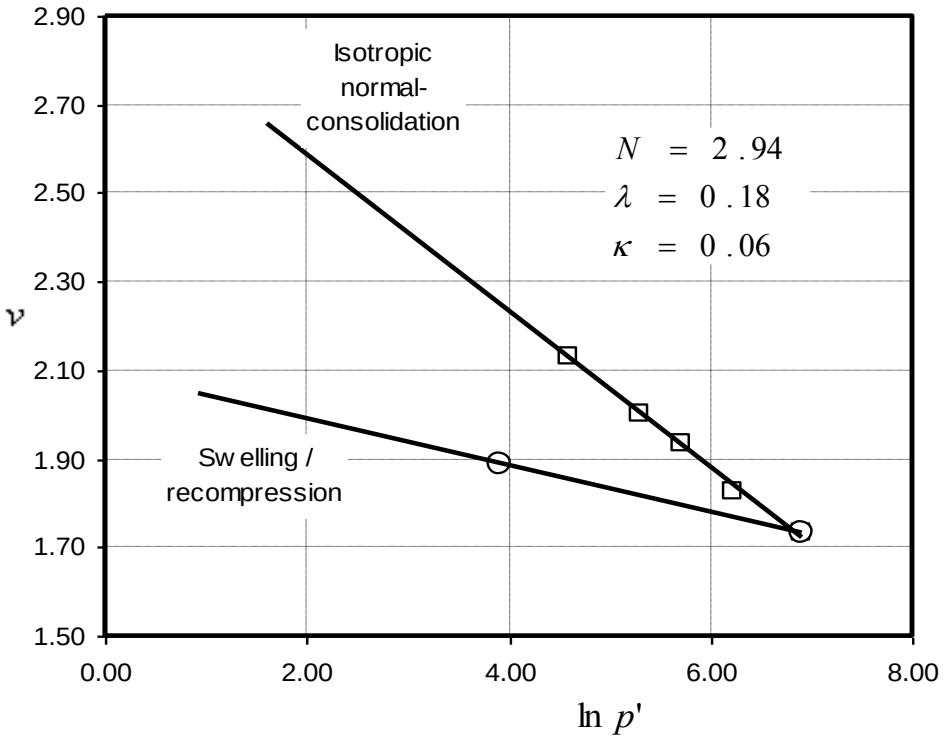

Figure 3-2 Isotropic consolidation of kaolin clay

3.3 *Apparatus and Equipment*

The experimental work on reconstituted kaolin clay was conducted using the cyclic triaxial testing facility in the geomachanics laboratory at the department of civil engineering at Curtin University of Technology (Australia). The cyclic triaxial testing System (Figure 3-3) consists of a triaxial cell, a load frame with computer-control platen, two computer-control flow pumps to control chamber pressure and back pressure, a high performance linear servo control electro actuator for cyclic loading with update rates of 500 times per second, a micro-processor for controlling cyclic loading, a PC with a Pentium processor to control the test and to log test data. The general layout of this cyclic triaxial equipment used in this study, together with the key apparatuses and aspects of the improved modification are presented below.

Figure 3-3 The cyclic triaxial testing system complete with a PC computer.

3.3.1 General Layout and overview

A schematic diagram showing the cyclic triaxial equipment systems is presented in Figure 3-4. The system consist of a load frame with computer-control platen, a triaxial cell, two flow pumps for controlling cell and sample volume and pressure, a linear electro-mechanical actuator with an external signal conditioning unit, and a PC computer that do the overall control. An external compressed air supply is required for producing cell pressure during the cyclic test.

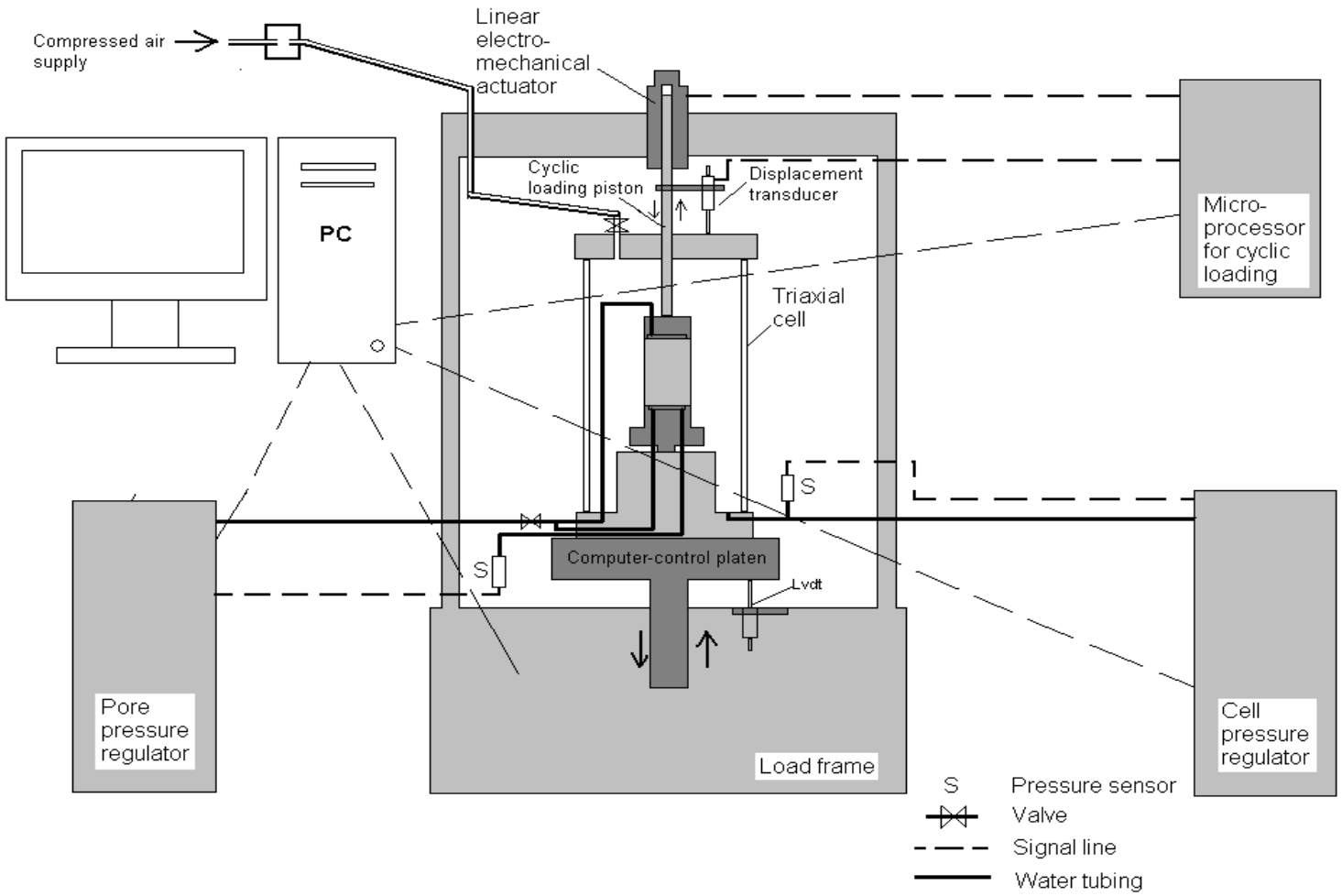

Figure 3-4 Schematic diagram of the cyclic triaxial equipment layout

3.3.2 Triaxial Cell

The triaxial cell consists of three main components, namely the cell base, cell body and top cell assembly. It enables specimen of cylindrical shape to be confined by uniformed all-round pressure, while an independent axial deviator stress can be applied to the specimen by the loading piston passing through the top cell assembly.

In the initial phase of cyclic triaxial testing, it was established that friction generated between loading piston and the top cell assembly was too great for the small specimen. The piston friction correction which the system allowed was only "one-way" which means that the specimen when undergo cyclic loading can only be correctly stressed in the loading cycle but become insufficiently unloaded in the unloading cycle, or vice-versa. To overcome this, modification of the triaxial cell was carried out to the cell base pedestal (Figure 3-5) to enable mounting of the load cell at the base of the specimen. This simple modified set up means the load cell will pick up and feedback only the stress actually experienced by the specimen, thereby completely eliminated the problem of piston friction during the downward and upward movement of the loading piston.

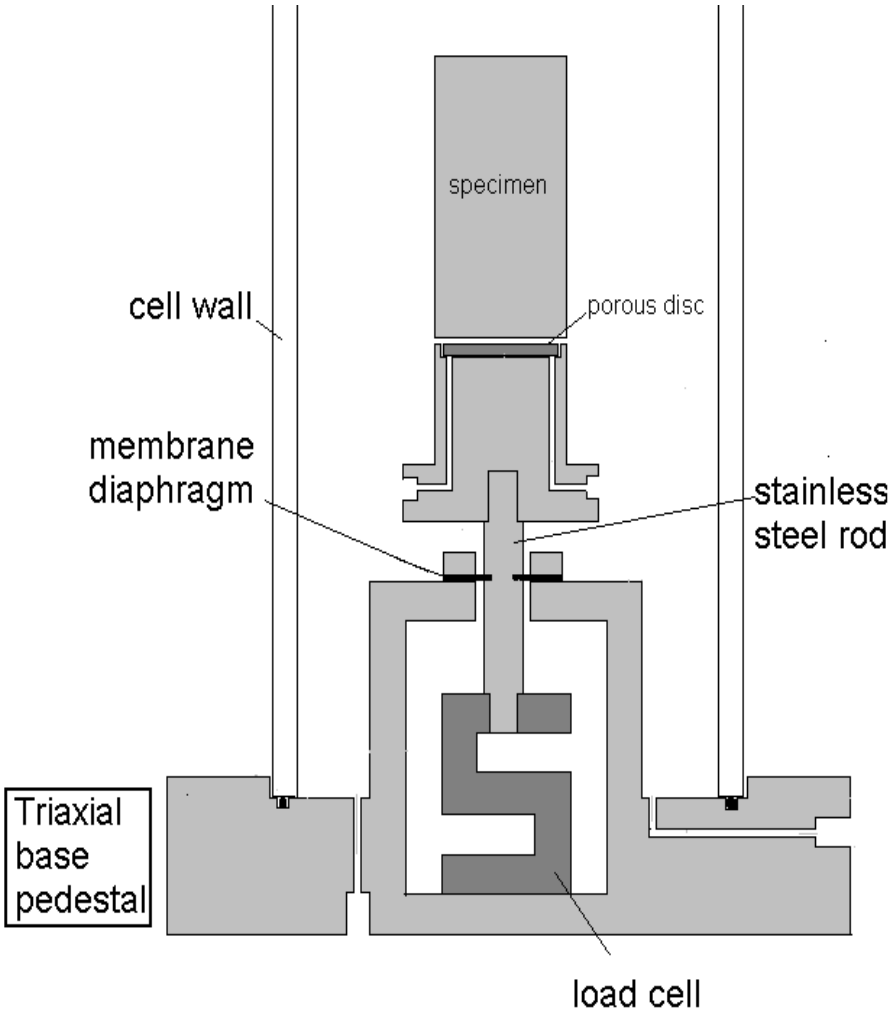

Figure 3-5 Schematic diagram of the triaxial base pedestal where load cell is installed

3.3.3 Loading Device

In this system, the cell pressure and the sample back pressure are provided by water pressure from separate flow pump, except during cyclic loading when external compressed air is used to maintain the cell pressure. The axial load for the static compression test is applied by the raising of computer-control platen, moving the triaxial cell with the specimen against the stationary top loading piston, thereby

generating the axial stress. For cyclic compression, the process is the opposite whereby the plate is being kept stationary, and axial load is applied by the movement of the top loading piston caused by the linear electro-mechanical actuator.

3.3.4 Measurement of Load, Displacement and Pressure

Various transducers are mounted in the system for measuring the axial load, confining pressure, pore water pressure and the axial strain (Figure 3-3 & Figure 3-4). An external 2.2kN capacity load cell is installed at the base of the specimen in order to measure the stress directly experienced by the specimen (Figure 3-5). Axial displacement is measured externally using LVDT displacement transducer via the movement of computer-control platen for static testing. During cyclic loading, another LVDT displacement transducer is mounted on the top loading piston to capture and measure its movement relative to the stationary triaxial cell. For the regulation of pressure and volume of water to the cell or specimen, flow pump utilizes a high speed, precision micro stepper motor to drive a piston in and out of sealed cylinder that filled with water. A pressure transducer at the end of the cylinder provides the feedback for control of pressure to within 0.35 kPa. The number of steps of the motor is used to compute and monitor volume change to within 0.001 cc. For cyclic testing, cell pressure is maintained using compressed air. Another set of pressure transducers was installed, one at the triaxial cell for measuring cell pressure and the other at the cell base pedestal for measuring specimen pressure.

3.4 *Testing Procedure*

3.4.1 Sample Preparation

3.4.1.1 Preparation of Sample from Slurry

Using a water content of about twice the liquid limit of kaolin clay, slurry is formed by mixing dry commercial grade kaolin powder with distilled water, using a motorized rotary mixer, for a period of two hours. The smooth and well mixed slurry is then sealed in a plastic container and cured for about a week to improve the homogeneity of the slurry mixture (Head 1982; Head 1986).

Upon curing, the slurry is pour into a Plunger cell (110 mm diameter by 300 mm in height) in layer of 50 mm depth (Figure 3-6). A Perspex lid with air vacuum connection is bolted to the flange of the cell body. Vacuum of 80 to 100 kPa is applied through the lid, and the surface of the slurry can be seen bubbling as air inside slurry is being removed.

After 20 minutes when the bubbling has virtually stopped, the vacuum is released and the Perspex lid removed. Further layer of slurry is evenly deposited in, and the above process repeated layer by layer until it reaches a level which is about 10 mm below the top flange.

The surface of the sample is levelled and just covered by a thin layer of de-aired water. The compression piston with embedded porous media is then placed on top and secured in position.

With the application of metal weights above the piston, the slurry is subjected to one-dimensional consolidation (Figure 3-7). An effective consolidation pressure of 75 kPa was attained after a week. Upon completion of the consolidation process and the removal of metal weight, and the soil is allowed to swell for 24 hours as it draws in water from both ends of the cell.

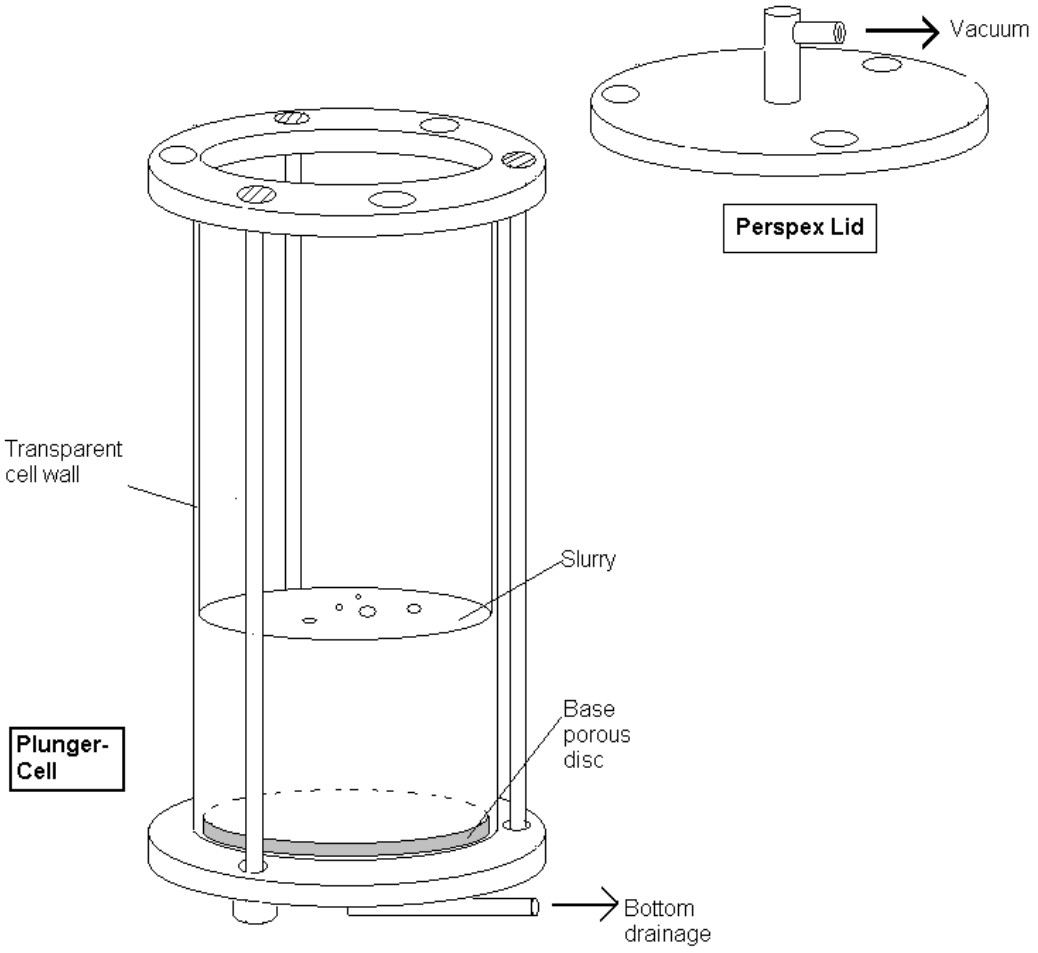

Figure 3-6 Plunger-cell for one-dimensional consolidation of kaolinite slurry

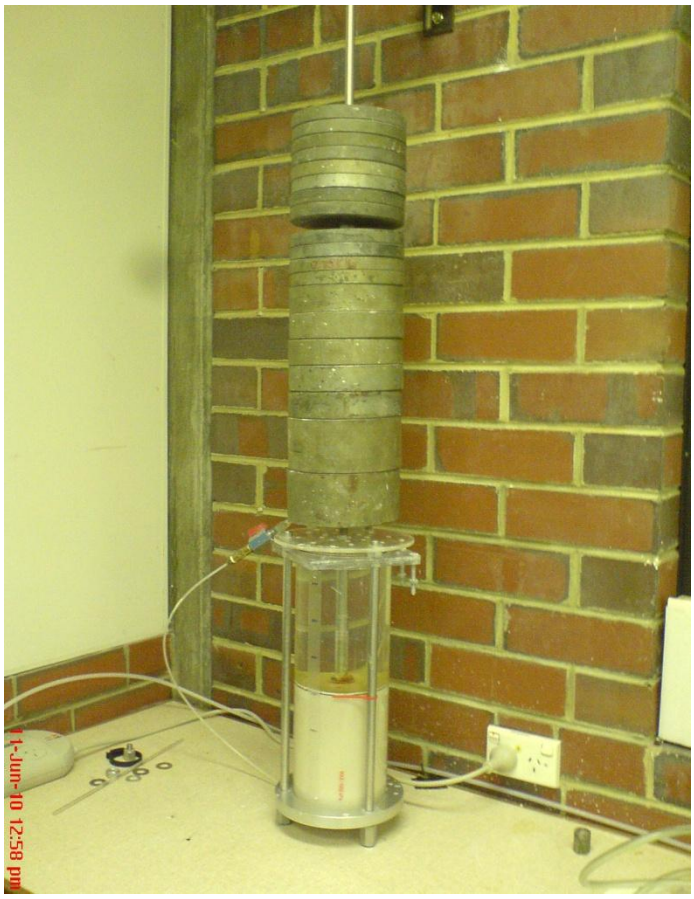

Figure 3-7 One-dimensional consolidation of kaolin slurry to form clay

3.4.1.2 Tube Sampling

A set of three 35 mm diameter stainless steel sample tubes are spaced and aligned vertically above the consolidated clay in plunger cell. Once in position, they are gently push into the clay until reaches the bottom of the cell. With the base flange of the plunger removed, the sample tubes with clay are carefully retracted, sealed and stored to avoid loss of moisture.

3.4.1.3 Sample Extrusion and Setting Up

Preparation of a 35 mm diameter saturated soft clay specimen for triaxial testing, require minimum disturbance to the soil and ensuring the moisture does not lost in the process of setting up the specimen for testing. First, a rubber membrane is placed and secured inside a 75 mm long cylindrical membrane stretcher of 38 mm diameter. A small vacuum of 5 kPa is then applied to bring the membrane in contact with the inner surface of the stretcher. Next, with the sample tube attached securely to a screw-type extruder, a 35 mm diameter x 70 mm long soil specimen is extruded into the cylindrical stretcher that was placed above the extruder. Then, vacuum is released. The specimen which is being held by the membrane is immediately placed on the triaxial base pedestal. To minimize disturbance to the specimen, split former is used to hold the specimen onto the base pedestal before the top cap can be securely placed on it and rubber rings installed (Head 1982; Lambe 1951).

3.4.2 **Saturation**

In view of the virtually fully-saturated state of soil sample prepared, saturation of kaolin specimen was to be reaffirmed and achieved by using “one-stage elevation of back pressure” procedure (Head 1986). Initial effective stress of the specimen was determined after the specimen was left to achieve pore pressure equilibrium under a cell pressure of 50 kPa. Keeping the initial effective stress constant, saturation was carried out by raising the cell pressure and the back pressure concurrently in one stage until the back pressure arrives at 200 kPa. Thereafter, the pore pressure coefficient (B-value) was taken. The back pressure at this level was sufficiently high to help in achieving full degree of saturation. The B-value of 0.99 – 1.0 was achieved in all cases.

3.4.3 Consolidation

3.4.3.1 Isotropic Normal Consolidation

After full saturation has been achieved, the specimen was initially having an effective stress state equal its "initial effective stress". Isotropic normal consolidation of specimen was carried out by gradually increasing the cell pressure (all-round pressure) to a pre-selected value depending on the intended effective consolidation pressure, while keeping the back pressure of 200 kPa constant (i.e. Effective consolidation pressure = Pre-selected cell pressure – Back pressure). For purpose of consistency, the process of consolidation was maintained for a period equal three times the duration required for 100 % primary consolidation t_{100} determined using "Volume change against square root of time" fitting method (Head 1986, Lambe 1951).

3.4.3.2 Isotropic Over-Consolidation

The process of over-consolidation required the specimen to be under normal-consolidation at the beginning to a pre-selected level as described in above paragraph 3.4.3.1. Following completion of normal-consolidation process, a pre-determined lower level of all-round pressure was applied gradually, during which the specimen was allowed to swell (be consolidated) for the duration equal three times the t_{100}.

3.4.4 Monotonic Undrained Compression

Monotonic undrained compression test was carried out to provide a benchmark for the cyclic test, in respect of its peak deviator stress and deformation characteristics. Tests were conducted at a control rate of strain between 0.0035 – 0.015 %/min for specimens of various consolidated state. The compression strain rate was guided by the time required to reach failure in undrained test, based on 95 % pore pressure equalization within the sample, given by Blight (1963) (Head 1986).

3.4.5 Cyclic Undrained Compression

In cyclic undrained compression, specimen was subjected to axial loading and unloading under constant cell pressure condition. Drainage was closed and variation of pore water pressure was measured at the top and bottom of specimen at regular interval within each cycle. The cyclic compression was a continuous application of cyclic deviator stress σ_d of sinusoidal shape (Figure 3-8).

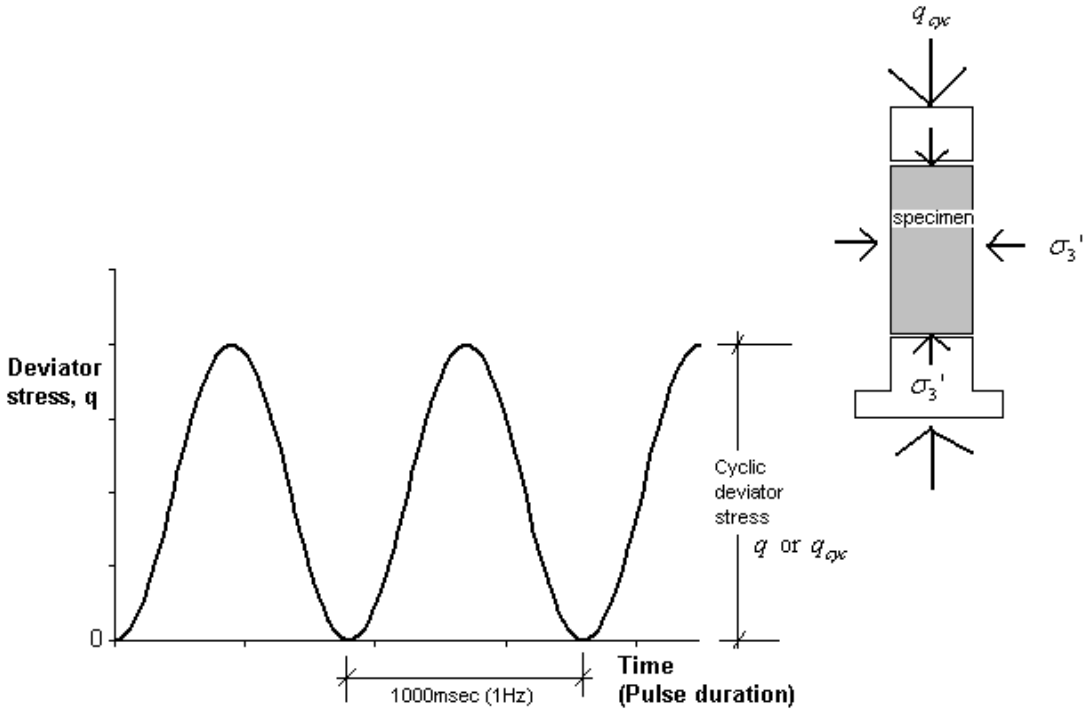

Figure 3-8 State of stress during cyclic compression

3.4.5.1 Level of Cyclic Deviator Stress

The first cyclic test normally begins with the magnitude of cyclic deviator stress at approximately one-third of the peak deviator stress from the monotonic compression test (i.e. well below the 60 % as reported for Grande Baleine sensitive clay (Lefebvre 1986)). The cyclic loading continued until it reaches a non-failure condition. For the subsequent tests, cyclic deviator stress of the consecutive test was stepped up approximately 10 to 15 kPa, until one of the tests has the specimen failed with large deformation.

3.4.5.2 Cyclic Loading Frequency

The tests were mainly conducted at a cyclic loading frequency of 1 Hz (one cycle per second) simulating the cyclic nature of stress near subgrade surface due to passing axles of train traveling at a speed of approximately 50 km/hour. Higher frequencies of 5 Hz and 10 Hz were also studied to identify the effect of frequency on the stress / strain response.

3.4.5.3 Step Compression Test

Two Step-compression tests CYC35(75)OC4step and CYC30(30)OC20step (refer to the Testing Program in paragraph 3.4.8) were conducted for the specimen of over-consolidated series OC4 and OC20 respectively. In these test, cyclic undrained compression test with relatively low magnitude of deviator stress, which had achieved a non-failure condition were given additional cyclic compression test with deviator stress a step (between 5 to 15 kPa) higher than the previous level of deviator stress. Further step-test is carried out until the specimen failed with large strain.

3.4.6 Temperature Setting

In order to isolate and eliminate the influence of temperature variation has on the tests, the testing including sample preparation, curing and storage and the actual triaxial testing were carried out in the triaxial room, with room temperature maintained at $22°C \pm 1°$ throughout the experimentation period.

3.4.7 Notes on Calculations

The calculations of stress and strain were performed assuming that the specimens deform as right cylinder (Bishop and Henkel 1957) in which uniform area correction was in place. In this study, correction for membrane stiffness was assumed negligible by the use of thin membrane of less than 0.01 inch in thickness, and the anticipated small axial deformation strain i.e. 5 mm is involved.

$$\sigma_d = \frac{P(1-\varepsilon_{vol})}{A_o(1-\varepsilon_v)} \tag{3-1}$$

where P = axial load (axial compression);

A_o = initial horizontal cross-sectional area of specimen;

ε_{vol} = Volumetric strain (reduction); and

ε_v = Axial strain (compression)

Since the clay specimens are mainly fully saturated, the initial horizontal cross-sectional area of specimen A_o can be corrected as follows:

$$A_o = \frac{W_s(1+e)}{G_s \cdot h} \times 10^3 \tag{3-2}$$

where W_s = dry weight of soil after test;

G_s = specific gravity of soil;

h = initial height of specimen (measured);

e = initial void ratio of soil = $\frac{wG_s}{S}$;

w = water content at the end of test; and

S = saturation of soil (S = 1 for full saturation).

3.4.8 Testing Program

The laboratory testing program consists of four series of tests that spanned across a wide range of stress history conducted on saturated reconstituted kaolin clay. There were isotropic normally consolidated (NC) series and isotropic over-consolidated (OC1.5, OC4 and OC20)) series which have the over-consolidation ratio of 1.5, 4 and 20 respectively. Each series included a monotonic undrained compression test and a set of cyclic undrained compression tests. The details of these tests are presented in Table 3-1.

Each test in Table 3-1 is given a name which is a set of characters consists of alphabets and numbers, e.g. **M** 30 **OC20**; and **CYC** 50(300) **OC1** ____, which indicates the monotonic test and cyclic test respectively. The naming system will be maintained throughout this thesis for easy reference. The first character / or set of characters is an alphabet(s) refer to the type of test performed, i.e. **M** for monotonic undrained compression test, and **CYC** for cyclic undrained compression test.

For monotonic undrained compression test, the second set of characters is numeric which refers to the confining stress, i.e. 30 means an effective isotropic consolidation of 30kPa. The third set of alphabet-numeric characters provides an indication of the stress history, i.e. **OC20** means an over-consolidation ratio of 20.

For cyclic undrained compression test, the second set of characters indicate the level of cyclic deviator stress and confining stress, i.e. 50(300) means a cycle deviator stress of 50 kPa and an effective consolidation of 300 kPa. The third set of

characters, i.e. **OC1** means an over-consolidation ratio of 1. The end of the name, i.e. ____, provides an indication of cyclic loading frequency other than 1 Hz; or indication of "step" when the test is a step test other than a single stage test.

Table 3-1 Summary of undrained compression triaxial tests on kaolin

Test No.	$p_i'(kPa)$	*q(kPa)*	*OCR*	*Frequency (Hz)*	*Type of test*
NC series					
M300OC1	300		1		Monotonic
CYC50(300)OC1	300	50	1	1	Cyclic
CYC65(300)OC1	300	65	1	1	Cyclic
CYC80(300)OC1	300	80	1	1	Cyclic
CYC90(300)OC1	300	90	1	1	Cyclic
CYC100(300)OC1	300	100	1	1	Cyclic
CYC50(300)OC1(5Hz)	300	50	1	5	Cyclic
CYC65(300)OC1(5Hz)	300	65	1	5	Cyclic
CYC50(300)OC1(10Hz)	300	50	1	10	Cyclic
CYC65(300)OC1(10Hz)	300	65	1	10	Cyclic
OC1.5 series					
M200OC1.5	200		1.5		Monotonic
CYC40(200)OC1.5	200	40	1.5	1	Cyclic
CYC55(200)OC1.5	200	55	1.5	1	Cyclic
CYC65(200)OC1.5	200	65	1.5	1	Cyclic
CYC70(200)OC1.5	200	70	1.5	1	Cyclic
CYC78(200)OC1.5	200	78	1.5	1	Cyclic

Table 3-1 Summay of undrained compression triaxial tests on kaolin **(Continued)**

Test No.	$p_i'(kPa)$	*q(kPa)*	*COR*	*Frequency (Hz)*	*Type of test*
OC4 series					
M75OC4	75		4		Monotonic
CYC20(75)OC4	75	20	4	1	Cyclic
CYC33(75)OC4	75	33	4	1	Cyclic
CYC45(75)OC4	75	45	4	1	Cyclic
CYC50(75)OC4	75	50	4	1	Cyclic
CYC60(75)OC4	75	60	4	1	Cyclic
CYC35(75)OC4step	75	35, 45 and 50	4	1	Cyclic-step
OC20 series					
M30OC20	30		20	1	Monotonic
CYC20(30)OC20	30	20	20	1	Cyclic
CYC30(30)OC20	30	30	20	1	Cyclic
CYC40(30)OC20	30	40	20	1	Cyclic
CYC55(30)OC20	30	55	20	1	Cyclic
CYC30(30)OC20step	30	30 and 40	20	1	Cyclic-step

3.4.9 Definition of Invariants and Terminology

The triaxial testing provides an axis-symmetric stress condition applied on a cylindrical specimen ($\sigma_2' = \sigma_3'$), with σ_{dev}= deviator stress and axial stress $\sigma_1' = \sigma_3' + \sigma_{dev}$.

The general stress invariants using "Cambridge $q - p'$ "stress parameters are as follows:

Mean effective stress (Effective spherical pressure), $p' = \frac{1}{3}\left(\sigma_1' + 2\sigma_3'\right)$ (3-3)

Axial deviator stress, $q = \sigma_{dev} = \sigma_1' - \sigma_3'$ (3-4)

where, the term σ_1' and σ_3' are the major and minor principal stress

respectively

The strain invariants used are:

Volumetric strain, $\varepsilon_v = (\varepsilon_1 + 2\varepsilon_3)$ (3-5)

Deviatoric strain, $\varepsilon_s = \frac{2}{3}(\varepsilon_1 - \varepsilon_3)$ (3-6)

where, ε_1 and ε_3 are the major and minor principal strain respectively.

In the case of undrained testing when the volumetric strain equal zero, the deviatoric strain is equal to major principal strain, i.e. $\varepsilon_s = \varepsilon_1$.

Other terminology used in this study includes:

$$\text{Cyclic stress ratio, CSR} = \frac{(\sigma_{dev})_{cyclic}}{(\sigma_{dev})_{static-\max.}} = \frac{q_{cyc}}{q_{\max}} \qquad (3\text{-}7)$$

Chapter 4 Presentation of the Experimental Results

4.1 *Introduction*

This chapter presents the results of tests carried out on saturated reconstituted kaolin clay under both monotonic and cyclic undrained compression. Having identified the possible parameters that influence the behaviour of soil under undrained cyclic loading, emphasis is placed upon the characterization of kaolin clay with respect to various consolidated states and stress history of soil. The presentation of the results was intended to be modular, with each module representing a series of tests conducted on saturated kaolin clay which were subjected to the same consolidation history prior to axial compression. There were altogether four series of tests results to be presented here, namely NC series, OC1.5 series, OC4 series and OC20 series, in sequence.

The typical behaviour of saturated kaolin clay under cyclic compression will be, as far as possible, explained in distinctive details particular to each series of the tests; with subsequent and later series(s) given a concise treatment without undue repetition. Except when bold similarity between tests series will be highlighted, little interrelation will be drawn upon in this chapter. A more general and coherent discussion will be presented in the ensuing chapter.

4.2 *Normally-Consolidated NC Series*

4.2.1 Introduction

In this series of tests, specimens were initially undergone an isotropic normally-consolidation at an effective stress of 300kPa. The stress and strain behaviour of the monotonic compression test and the typical tests of cyclic compression will be described. This is followed by the illustration of the behaviour pattern and relationship of / amongst all tests in the same series. These include description of strain development and stabilization, excess pore water pressure response and development, the notion of state of stress equilibrium and state of resiliency, the identification of threshold stress, the total strain and elastic strain characteristics, and the influence of cyclic loading rate (frequency) on stress /strain response of clay soil.

Tests included in the NC series are:
M300OC1
CYC50(300)OC1
CYC65(300)OC1
CYC80(300)OC1
CYC90(300)OC1
CYC100(300)OC1
CYC50(300)OC1(5Hz)
CYC65(300)OC1(5Hz)
CYC50(300)OC1(10Hz)
CYC65(300)OC1(10Hz)

4.2.2 Monotonic Compression

The result of test M300OC1 described the monotonic strength and the strain characteristic for the NC series clay under axial compression. The magnitude of peak strength provides a prior indication of the maximum stress level from which various cyclic deviator stress levels were apportioned. In addition, the peak strength in normally-consolidated NC series was used to work out the fundamental strength

parameter M which is the slope of critical state line in the $p' - q$ plot for tests of all series in general (Atkinson 1993).

Figure 4-1 showed the variation of deviator stress and excess pore pressure with respect to axial strain for the test. As axial strain was applied on the specimen at a controlled rate, deviator stress began to build up at a reducing rate with respect to the strain. At the same time, there was an increase in the excess pore water pressure until it reached the maximum of 170 kPa at about 17 % strain. Thereafter, the pore water pressure remained constant till end of the test. At 12 % strain, the build-up of deviator stress had slow down substantially, but continued to peak at 15 % strain. The peak deviator stress of 140 kPa was observed and taken as the monotonic undrained compression strength for the NC series. The final moisture content of specimen was 35.3 %.

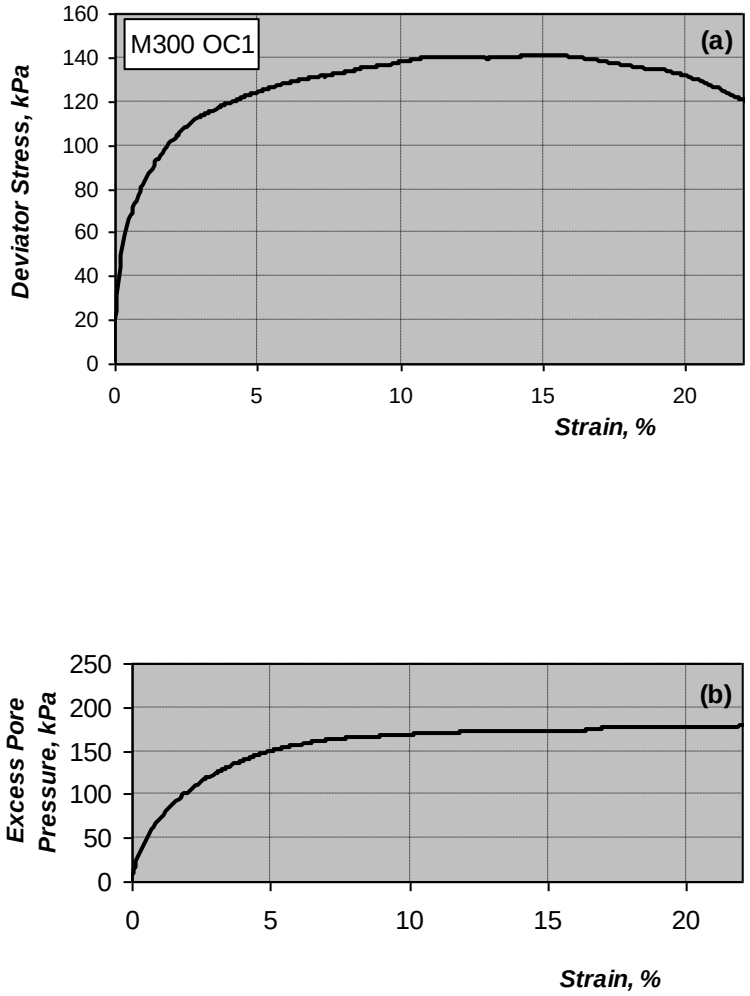

Figure 4-1 Test result of the monotonic undrained compression: (a) Deviator stress verses axial strain; (b) Excess pore water pressure verses axial strain. (NC series, consolidation = 300 kPa)

The data of the slow strain-controlled monotonic undrained compression test when plotted on p'- q stress plane is shown in Figure 4-2. The specimen of saturated kaolin clay was initially in a state of isotropic normal-consolidation. The pattern of stress path which is characteristic of a normal-consolidated soil, moved upward towards the left due to increase in pore water pressure of substantial proportion, i.e. more than one-third of the deviator stress. As soon as it reached the critical state line (CSL), the stress path became stationary before it began to move down along the CSL as the specimen began to yield. At the vertex of the stress path, the obliquity ($\eta = q/p'$) or

the stress ratio (q/p') is the maximum, and it coincides with the gradient of the critical state line *M*. The deviator stress at which it reached the CSL represents the peak deviator stress of 140 kPa. The strength parameters thus obtained are:

Peak deviator stress, $\sigma_{d(static-\max.)}$ = 140 kPa

Slope of critical state line in $p'-q$ plane, M = 0.803

Coulomb effective friction angle, ϕ' = 20.75°

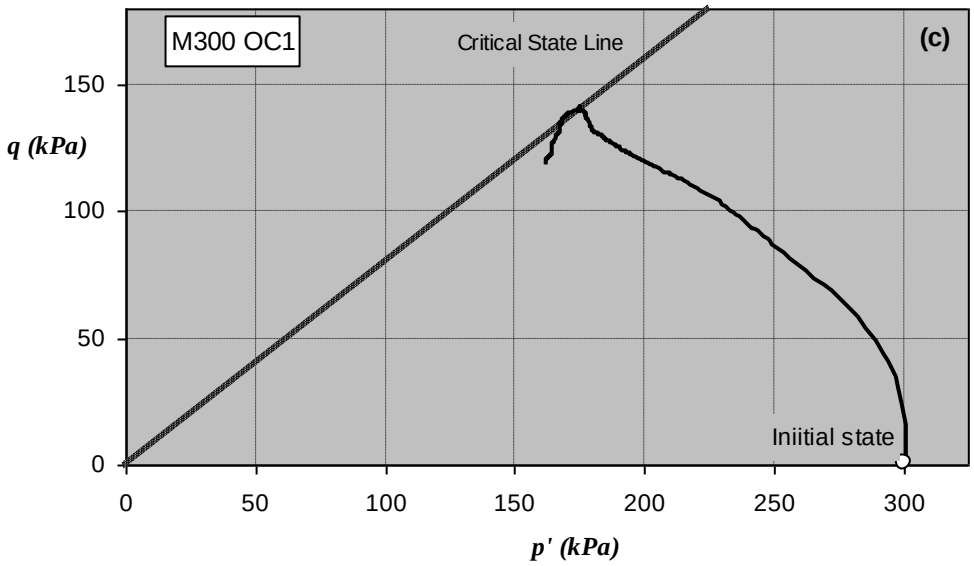

Figure 4-2 Stress path for monotonic undrained compression on saturated kaolin clay (normal-consolidated at 300 kPa)

4.2.3 Cyclic Compression Leading to Resilient State

All of the cyclic compression tests were conducted at a cyclic deviator stress apportioned from the peak deviator stress of 140 kPa obtained from monotonic compression test. Cyclic compression tests in which the specimens had arrived at an non-failure condition are typified by test CYC50(300)OC1. Specimen of CYC50(300)OC1 exhibited cyclic stress responses (Figure 4-3) which was characteristic of all tests that had led to a resilient state (a non-failure state in which both state of stress equilibrium and strain stabilization exists).

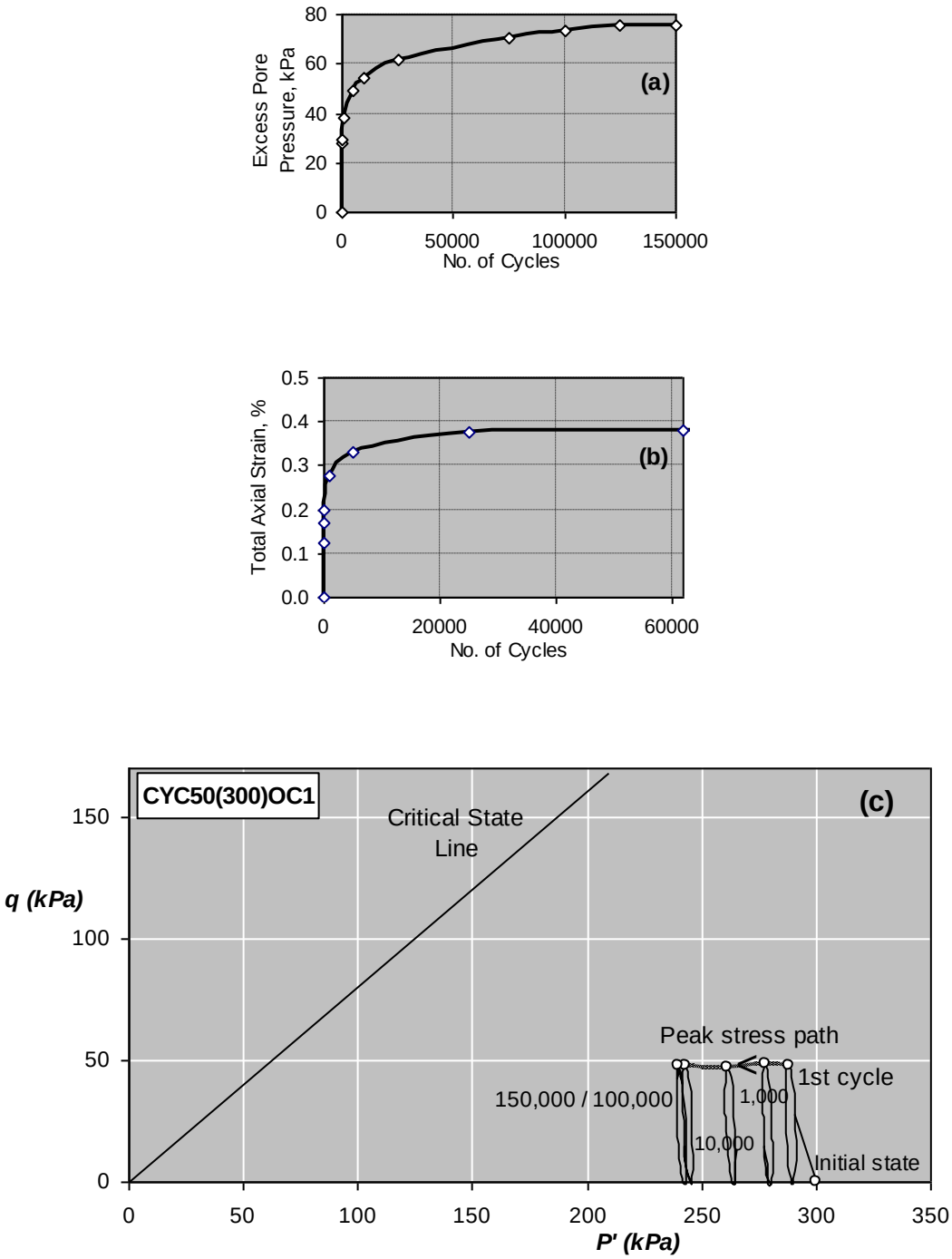

Figure 4-3 Results of cyclic undrained compression test on kaolinite clay that led to a resilient state (normally consolidated at 300 kPa, with cyclic deviator stress = 50 kPa, CSR = 0.36)

Under a cyclic deviator stress of 50 kPa (cyclic stress ratio CSR equal 0.36), the specimen built up excess pore pressure over each cycle of deviator stress application. As the deviator stress oscillated in a sinusoidal way between 50 kPa and the near zero value, the excess pore water pressure gradually built up and oscillated approximately in the same phase as the deviator stress despites it being transient and unequalized within the specimen.

Figure 4-3a showed the maximum excess pore pressure corresponding to the peak deviator stress of each loading cycle. The excess pore pressure was building up at a reducing rate until it reached the maximum at 75 kPa at about 100,000 cycles of loading application, and remained constant thereafter. The total axial strain (which includes both the non-recoverable plastic strain and the recoverable elastic axial strain) was also increasing with the numbers of loading cycles, but began to show sign of stabilization (plateau-off) at 60,000 cycles (in Figure 4-3b).

Presented in a p'- q plane, Figure 4-3c showed the cyclic stress path of the 1^{st}, 1000^{th}, $10{,}000^{th}$, $100{,}000^{th}$ and $150{,}000^{th}$ cycle of loading application. Due to the increasing pore water pressure and the consequent reduction in mean effective stress p', the stress path of each cycle gradually migrated to the left and began to form hysteresis loop at about $100{,}000^{th}$ cycle. By this time, the total axial strain of the specimen had also achieved strain stabilization as shown in Figure 4-3b. At this stage, a state of resiliency had arrived in which both the state of stress equilibrium and the strain stabilization exist. The term "Peak stress path" is introduced here which represents the state of stress in each cycle when the deviator stress is at the maximum. In this test, the peak stress path of the cyclic undrained compression test moved horizontally to the left and became stationary at $100{,}000^{th}$ cycle without reaching the critical state line (CSL). The excess pore water pressure within the specimen had attained equilibrium and the cumulative total axial strain had stabilized.

Upon arriving at the resilient state when the effective stress was in equilibrium, the variation of pore water pressure appeared to be about 20kPa which was $2/5$ of the axial deviator stress. This was higher than the $1/3$ ratio which was expected of an ideal elastic response from an isotropic consolidated soil under undrained compression (Lambe and Whitman 1969). The higher excess pore water pressure to

deviator stress ratio i.e. 2/5 verses 1/3 at the state of stress equilibrium can be attributed to the anisotropic nature of soil specimen due to the fact that the test sample was prepared using one dimensional axial consolidation and consolidated subsequently with only top and bottom drainage, which caused the specimen to be more compressible in the axial than the radial direction (Wood 1990).

In general, the behaviour of the clay specimens in the normally-consolidated (NC) series which led to a resilient state under undrained cyclic compression can be typified by this: Under cyclic compression, soil builds up pore water pressure and total strain as the application of cyclic compression continues and causes a tendency for densification. The increase in pore water pressure and total strain finally cease approximately at the same number of cycles, as clay specimen got remoulded into a state where tendency for densification no longer exists and equalization of pore water pressure within the specimen taken place. As both the pore water pressure and the total strain become stabilized, a state of resiliency has arrived in which both stress equilibrium and strain stabilization exist. At this state, further application of cyclic loading produces constant (or recoverable) variation of the pore water pressure and the axial strain within each loading cycle in an elastic manner. At the state of resiliency, the stress path form hysteresis (in $p'-q$ plane) and the peak stress path become stationary before the critical state line (CSL) and it has an obliquity (η) less than the gradient of critical state path (M).

4.2.4 Cyclic Compression Leading to Ultimate Failure

Following the test which led to resilient state as described in above 4.2.3, subsequent tests were carried out expecting a non-failure outcome whereby each clay specimen was under cyclic compression with deviator stress level a small step increment of 10 to 15 kPa to that of the previous test. The tests continued until a “failure condition” was encountered when a test specimen exhibited ultimate failure with large strain. Test CYC100(300)OC1 was such test that led to failure when the specimen was given a cyclic deviator stress of 100 kPa (cyclic stress ratio, CSR = 0.71).

For test CYC100(300)OC1 (Figure 4-4), the initial response of specimen was essentially similar to that described for test CYC50(300)OC1. Under cyclic compression, the excess pore water built up quickly at a reducing rate and reached the maximum at 240kPa after an indicative 5,000 loading cycles. However, the cumulative total strain initially appeared to increase at a reducing rate to 4% strain after 1,000 cycles. It then maintained the same rate of increment until it reached 6% at 3,000th cycles, before it built up at increasing rate and led to ultimate failure with large strain.

On the p'- q plot, the increase in excess pore water pressure caused the stress path (loop) and the peak stress path to migrate horizontally to the left. The excess pore water pressure continued to increase until the peak stress path reached the critical state line (CSL) upon which cumulative total axial strain began to develop at an increasing rate. Due to the high rate of cyclic loading, the non-equalization of pore water pressure within the specimen had produced a higher measured pore water pressure than the actual equivalent pore water pressure within the specimen. As a result, the peak stress path which supposed to terminate on the CSL was depicted as appeared to have crossed the CSL before moving down slightly.

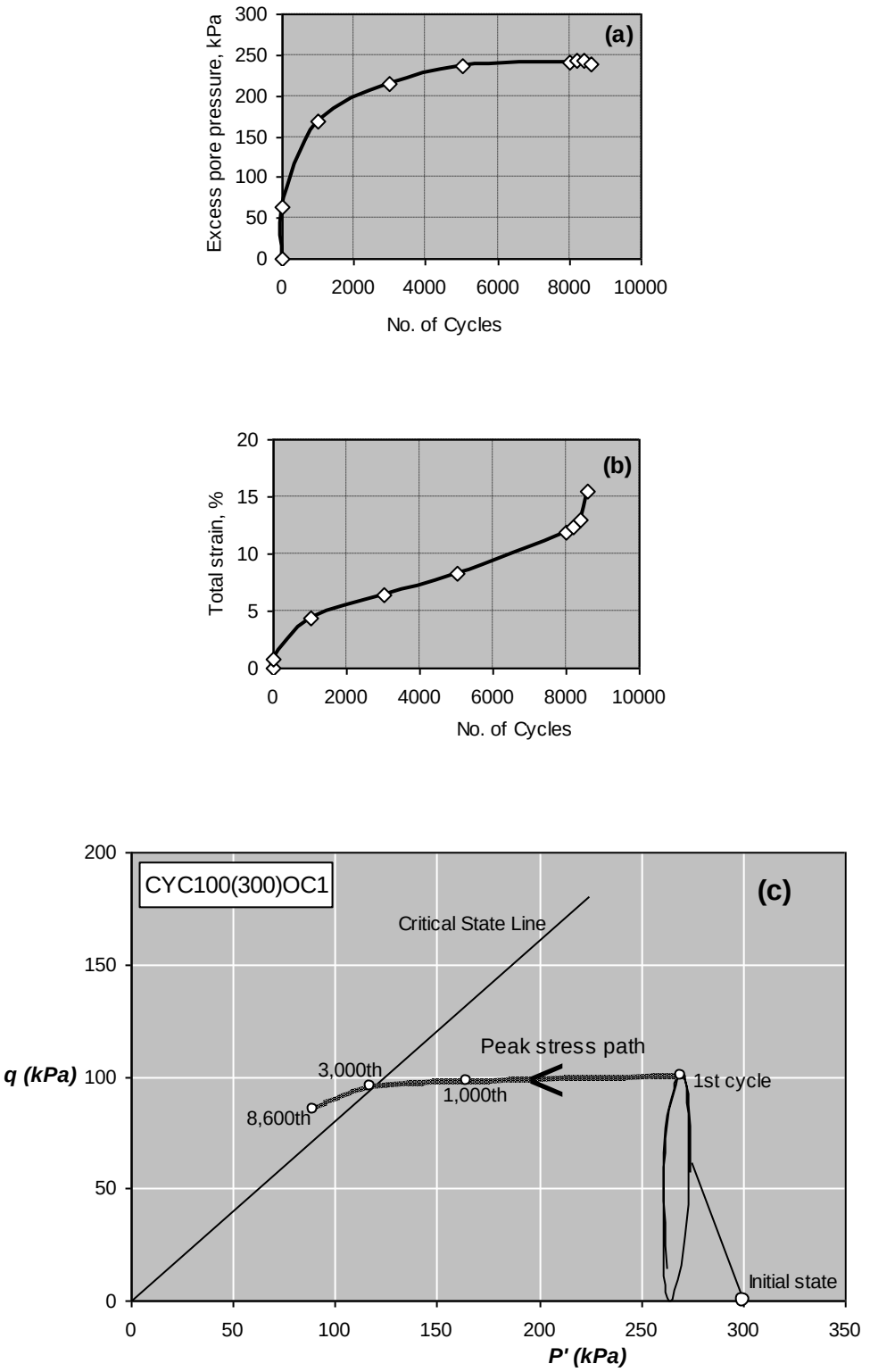

Figure 4-4 Results of a cyclic undrained compression test on kaolinite clay that led to ultimate failure (normal-consolidation = 300 kPa, with cyclic deviator stress = 100 kPa, CSR = 0.71)

In general, when clay specimen of the normally-consolidated (NC) series is subjected to cyclic compression which led to ultimate failure, excess pore water pressure (the equivalent excess pore water pressure) builds up at a reducing rate within the specimen. The axial strain develops quickly initially at reducing rate and then remains at constant rate as the peak stress moves toward the critical state line. The equivalent excess pore water pressure within the specimen continues to increase until the peak stress path eventually reaches the critical state line, where the stress obliquity (η) at the stagnated end of the peak stress path equal the gradient of the critical stress line (M). At this state, specimen begins to deform at a significantly increasing rate until it ultimately failed with large strain. Unless an equivalent pore water pressure within specimen can be ascertained, the non-equalization of pore water pressure within the specimen will cause the depiction of the peak stress path appeared to have crossed, when it should have terminated on, the CSL.

4.2.5 Line of Cyclic Stress Equilibrium State and the Threshold Stress

All tests which arrived at the resilient state are typified by test CYC50(300)OC1 as described in above 4.2.3. They include:

CYC50(300)OC1, (with cyclic deviator stress = 50kPa, CSR = 0.36);
CYC65(300)OC1, (with cyclic deviator stress = 65kPa, CSR = 0.46);
CYC80(300)OC1, (with cyclic deviator stress = 80kPa, CSR = 0.57); and

CYC90(300)OC1, (with cyclic deviator stress = 90kPa, CSR = 0.63).Figure 4-5 and Figure 4-6 showed the built-up of excess pore water pressure and the total strain, corresponding to the peak stress within a cycle for all the above tests which arrived at a resilient state. There was a maximum excess pore water pressure that could possibly be accumulated for each test, and the associate maximum total strain that each specimen could sustain, irrespective of further number of loading applications once attained. The maximum pore water pressure dictates the end point of peak stress path where it signifies the arrival of a state of stress equilibrium in response to the cyclic compression.

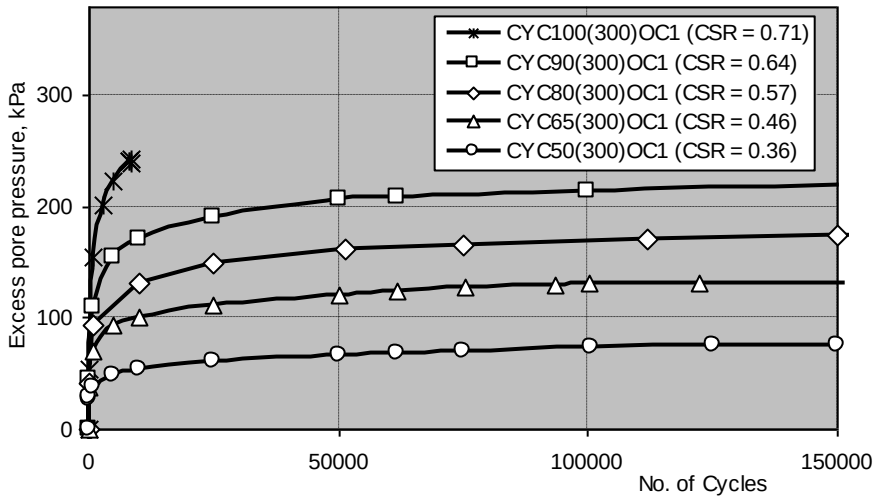

Figure 4-5 Accumulation of peak excess pore water pressure over each cycle (NC series)

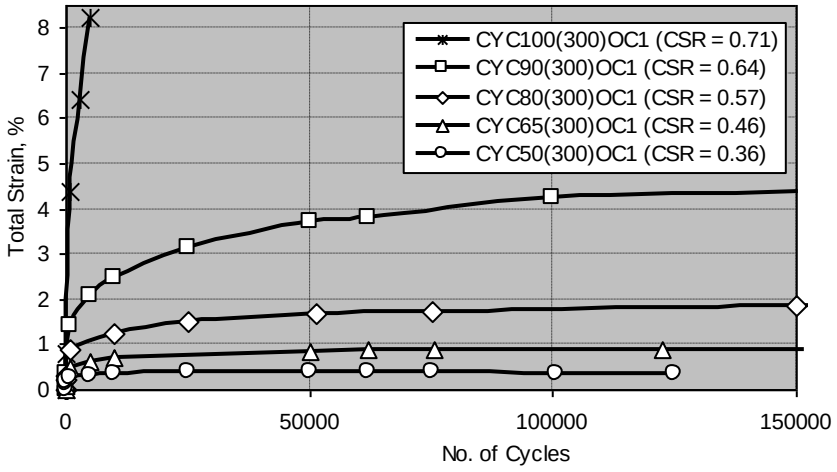

Figure 4-6 Development of peak total strain over each cycle (NC series)

An overall view of the peak stress path for the above tests that arrived at the state of stress equilibrium and the test CYC100(300)OC1 which failed ultimately is shown in Figure 4-7. The peak stress path of all tests became stationary between 100,000 and 150,000 cycles indicated that the state of stress equilibrium within soil specimen had arrived, except that the peak stress path for test (with CSR = 0.71) moved towards and reached the critical state line CSL, causing ultimate compression failure as specimen failed with high axial strain.

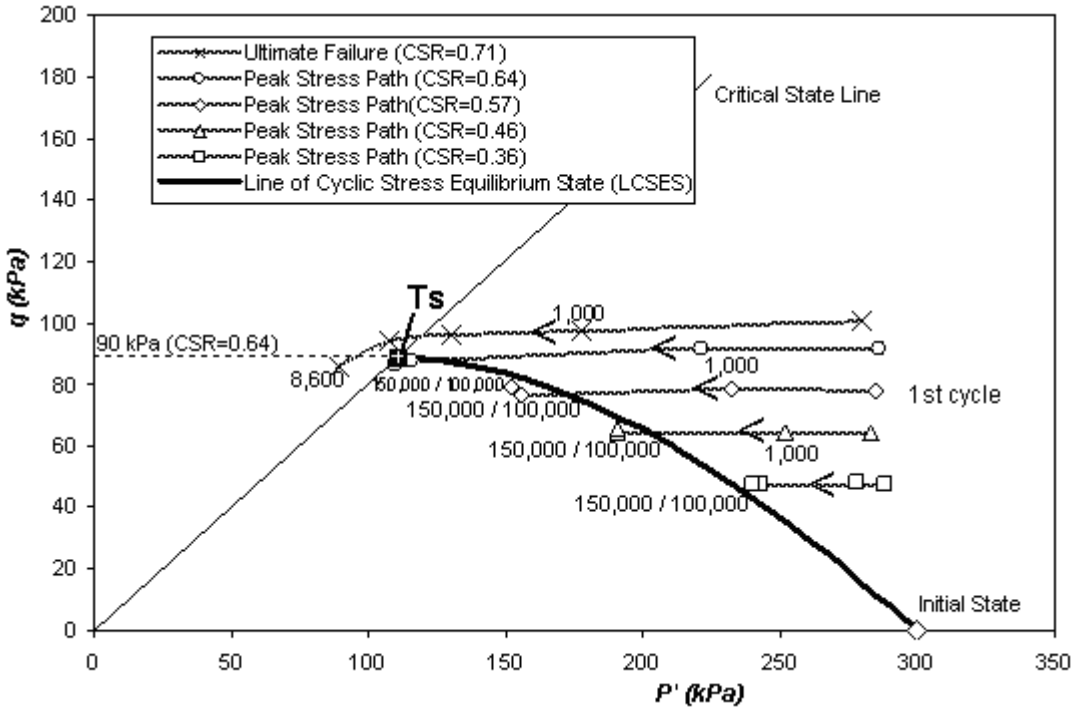

Figure 4-7 The locus of stationary ends of peak stress paths connected to form line of cyclic stress equilibrium state. (Normally-consolidated NC series)

Of interest in this study is the identification of the maximum deviator stress (threshold stress) amongst all possible stationary ends of peak stress paths where

state of stress equilibrium has arrived. By examined the locus (where the stationary points of the peak stress paths are) at the end of the peak stress paths which indicates state of stress equilibrium, these locus can be connected together to form a non-straight line (Refereed hereinafter as the line of cyclic stress equilibrium state LCSES). The LCSES can be extrapolated to intercept the critical state line (CSL) at the point "Ts" at which the deviator stress represents the threshold stress (q_t) of the kaolinite clay that had been normally-consolidated to 300 kPa.

For normally-consolidated NC series clay under undrained cyclic compression, the locus at the stagnating end of all possible peak stress paths where it becomes stationary before reaching the critical state line CSL can be connected to form a line of cyclic stress equilibrium state. The LCSES therefore represents the peak stress state where excess pore water pressure ceases to increase and development of strain stabilized. The level of deviator stress of LCSES at the intersection of LCSES extrapolation and CSL is the maximum possible cyclic deviator stress (the threshold stress, q_t) that normally-consolidated clay soil specimen will attain in the resilient state.

4.2.6 Development of Axial Strain

The development of the total strain consists of plastic (permanent or non-recoverable) and elastic (temporary or recoverable) strain. The accumulation of total axial strain with respect the number of cyclic loading applications had been described and shown in Figure 4-6 for the cyclic compression tests. Figure 4-8 showed the relationship of the stabilized total strain (maximum total strain) of each test with the level of deviator stress at stress equilibrium state. A way to apprehend the axial deformation characteristics of saturated clay under undrained compression had been attempted by correlating the stabilized total strain of cyclic compression test to the static axial strain of the monotonic compression test in a p'- q - v stress state space.

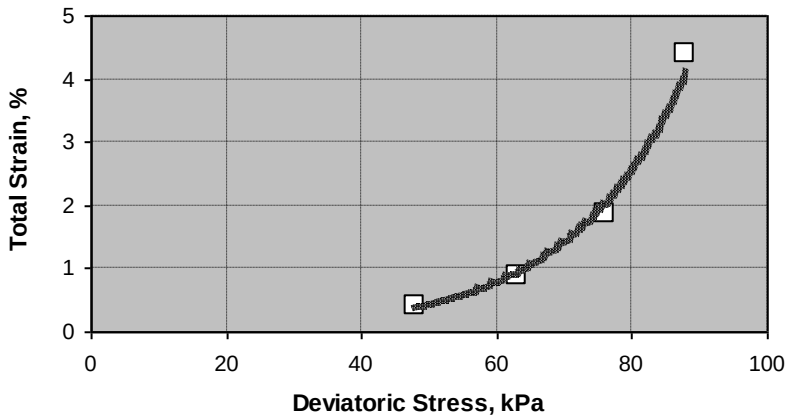

Figure 4-8 Variation of the stabilized total strain with deviator stress (NC series)

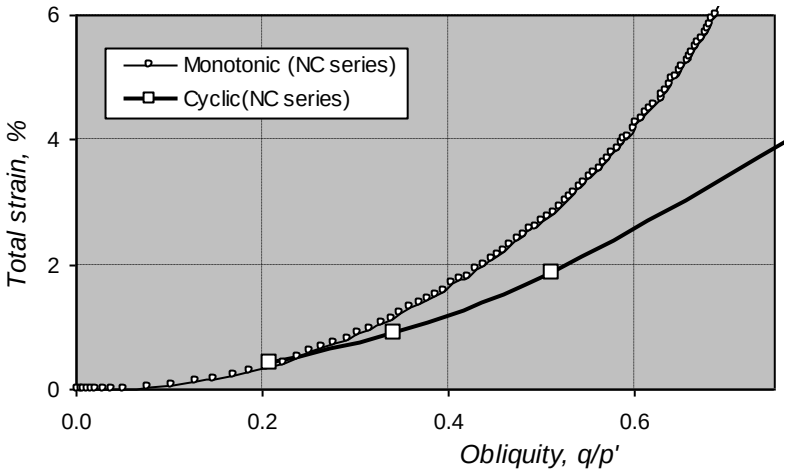

Figure 4-9 Variation of total strain (stabilized in cyclic tests) with stress obliquity (NC series)

First of all, the constant-strain contours were derived from the strain data of the basic monotonic compression test. Figure 4-10 showed the constant-strain contours derived from the test M300OC1, where each contour is a straight line radiates from the 'zero' point in a p'- q plot. For normally-consolidated clay under monotonic compression, the shapes of the stress path are identical and the relationship between the strain and the stress obliquity q/p' is expected to be the same irrespective of the consolidation pressure within a fair range i.e. up to 400 kPa (Lambe and Whitman 1969). On the constant-strain contours in Figure 4-10, data points of the actual stabilized total strain of cyclic compression tests at their respective stress equilibrium state were superimposed. It was found that, except at the very low end of strain scale (up to 0.5 %), the stabilized total strain of cyclic compression tests did not matched well with the constant-strain contours derived from the monotonic test strain data. When the strain data was plotted against the stress obliquity q/p' as shown in Figure 4-9, the relationship of the stabilized total strain with respect to its stress obliquity q/p' for cyclic compression clearly did not resemble that of monotonic test (except when the stress obliquity $q/p' < 0.2$).

As part of the total axial strain, the recoverable or elastic strain may be referred to as the resilient strain under certain circumstances (i.e. the magnitude of cyclic loading) within each loading cycle. In general, the elastic strain of clay specimen under cyclic compression is the difference in strain at the peak compressive stress and the strain when the test specimen is fully unloaded. Under undrained cyclic compression, the elastic strain of the soil gradually increased until it become stabilized as the peak stress path arrived at the cyclic stress equilibrium state. It is at this final state that the elastic strain is referred to as the resilient strain. The resilient strain under cyclic compression increased with respect to the level of cyclic deviator stress as in Figure 4-11. There appeared to be a linear relationship between the resilient strain and the stress obliquity at cyclic stress equilibrium state as shown in Figure 4-12.

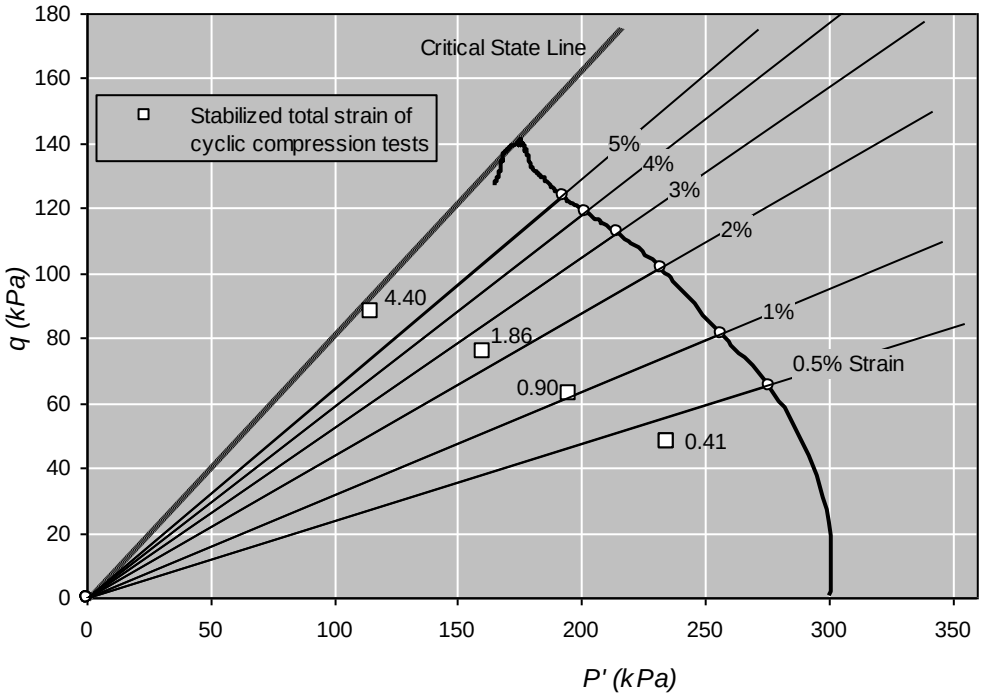

Figure 4-10 Constant-strain contours of test M300OC1 superimposed on the effective stress path (Kaolin clay, normal-consolidated at 300 kPa)

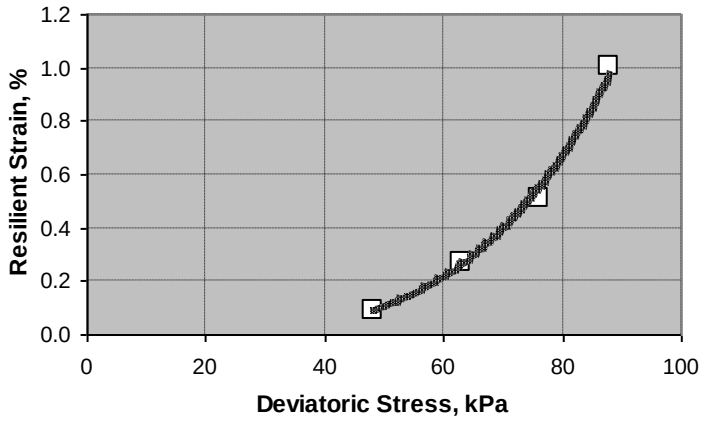

Figure 4-11 Variation of resilient strain with cyclic deviator stress (NC series)

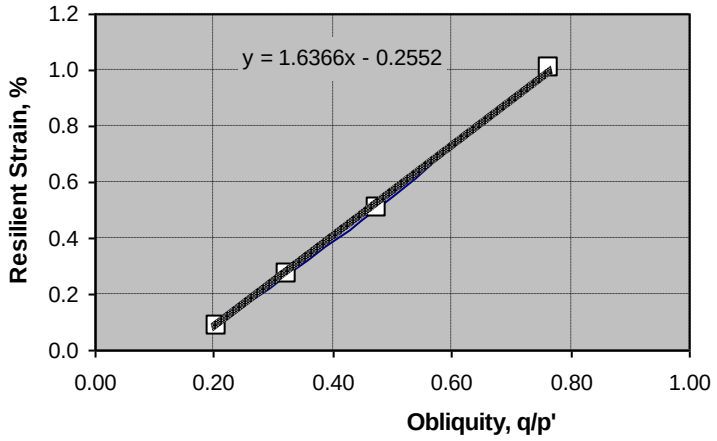

Figure 4-12 Variation of resilient strain with stress obliquity at equilibrium state (NC series)

4.2.7 Undrained Resilient Modulus

The undrained resilient modulus is the elastic modulus of the soil specimen under undrained cyclic compression that has arrived at the resilient state where both the stress equilibrium and the strain stabilization co-exist. At the beginning of the test, the elastic modulus of soil was decreasing with the number of cyclic loading applications (refer to Figure 4-13) due to the increasing elastic strain in each loading cycle. As the total strain hence the elastic strain became stabilized, the elastic modulus at this point is referred as the undrained resilient modulus which is defined as follows:

$$\text{Resilient Modulus (undrained), } E_r = \frac{q_{cyc}}{\varepsilon_r} \qquad (3\text{-}1)$$

where, q_{cyc} = cyclic deviator stress, and

ε_r = resilient strain (or elastic strain at resilient state)

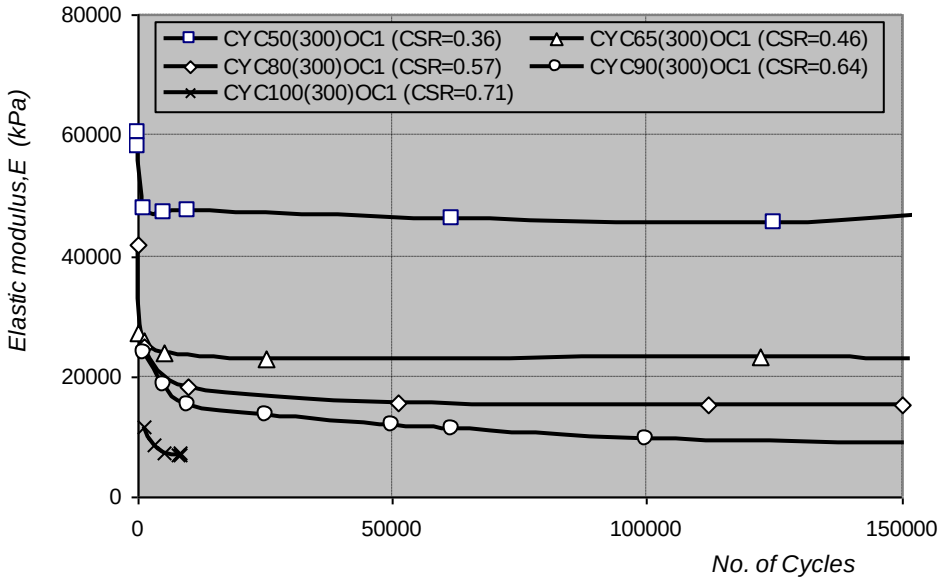

Figure 4-13 Variation of elastic modulus with no. of cycles – NC series (kaolin clay normal-consolidated at 300 kPa)

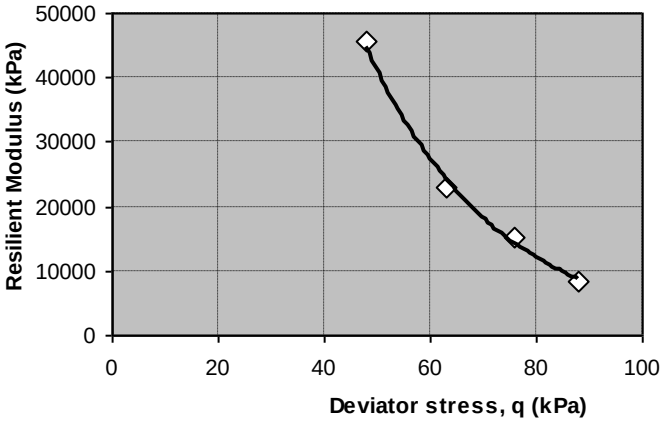

Figure 4-14 Result showing the decrease in resilient modulus as cyclic deviator stress increases (kaolin clay normally consolidated at 300 kPa)

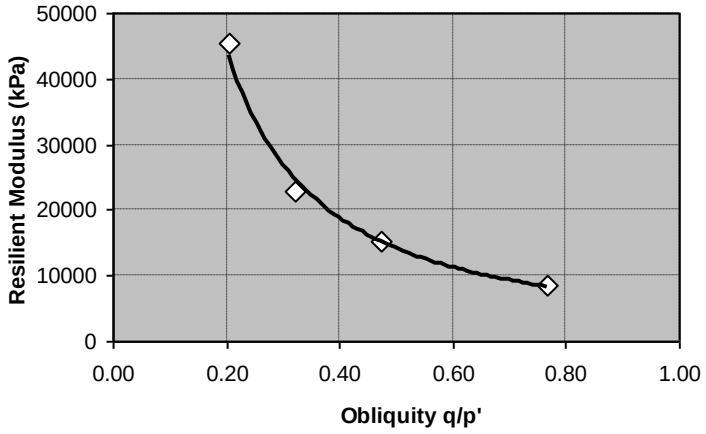

Figure 4-15 The relationship of resilient modulus with stress obliquity at cyclic stress equilibrium state

Figure 4-14 showed the variation of resilient modulus with respect to the level of cyclic deviator stress. The higher cyclic deviator stress will eventually cause the specimen under undrained cyclic compression to have a lower resilient modulus. The correlation of the resilient modulus (E_r) with the cyclic deviator stress (q) had been able to provide direct and practical information, as compared to correlating with the mean effective stress (p') which requires the knowledge of excess pore water pressure at the state of stress equilibrium. However, the variation of resilient modulus with respect to the stress obliquity (η) appeared also to correlate well as shown in Figure 4-15. The fundamental relationship between the resilient modulus and the stress obliquity at cyclic stress equilibrium state will be further illustrated in the next chapter.

4.2.8 Effect of Cyclic Loading Frequency

Up until this stage, the test data and results presented were from tests conducted at the cyclic loading frequency of 1 Hz (one cycle per second). Four other tests were carried out at higher cyclic loading frequency in order to study the influence of different cyclic loading frequency has on the stress /strain response of soil. Tests CYC50OC1(5Hz) and CYC65OC1(5Hz) were conducted at 5 Hz (five cycles per second) with a deviator stress of 50 kPa (CSR = 0.36) and 65 kPa (CSR = 0.46) respectively, whilst test CYC50(300)OC1(10Hz) and CYC65(300)OC1(10Hz) were both conducted at 10 Hz (10 cycles per second) with a cyclic deviator stress of 50 kPa and 65 kPa respectively.

Comparison was made on the build-up of peak excess pore water pressure for tests carried out at the cyclic deviator stress of 65 kPa with cyclic loading frequency of 1 Hz (from the earlier test CYC65(300)OC1), 5 Hz and 10 Hz. Figure 4-16 showed the accumulation of peak excess pore water pressure for the early part of the cyclic loading up to 150,000 cycles. For the same number of loading applications, the excess pore pressure was lower for test conducted at higher loading frequency where the total loaded duration (approximately equivalent to the number of cycles x (1 / cyclic loading frequency)) was lower. In view of this, it can be reasonably deduced that the build-up of excess pore water pressure will be closely proportionate to the total loaded duration, for the range of cyclic loading frequency considered.

A similar comparison was made for the build-up of the total strain at constant number of loading cycles (Figure 4-17). It was observed that for any given number of loading applications, higher cyclic loading frequency produced lower total strain. This also indicates that the development and accumulation of total strain is directly proportionate to the actual total loaded duration.

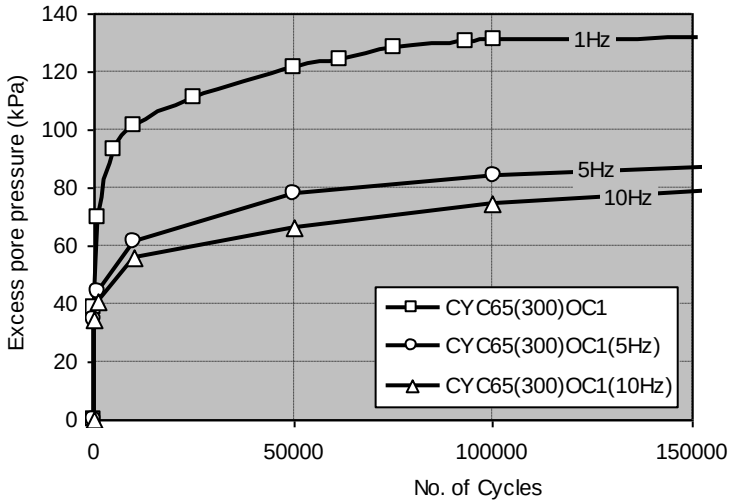

Figure 4-16 Results showing the building up of peak excess pore water pressure over each cycle under cyclic loading frequency of 1 Hz, 5 Hz and 10 Hz. (kaolin clay normal-consolidated to 300 kPa, deviator stress = 65 kPa)

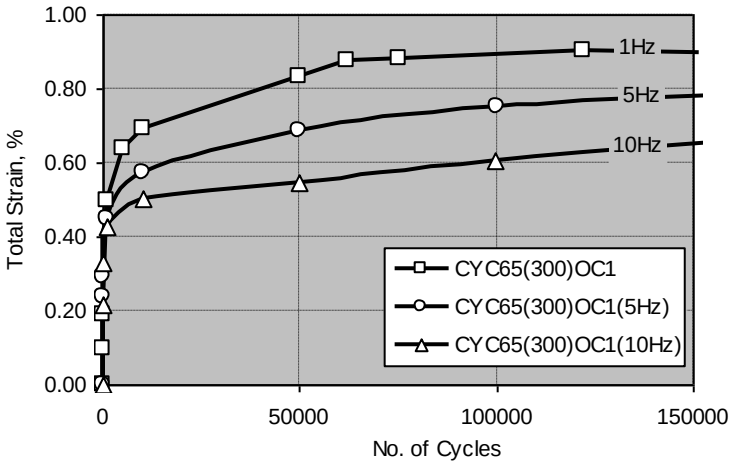

Figure 4-17 Results showing the development of peak total strain over each cycle under cyclic loading frequency of 1 Hz, 5 Hz and 10 Hz. (kaolin clay normal-consolidated to 300 kPa, deviator stress = 65 kPa)

In general, given the same number of loading applications, the effect of higher cyclic loading frequency, i.e. from 1 Hz to 10 Hz, has on undrained cyclic compression reduces the build-up level for peak excess pore water pressure and the total axial strain. However, when tests with higher cyclic loading frequency were subjected to further number of cyclic loading applications which increased the total loaded duration, levels of the peak excess pore water pressure and the total strain continue to increase. Specimens under cyclic loading frequencies of 5 Hz and 10 Hz, all arrived at approximately same level of maximum excess pore water pressure and the stabilized total strain (refer to Figure 4-18, Figure 4-19 & Figure 4-20) as the specimen under cyclic frequency of 1 Hz; with the higher number of cycles applications associate with higher cyclic loading frequency.

In Figure 4-18, under cyclic deviator stress of 50 kPa, specimen cycled at 1 Hz attained the maximum excess pore water pressure of 75 kPa at about 100,000 cycles, whereas the other specimen cycled at 5 Hz only reached the same maximum excess pore pressure at approximately 300,000 cycles. Under cyclic deviator stress of 65 kPa (Figure 4-19), a maximum pore pressure of 100 kPa was arrived at 400,000 cycles for the specimen cycled at 5 Hz. The same maximum excess pore pressure was only attained after 800,000 cycles for the specimen cycled at 10 Hz. In terms of total strain, Figure 4-20 showed the result of three tests cycled at 1 Hz, 5 Hz and 10 Hz respectively, under a cyclic deviator stress of 65 kPa. The stabilized total strain of 0.8 % was arrived for the three specimens at about 100,000 cycles, 400,000 cycles and 800,000 cycles respectively.

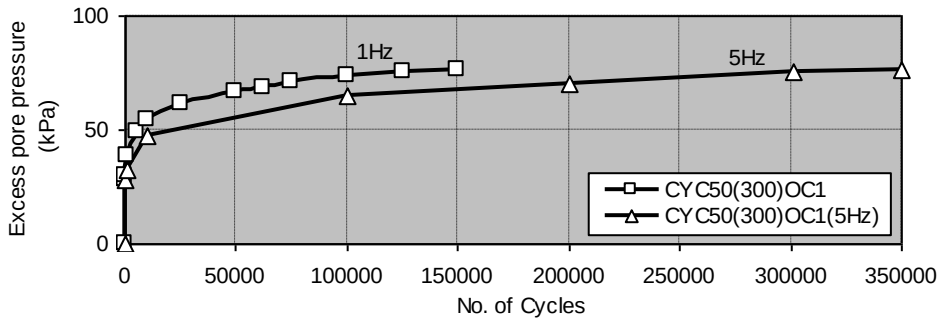

Figure 4-18 Number of loading cycles taken to reach the same level of peak excess pore water pressure for test carried out under loading frequency of 1Hz and 5Hz (normal-consolidated at 300 kPa, cyclic deviator stress = 50 kPa)

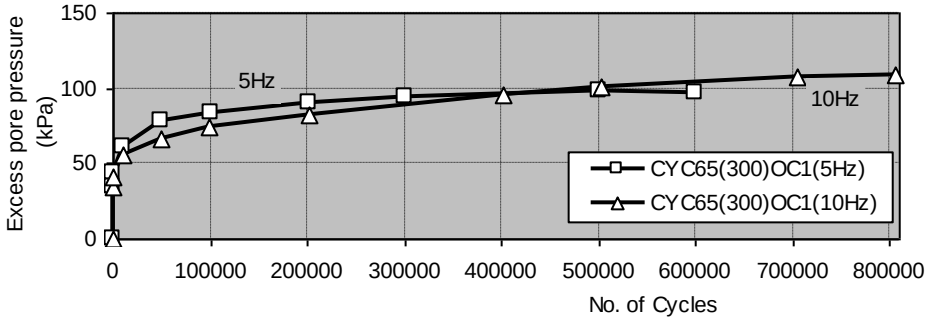

Figure 4-19 Number of loading cycles taken to reach the same level of peak excess pore water pressure for test carried out under loading frequency of 5Hz and 10Hz (normal-consolidated at 300 kPa, cyclic deviator stress = 65 kPa)

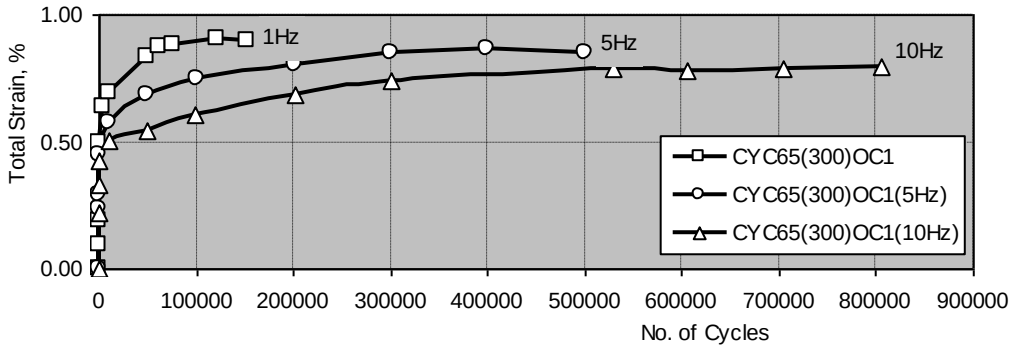

Figure 4-20 Results demonstrates different number of cycles required to achieve approximately same level of the stabilized strain under cyclic loading frequency of 1 Hz, 5 Hz and 10 Hz (kaolin clay normally-consolidated at 300 kPa, cyclic deviator stress = 65 kPa)

In summary, under cyclic compression with constant deviator stress of various loading frequencies, i.e. 1 Hz to 10 Hz, effect of the number of loading cycles on the excess pore pressure build-up and the total strain development will be apparent during the transient cycles prior to arriving at the resilient state. At the same number of cyclic loading applications, higher loading frequency generates lesser strain energy to the soil, and therefore the soil responds with lower excess pore pressure and lower total strain. However, continuous application of cyclic loading will eventually lead to the resilient state where all soil specimens under various cyclic loading frequencies i.e. 1 to 10 Hz will build up the equivalent level of maximum excess pore water pressure and the stabilized total strain. In other words, the peak stress path of these tests will arrive at same cyclic stress equilibrium state. Figure 4-21 showed the peak stress path of test specimens conducted under different cyclic deviator stress and loading frequency, all arrived at the same line of cyclic stress equilibrium state LCSES described in Figure 4-7. As such, variation of cyclic loading frequency will have no effect on the level of threshold stress in undrained cyclic compression.

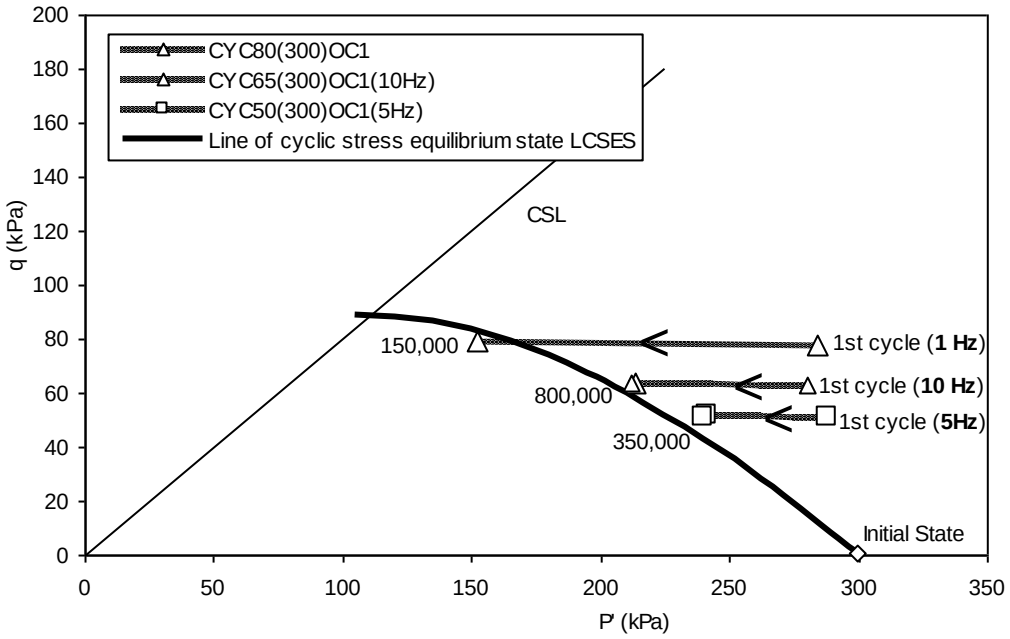

Figure 4-21 Locus of the stationary ends of peak stress paths for tests of various deviator stress and loading frequencies, arrived at the same line of cyclic stress equilibrium state LCSES under 1 Hz. (NC series)

4.3 *Over-Consolidated OC1.5 Series*

4.3.1 Introduction

Test specimens of over-consolidated OC1.5 series were initially undergone an isotropic normal-consolidation at an effective stress of 300 kPa. The specimens were then allowed to swell under an effective consolidation pressure of 200 kPa, giving an over consolidation ratio (OCR) of 1.5. The following presentation mainly focuses on the pore water pressure development, equilibrium stress and strain pattern which was atypical to the NC series. Summarized description will be presented when there was similarity with the NC series.

Tests included in this series are:

M200 OC1.5	
CYC40(200)OC1.5	(CSR = 0.35)
CYC55(200)OC1.5	(CSR = 0.48)
CYC65(200)OC1.5	(CSR = 0.56)
CYC70(200)OC1.5	(CSR = 0.61)
CYC78(200)OC1.5	(CSR = 0.66)

4.3.2 Monotonic Compression

Figure 4-22 showed the development of the deviator stress and the excess pore water pressure verses the axial strain for test M200OC1.5. As the deviator stress increased under a controlled strain rate, there was a less steep build-up (compared with the normally-consolidated soil in NC series) of the excess pore water pressure until it reached the maximum of 100 kPa at about 16 % strain. The increase of the deviator stress slow down substantially after 10 % strain and peak at about 14 % strain where the maximum deviator stress of 115 kPa was taken as the peak undrained compression strength for the OC1.5 series. The specimen had a final moisture content of 35.7 %.

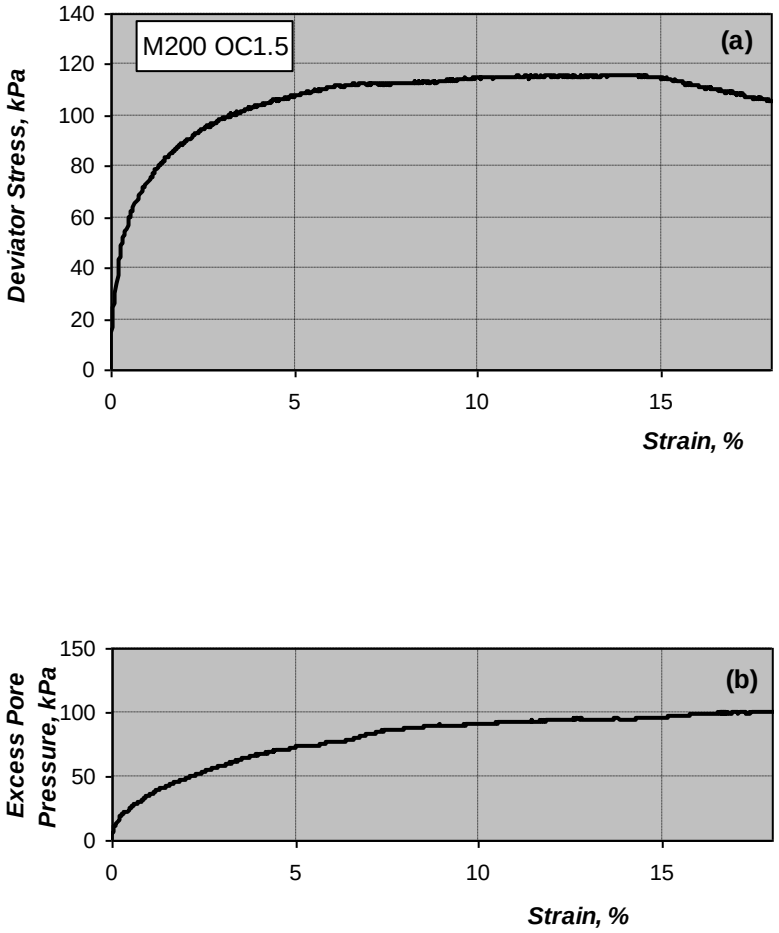

Figure 4-22 Result of the monotonic undrained compression (OC1.5 series, consolidation = 200kPa)

Plotted on *p'- q* stress plane as shown in Figure 4-23, the slow and gradual increase in excess pore water pressure has caused the pattern of stress path to move vertically upward until it reached the deviator stress of 65 kPa. Then the upward movement continued as it begun to sway leftward towards critical state line (CSL). The deviator stress at the vertex of stress path represents the peak deviator stress of 115 kPa where it has the same stress obliquity as the CSL.

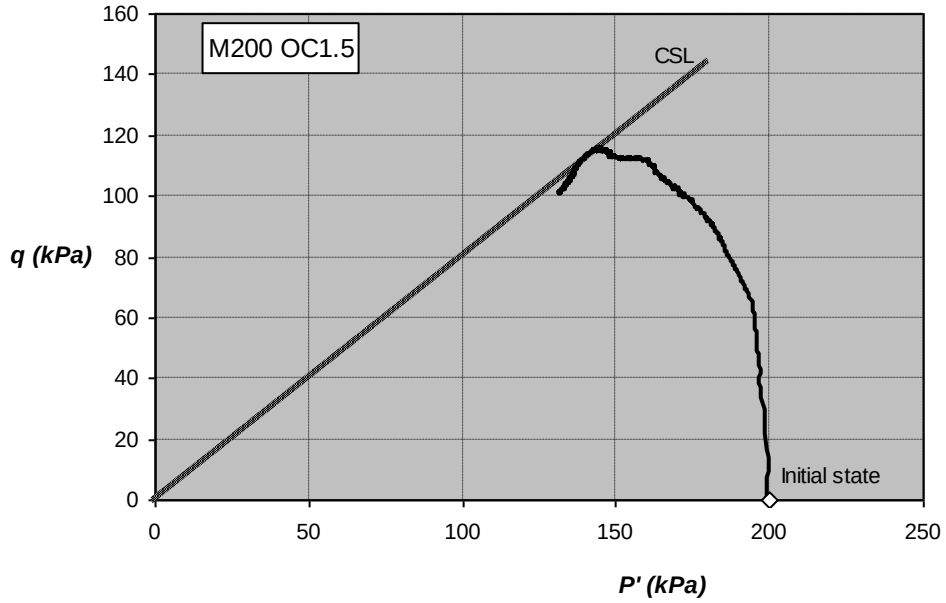

Figure 4-23 Stress path for monotonic undrained compression on saturated kaolin clay (consolidated at 200kPa, OCR=1.5)

4.3.3 Cyclic Compression Leading to Resilient State

In the lightly over-consolidated OC1.5 series, there were two different characteristic cyclic stress responses for soil specimen that had led to the resilient state. Typically, they can be represented by test CYC65(200)OC1.5, and test CYC40(200)OC1.5.

(1) TEST CYC65(200)OC1.5

Specimen of test CYC65(200)OC1.5 has the behavioural pattern which was characteristic of the tests with higher cyclic deviator stress, i.e. CYC55(200)OC1.5, CYC65(200)OC1.5 and CYC70(200)OC1.5, which had led to the resilient state. In general, these tests exhibited cyclic stress responses similar to those in the NC series. Under cyclic compression, the specimen built up excess pore pressure and total strain over each cycle of loading application (Figure 4-24 (a) & (b)). The only difference

was the rate of the increment for both excess pore pressure and the total strain was significantly slower in the early part of the loading application, i.e. up to 1000 cycles or so (Figure 4-24). This can be noticeable by examining the gap between 1st and the 1000th cycle, and between 1000th and 10,000th cycles. The relatively closer gap of the 1st and 1000th cycle suggested a smaller excess pore pressure built-up during this period of loading application.

As the accumulation of excess pore water pressure and total axial strain stabilized, a state of resiliency arrived in which both stress equilibrium and strain stabilization exist. Further application of cyclic loading produces only constant variation of pore water pressure and total axial strain within each loading cycle as the peak stress path became stationary before the critical state line. The state of stress at the stagnated end of peak stress path has a stress ratio (η) less than the gradient of critical state path (M).

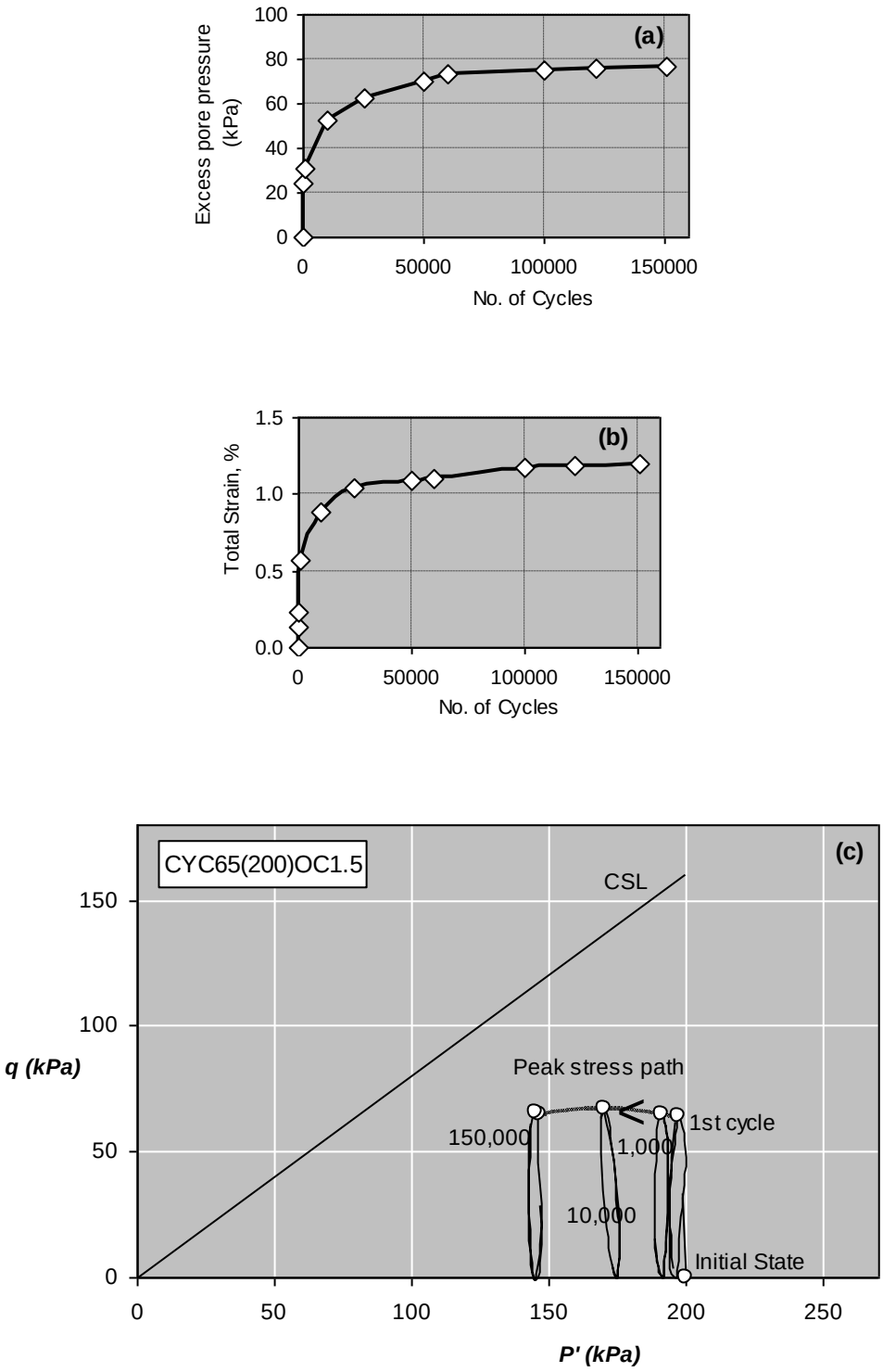

Figure 4-24 Results of cyclic undrained compression test on kaolinite clay that led to a resilient state (OC1.5 series, consolidated at 200 kPa (OCR = 1.5), cyclic deviator stress = 65 kPa and CSR=0.56)

(2) TEST CYC40(200)OC1.5

Under cyclic compression with deviator stress of 40 kPa (CSR = 0.35), the excess pore pressure immediately surged to 14 kPa (a level slightly higher than one-third that of deviator stress) at the very first cycle (Figure 4-25(a)). The excess pore pressure showed no sign of building up and it remained approximately constant throughout the entire test duration. The total axial strain, however, appeared to have increased with the numbers of loading cycles but became stabilized at a relatively early stage of the loading cycles (Figure 4-25(b)).

On the p'- q plane plot (Figure 4-25(c)), cyclic stress path formed hysteresis loop from 1st to 150,000th cycle due to the non-incremental and constant-amplitude variation of excess pore water pressure within each cycle. The peak stress path presented itself as a stationary peak stress state as no migration of peak stress path was visible. The state of cyclic stress equilibrium appeared to be inherent as soon as the cyclic loading began. However, as the total axial strain of the specimen appeared only became stabilized after shortly after the test began (approximately within 10,000 cycles), it can only be speculated that the arrival of state of resiliency therefore only follow the arrival of strain stabilization.

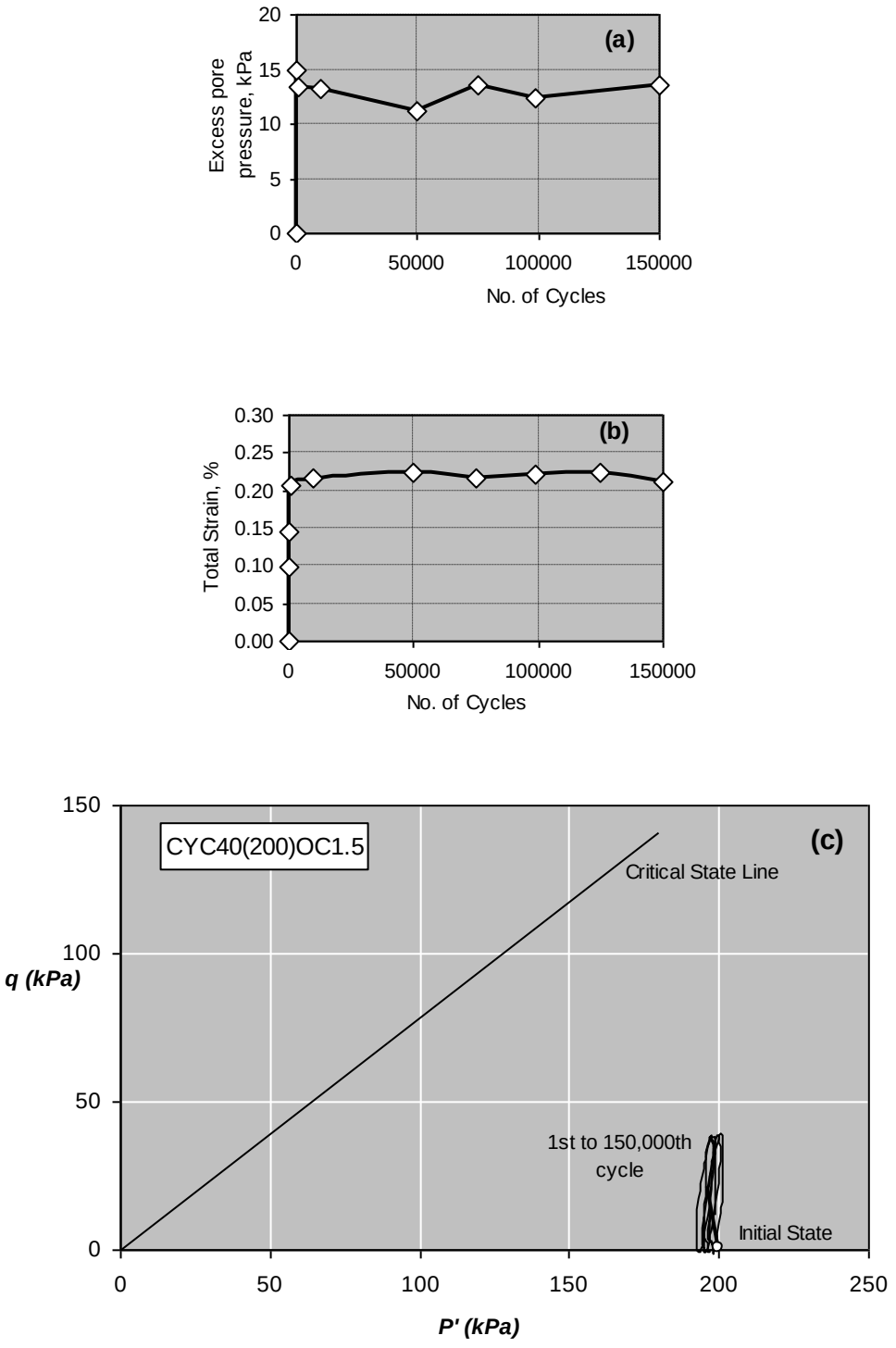

Figure 4-25 Results of cyclic undrained compression test on kaolinite clay that led to a resilient state (OC1.5 series, consolidated at 200 kPa (OCR = 1.5), cyclic deviator stress = 40 kPa and CSR = 0.35)

In general, the behaviour of the clay specimens in the over-consolidated OC1.5 series, which led to a resilient state under undrained cyclic compression, can be summarized as follows:

(1) Under cyclic deviator stress above a specific level, soil builds up excess pore water pressure and total axial strain in a way similar to the normally-consolidated soil, except that the accumulation rate of excess pore water pressure is remarkably slower during the early cycles. As soon as the resilient state arrived, the stress path form hysteresis and the peak stress path became stationary before the critical state line. The stationary end of peak stress path has a stress ratio (η) less than the gradient of critical state path (M). A state of resiliency exists after the arrival of both stress equilibrium and strain stabilization.

(2) Under cyclic deviator stress below a specific level, no accumulation of excess pore water pressure occurs, except constant-amplitude variation of excess pore pressure within each cycle. The peak stress path is stationary without migration and it has a stress ratio (η) less than the gradient of critical state path (M). There is, however, a relatively early accumulation and stabilization of the total axial strain after the cyclic loading began. Hence, the state of cyclic stress equilibrium is inherent and the state of resiliency exists only after an early arrival of strain stabilization.

4.3.4 Cyclic Compression Leading to Ultimate Failure

Test CYC78(200)OC1.5 was given cyclic deviator stress of 78 kPa (cyclic stress ratio CSR = 0.66) at which the specimen led to ultimate failure.

The initial response of specimen was essential similar to that described for CYC100(300)OC1 of the NC series. Under cyclic compression, the excess pore water built up at relatively slower but a reducing rate with respect to the number of cycles. It reached the maximum at 170 kPa after 100,000 loading cycles. The total strain initially increased at a reducing rate to 4 % after 40,000 cycles. The same rate of increment was maintained until it reached 7 % after 90,000 cycles. It then built up at an increasing rate and ultimately led the specimen to fail with large strain.

Similar to the cyclic compression tests which led to resilient state, the p'- q plot (Figure 4-26(c)) showed the relatively closer distance between the peak stress state of 1st and 1000th cycle due to the slower rate of excess pore pressure accumulation during the early-stage cycles (characteristic of lightly over-consolidated soil). The depicted crossing of critical state line by the peak stress path at 50,000th cycle appeared premature (Compared to the yielding of specimen marked by the sudden increasing rate of total axial strain at the 100,000th cycle as shown in Figure 4-26(b)) and it may suggests that the actual equivalent excess pore water pressure within specimen at the 50,000th cycle was likely to be lower than the measured value of excess pore water pressure.

When specimen of the over-consolidated OC1.5 series is subjected to undrained cyclic compression leading to ultimate failure, specimen builds up excess pore water pressure at reducing rate as the peak stress migrates horizontally towards the critical state line (CSL). Similar to that of normally-consolidated soil in the NC series, the axial strain develops at a reducing rate initially but remains at constant rate of increment thereafter. The actual equivalent excess pore water pressure which increases with a lag to the measured value accumulates until it reaches a plateau. Upon which, the peak stress eventually reaches the CSL where specimen deforms at a significantly increasing rate and failed ultimately.

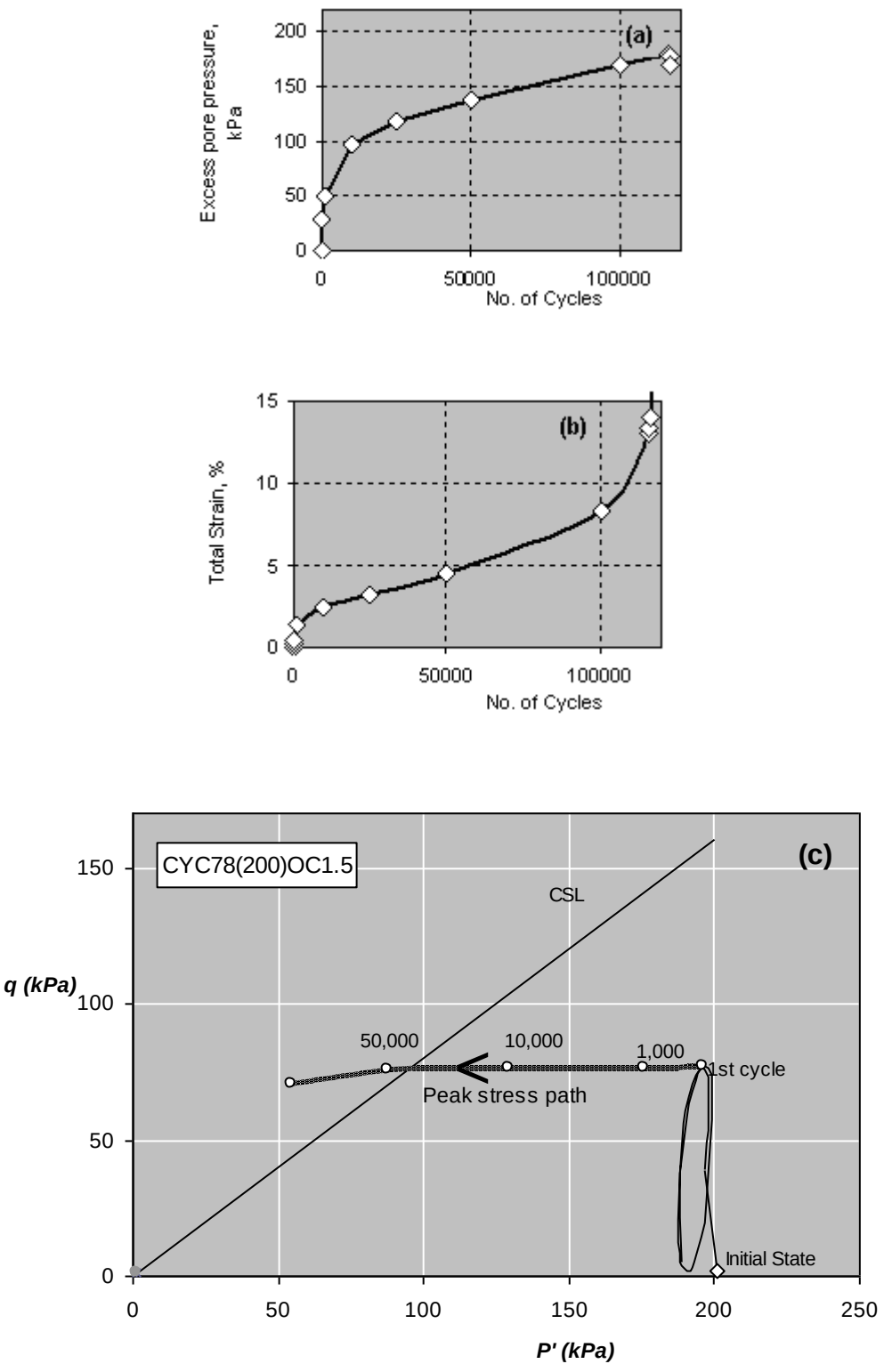

Figure 4-26 Results of a cyclic undrained compression test on kaolinite clay that led to ultimate failure (consolidation = 200 kPa, OCR = 1.5, with cyclic deviator stress = 78 kPa, CSR = 0.66)

4.3.5 Line of Cyclic Stress Equilibrium State and the Threshold Stress

Tests included in this series which arrived at the resilient state are:

CYC40(200)OC1.5 (CSR = 0.35),
CYC55(200)OC1.5 (CSR = 0.48),
CYC65(200)OC1.5 (CSR = 0.56) and
CYC72(200)OC1.5 (CSR = 0.61).

Figure 4-27 provides an overall view of the peak stress paths for above tests that arrived at the state of stress equilibrium, including the stationary peak stress state for test CYC40(200)OC1.5 and the peak stress path of the failure test CYC78(200)OC1.5. As described in 4.3.3, the two different characteristic response of the soil under undrained cyclic compression produced the line cyclic stress equilibrium state (LCSES) unique to this series of lightly over-consolidated clay and it is likely to the be characteristic of all lightly over-consolidated clay. By connecting the locus of stationary end of all the peak stress paths, the stationary peak stress state and the initial consolidated state (p'= 200 kPa, q = 0), the LCSES extended vertically upward from the initial consolidated stress state connecting the stationary peak stress state, to join another curve which bends gently toward the left. As with the NC series, the extrapolation of the curved LCSES intercepted the critical state line (CSL) at point "Ts", at which the deviator stress represents the threshold stress (q_t) of the lightly over-consolidated OC1.5 series soil.

For the lightly over-consolidated OC1.5 series clay under undrained cyclic compression, the locus at the end of all possible peak stress paths form a unique line pattern consists of a near vertical straight line rising from the initial stress state and a curve bending leftward above the tip of straight line, to a point on the critical state line. While the curving portion of LCSES represents a resilient state at which excess pore water pressure ceased building up and total axial strain stabilized. The vertical portion of LCSES does not necessarily signal the resilient state until the development of total strain has also been stabilized. Similar to the NC series, the level of deviator

stress of LCSES at the intersection of LCSES extrapolation and CSL indicates the threshold stress (q_t) of clay soil for the OC1.5 series.

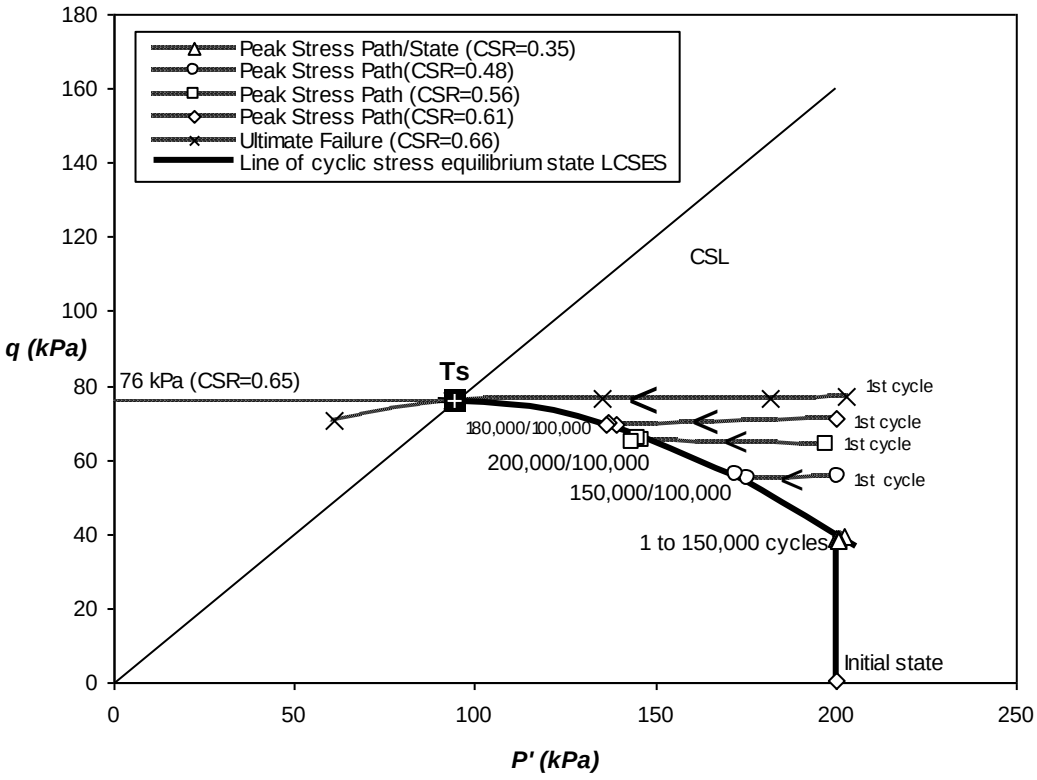

Figure 4-27 The locus of stationary ends of peak stress paths, the peak stress state and the initial state are connected to form line of cyclic stress equilibrium state. (OC1.5 series: consolidation = 200kPa, OCR=1.5)

4.3.6 Deformation Characteristic and Resilient Modulus

Figure 4-28 presents and describes the accumulation of total axial strain with respect to the number of cyclic loading application for the cyclic compression tests. The

relationship of the stabilized total axial strain (maximum total axial strain) with the level of cyclic deviator stress is shown in Figure 4-29.

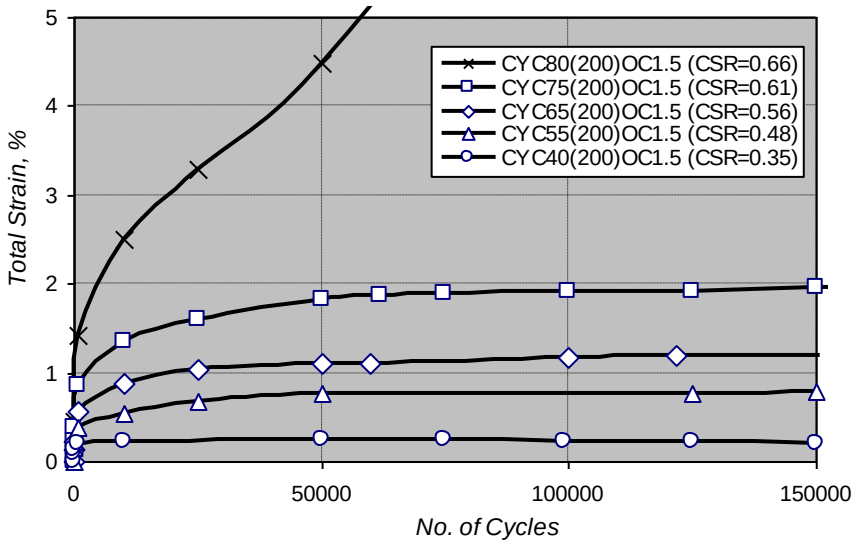

Figure 4-28 Development of peak total strain over each cycle (NC series)

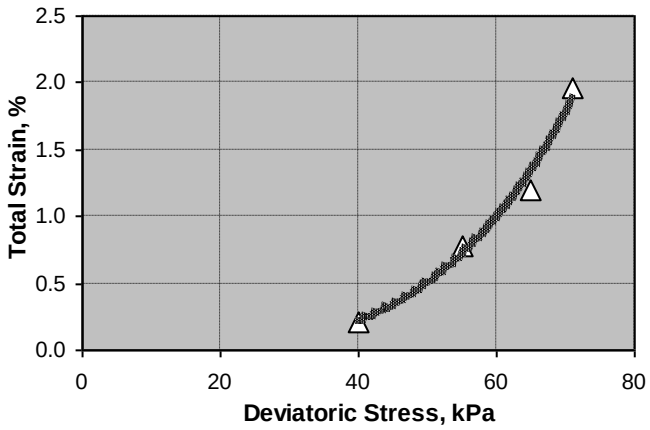

Figure 4-29 Variation of stabilized total strain with level of cyclic deviator stress (OC1.5 series: consolidation = 200kPa, OCR = 1.5)

Attempt was made to correlate the stabilized total strain of cyclic compression test to the static axial strain of the monotonic compression test in a p'- q - v stress state space. The constant-strain contours that were derived from the strain data of the basic monotonic compression test M200OC1.5 was shown in Figure 4-30. As in normally-consolidated series soil described in paragraph 4.2.6, over-consolidated soil of same over-consolidation ratio under monotonic compression is expected to have stress path of identical shape. Also, the relationship between the axial strain and the stress obliquity q/p' is expected to be the same irrespective of the consolidation pressure within a fair range. The superimposition of the stabilized total axial strain of cyclic compression tests at their respective stress equilibrium state produced reasonably good matching for strain level below 1%. Above the 1% strain level, however, the stabilized total strain data and the static strain contours did not match well. Comparing with the normally-consolidated NC series, this suggested that the lightly over-consolidated OC1.5 series has a better resemblance on the $p'-q$ plot between the data points of the stabilized total strains of cyclic compression tests and the constant-strain contours of the static axial strain of the monotonic compression test. Figure 4-31 showed the stabilized axial strain data plotted against the stress obliquity q/p' for the lightly over-consolidated OC1.5 series soil, where the curve for the cyclic compression tests and the monotonic test matched well by overlapped each other for the strain below 1 %.

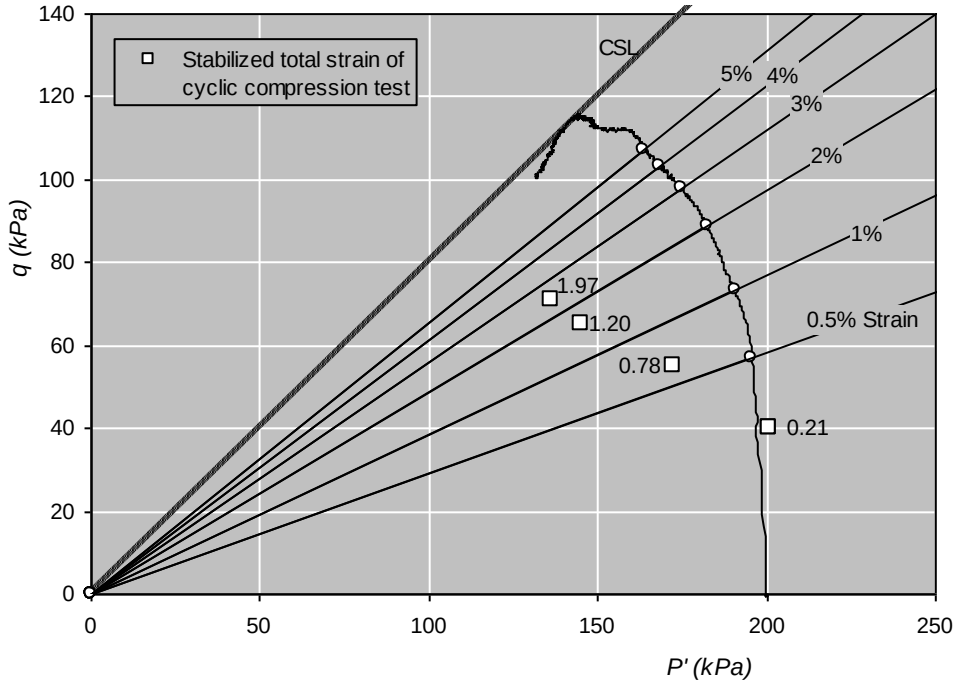

Figure 4-30 Constant-strain contours of test M200OC1.5 superimposed on the effective stress path (Kaolin clay, consolidated at 200kPa, OCR = 1.5)

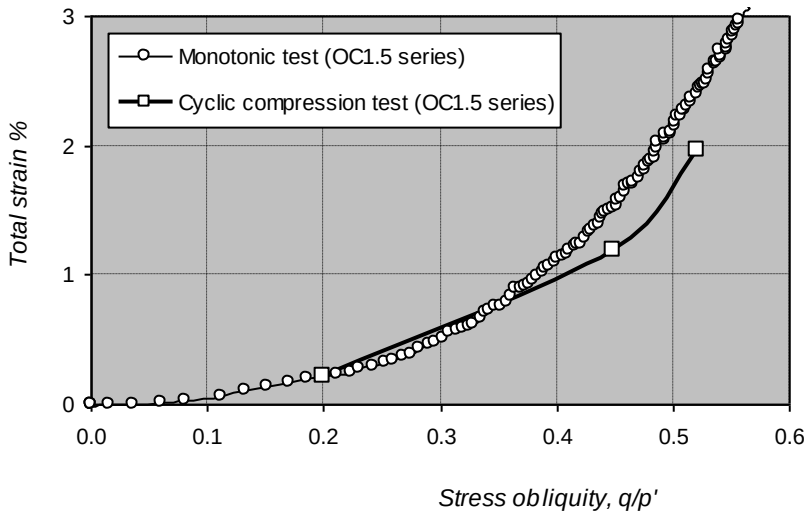

Figure 4-31 Variation of total strain (stabilized in cyclic tests) with stress obliquity (OC1.5 series)

Under cyclic undrained compression, the elastic axial strain of the soil gradually increases until it stabilizes as the peak stress path arrived at the cyclic stress equilibrium state. However, the elastic strain of soil for test CYC40(200)OC1.5 with an inherent state of cyclic stress equilibrium, appeared to be fairly constant throughout the test. This can be noticeable from Figure 4-32 which showed the variation of elastic modulus with the number of loading cycles where the elastic modulus for CYC40(200)OC1.5 appeared to be constant throughout. The resilient strain (the stabilized elastic strain) under cyclic compression increased with respect to the level of cyclic deviator stress as in Figure 4-33. The resilient strain and the stress obliquity at cyclic stress equilibrium state have a linear relationship as shown in Figure 4-34.

The variation of resilient modulus with respect to the level of cyclic deviator stress and the stress obliquity are shown in Figure 4-35 and Figure 4-36. As in normally-consolidated NC series, the higher cyclic deviator stress and the higher stress obliquity at equilibrium state associate with the lower resilient modulus.

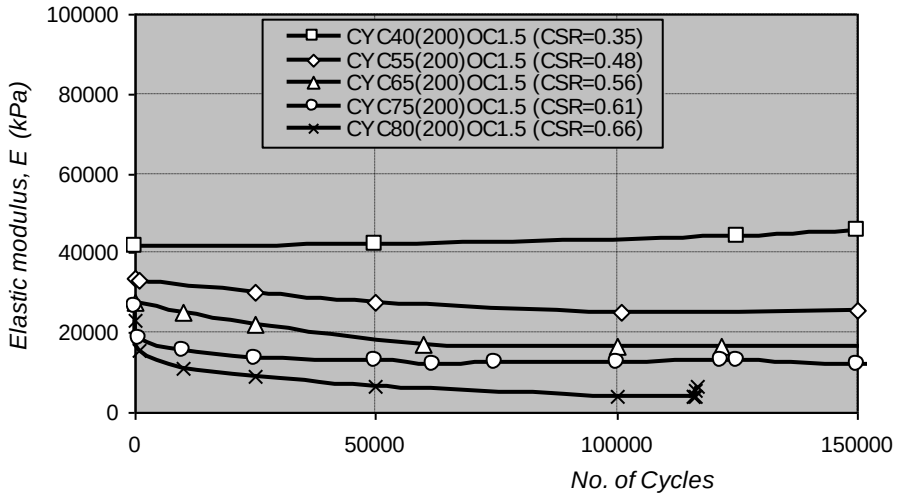

Figure 4-32 Variation of elastic modulus with number of cycles – OC1.5 series (kaolin clay, consolidated at 200kPa, OCR = 1.5)

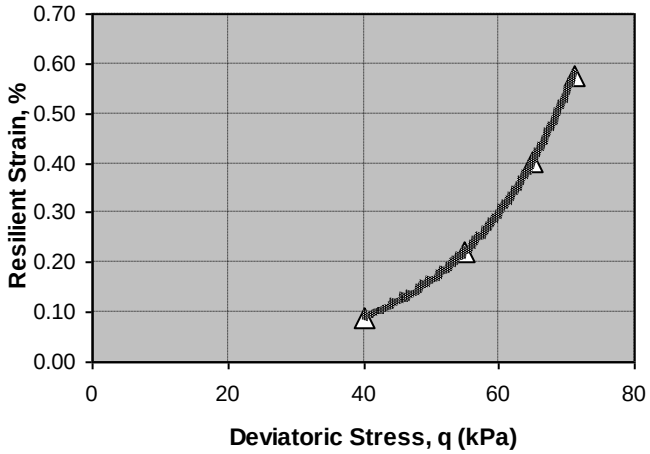

Figure 4-33 Variation of resilient strain with the level cyclic deviator stress (OC 1.5 series: consolidation = 200kPa, OCR = 1.5)

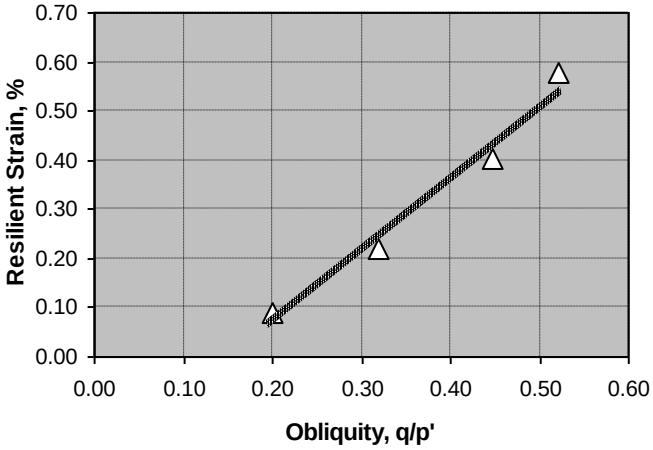

Figure 4-34 Variation of resilient strain with the stress obliquity at equilibrium (OC 1.5 series)

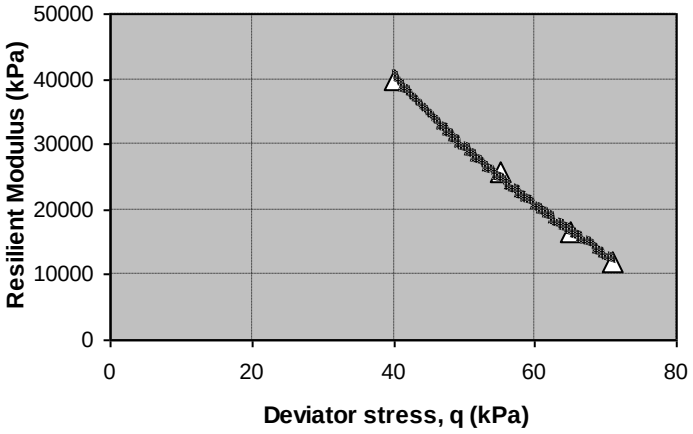

Figure 4-35 Variation of resilient modulus with level of cyclic deviator stress (OC1.5 series: consolidation = 200kPa, OCR = 1.5)

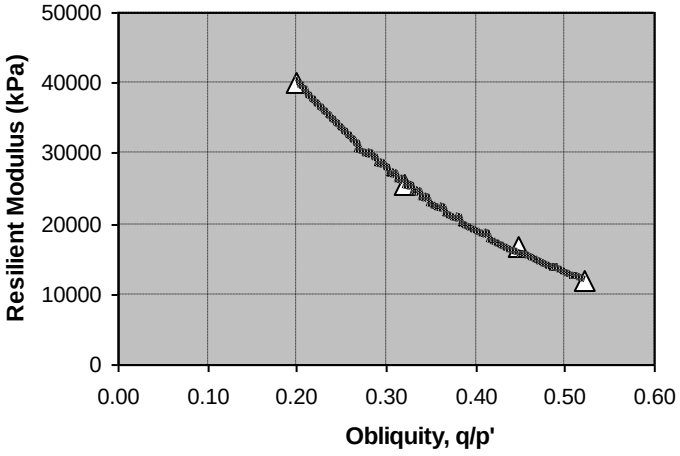

Figure 4-36 Variation of resilient modulus with stress obliquity at equilibrium (OC1.5 series)

4.4 *Over-Consolidated OC4 Series*

4.4.1 Introduction

In OC4 series, tests specimens were initially undergone an isotropic normal-consolidation at an effective stress of 300 kPa, followed by swelling to an effective consolidation pressure of 75 kPa, giving an over consolidation ratio OCR of 4. Tests included in this series were:

M75OC4	
CYC20(75)OC4	(CSR = 0.24)
CYC35(75)OC4	(CSR = 0.43)
CYC45(75)OC4	(CSR = 0.55)
CYC50(75)OC4	(CSR = 0.60)
CYC60(75)OC4	(CSR = 0.73)
CYC35(75)OC4Step	

4.4.2 Monotonic Compression

Figure 4-37 showed the development of the deviator stress and the build-up of excess pore water pressure with respect to the axial strain for test M75OC4. As deviator stress gradually increased under a slow controlled strain rate, there was a steep but small increase in the excess pore water pressure of 13 kPa at 2 % strain followed by an immediate reduction. By 5 % strain, the excess pore pressure had reduced to 10 kPa and remained constant till the end of the test. The deviator stress continued to increase at a reducing rate until it reached the peak of 82 kPa at 12 % strain. The final moisture content of the specimen was 37.6 %.

On the p'- q stress plane (Figure 4-38), the small and sharp increase in excess pore water pressure has caused the pattern of stress path to move upward initially until q = 20 kPa. It then moved up and slightly rightward as excess pore pressure remained at a constant level. The stress path crossed the critical state line and reached the

maximum at 82 kPa. It then moved downward along the early stress path towards the critical state line as the specimen failed with large strain.

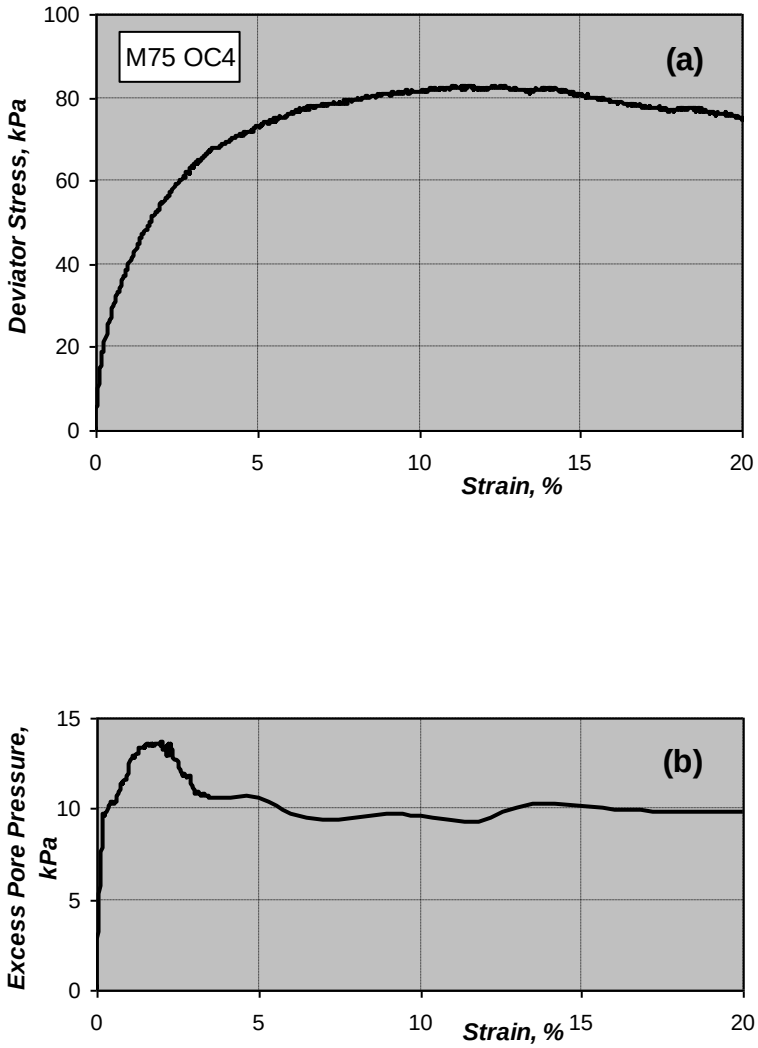

Figure 4-37 Result of the monotonic undrained compression (OC4 series: consolidation = 75kPa, OCR = 4)

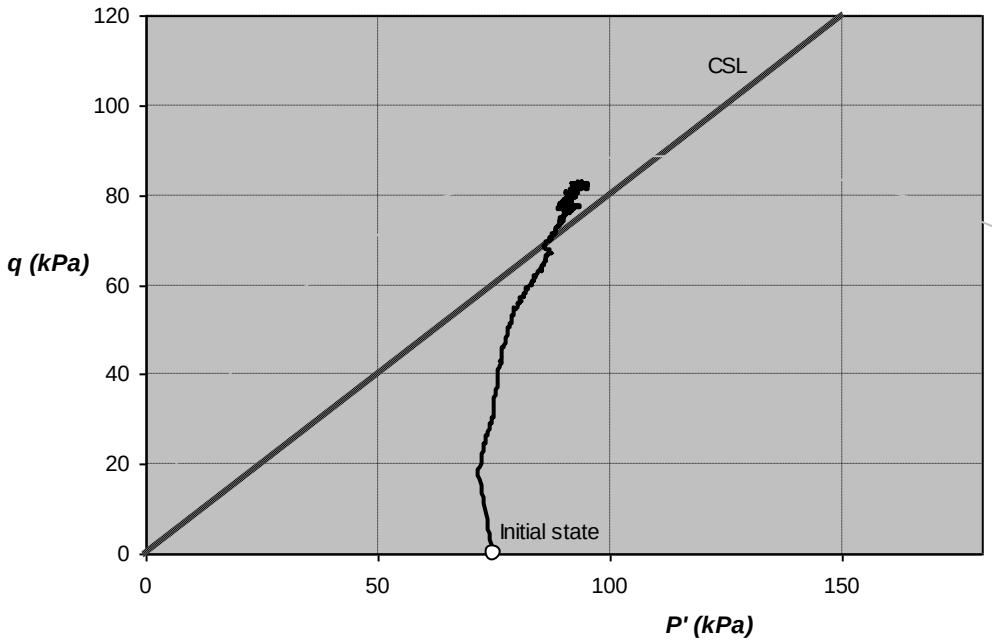

Figure 4-38 Stress path for monotonic undrained compression on saturated kaolin clay (consolidated at 75kPa, OCR=4)

4.4.3 Cyclic Compression

Cyclic stress responses for soil specimens of the over-consolidated series OC4 series (over consolidation ratio (OCR) = 4) that led to the resilient state can be typified by test CYC20(75)OC4, which has the similar response to CYC40(200)OC1.5 as described in OC1.5 series (4.3.3). Under cyclic compression, excess pore pressure of the specimen surged immediately on the first cycle (Figure 4-39(a)) and remained approximately constant throughout the entire test duration, while the total axial strain had an abrupt and reducing rate of increment but soon became stabilized at approximately 15,000th cycle, with respect to the numbers of loading cycles (Figure 4-39(b)).

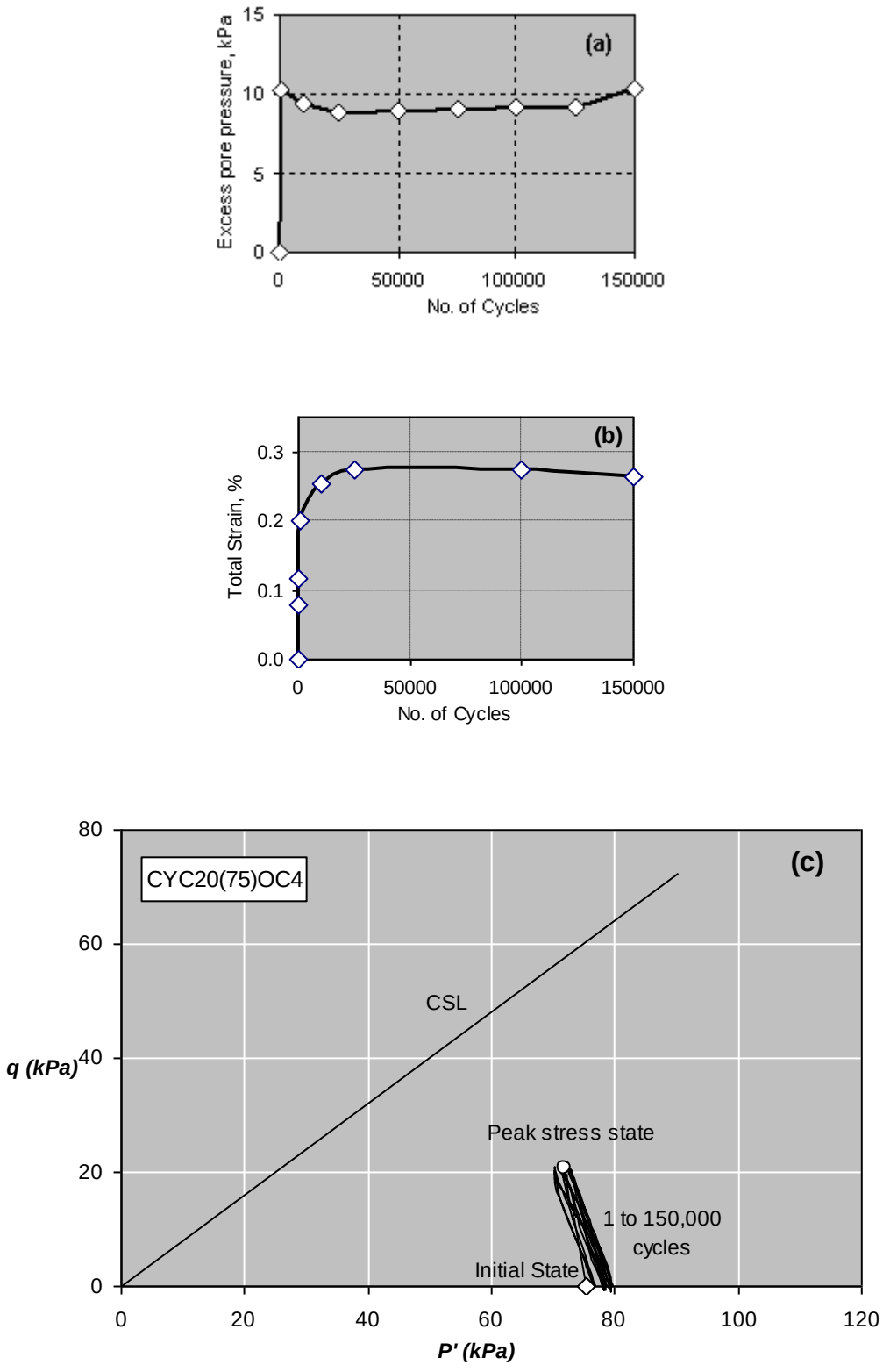

Figure 4-39 Results of cyclic undrained compression test on kaolinite clay that led to a resilient state (OC4 series: consolidated at 75 kPa, OCR = 4, cyclic deviator stress = 20 kPa, CSR = 0.24)

On *p'- q* plane plot (Figure 4-39(c)), the state of cyclic stress equilibrium appeared to be inherent as soon as the cyclic loading began. The amplitude of constant variation in the excess pore water pressure was 1/2 of the level of cyclic deviator stress, whereby it caused the depiction of the stress path loop to be inclined towards the left.

However, as an exceptional observation, test CYC45(75)OC4 with a higher cyclic deviator stress at 45 kPa (CSR = 0.55), the inherent state of stress equilibrium appeared unstable, as stress path loop moved slightly to the right before it finally settled to the left (Figure 4-40). The reason for this may be due to that the consolidated clay specimen of OC4 series had a state of stress exists near the wet and dry division of the critical state line, where the clay soil particles under remoulding action was balancing between the tendency of volume reduction for 'wet' soil (with positive excess pore water pressure) and dilation for 'dry' soil (with negative excess pore water pressure).

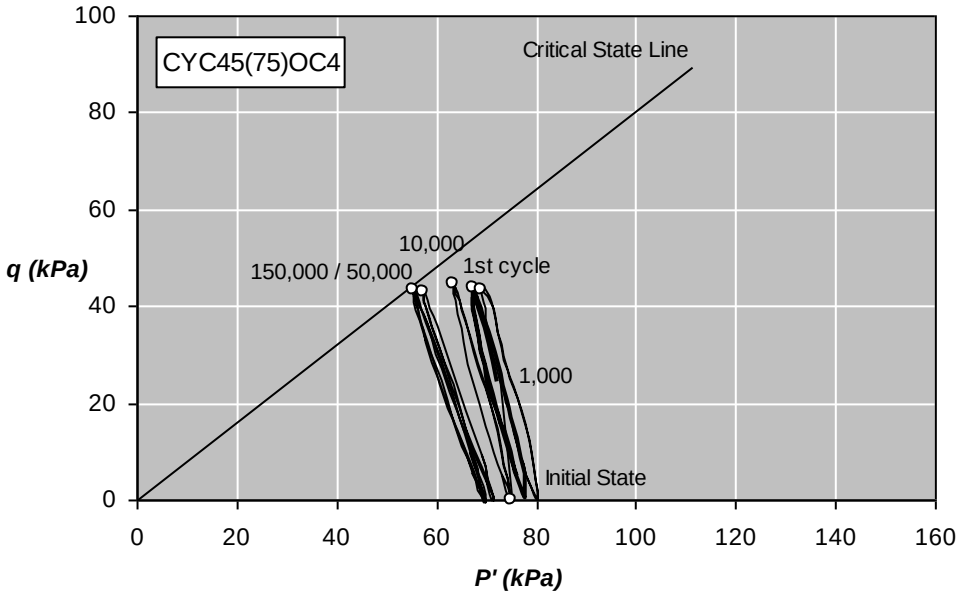

Figure 4-40 Results of cyclic undrained compression test on kaolinite clay that led to a resilient state (OC4 series: consolidated at 75 kPa, OCR = 4, cyclic deviator stress = 45 kPa, CSR=0.55)

At the inherent state of stress equilibrium where the resilient state was subsequently developed, the peak stress state of the tests conducted generally had a stress obliquity ($\eta = q/p'$) smaller than or near the gradient of critical state line (CSL). However, test CYC50(75)OC4, with a deviator stress of 50 kPa which was the highest to achieve resilient state, appeared to have its stagnated end of the peak stress path (the peak stress) existed at a stress obliquity slightly above that of the CSL.

Test CYC60(75)OC4 was the ultimate failure test where the specimen was given cyclic deviator stress of 60 kPa (cyclic stress ratio CSR = 0.73). Under cyclic compression, the excess pore water pressure surged up immediately and increased slightly before becoming constant at 40 kPa (Figure 4-41(a)). For the total axial strain, it increased sharply initially but briefly increased at a reducing rate for 1,000 cycles. Then it maintained and stayed at the same rate of increment for the next 2000 cycles to 8% strain before it built up at increasing rate to about 15% strain at 5000th cycle (Figure 4-41(b)) as the specimen led suddenly to ultimate failure with large strain.

On the *p'- q* plot (Figure 4-41(c)), the peak stress state of 1st cycle exists above the critical state line and the peak stress path was depicted as appeared to be migrated leftward initially (due to the time-lead effect of the measured excess pore pressure over the actual equivalent excess pore pressure within specimen, as described in the NC and OC1.5 series) before moving down towards the critical state line.

In the over-consolidated OC4 series, specimen under cyclic compression that led to failure built up excess pore water pressure immediately and appeared to increase slightly before remained constant throughout the test. Typified by test CYC60(75)OC4, the axial strain built up quickly at reducing rate initially and stayed at the same rate of strain increment as specimen yielded progressively. The peak stress path which commenced at a stress state above critical state line moved down towards critical state line as specimen began to deform at a significantly increasing rate and failed with large strain ultimately.

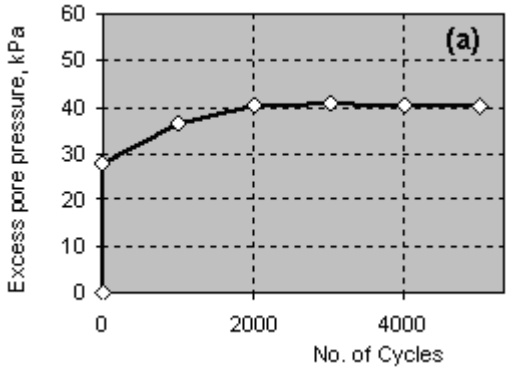

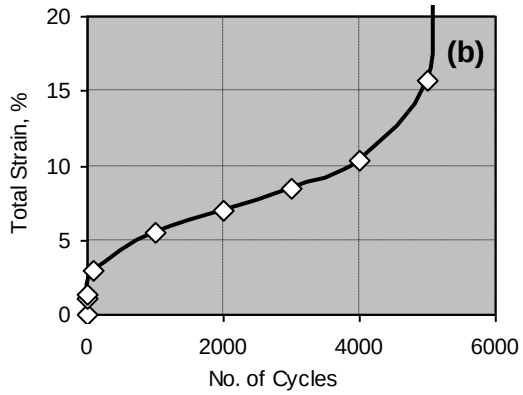

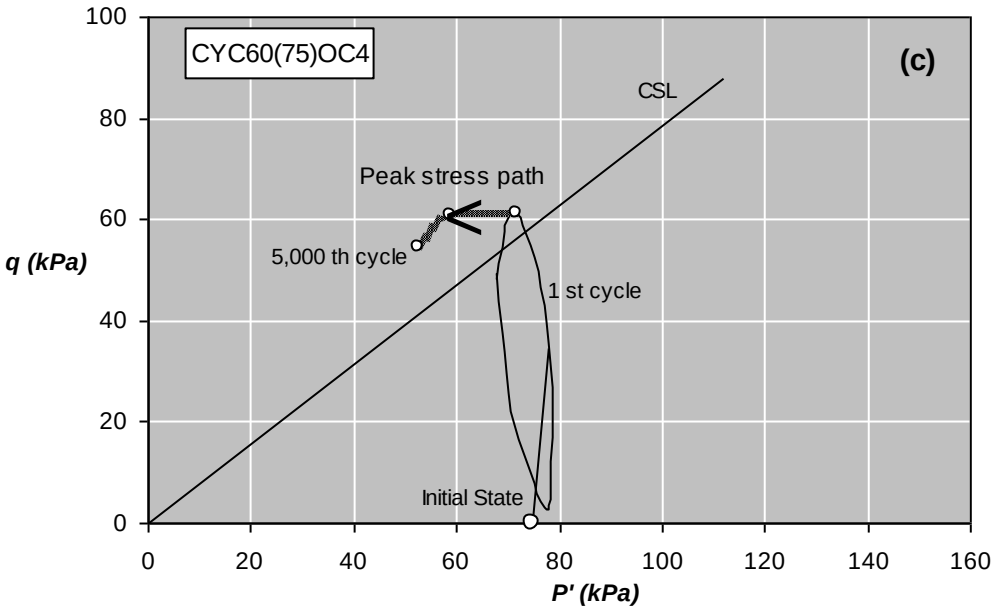

Figure 4-41 Results of a cyclic undrained compression test on kaolinite clay that led to ultimate failure (consolidation = 75 kPa, OCR = 4, with cyclic deviator stress = 60 kPa , CSR=0.73)

4.4.4 Step-Cyclic Compression Test

A step-cyclic compression test was carried out for OC4 series. CYC35(75)OC4step began with a cyclic deviator stress of 35 kPa, followed by 45 kPa and 50 kPa. The test was conducted as a confirmation test to test CYC50(75)OC4 which had attained a stabilized strain and resilient state, and a means to locate the maximum level of deviator stress that divides the failure and non-failure condition. This was done by assessing the development of total axial strain with respect to the repeated loading applications. From Figure 4-42, both the 1st and 2nd step-test with cyclic deviator stress of 35 kPa and 45 kPa respectively achieved stabilized strain after prolong application of loading in excess of 100,000 cycles. However, the 3rd step-test with deviator stress at 50 kPa has produced additional 10 % strain after 60,000 cycles of loading application, and it looked set to develop further. This provided an indication that the level of deviator stress for test CYC50(75)OC4 conducted earlier may be the highest possible to attain a stabilized strain and resilient state, and that the maximum level of deviator stress which divides the failure and non-failure condition (threshold stress) would be very close to 50 kPa or slightly lower.

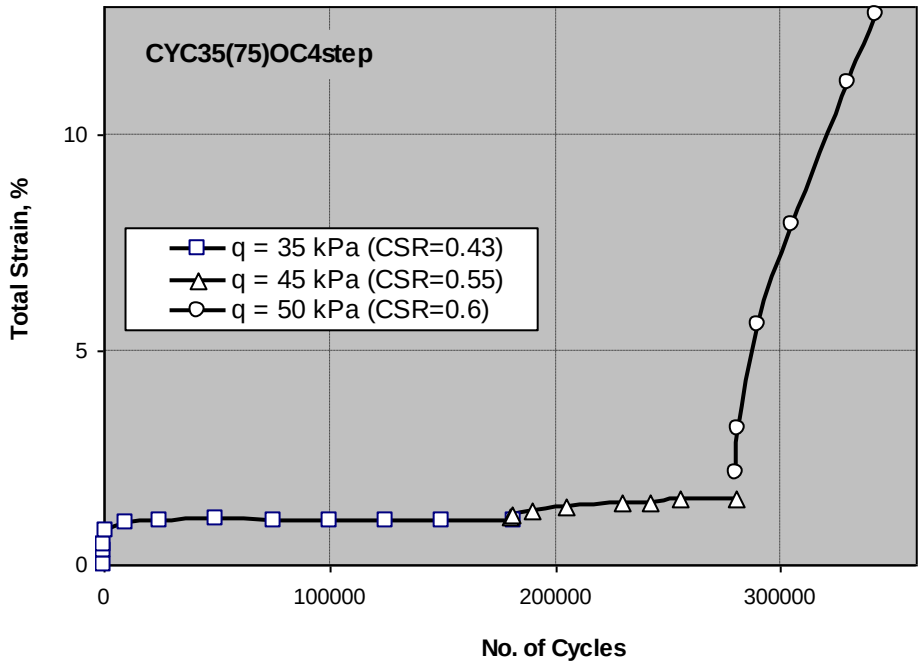

Figure 4-42 Development of total strain for the step-cyclic compression test

4.4.5 Cyclic Stress Equilibrium, Resilient State and the Threshold Stress

An overall view of the peak stress states for the tests of OC4 series that arrived at the resilient state and the failure test CYC60(75)OC1.5 is shown in Figure 4-43. The inherent state of cyclic stress equilibrium in tests that attained resilient state means that the peak stress path will show out in the p'- q plot as adjacent dot points or single dot, except for tests with high deviator, i.e. CYC45(75)OC4 where slight instability of the clay internal structure may have caused it to appear as a short peak stress path. By taking the best fit of these dot points, the line of cyclic stress equilibrium state (LCSES) appeared to be a straight line rising vertically at a slight incline to the left. Confirmed by the step-cyclic compression test (as described in above paragraph 4.4.4) which indicated the maximum possible level of cyclic deviator stress (threshold stress), the upper end of LCSES where the level of the deviator stress representing the threshold stress appeared to have coincidentally

intercepted and terminated on the critical state line at the point "Ts" (where the mid-point of peak stress path for test CYC50(75)OC4, with a deviator stress of 50 kPa (CSR = 0.61) was). The relatively high level of stabilized total strain for test CYC50(75)OC4 at 4.05 % (Figure 4-44), provided an indication that the level of cyclic deviator stress of 50 kPa can be taken as the best prediction of threshold stress for the OC4 series.

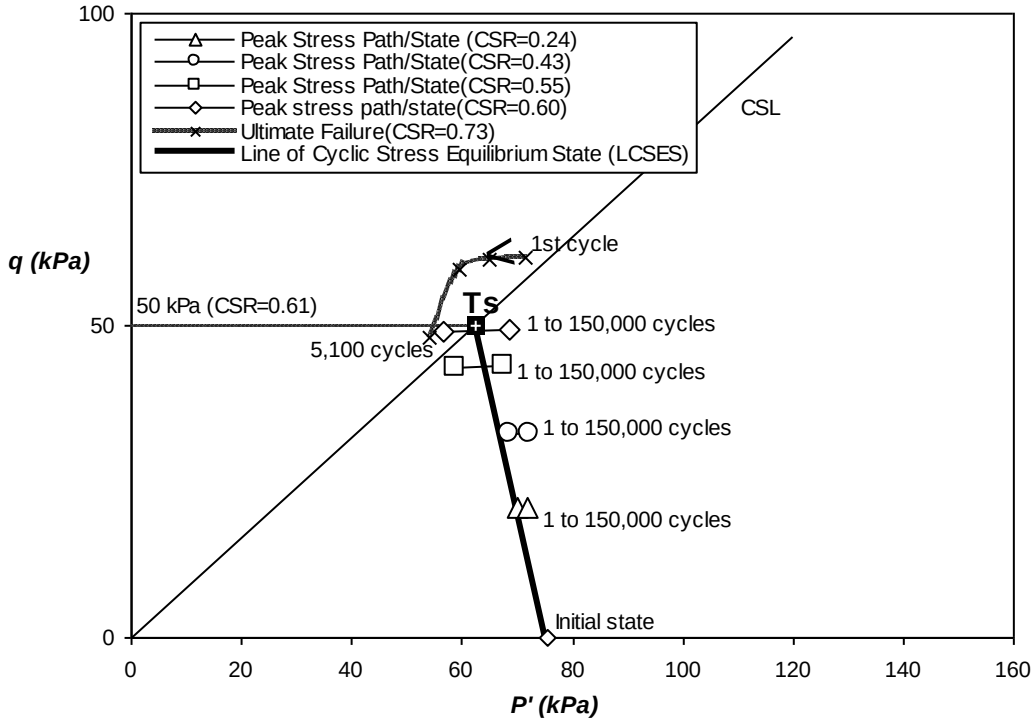

Figure 4-43 The initial state, the inherent peak stress equilibrium states and mid-point of peak stress paths are connected to form a straight line of cyclic stress equilibrium state. (OC4 series: consolidation = 75Pa, OCR = 4)

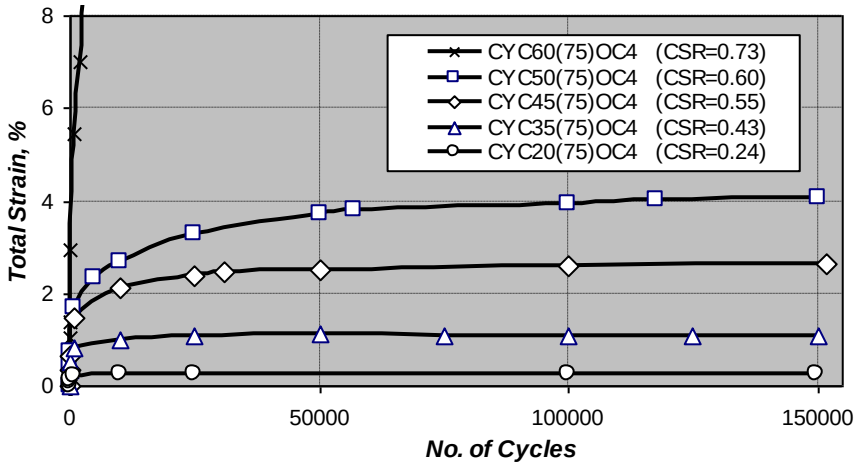

Figure 4-44 Development of peak total strain over each cycle (OC4 series)

For the over-consolidated OC4 series, the locus of the inherent peak stress states for tests specimen which led to resilient state can be connected to form the LCSES in a straight line pattern. Rising vertically at a slight inclination to the left, the terminated end of LCSES at which the level of deviator stress represents the threshold stress, appeared intercepting the critical state line (CSL) at a stress state coincides with the peak stress state of test CYC50(75)OC4 that had led to a resilient state. Therefore, in general, the maximum peak stress state (threshold stress) in the over-consolidated OC4 series existed at a stress obliquity ($\eta = q/p'$) on or slightly above that of the CSL, where the threshold stress can be identified near the intercept of the LCSES and the CSL.

4.4.6 Deformation Characteristic and Resilient Modulus

Figure 4-45 depicted the relationship of the stabilized total axial strain with respect to the level of deviator stress for the OC4 series. The constant-strain contours plot which derived from the monotonic test strain data was produced in Figure 4-46. The superimposition of the stabilized total strain of cyclic compression tests at their respective stress equilibrium state on the constant-strain contours showed an improved matching compared with the two previous series i.e. NC series and the

OC1.5 series. The correlation of stabilized total axial strain for cyclic compression tests and the static axial strain of monotonic compression test was further illustrated with respect to the stress obliquity in Figure 4-47. It can be seen that below 2% axial strain and for stress obliquity less than 0.7, the two curves approximately overlapped each other.

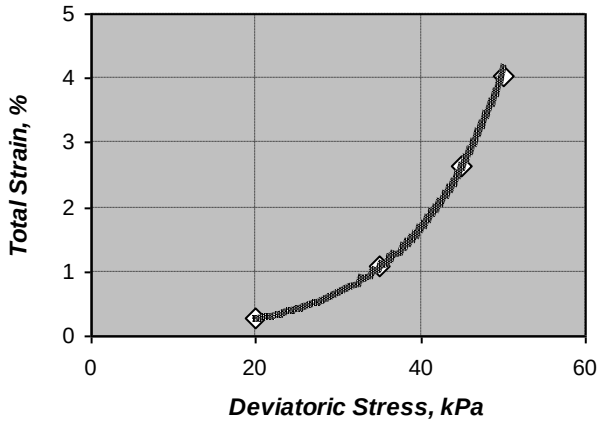

Figure 4-45 Variation of stabilized total strain with level of cyclic deviator stress (OC4 series: consolidation = 75kPa, OCR = 4)

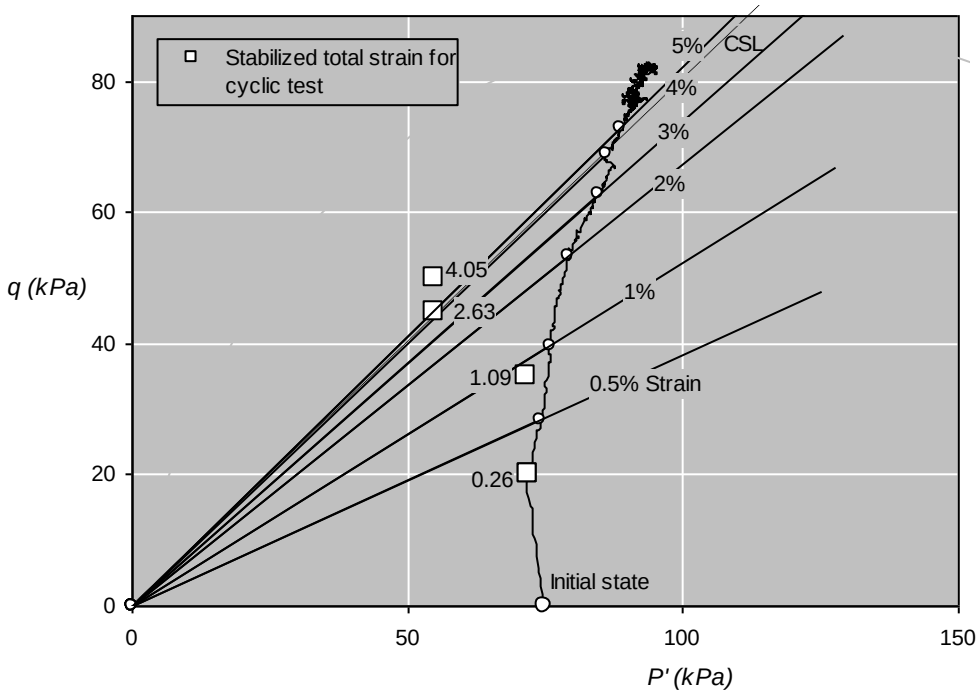

Figure 4-46 Constant-strain contours of test M75OC4 superimposed on the effective stress path (Kaolin clay, consolidated at 75kPa, OCR = 4)

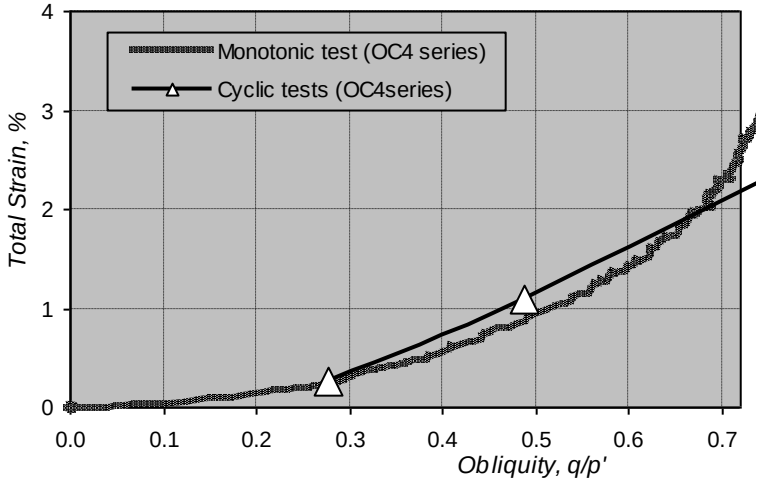

Figure 4-47 Variation of total strain (stabilized in cyclic tests) with stress obliquity (OC4 series)

As in test CYC40(200))C1.5 of OC 1.5 series, the elastic strain of tests specimen that achieved resilient state were constant throughout the test, as were implicit in the plot of elastic modulus verses number of loading cycles shown in Figure 4-48, where the elastic modulus was constant throughout the cyclic compression. Figure 4-49 showed that the resilient strain (which is the same as elastic strain for the OC4 series) under cyclic compression increased with respect to the level of cyclic deviator stress. The resilient strain and the stress obliquity of the peak stress state have a linear relationship as shown in Figure 4-50.

The variation (non-linear) of resilient modulus with respect to the level of cyclic deviator stress and the stress obliquity are shown in Figure 4-51 and Figure 4-52 respectively. Consistent with the NC series and OC1.5 series, higher cyclic deviator stress and higher stress obliquity of the peak stress state at equilibrium associate with lower resilient modulus.

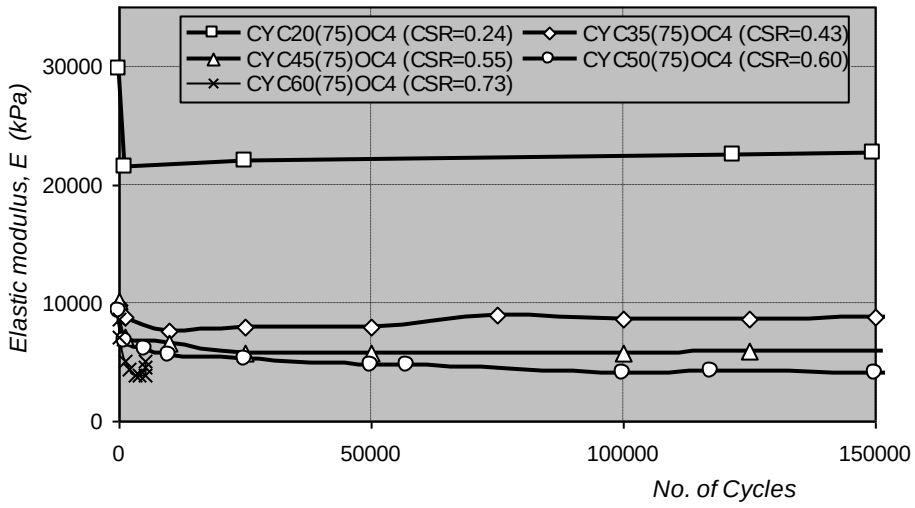

Figure 4-48 Variation of elastic modulus with number of cycles – OC4 series (kaolin clay, consolidated at 75 kPa, OCR = 4)

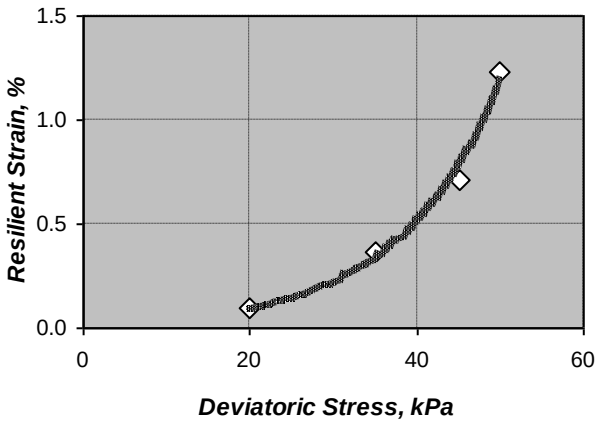

Figure 4-49 Variation of resilient strain with the level cyclic deviator stress (OC 4 series: consolidation = 75 kPa, OCR = 4)

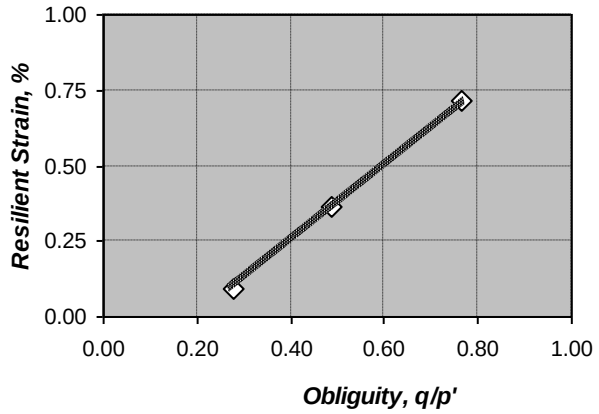

Figure 4-50 Variation of resilient strain with the stress obliquity at equilibrium (OC4 series)

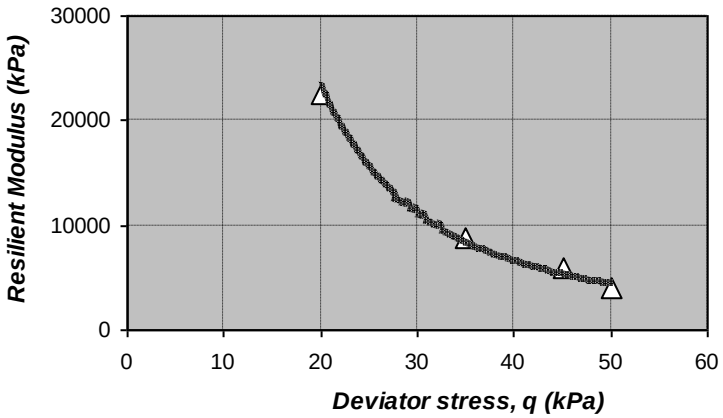

Figure 4-51 Variation of resilient modulus with level of cyclic deviator stress (OC4 series: consolidation = 75 kPa, OCR = 4)

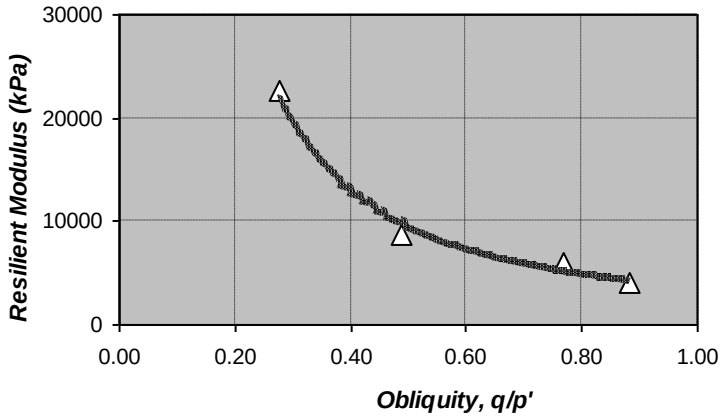

Figure 4-52 Variation of resilient modulus with stress obliquity at equilibrium (OC4 series)

4.5 *Over-Consolidated OC20 Series*

4.5.1 Introduction

Test specimens of the heavily over-consolidated OC20 series were initially given an isotropic normal-consolidation of 600 kPa (double that of all other tests series), before they were allowed to swell to an effective consolidation pressure of 30 kPa, giving an over consolidation ratio (OCR) of 20. Tests included in this series were:

M30 OC20	
CYC20(30)OC20	(CSR = 0.29)
CYC30(30)OC20	(CSR = 0.44)
CYC40(30)OC20	(CSR = 0.58)
CYC55(30)OC20	(CSR = 0.80)
CYC30(30)OC20step	

4.5.2 Monotonic Compression

The development of the deviator stress and the excess pore pressure with respect to the controlled axial strain for test M30OC20 is shown in Figure 4-53. Under slow constant axial strain, the deviator stress increased gently with the strain and reached the peak of 69 kPa at about 12 % strain, while the excess pore pressure increased to a small peak of 7 kPa at 1 % and gradually went all way down into negative region from 4 % strain onward. The excess pore pressure continued to decrease at reducing rate until it reached the maximum negative excess pore pressure of 21 kPa at 15 % strain and remained constant throughout. The specimen had a final moisture content of 36.8 %.

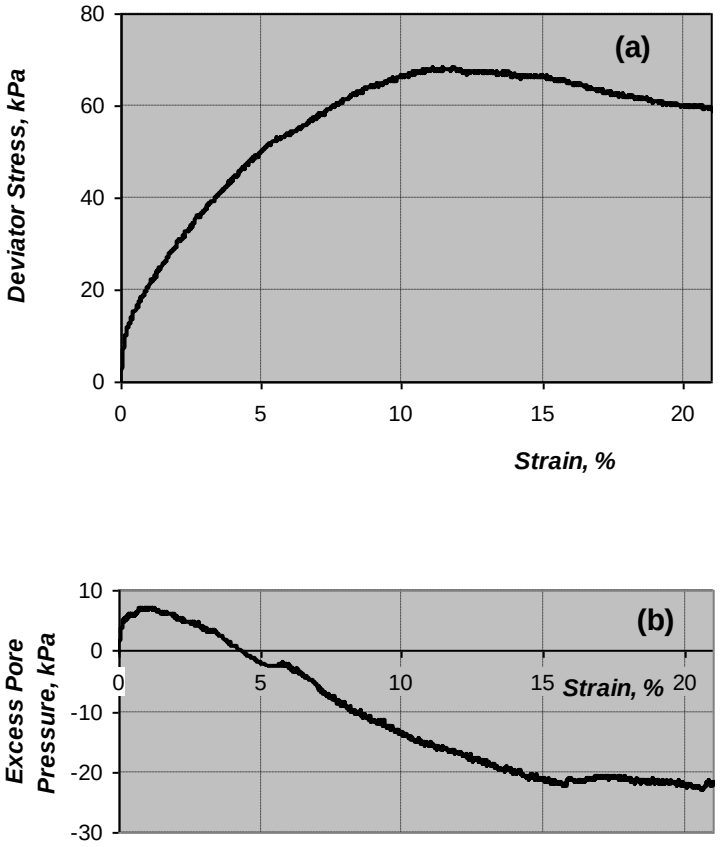

Figure 4-53 Result of the monotonic undrained compression (consolidation = 30 kPa, OCR = 20)

On the *p'- q* stress plane (Figure 4-54), the initial small and steep increase in excess pore water pressure caused the pattern of stress path to move vertically upward at the beginning until q = 10 kPa. However, the relatively larger decrease in excess pore pressure caused the stress path to then move right and upward as excess pore pressure continued decreasing. The stress path crossed the critical state line and eventually reached the maximum of 69 kPa before it moved straight down and rightward towards the critical state line as the specimen failed with large strain.

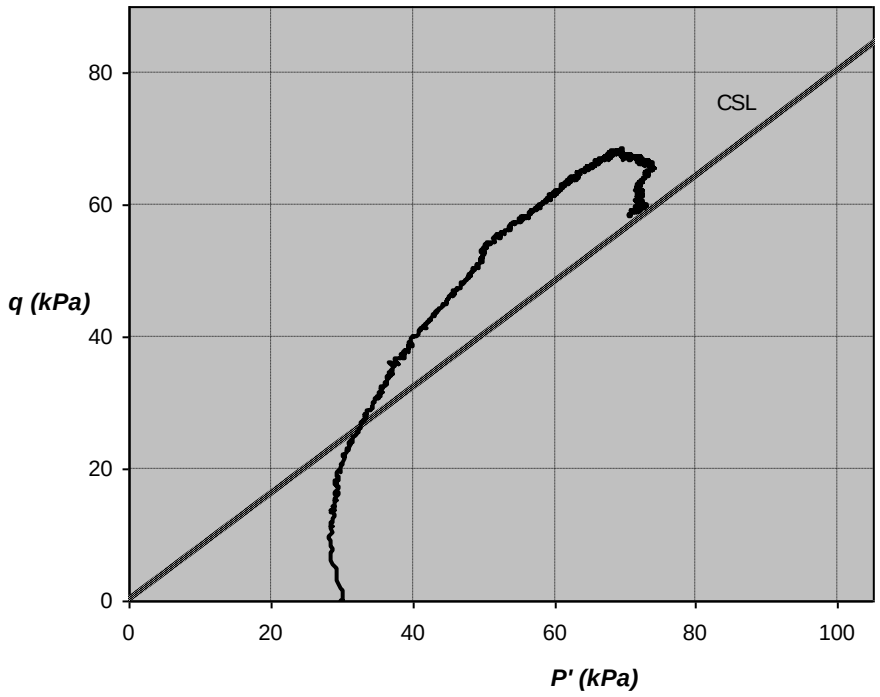

Figure 4-54 Stress path for monotonic undrained compression on saturated kaolin clay (consolidation = 30 kPa, OCR = 20)

4.5.3 Cyclic Compression

The cyclic stress responses for soil specimens of OC20 series generally resembled many aspects of the characteristic for the OC4 series. Test CYC30(30)OC20 was typical of the tests which arrived at the resilient state. Under cyclic compression, excess pore pressure surged immediately on the first cycle (Figure 4-55(a)) and remained constant throughout the entire test duration. At the same time, the total axial strain increased at a reducing rate with respect to the numbers of loading cycles (Figure 4-55(b)). It soon became stabilized in less than 50,000 cycles. The state of cyclic stress equilibrium in test CYC30(30)OC20 was inherent as soon as cyclic compression began, and it exhibited a rather stable state of stress equilibrium as cyclic stress path formed close hysteresis (Figure 4-55(c)). In OC20 series, test with

higher cyclic deviator stress at 40 kPa (test CYC40(30)OC20) also arrived at the resilient state and, together with test CYC30(30)OC20), had the peak stress state (inherent) exists above the critical state line (CSL) with the stress obliquity larger than the gradient of CSL.

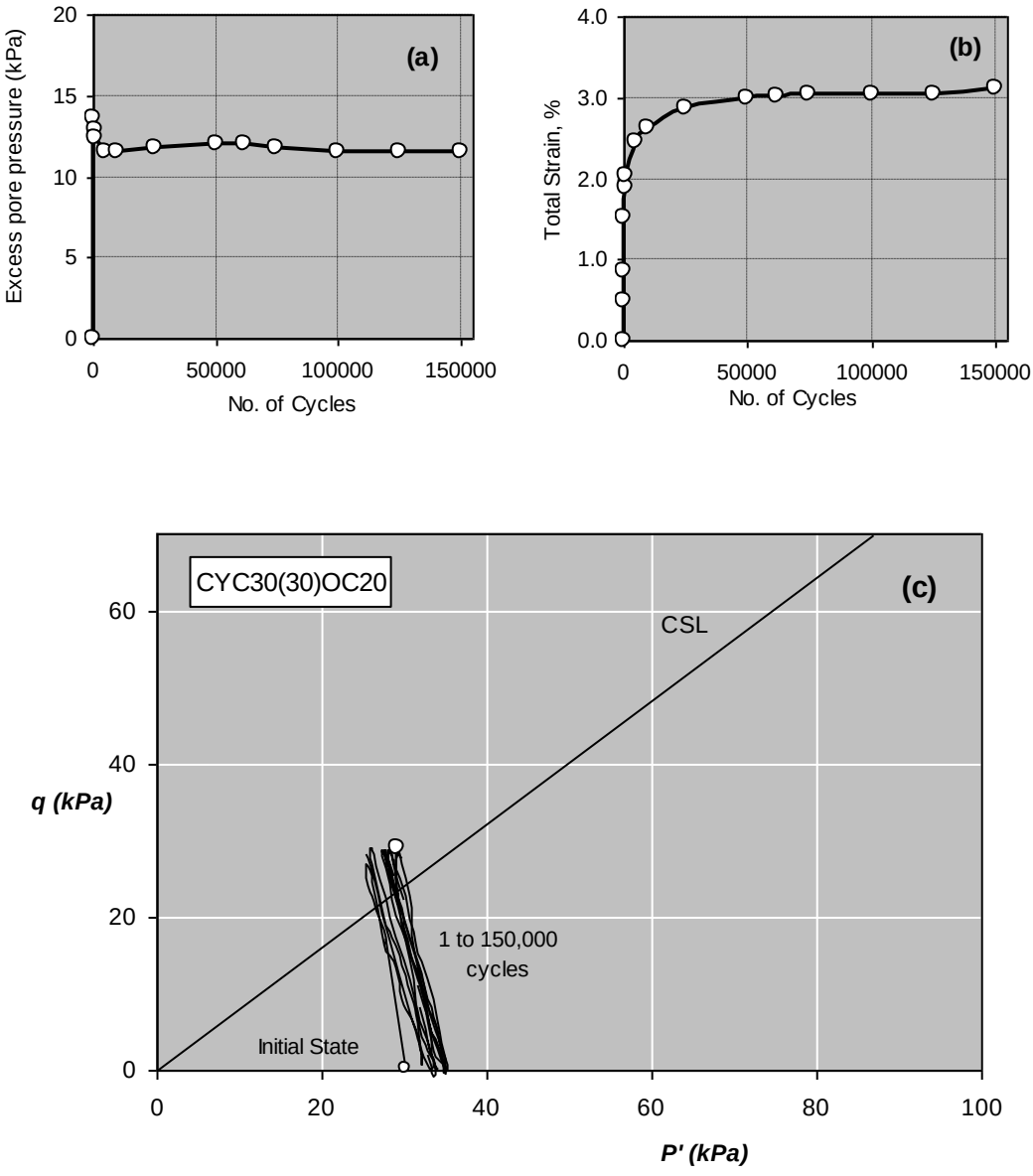

Figure 4-55 Results of cyclic undrained compression test on kaolinite clay that led to a resilient state (OC20 series: consolidation = 30 kPa, OCR = 20, cyclic deviator stress = 30 kPa and CSR = 0.44)

For the ultimate failure test CYC55(30)OC20 (Figure 4-56) when the specimen was given a cyclic deviator stress of 55 kPa (cyclic stress ratio CSR = 0.80), excess pore water surged up immediately and decreased progressively to about 16 kPa at 100th cycle. The total strain increased sharply and briefly stayed at a reducing rate for 10 cycles. It then maintained at the same rate of increment for the next 30 cycles to 10 % strain before it built up at increasing rate and led to ultimate failure with large strain. The peak stress state of 1st cycle began above the critical state line (Figure 4-56 (c)) and the peak stress path appeared to migrate vertically downward.

4.5.4 Step-Cyclic Compression Test

As a means to locate the maximum level of cyclic deviator stress that divide non-failure and failure tests (threshold stress) in confirmation of tests CYC4)(30)OC20, step compression test CYC30(30)OC20step was carried out with the initial cyclic deviator stress of 30 kPa which was stepped up to 40 kPa. The development of the total axial strain with respect to the number of loading cycles was shown in Figure 4-57. Test began with an initial cyclic deviator stress of 30 kPa had attained a stabilized axial strain of 3 % as earlier as at 50,000th cycle. The subsequent step-test with the deviator stress of 40 kPa however developed additional 10 % strain after a further 120,000 cycles and appeared to be increasing further when decision was made to terminate the test. Based on this observed axial strain development, the level of deviator stress for the earlier test CYC40(30)OC20 which had attained stabilized state, was taken to be the threshold stress for the heavily over-consolidated OC20 series clay soil.

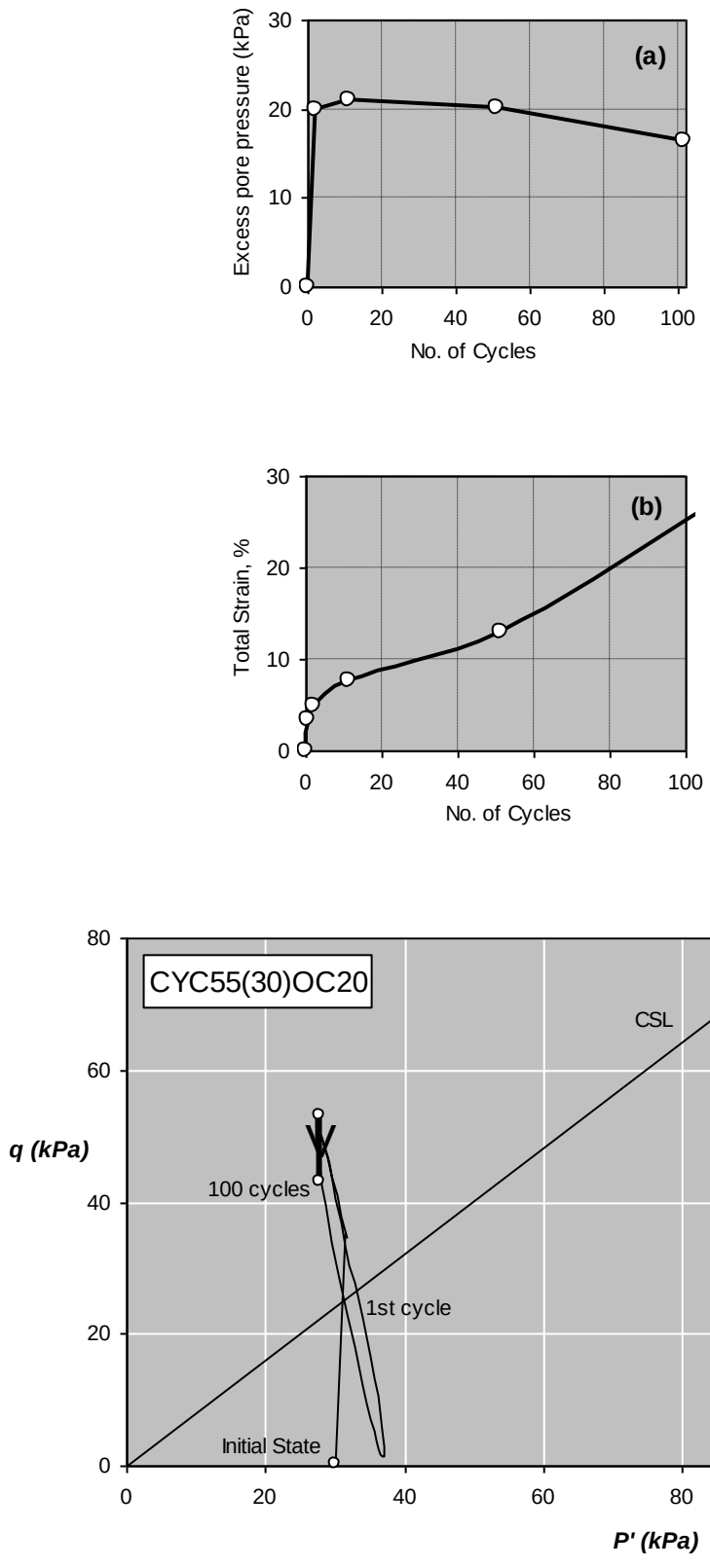

Figure 4-56 Results of a cyclic undrained compression test on kaolinite clay that led to ultimate failure (consolidation = 30 kPa, OCR = 20, with cyclic deviator stress = 55 kPa , CSR = 0.8)

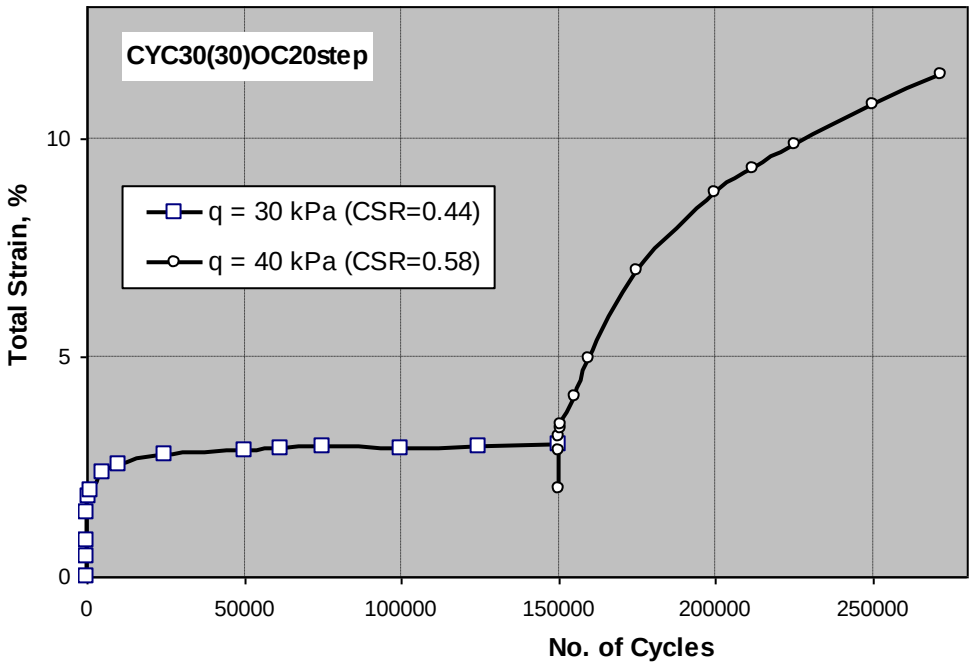

Figure 4-57 Development of total strain for the step compression test

4.5.5 Cyclic Stress Equilibrium, Resilient State and the Threshold Stress

Under cyclic compression, the inherent state of cyclic stress equilibrium in the heavily over-consolidated OC20 series means that the locus of all possible peak stress states forms the LCSES in a straight line (Figure 4-58). Rising vertically at a slight inclination to the left, the LCSES crossed the critical state line, but terminated at a specific (maximum possible) peak stress state at which the level of deviator stress represents the threshold stress. The specific peak stress state (threshold stress) can only be ascertained by obtaining the maximum possible deviator stress that would arrive at a stabilized total strain. Determined from the highest cyclic deviator stress obtained from the non-failure tests, and the further confirmation by the step-cyclic compression test as described in above paragraph 4.5.3, the cyclic deviator stress of 40 kPa (CSR = 0.58) from test CYC40(30)OC20 that produced a stabilized

total strain of 9.57 %, was taken to be the best estimate of threshold stress for the OC20 series.

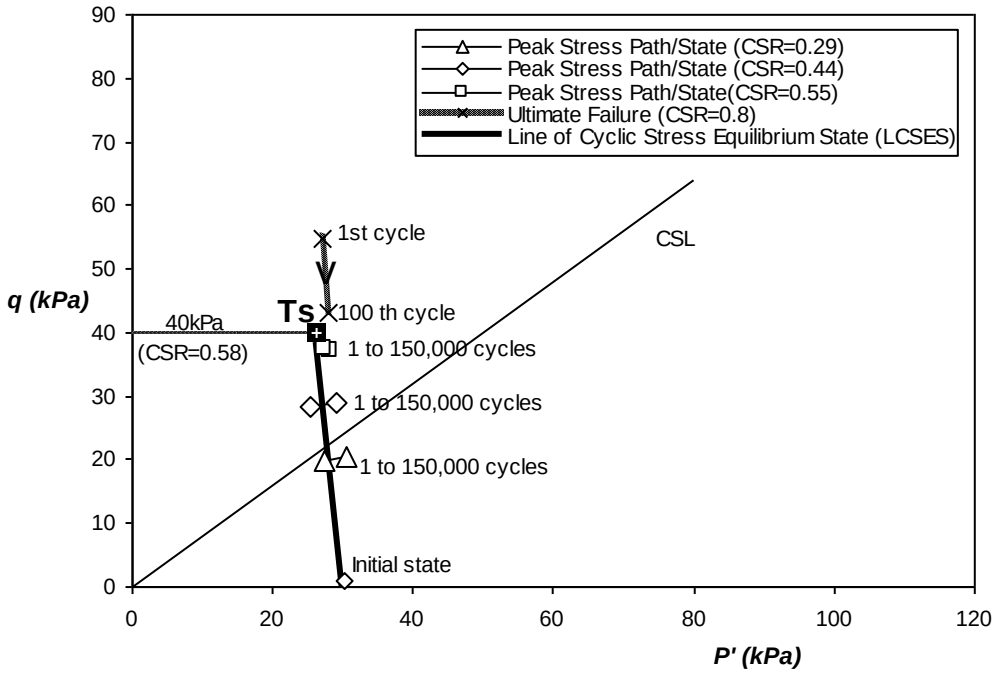

Figure 4-58 The initial state and the inherent peak stress equilibrium states are connected to form a straight line of cyclic stress equilibrium state. (OC20 series: consolidation = 30 kPa, OCR = 20)

4.5.6 Deformation Characteristic and Resilient Modulus

Figure 4-59 described the development of the total axial strain with respect to the number of load cycles for the OC20 series. There appeared to be a non-linear relationship between the stabilized total axial strain and the level of deviator stress as shown in Figure 4-60. The constant-strain contours of the static axial strain from the

monotonic compression test was able to represent the data points of the stabilized total axial strain when both were superimposed on a p'–q plot as shown in Figure 4-61. The relationship when re-interpreted in Figure 4-62 described the amount of stabilized total axial strain and the static axial strain with respect to stress obliquity. It can be observed that up to 3 % strain and with the stress obliquity less than 1, the plot showed good resemblance between the cyclic stabilized total axial strain and the static axial strain, with respect to the stress obliquity.

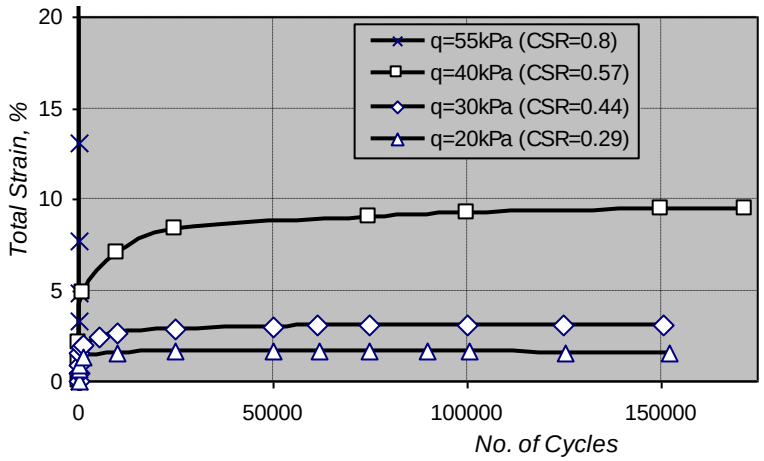

Figure 4-59 Development of peak total strain over each cycle (OC20 series)

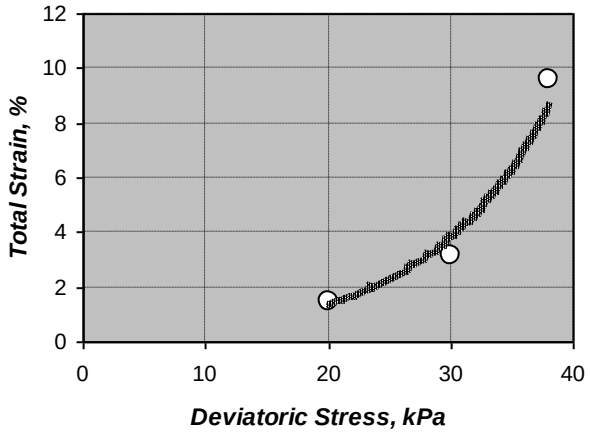

Figure 4-60 Variation of stabilized total strain with level of cyclic deviator stress (OC20 series: consolidation = 30 kPa, OCR = 20)

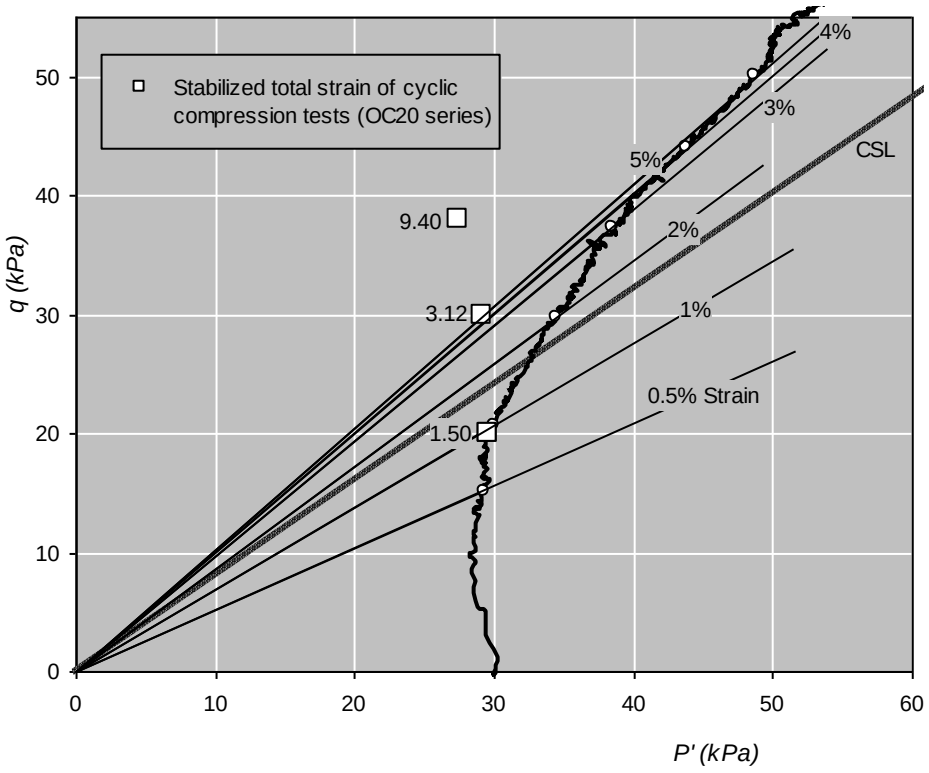

Figure 4-61 Constant-strain contours of test M30OC20 superimposed on the effective stress path (Kaolin clay, consolidated at 30 kPa, OCR = 20)

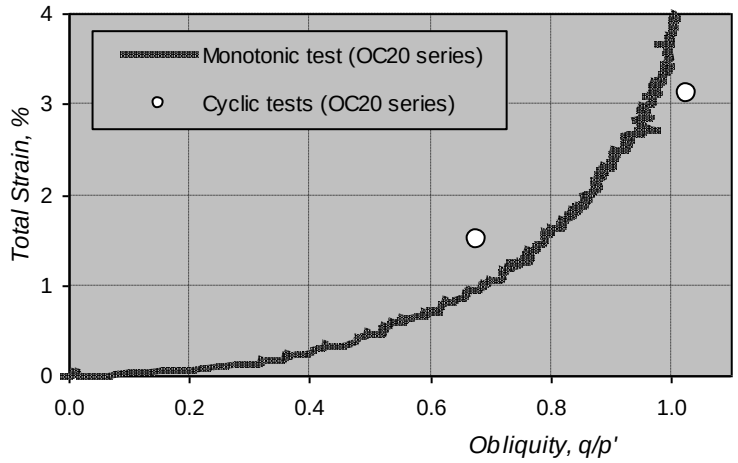

Figure 4-62 Variation of total strain (stabilized in cyclic tests) with stress obliquity (OC20 series)

Similar to OC4 series and as reflected in Figure 4-63 showing the elastic modulus verses the number of loading cycles, the elastic strain in the tests specimen of OC20 series was observed to be constant throughout the test. Figure 4-64 and Figure 4-65 showed the relationship of resilient strain with the level of deviator stress and stress obliquity respectively. The magnitude of resilient strain was noted to be increasing with the level of deviator stress and the stress obliquity of the inherently stabilized peak stress state.

The variation of resilient modulus with the level of cyclic deviator stress and the stress obliquity at equilibrium were shown in Figure 4-66 and Figure 4-67 respectively. As in all the earlier series, higher cyclic deviator stress or stress obliquity resulted in lower resilient modulus, except that for stress obliquity above the gradient of critical state line (i.e. $\eta >$ M), resilient modulus appeared to become constant (also refer to Figure 4-63).

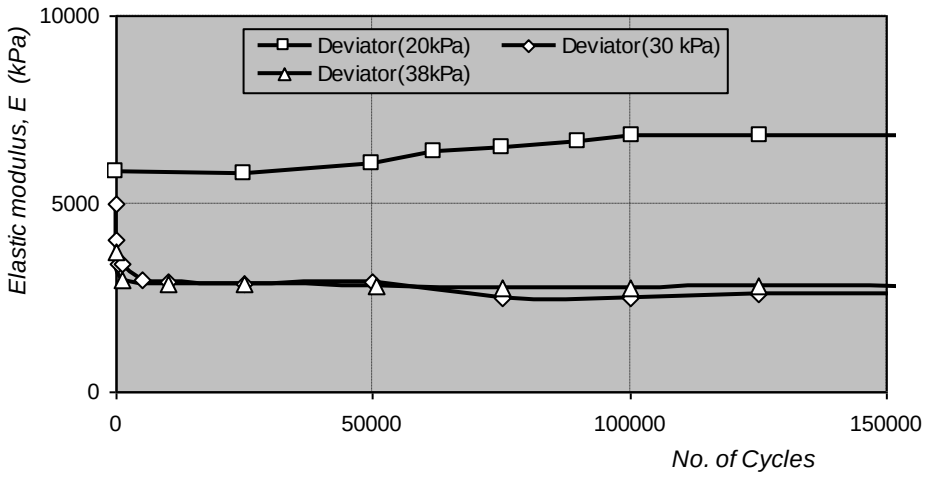

Figure 4-63 Variation of elastic modulus with number of cycles – OC20 series (kaolin clay, consolidated at 30 kPa, OCR = 20)

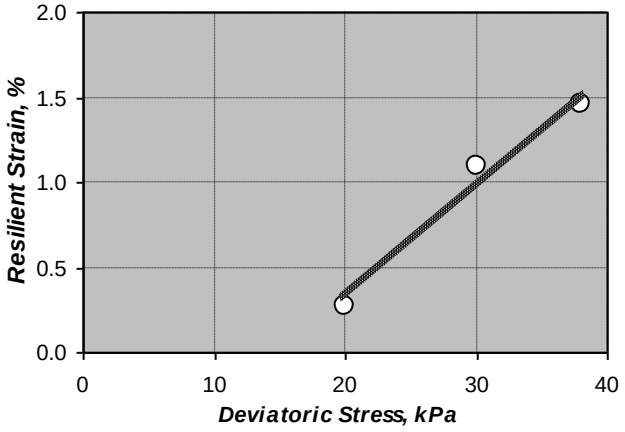

Figure 4-64 Variation of resilient strain with the level cyclic deviator stress (OC 20 series: consolidation = 30 kPa, OCR = 20)

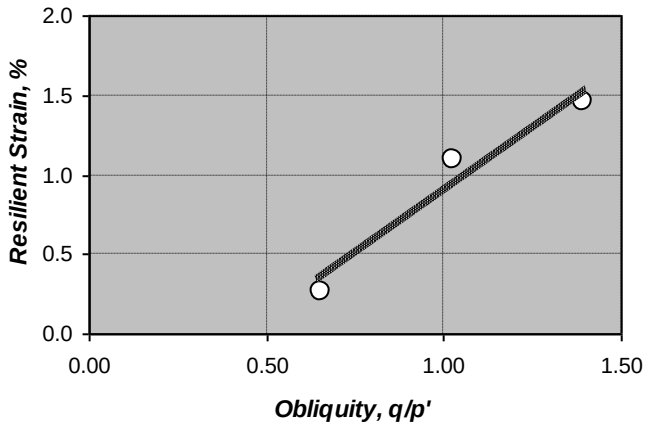

Figure 4-65 Variation of resilient strain with the stress obliquity at equilibrium (OC 20 series)

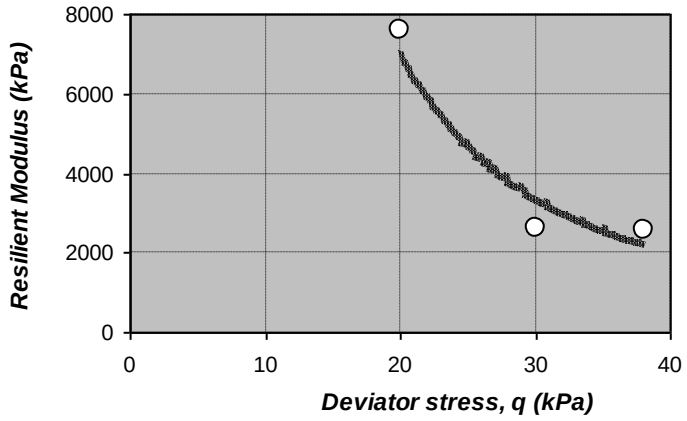

Figure 4-66 Variation of resilient modulus with level of cyclic deviator stress (OC20 series: consolidation = 30 kPa, OCR = 20)

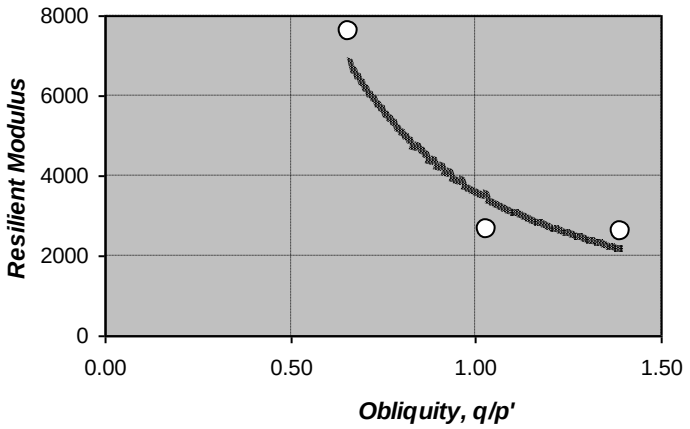

Figure 4-67 Variation of resilient modulus with stress obliquity at equilibrium (OC20 series)

Chapter 5 Discussion of the Results

5.1 *Introduction*

The presentation of the experimental results in the previous chapter has been discussed and elaborated in details particularly for those aspects which were relevant in the design of railway track foundation with clay subgrade and that required for continued development of the presentation. It has so far been limited to the general and specific behaviour related to any one of the tests series. In this chapter, attempt was made to synthesize the characteristics and behaviour of clay under undrained compression across all of the tests series of wide-ranging degree of over-consolidation that will be coherently presented and discussed.

5.2 *Validity of Effective Stress Analysis for Cyclic Loading*

Use of effective stress analysis for undrained loading of repeated or cyclic nature on saturated clay had been for those with very slow cyclic loading rate (or frequency), where the excess pore water pressure was allowed sufficient time to become equalized within the specimen (Sangrey 1969; Sangrey 1978) before its measurement can be meaningfully taken. In this study, fast cyclic loading rate of 1Hz and in excess was applied to the clay specimen to simulate the stress characteristics near the subgrade surface caused by the moving train wheels. Use of effective stress analysis, in this case, will be appropriate if the equilibrium state of stress, rather than the transient state of presiding loading cycles, is of prime interest (Seed and Martin 1966). In view of this, the effective stress plots (including the measured excess pore water pressure) presented so far in the previous chapter that described the cyclic responses prior to achieving the cyclic stress equilibrium state or the resilient state, were by and large a qualitative description and an indication of the state of stress the

specimen may be experienced. Upon arriving or at the stress equilibrium and resilient state when the measured excess pore water pressure reflects the equalized pore water pressure within the soil specimen, the state of stress (p', q) then represents the actual and true value of the stress exists, both qualitatively and quantitatively.

5.3 *Relevance to Design of Railway Track Foundation Subgrade*

A typical saturated kaolinite clay specimen under undrained compression (as in test CYC100(300)OC1 described in paragraph 4.2.4) with cyclic deviator stress slightly above its threshold stress i.e. 10 % higher, and at a loading rate of 1 Hz, can build up its full excess pore water pressure within an hour that lead to ultimate failure with large strain. In the real case, clay subgrade though normally exist in partial saturation state can become highly saturated in wet weather / season. The dissipation of the excess pore water pressure built up in the subgrade will likely be a slow process compared to the test specimen, due to the relatively thicker strata with consequent longer drainage path. Therefore, characterization of subgrade strength on assumption of full saturation and "undrained" condition under cyclic compression can be justified. Such assumption generates stabilized threshold stress of the lower-bound, when possible densification (for the normal to lightly over-consolidated soil) is discarded and negative excess pore water pressure (for the heavily over-consolidated soil) would have been unsustainable (for reason(s) as described in the following paragraph 5.4). Therefore, it represents the most vulnerable and possible condition for the fine-grained subgrade in general. For railway tracks on the lowland or in the wet-climate region, the assumptions made are in fact the reality.

Notwithstanding that the subgrade of fine-grained soil may originally exists in a naturally undisturbed consolidated state or compacted state, it is commonly given a standard in-situ compaction. The compaction of subgrade soil literally alter the stress history of soil exists prior to the compaction in the same way that cyclic loading causes over-consolidation of an otherwise normally-consolidated clay (Lefebvre

1986). In this regards, the tests were deliberately designed with parametric reference to wide-ranging stress history i.e. over-consolidation ratio, in order to provide the fundamental understanding for the behaviour of a clay subgrade in general. The new stress history i.e. over-consolidation ratio or maximum past consolidation stress, can be estimated on assumption of a near isotropic consolidation taken place as a result of compaction process.

5.4 *General Stress and Strain Responses under Undrained Cyclic Compression*

For saturated clay under undrained cyclic compression, depending on the consolidated state (p_i', p_o') and the level of cyclic deviator stress (σ_{dev}), the stress and strain response of soil followed certain behaviour pattern. Generally, as the deviator stress (compression) cycled at a particular loading shape, i.e. sinusoidal, with respect to time duration, so were the excess pore water pressure and the total axial strain; both of which appeared to be cycled at the same phase as the cyclic deviator stress.

For normally-consolidated clay, the excess pore water pressure and the total axial strain develop at a reducing rate as loading cycles continue. Depending on the level of deviator stress, the specimen with a deviator stress higher than its threshold stress (q_t) continues the accumulation of the excess pore water pressure and the total axial strain, until the specimen ultimately failed with large strain. Whereas the specimen with a deviator stress lower than the threshold stress (q_t), has the excess pore water pressure and the total strain gradually become stabilized and remained constant after a certain number of loading cycles. The arrival of stress equilibrium state signals the arrival of resilient state of soil during which both the excess pore water pressure and the axial strain (resilient strain) varies and cycles about a fixed reference within a constant amplitude. For lightly over-consolidated clay, similar behaviour pattern applies, except for cyclic deviator stress below a specific level lower than the threshold stress (q_t), excess pore water pressure oscillates and varies within a

constant level without accumulation of excess pore water pressure taking place, as the total axial strain soon become stabilized after a relatively shorter number of cycles.

For over-consolidated clay (i.e. OCR = 20), excess pore water pressure oscillates within a constant level as soon as the cyclic compression begins. The state of stress equilibrium is inherent for the heavily over-consolidated clay under cyclic compression. No accumulation of excess pore water pressure but the total axial strain takes place. Test specimen with cyclic deviator stress higher than its threshold stress showed little sign of the excess pore water pressure accumulation or regression, with total axial strain increases initially at a reducing rate with respect to the number of cycles. The rate of strain increment then briefly becomes constant before it increases as the specimen fails with large strain (Figure 4-56). The measured excess pore water pressure was unlike that of the monotonic undrained compression (as shown in Figure 4-53) in which negative excess pore water pressure (or suction) developed long before peak stress is reached. Under successive application of undrained compression at fast loading rate, the dilative tendency permits constant rearrangement of clay particles such that any transient negative excess pore water pressure within the specimen soon diminishes, rendering the capacity to withstand compression unsustainable and soil fails with large deformation. In the case when the cyclic deviator stress is lower than the threshold stress (q_t), the total axial strain increases initially and become stabilized after certain number of cycles, signalling the arrival of the resilient state.

Upon the stabilization of total axial strain and resilient state, clay specimen of all consolidated series behaves elastically in terms of the strain response and the variation in its excess pore water pressure within the specimen. At resilient state, the total axial strain ceased to increase and it consists of the permanent strain which has remained constant and the elastic strain which oscillates within constant amplitude in the cycle. The excess pore water pressure also oscillates within constant amplitude which is a proportion of the level of deviator stress, with no accumulation. The proportion is normally closed to one-third of the deviator stress if the specimen was truly isotropic. However, in the cyclic compression tests series that were conducted, the proportion of the oscillating excess pore water pressure to the level deviator

stress were found to be in the range between 1/3 (for normal-consolidated soil) to ½ (for over-consolidated OC20 series. The reason is likely due to the anisotropic effect of the way soil sample were prepared and consolidated. With the clay sample prepared from one-dimensional slurry consolidation and the subsequent consolidation / swelling of soil specimen, both of which using top and bottom drainage, soil specimen will be more compressible in the axial direction, thereby causing a higher proportion of excess pore water pressure in excess of 1/3.

5.5 *State of Cyclic Stress Equilibrium and the Resilient State*

The stationary end of peak stress path / state for tests which did not fail after a large number loading cycles, i.e. up to150,000 cycles were used to define the line of cyclic stress equilibrium state (LCSES) for the tests series of various over-consolidation ratio. It is important to note that the arrival at the stress equilibrium state implies also the resilient state for normally-consolidated clay and generally for lightly over-consolidated clay when deviator stress is above a specific level. But in the case of heavily over-consolidated clay, the state of stress equilibrium is inherent under cyclic compression, as the total axial strain accumulates prior to become stabilized in a relatively early stage of cyclic loading.

In the same p'–q plot, the LCSES for the four series of tests were shown in Figure 5-1. Each of the four LCSES appeared to be unique to the consolidated state and stress history of the soil specimen had undergone. For the normally-consolidated clay, the LCSES is a gentle curve bending towards the left and intercepts the critical state line (CSL) at which the threshold stress can be identified. The LCSES for the lightly over-consolidated clay (up to OCR = 4) is a dual-gradient line, with the first line rising vertically from where the initial consolidation state (p_i') is until it reaches a specific state of stress (p', q), followed by a gentle curve bending towards the left and intercepts the CSL to locate the threshold stress. The over-consolidated OC4 series (OCR = 4), with its state of stress exists near the wet / dry divisional line of the

CSL (i.e. wet / dry division occurs approximately when OCR = 2.718 (Schofield and Wroth 1968)), has the LCSES which is a straight line rising near vertically towards the CSL, where the threshold stress can be identified near the intercept. For heavily over-consolidated OC20 series, the LCSES rises near vertically beyond CSL, where the terminated end of the LCSES locates the level of threshold stress. The threshold stress for the heavily over-consolidated soil, i.e. OC20 series (may include also the medium over-consolidated soil, i.e. OC4 series) will be best identified using total strain stabilization criteria to determine the highest deviator stress possible that will attain stabilized total strain. This can be accomplished by carrying out additional tests at level between the highest cyclic deviator stress which has achieved strain stabilization and that which has failed with high deformation.

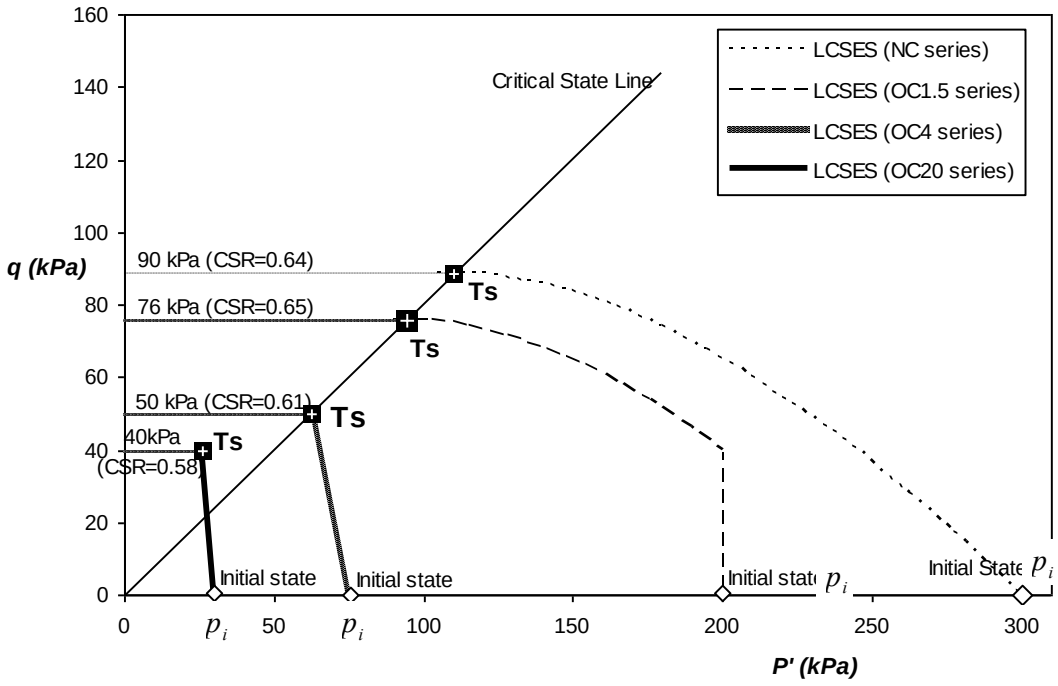

Figure 5-1 Line of cyclic stress equilibrium state for all test series of various consolidated state and stress history

In Figure 5-1, higher initial consolidation state (p_i') though appeared to have higher threshold stress (q_t) at point "Ts", it need not necessarily be the case in general as the level of threshold stress is also influenced by the past maximum pre-consolidation pressure (p_o'). A better illustration can be made using the normalized plot. Normalized with the past maximum pre-consolidation pressure (p_o'), Figure 5-2 showed that the higher the over-consolidation ratio (the inverse of p_i'/p_o'), the lower the normalized threshold stress (q_t/p_o') will be. In terms of the cyclic stress ratio (CSR) of threshold stress (Figure 5-3), specimen with higher over-consolidation ratio (i.e. OC20 series) appeared to have the threshold stress with lower CSR (i.e. CSR = 0.58 as compared to 0.64 for NC series).

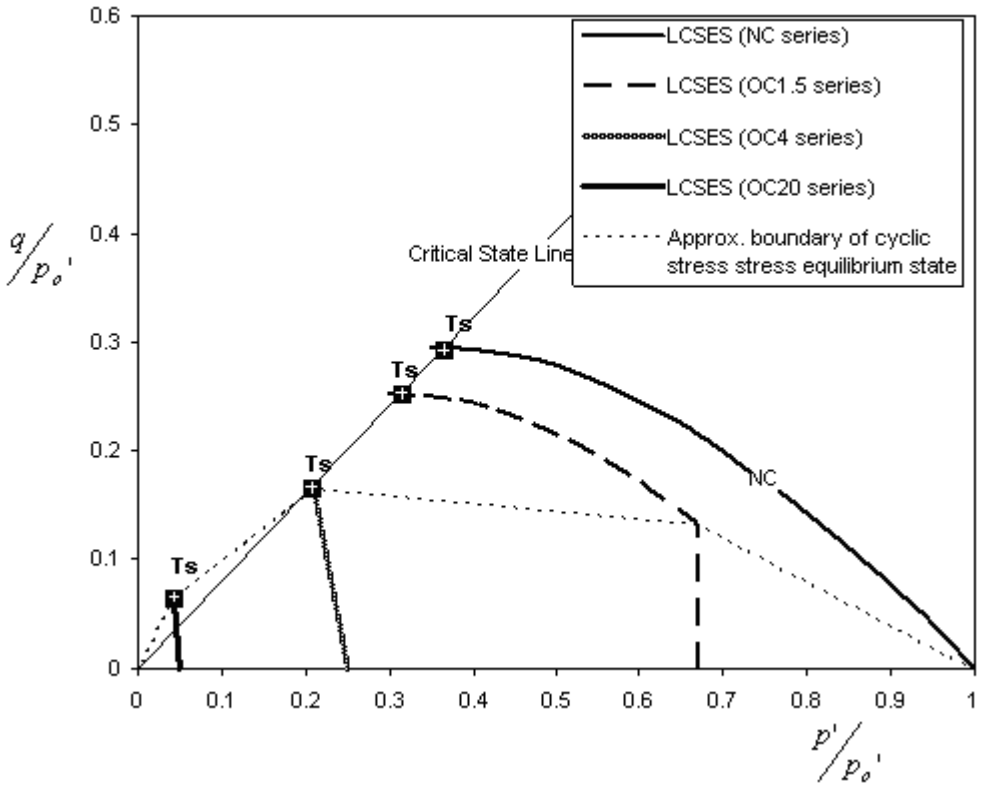

Figure 5-2 Normalized plot of line of cyclic stress equilibrium state for all test series

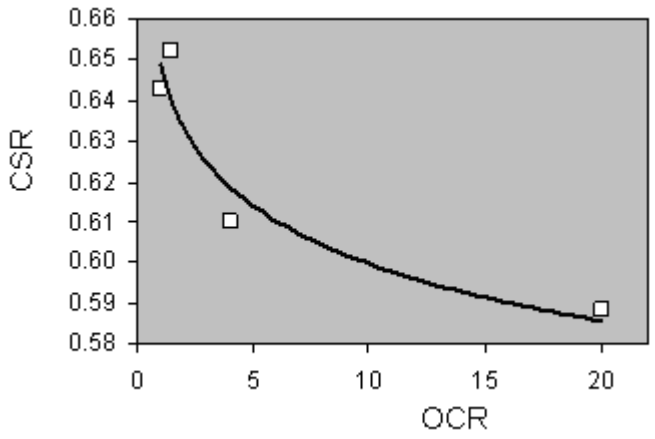

Figure 5-3 The cyclic stress ratio of threshold stress with respect to over-consolidation ratio (kaolinite clay)

5.6 *Compressibility and Resilient behaviour*

5.6.1 General Expression for Axial Deformation

The total axial strain (ε_a) of test specimen which achieved stabilization can be seen to relate to stress obliquity ($\eta = q/p'$) for each test series differently, as shown in Figure 5-4. The relationships in general may be expressed in the following form:

$$\varepsilon_a = A\left(q/p'\right)^{B}_{equiv.} \qquad \% \qquad (5\text{-}1)$$

where $\left(q/p'\right)_{equiv.}$ is the effective stress obliquity at the state of stress

equilibrium and the resilient state. *A*, *B* are the constants from the regression analysis of the tests results.

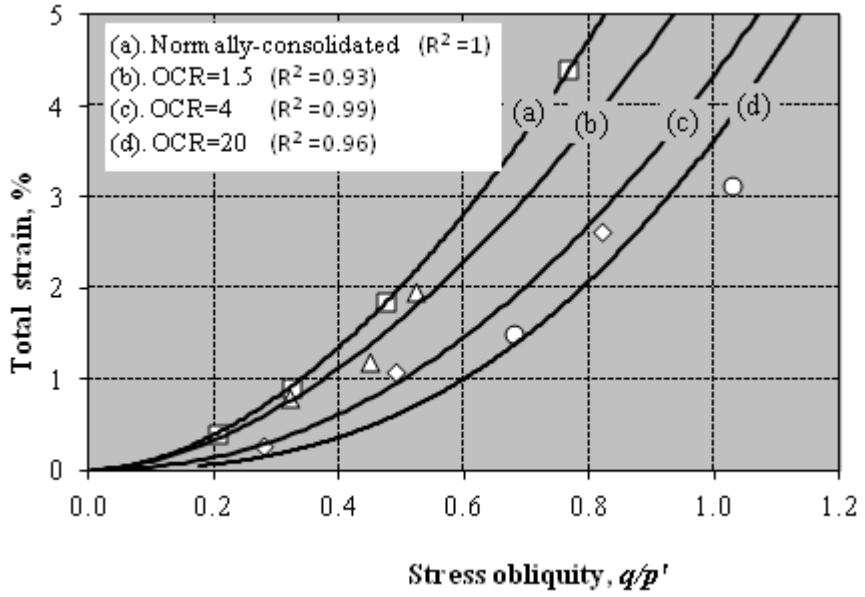

Figure 5-4 The relationship of total axial strain with respect to effective stress obliquity at stress equilibrium state for various test series (kaolin clay)

The experimental models obtained for the respective tests series (in Figure 5-4) are given as follows:

$$\varepsilon_a = 7.11\left(q/p'\right)^{1.81} \quad \%$$

(for normally-consolidated series, with $R^2 = 1$);

$$\varepsilon_a = 5.65\left(q/p'\right)^{1.77} \quad \%$$

(for OC1.5 series, with $R^2 = 0.93$);

$$\varepsilon_a = 4.34\left(q/p'\right)^{2.13} \quad \%$$

(for OC4 series, with $R^2 = 0.99$); and

$$\varepsilon_a = 3.64\left(q/p'\right)^{2.52} \quad \%$$

(for OC20 series, with $R^2 = 0.96$)

The stabilized total axial strain for the kaolin clay tested appeared to be dependant not only on its effective stress obliquity; it is also dependent on its stress history in terms of over-consolidation ratio.

5.6.2 Characteristic and Determination of Axial Strain

It is generally known that, the linear relationship between axial strain and stress obliquity exists for the normally-consolidated clays (such as the remoulded Boston blue clay) of the various consolidated states under monotonic undrained compression (Lambe and Whitman 1969). When a set of constant strain contours radiating from the origin is drawn (such as in Figure 4-10, Figure 4-30, Figure 4-46 and Figure 4-61), it will be good for soil of the same over-consolidation ratio under monotonic compression, irregardless of pre-consolidation pressure within a fair range. However, the derived relationship for each monotonic compression may not directly represent the relationship between stabilized total strain and stress obliquity for cyclic compression of the same consolidated series; notwithstanding that for soil of heavily over-consolidated state and, at the low stress obliquity of normally-consolidated and lightly over-consolidated state, the two sets of relationship appeared to be in close resemblance (Figure 4-9, Figure 4-31, Figure 4-47 and Figure 4-62).

In the case of normally-consolidated soil, under monotonic compression (Figure 4-2), the stress path moves on the surface of stress state boundary surface (SSBS) of the "p'–q'–v" space. Normalization with the pre-consolidation pressure ($p_o' = p_i'$ in

this case) produced a constant-strain plot where each of the constant-strain contours previously described in Figure 4-10 will appear as a chain of strain-dots (Figure 5-5). However, under cyclic undrained compression, the peak stress path moves into and within stress state boundary surface (SSBS) (as shown in Figure 4-24), rather than on surface of SSBS as in monotonic loading (Smith 2006). When normalized with the pre-consolidation pressure (p_o'), the stagnated end of the peak stress path (upon attaining the equilibrium state) is nowhere coincides with the same strain-dot as that of the monotonic compression. Constant-strain contours or Normalized strain-dots of different characteristic pattern from the monotonic compression (as in Figure 4-10 and Figure 5-5) can therefore be expected for the normally-consolidated clay (including the lightly over-consolidated clay) under cyclic compression.

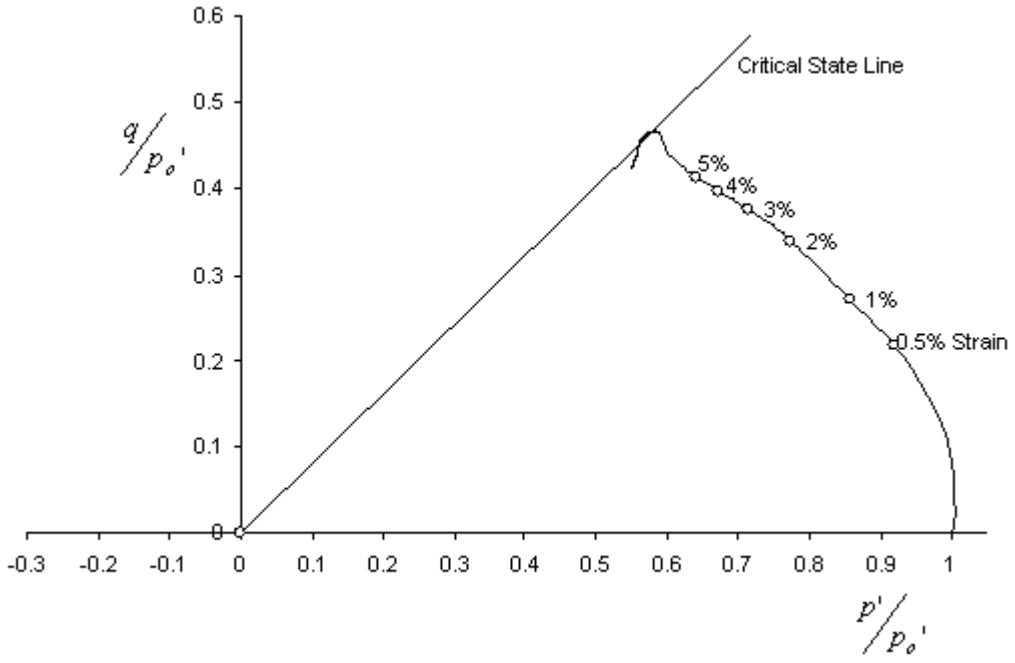

Figure 5-5 Normalized plot showing the constant-strain contours appear as strain-dots for the normally-consolidated kaolin clay under monotonic compression

Attempt was made to devise a means that enable the determination of stabilized total axial strain of cyclic compression (or the total axial strain during cyclic compression) without necessarily carrying out the lengthy cyclic loading tests. In order to produce a normalized constant-strain contours plot that is applicable to clay soil (kaolinite clay) of all stress history under cyclic compression, a graphical representation of the correlation between the stabilized total axial strain and the state of stress at equilibrium for clay soil of various consolidated states (within a fair range) is plausible. Based on the characteristics and the relationship between the static axial strain of monotonic compression and the stabilized total axial strain of cyclic compression described before, it can be postulated that:

a) For soil that is normally-consolidated to lightly over-consolidated, the straight lines which connect the strain-dots of the normally-consolidated NC series clay under monotonic compression to the strain-dots of an over-consolidated series exists near the wet /dry divide (i.e. OC4 series was selected in this case) on a normalized $p'-q$ plot, provides the constant-strain contours for cyclic compression from which the stabilized total axial strain of cyclic compression (or the total axial strain during cyclic compression in general)) can be determined knowing the peak stress state at equilibrium.

b) For the heavily over-consolidated soil, the constant-strain contours for cyclic compression radiates from the origin of the normalized plot, to connect to the constant strain contour at the wet/ dry divide (strain-dots of the over-consolidated series OC4).

In addition, it was postulated that the pattern and configuration of constant-strain contours plot for the resilient strain may resembles that of the stabilized total strain contours.

From the above postulations, strain data of the monotonic test from the normally-consolidated NC series (Figure 5-5) and additional set of strain data from the over-

consolidated OC4 series (Figure 4-46) where the stress path routed completely within the stress state boundary surface (SSBS) were used. A partial plot of the constant-strain contours for cyclic compression (NC to OC4 series soil) which takes into consideration of the different strain characteristic for stress state within the SSBS can be produced. Figure 5-6 showed a normalized plot of the constant-strain contours for total axial strain, where the straight-line contours appeared to have radiated from an arbitrary point to the left of the zero. For all of the tests which led to state of stress equilibrium in the NC series and OC1.5 series, the states of stresses at equilibrium were normalized and superimposed on the constant-strain contours plot for total axial strain (Figure 5-7). The mapping of the stabilized total axial strains at the respective peak stress states at equilibrium were found to be in reasonably good agreement with that of the derived constant-strain contours plot for total strain under cyclic compression.

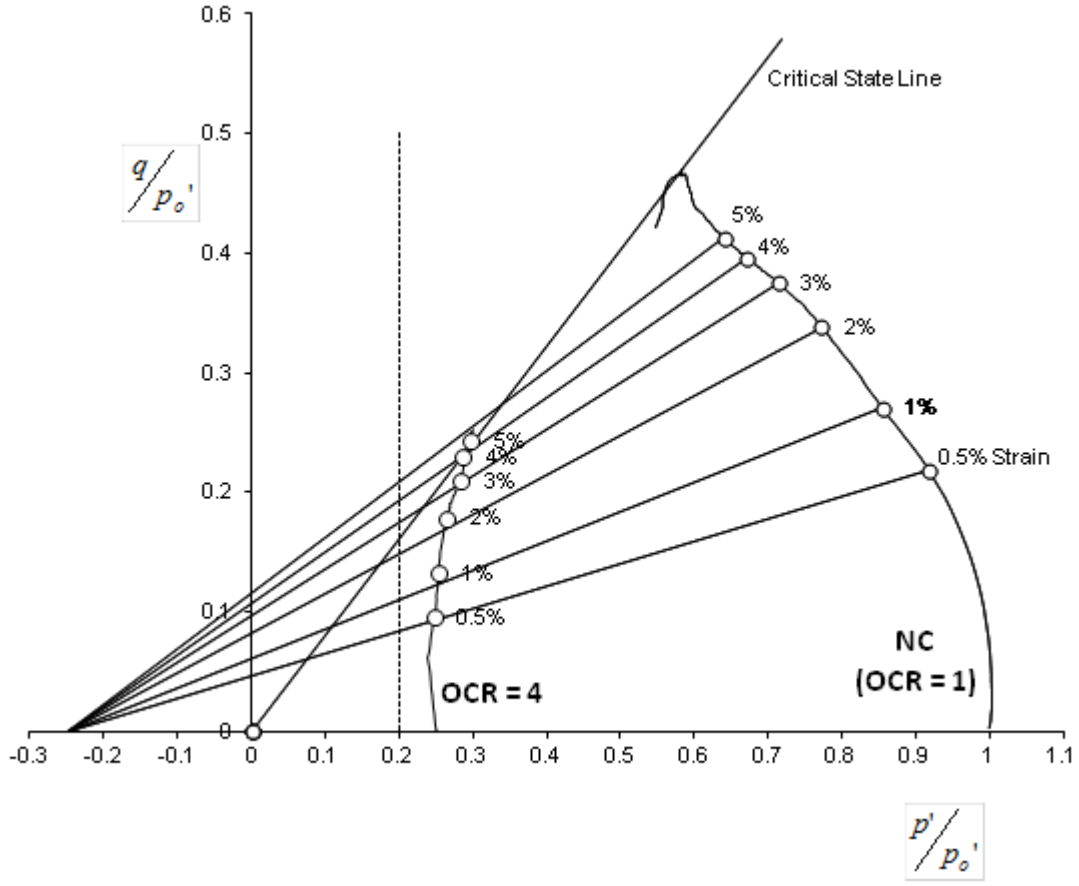

Figure 5-6 Normalized partial plot of the constant-strain contours for total axial strain under cyclic compression (for 0 < OCR < 4)

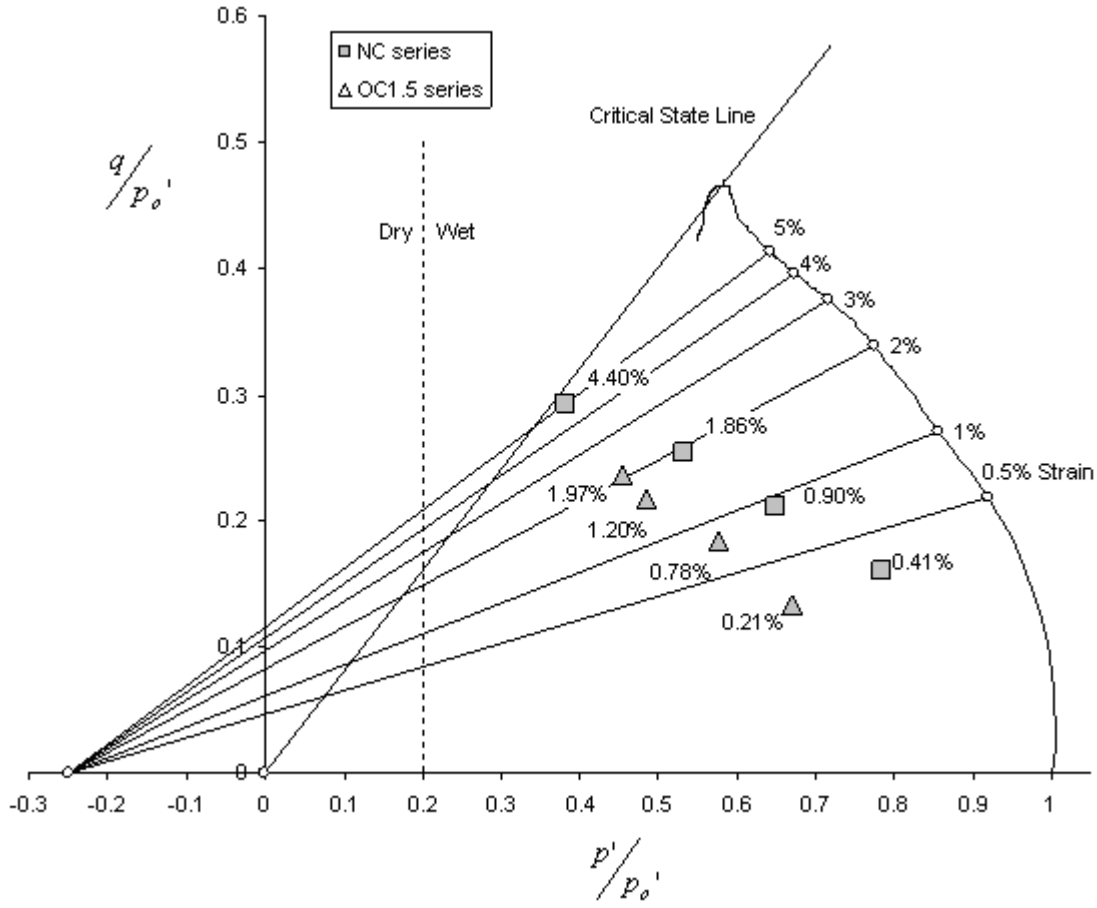

Figure 5-7 The superimposition of the stabilized total axial strain of the respective peak stress states at equilibrium (for the NC and the OC1.5 series) on the normalized partial plot of the constant-strain contours for total axial strain (kaolin clay)

The above partial normalized plot of the constant-strain contours was further improved and adjusted to take account of the deformation characteristic of soil specimen with state of stress exists on the "dry" side of the critical state. The

adjusted complete plot of the constant-strain contours has the straight line contours radiated from the origin of the plot and linked up the previously derived contours along the dry / wet division line, i.e. at approximately $p'/p_o' = 0.2$ (Figure 5-8). Superimposition of the stabilized total axial strain of the respective normalized stress states for specimen of the OC4 and OC20 series soil has apparently shown good mapping on the constant-strain contours (Figure 5-9). The characteristic normalized $p'-q$ plot of constant-strain contours for total strain has provided a good graphical representation of the stabilized total axial strain (and perhaps the total axial strain at any one time during cyclic compression, knowing the effective states of stress) that will develop with respect to the peak stress state (or stress obliquity for the heavily over-consolidated soil) under cyclic compression for kaolin clay of various consolidated state and stress history.

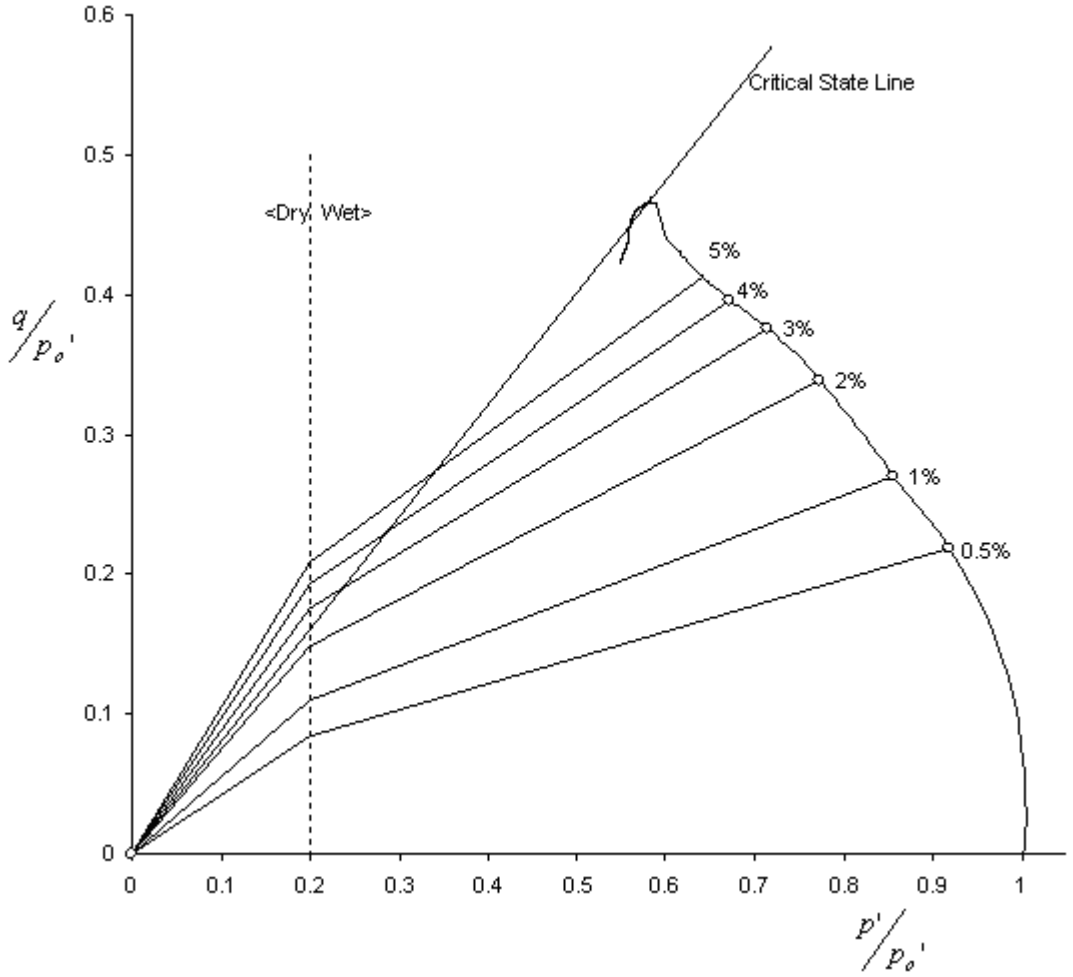

Figure 5-8 The normalized plot of the constant-strain contours for total axial strain (kaolin clay)

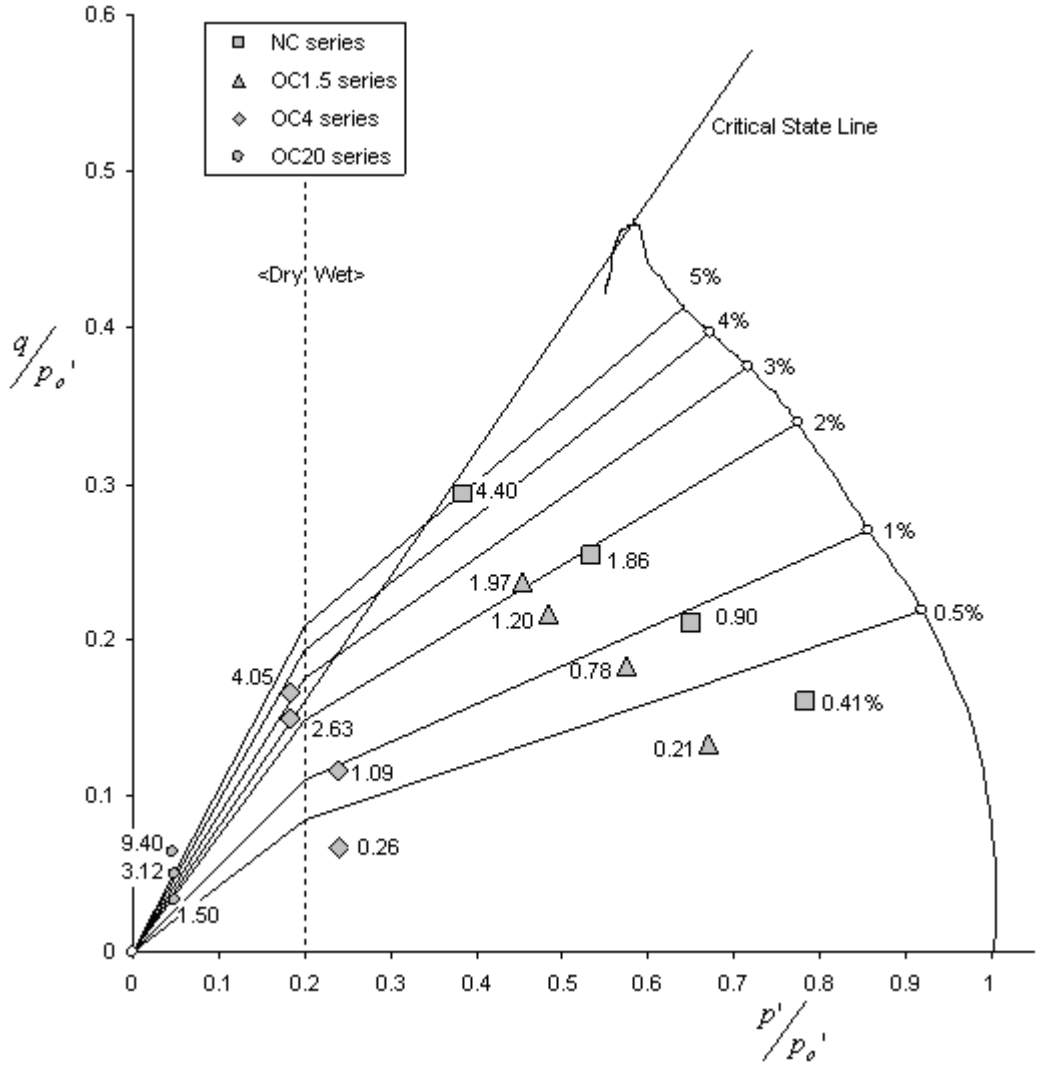

Figure 5-9 The superimposition of the stabilized total axial strain of the respective peak stress states at equilibrium (for all tests series) on the normalized plot of the constant-strain contours for total axial strain (kaolin clay)

5.6.3 Characteristic of Elastic Strain

In the similar way that the stabilized total strain forms distinctive constant-strain contours on a normalized p'–q plot, constant-strain contours can also be drawn to describe the relationship of the resilient strain with the respective state of stress (and the stress obliquity). Unlike the use of static axial strain data from the monotonic tests that will derive the constant-strain contours plot for total axial strain of cyclic compression (as shown in Figure 5-9), the static axial strain data of the monotonic test provides little clue to the elastic strain behaviour of the cyclic compression. Nevertheless, it has been postulated that the normalized plot of the constant-strain contours for elastic and resilient axial strain will take the similar pattern and configuration, i.e. constant-strain contours radiate from the same point of origin (Figure 5-6 and Figure 5-8), as that of the total strain described in the previous paragraph 5.6.2. Based upon the postulation and using the resilient strain data from one of the test series i.e. NC series (Figure 4-12) where the variation of the resilient strain with the peak stress state (can be deduced from Figure 4-11 and Figure 4-12) was known, a partial normalized plot of the constant-strain contours for elastic axial strain, applicable to normally-consolidated NC series to over-consolidated OC4 series clay soil , can be derived as shown in Figure 5-10. The partial constant-strain contours plot in Figure 5-10 was further adjusted to account for the heavily over-consolidated soil in the same way as the total axial strain plot shown in Figure 5-8. The complete plot of the constant-strain contours for elastic axial strain was developed as shown in Figure 5-11. The validity of the plot was examined by the superimposition of the resilient strain of the respective normalized stress states for tests specimen of all four tests series that arrived at the resilient state (Figure 4-34, Figure 4-50 and Figure 4-65) on the developed constant-strain contours plot for elastic axial strain. The mapping was found to be in good agreement (Figure 5-12).

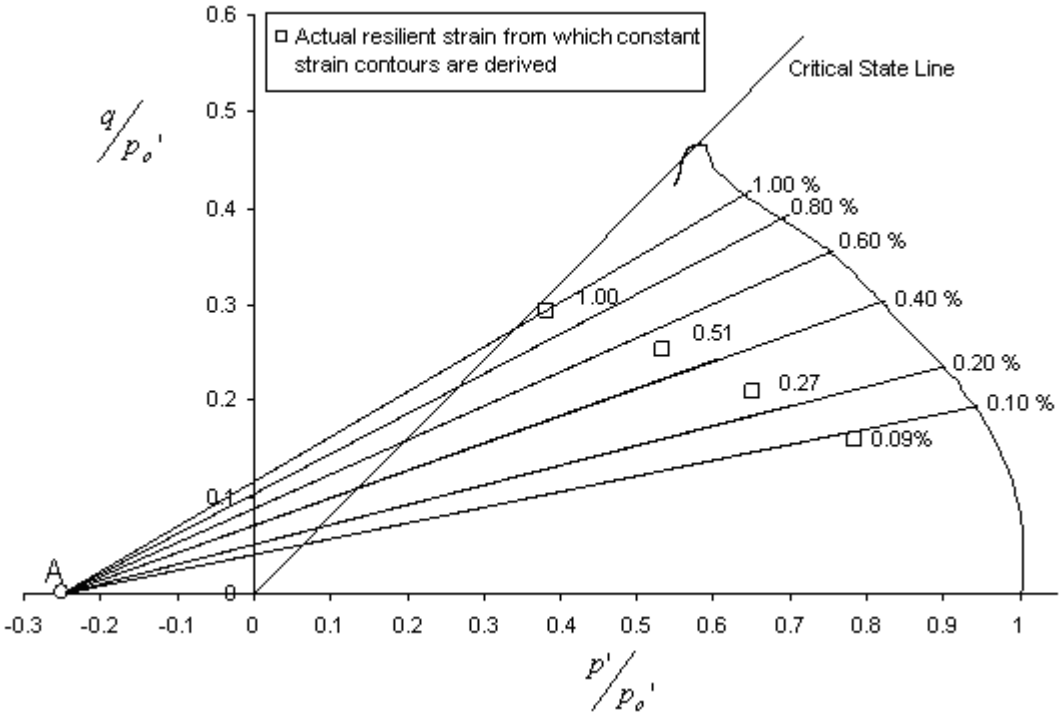

Figure 5-10 Normalized partial plot of the constant-strain contours for elastic axial strain under cyclic compression (kaolin clay)

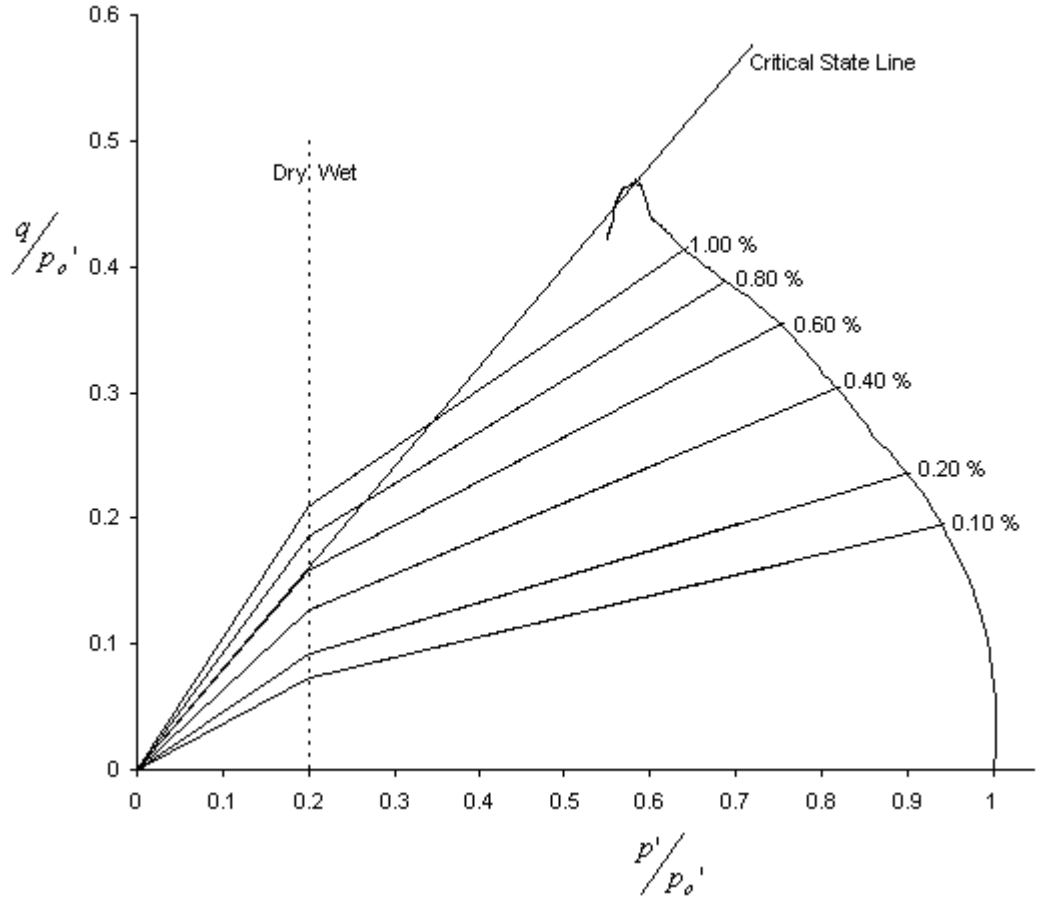

Figure 5-11 Normalized plot of the characteristic constant-strain contours for elastic axial strain (kaolin clay)

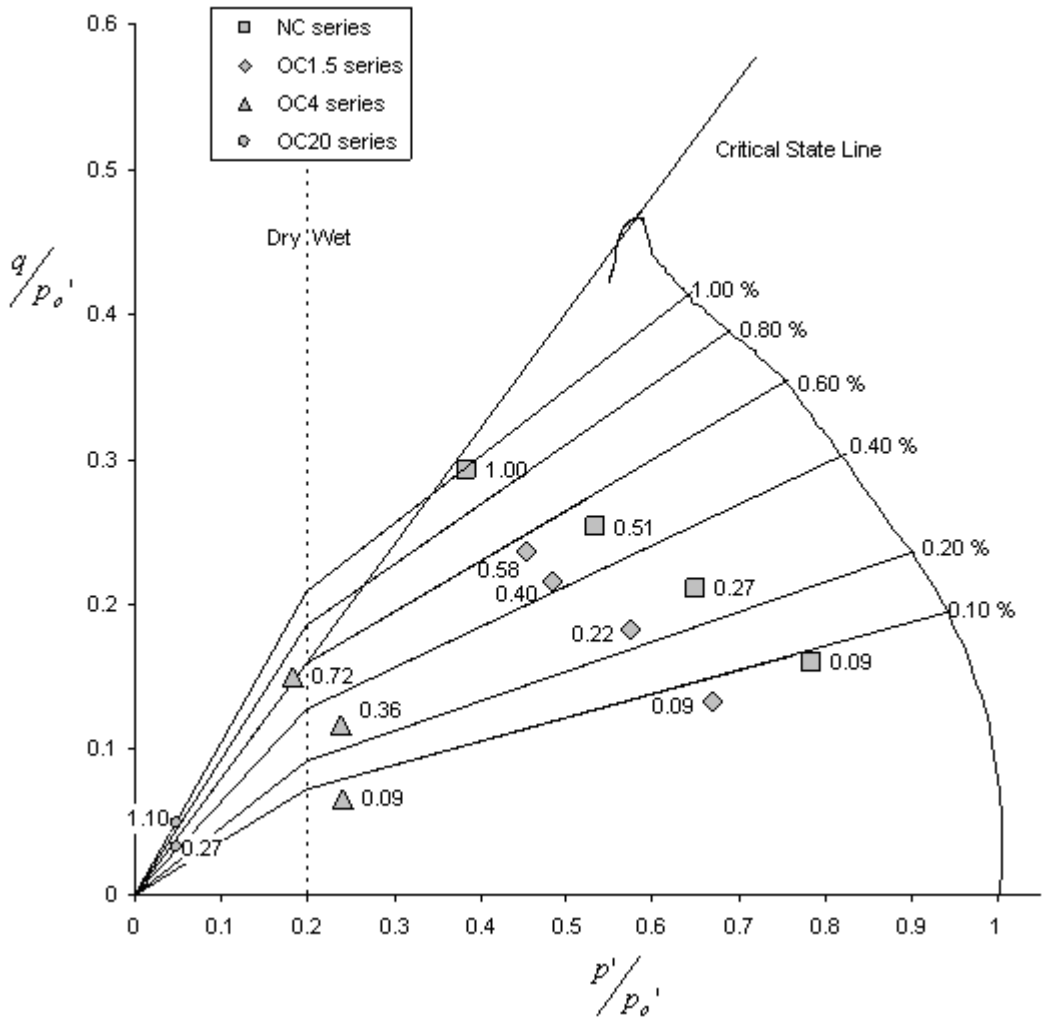

Figure 5-12 Superimposition of the resilient strains data of respective peak stress states on the normalized constant-strain contours plot for elastic axial strain (kaolin clay)

The normalized plots of the constant strain contours for the total strain, and the elastic strain, as described above provides a characteristic and graphical illustration of the axial deformation behaviour of the saturated clay under cyclic undrained compression. With the superimposition of the line of cyclic stress equilibrium state

LCSES for each of the consolidated series, the amount of stabilized total axial strain and the resilient axial strain can be obtained by directly read from the graphs (Figure 5-13 and Figure 5-14) for any specific level of cyclic deviator stress. Inferring from Figure 5-13 and Figure 5-14, the amount of axial strain (total and resilient) given the same level of cyclic deviator stress will be larger for soil with higher over-consolidation ratio (see also Figure 5-15 and Figure 5-16).

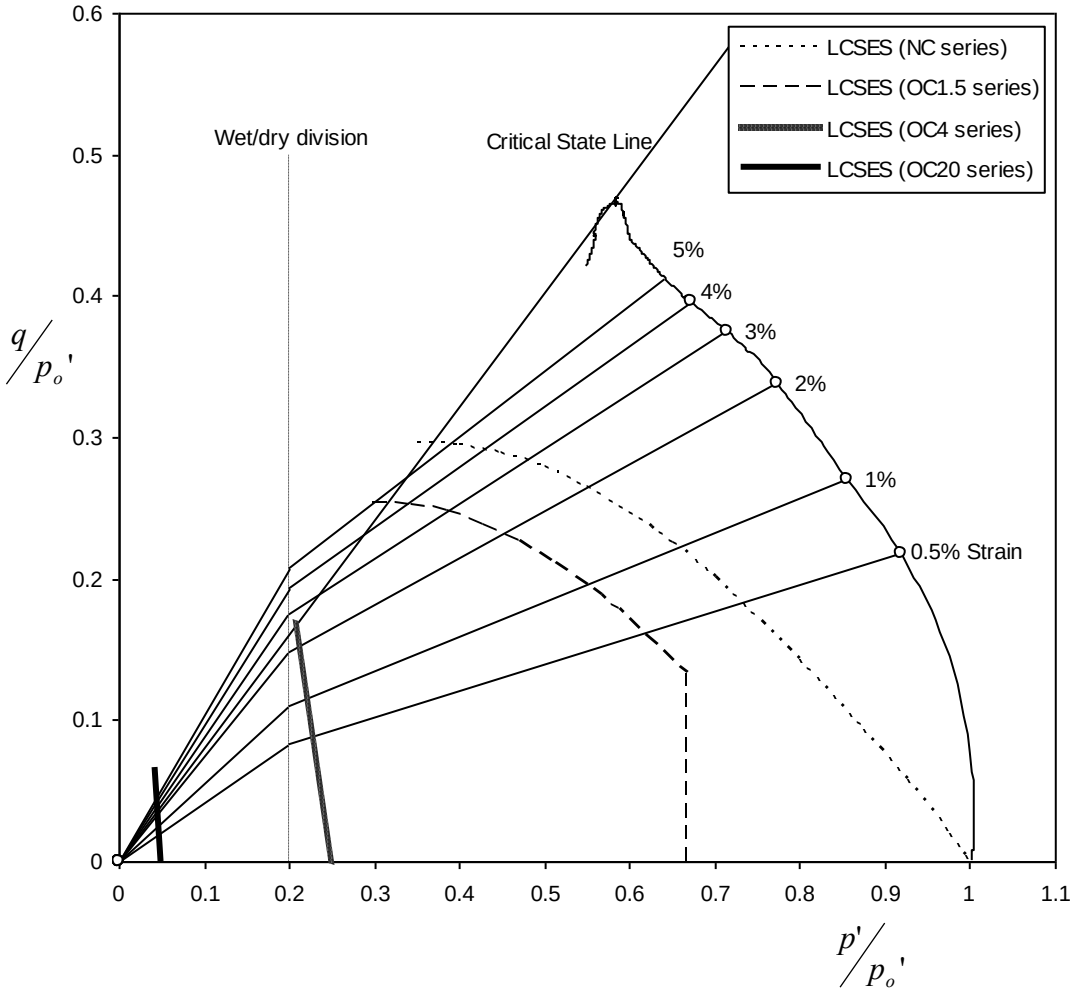

Figure 5-13 Superimposition of the line of cyclic stress equilibrium state (LCSES) on the normalized plot of the constant-strain contours for total strain (kaolin clay)

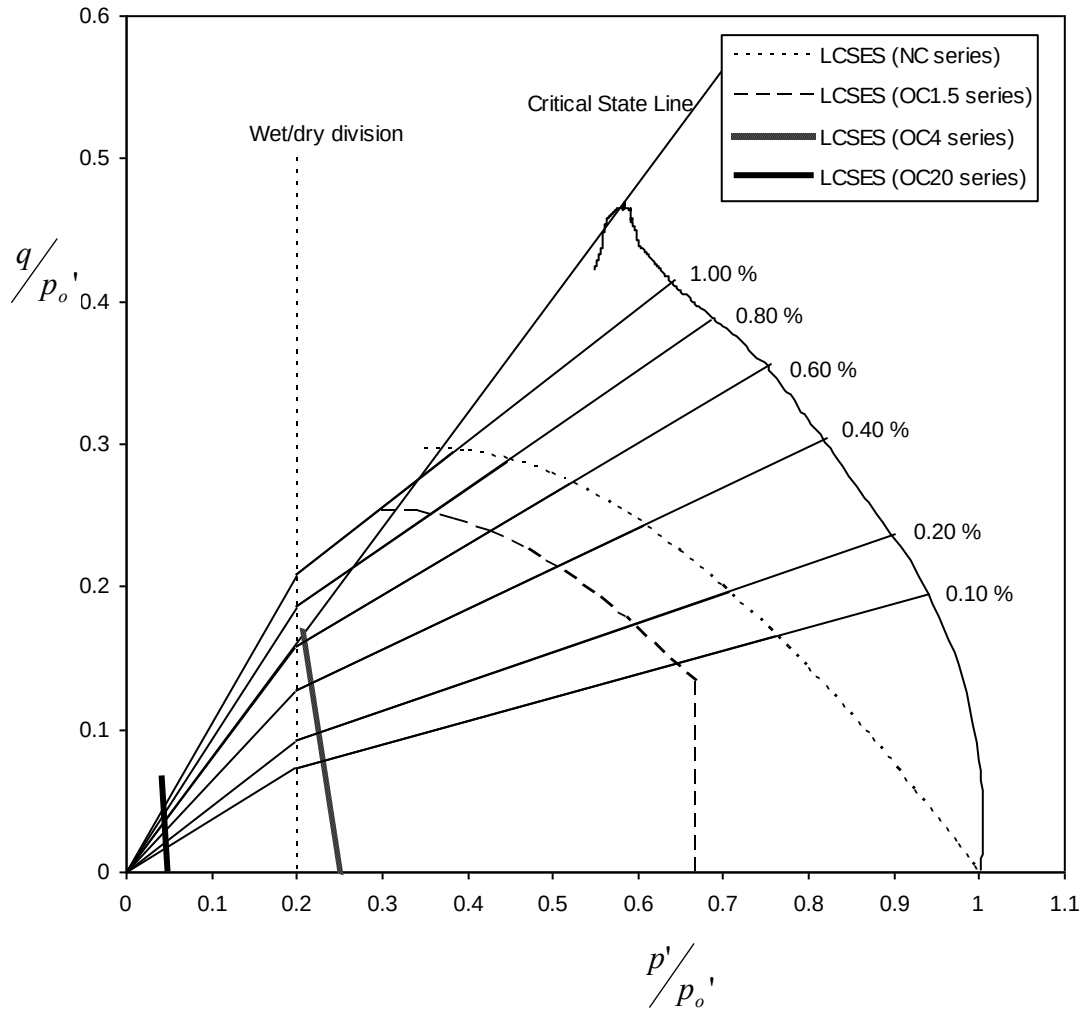

Figure 5-14 Superimposition of the line of cyclic stress equilibrium state (LCSES) on the normalized plot of the constant-strain contours for elastic axial strain (kaolin clay)

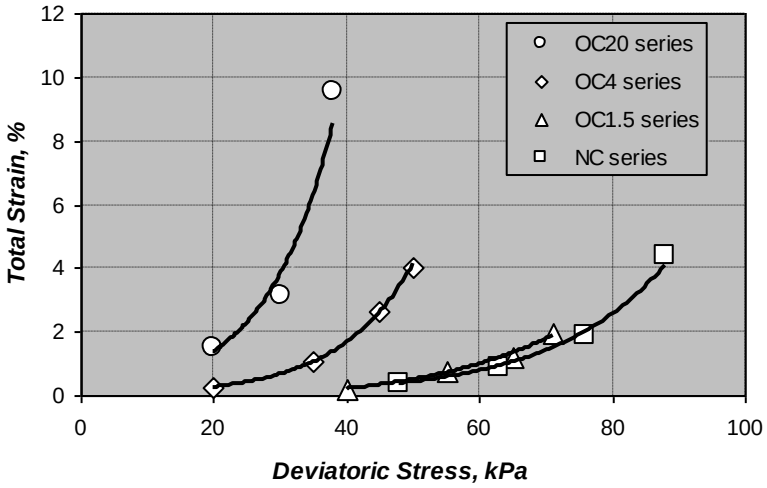

Figure 5-15 Comparison of the relationship for stabilized strain verses level of deviator stress

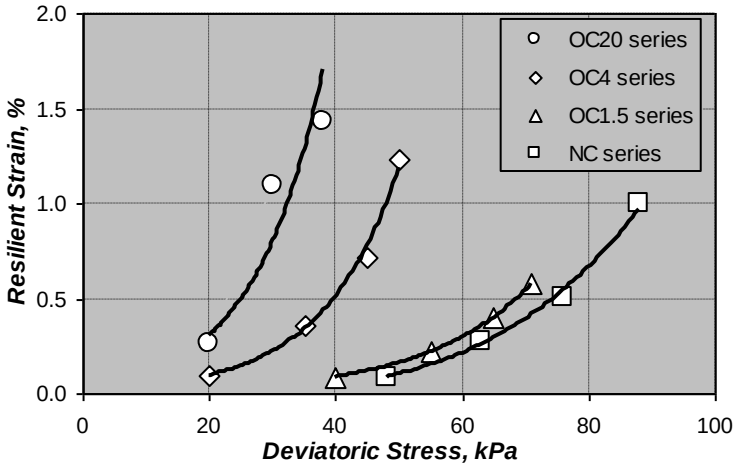

Figure 5-16 Comparison of the relationship of resilient strain verses level of deviator stress

5.6.4 Resilient Modulus

Figure 5-17 provided an overall comparison on the variation of resilient modulus of undrained cyclic compression with respect to the level of deviator stress, for the four tests series of wide-ranging over-consolidated state. The direction of each curve and their relative position has a trend completely opposite of the resilient strain, where lower resilient modulus seemed to associate with higher over-consolidation ratio, not withstanding the dependency on the level of past maximum pre-consolidation pressure (p_o') i.e. OC20 series has a higher past maximum pre-consolidation pressure of 600 kPa as compared to 300 kPa for all the other series. Using a similar expression (Equation (2-12)) as proposed by Brown et al.(1975), a more general correlation can be described of the resilient modulus (undrained) with respect to the stress obliquity at equilibrium (with σ_3' replaced by effective mean stress p'). The correlation appeared to be strong as can be seen from Figure 5-18, with higher stress obliquity at equilibrium produces lower resilient modulus. The resilient modulus of the saturated kaolin clay under cyclic undrained compression hence can be expressed in the following equation (with $R^2 = 0.9$):

$$E_r = 4092\left(q/p'\right)_{equi}^{-1.5} \qquad \text{(kPa)} \qquad \text{(5-2)}$$

where $\left(q/p'\right)_{equi}$ is the stress obliquity at cyclic stress equilibrium state

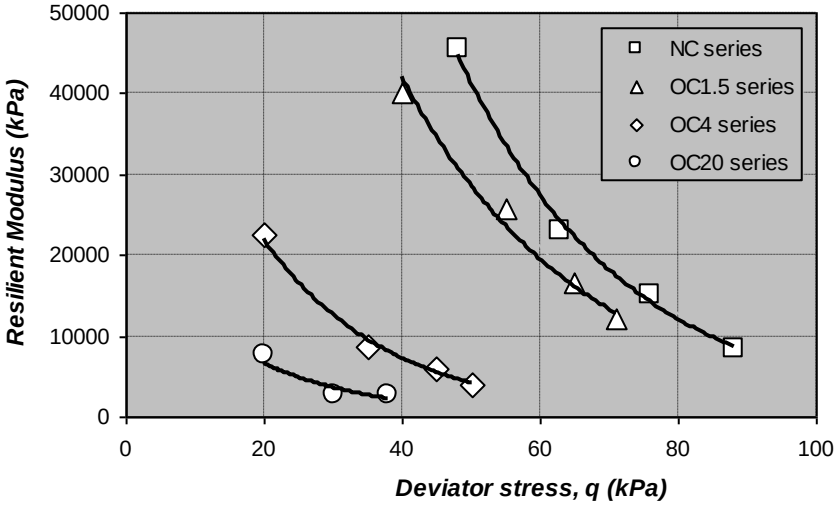

Figure 5-17 Comparison of the relationship of resilient modulus verses level of deviator stress

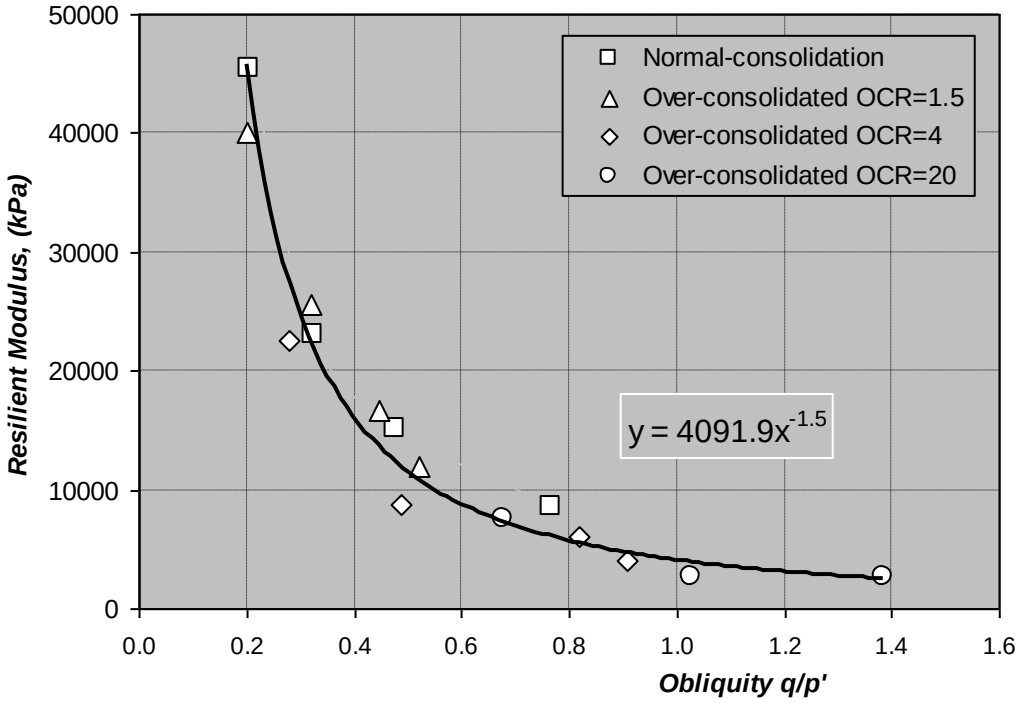

Figure 5-18 The variation of resilient modulus with respect to stress obliquity at equilibrium (kaolin clay)

Chapter 6 Critical State Model for Predicting Cyclic Threshold Stress

6.1 *Introduction*

The development of original Cam-clay model by Schofield and Wroth (1968) and subsequently the modified Cam-clay critical state model by Wood (1990) offered a means by which various simple mechanical models that represent the laboratory behaviour of remoulded soil can be explained. It has enabled many aspects of monotonic stress / strain behaviour of soil to be studied and appreciated before any experimental testing. So far, these models were able to match well the observed behaviour of insensitive or non-structured clay subjected to monotonic loading. There have been constant attempts in making improvement to these early and fundamental models that will simulate the behaviour of soil responds under cyclic stress. While many empirical and constitutive models have since been developed for cyclic loading (Carter et al. 1982; Egan and Sangrey 1978; Indraratna and Salim 2005), they were largely set out to fulfil a specific aspect of engineering objectives. Some were intricate and overly complex for any possible practical application. The original Cam-clay despites being an earlier and basic model has been a rational constitutive relationship developed from first principles. It provides a good fundamental and potential for developing further understanding on many aspects of cyclic loading behaviour.

In this study, the proposed theoretical model which is extended and developed from the original Cam-clay model, intended only to model the existence of the cyclic stress equilibrium state from which the level of threshold stress can be derived.

6.2 *Review of Original Cam-Clay Model*

The core idea in the concept of critical state is that soil and granular materials if continuously distorted until they flow as a frictional fluid, will be in a "critical state" defined by the following two equations (Schofield and Wroth 1968):

$$q = Mp' \tag{6-1}$$

$$\Gamma = v + \lambda \ln p' \tag{6-2}$$

where the variables p' and q and the constant M are as defined in the previous chapters. The constant Γ is the specific volume at p' = 1 kPa on the critical state line (CSL), λ is the gradient of the compression (or normal-consolidation) line, and v is the specific volume of soil (v = 1 + e) with e being the void ratio of soil.

The original Cam-clay model required the four parameters: λ, κ, Γ and M to be specified, where κ is the gradient of swelling / recompression line on the v - p' plane. They are the fundamental properties that can be obtained from a standard static triaxial test. In addition, it requires the elastic shear modulus G to be estimated.

The current yield function of the soil represents the volumetric yield locus (yield curve) on the $p' - q$ plane with its isotropic state base line (q = 0) coincides with a specific swelling / recompression line defined by its normal pre-consolidation pressure (p_o') (Figure 6-1). Yielding of the soil occurs whenever the stress state of soil satisfies the criterion as follows:

$$\frac{q}{Mp'} + \ln\left(\frac{p'}{p_{cr}'}\right) = 1 \qquad (6\text{-}3)$$

where p_{cr}' is the mean effective stress at the intersection of the CSL and the yield curve

For any change of stress state within the current yield curve, the soil responds elastically in terms of its volume change.

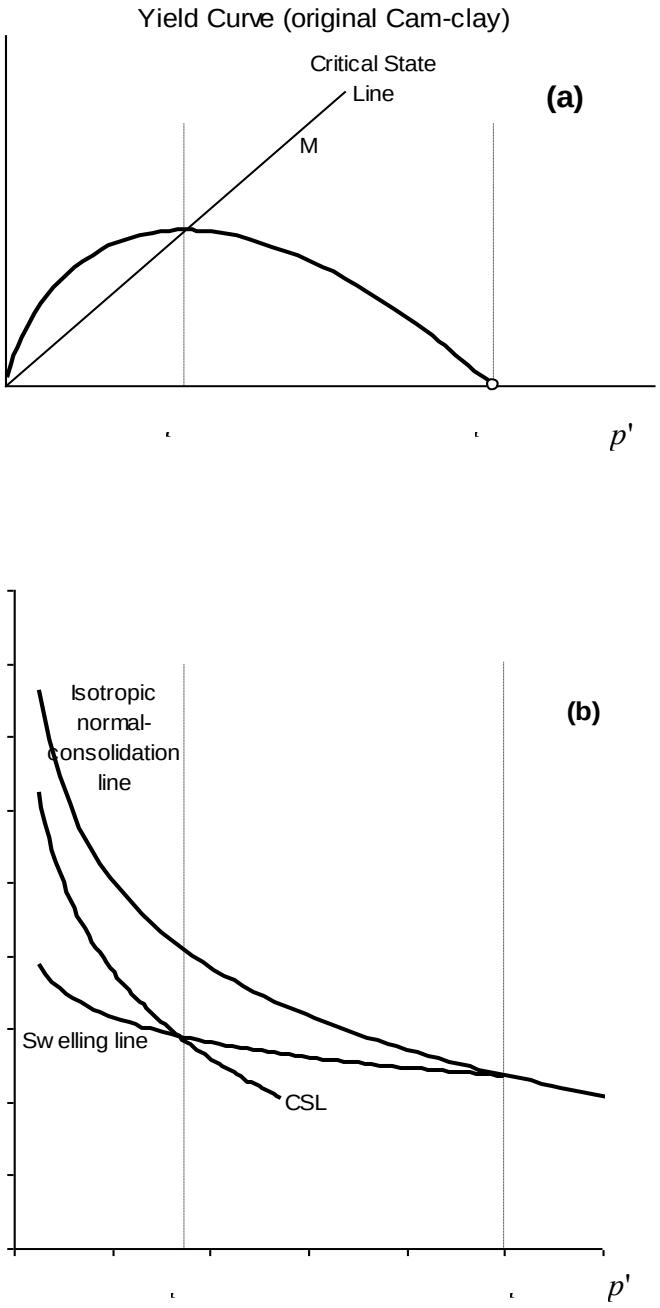

Figure 6-1 Yield curve for original Cam-clay (Schofield and Wroth 1968)

6.3 *A Theoretical Extension from Original Cam-clay Model*

The tests results and the *p'- q* stress plots presented and discussed in the previous chapters (4 and 5) has clearly illustrated and confirmed two of the specific characteristics of stress responses unique to saturated clay in both sub- and critical region, under cyclic undrained compression. Firstly, there is an elasto-plastic response in which peak stress path migrates to the left before it become stagnated on the line of cyclic stress equilibrium state (LCSES). (Such as on the LCSES of normally-consolidated NC series and, the curved portion of the LCSES of over-consolidated OC1.5 series (Figure 5-2)). Next, there is an elastic response where the Peak stress state which occurs below a specific level (at which the LCSES either abruptly changed its course (as in OC1.5 series) or terminates beyond the critical state line (as in OC20 series)) of stress state is inherently stagnated (without migration). The phenomenon allows us to postulate that some kind of cyclic stress equilibrium state surface (CSESS) within the *p'- q – v* space (depicted as the approximate boundary of cyclic stress equilibrium state surface in Figure 5-2) may be inherent for saturated clay under cyclic undrained compression. Developed from and as an extension to the basic original Cam-clay model, the following section therefore intended to describe and substantiate the existence of CSESS, from which to develop a theoretical model that enables cyclic threshold stress to be predicted without resort to carrying out lengthy experimentation of the cyclic load tests.

6.3.1 Cyclic Stress Equilibrium State

The establishment of the functional relationship representing cyclic stress equilibrium state in the $p' - q$ plane at constant volume was spurred on by the observed effective stress response of the saturated kaolinite clay under cyclic undrained compression. It was built on the understanding of volumetric compressibility and the basic idea of volumetric compatibility within the soil mass. That is, if a change in the soil volume (Δv) involves plastic volumetric change (Δv_p) and elastic volumetric change (Δv_e), then the total volume change (Δv) will be,

$$\Delta v = \Delta v_p + \Delta v_e \qquad (6\text{-}4)$$

For undrained triaxial (cyclic) compression, $\Delta v = 0$. Equation (6-4) becomes,

$$\Delta v_p = -\Delta v_e \qquad (6\text{-}5)$$

For a clay that has been normally-consolidated to a pre-consolidation pressure (p_o'), the size of current yield function (Equation (6-3)) represents the boundary of the possible stress states (p', q) in the " $p' - q - v$ "space, within which there can only be elastic swelling $(\Delta v_e)_{swelling}$ occurs prior to any possible elastic contraction $(\Delta v_e)_{contraction}$ (see Figure 6-2).

For a perfectly isotropic consolidated clay, any change in the deviator stress Δq (when $\Delta p' = 0$) within the current yield function produces no volume change. That is,

$$\Delta v = (\Delta v_e)_{swelling} = (\Delta v_e)_{contraction} = 0. \qquad (6\text{-}6)$$

Under undrained cyclic compression, the remoulding of clay causes an apparent over-consolidation for a normally-consolidated clay (Lefebvre 1986). This implies that the size of current yield function (represented by the p'_o) will constantly be enlarged with each loading cycle, while the mean effective stress (p') is decreasing due to increase in excess pore water pressure. For this to have occurred, plastic contraction $(\Delta v_p)_{contraction}$ must have taken place in each loading cycle, and it can only be balanced by elastic swelling $(\Delta v_e)_{swelling}$, such that it appeared no net change in volume (see Figure 6-2). From Equation (6-5),

$$(\Delta v_p)_{contraction} = (\Delta v_e)_{swelling} \qquad (6\text{-}7)$$

Since plastic volumetric change i.e. plastic contraction $\left(\Delta v_p\right)_{contraction}$ appeared to be a non-reversible process in an undrained compression (i.e. as in normal-consolidation), Equation (6-7) implies there will be no elastic contraction $\left(\Delta v_e\right)_{contraction}$ during the unloading process.

As illustrated in Figure 6-2, the process of plastic contraction will, in general, continues until it equal to the total elastic swelling $\Sigma\left(\Delta v_e\right)_{swelling}$ that can possibly occur with the original yield function (referred to previously as current yield function in Equation (6-3)), whereby the stress state (p', q) boundary defined by the original yield function also defines the boundary ($p', q, (v = 0)$) of the cyclic stress equilibrium state under a constant volume. At this time,

$$\Sigma\left(\Delta v_p\right)_{contraction} = \Sigma\left(\Delta v_e\right)_{swelling} = \text{Function of} \left\{ \lambda, \kappa, \left(p', q_{cyc} \right)^{original\ yield\ function}_{} \right\} \qquad (6\text{-}8)$$

Thus, the boundary of cyclic stress equilibrium state on the p'- q plane ($v = 0$) will have a function identical to the original yield function as follows:

$$q = Mp' \ln\left(p_o' \Big/ p' \right) \qquad (6\text{-}9)$$

The above Equation (6-9) defines the boundary of cyclic stress equilibrium state for normally-consolidated saturated clay at constant volume in an undrained cyclic compression. Based on this, it is reasonable to postulate that cyclic stress equilibrium state boundaries of respective sizes exist for each pre-consolidation pressure (p_o') along the normal-consolidation line, forming a cyclic stress equilibrium state surface (CSESS) within the stress state boundary surface (SSBS).

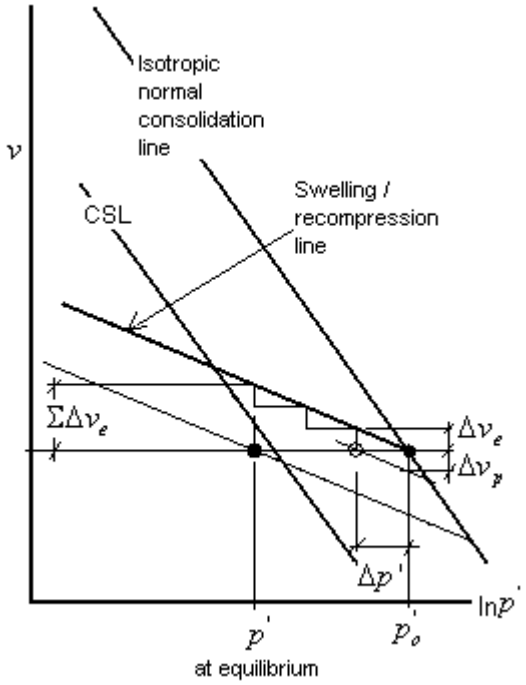

Figure 6-2 Volumetric compressibility and volumetric compatibility within soil mass

6.3.2 Equation of Cyclic Stress Equilibrium State Surface

Figure 6-3 showed a p'–q plot of the cyclic stress equilibrium state surface (CSESS) normalized with the equivalent pre-consolidation pressure (p_e') (which is the same as the pre-consolidation pressure (p_o') for normal-consolidation), in relation to the Roscoe surface and Hvorslev surface (Smith 2006). The CSESS for undrained cyclic compression appeared to exist within the overall stress state boundary surface (SSBS). Re-writing Equation (6-9), the general equation of the cyclic stress equilibrium state surface (CSESS) at constant volume ($\Delta v = 0$) for saturated clay soil in both sub- and critical region, can be written as,

$$q = Mp' \ln\left(p_e' \Big/ p' \right) \tag{6-10}$$

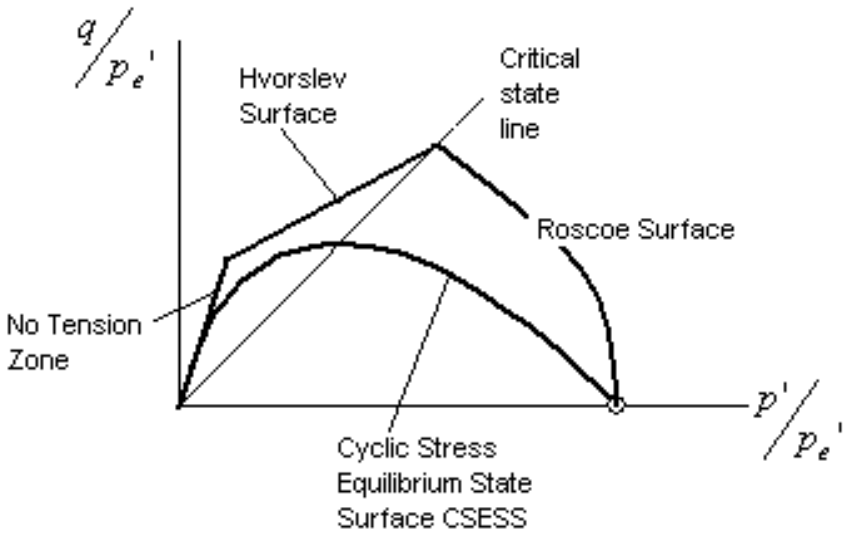

Figure 6-3 The existence of cyclic stress equilibrium state surface (CSESS) within the overall stress state boundary surface (SSBS).

6.3.3 Significance of Cyclic Stress Equilibrium State Surface

Under undrained cyclic compression, the state of cyclic stress path relative to the cyclic stress equilibrium state surface (CSESS) determines the specific effective stress response and strain development as follows:

a) Cyclic Stress State within CSESS

In the case of over-consolidated clay soil under a relatively low cyclic deviator stress, the state of cyclic stress path originates and looping within the CSESS (as in stress path 'a' in Figure 6-4). Except for volumetric distortion, there is no change in volume (either plastic or elastic) internally within the soil. Hence,

$$\Sigma\left(\Delta v_e\right)_{swelling} = \Sigma\left(\Delta v_p\right)_{contraction} = 0 \qquad (6\text{-}11)$$

The excess pore water pressure and hence the cyclic stress state responds in an elastic and reversible manner in each cycle of loading application as cyclic stress path forms hysteresis loop. The state of stress equilibrium is said to be inherent for cyclic stress path which originates and loops within the CSESS. There will be an early build-up of axial strain after a relatively short number of loading cycles, but it soon becomes stabilized.

b) Cyclic Stress State beyond CSESS

For cyclic compression when the whole or partial cyclic stress path forms and looping outside the CSESS, cyclic stress responses which largely depend on the consolidated state and the stress history of soil (i.e. over-consolidation ratio) are as follows:

- Normally and Lightly Over-consolidated Soil

Clay soil which exists in sub-critical region has a contractive tendency under compression that builds up excess pore water pressure. As a result, peak stress path migrates horizontally to the left (as shown in Figure 4-7 & Figure 4-27). Two distinctive behavioural patterns can possibly occur depending on the level of cyclic deviator. One in which the peak stress path first reaches the critical state line (CSL) where large soil deformation follows (as in path 'b' in Figure 6-4). In the other, the peak stress path reaches the cyclic stress equilibrium state surface (or the line of cyclic stress equilibrium states as described in previous chapters) where stress hysteresis loop will be formed (path 'c' in Figure 6-4). The threshold stress q_t (or critical level of cyclic loading) will be the maximum possible cyclic deviator stress that will arrive at the cyclic stress equilibrium surface, beyond which the peak stress path will approach the CSL where soil deforms with large strain.

- Heavily Over-consolidated Soil

The tendency of over-consolidated clay to dilate under compression means that the plastic swelling $(\Delta v_p)_{swelling}$ of soil (if any) will have to be balanced by the elastic contraction $(\Delta v_e)_{contraction}$ at constant volume, such that,

$$(\Delta v_p)_{swelling} = (\Delta v_e)_{contraction} \tag{6-12}$$

However, the above Equation (6-12) violates the basic internal mechanism for volumetric change for soil under undrained cyclic compression described in paragraph 6.3.1 (Equation (6-7) & (6-8)), causing instability within soil mass. The peak stress path migrates downward towards CSESS with large strain failure (path'd' in Figure 6-4). Therefore, the peak stress path of an undrained cyclic compression which originates outside the CSESS is transient and unsustainable. It will not migrate horizontally towards the cyclic stress equilibrium state surface. Instead, move downward fairly quickly as soil fails with large strain (see Figure 4-56c).

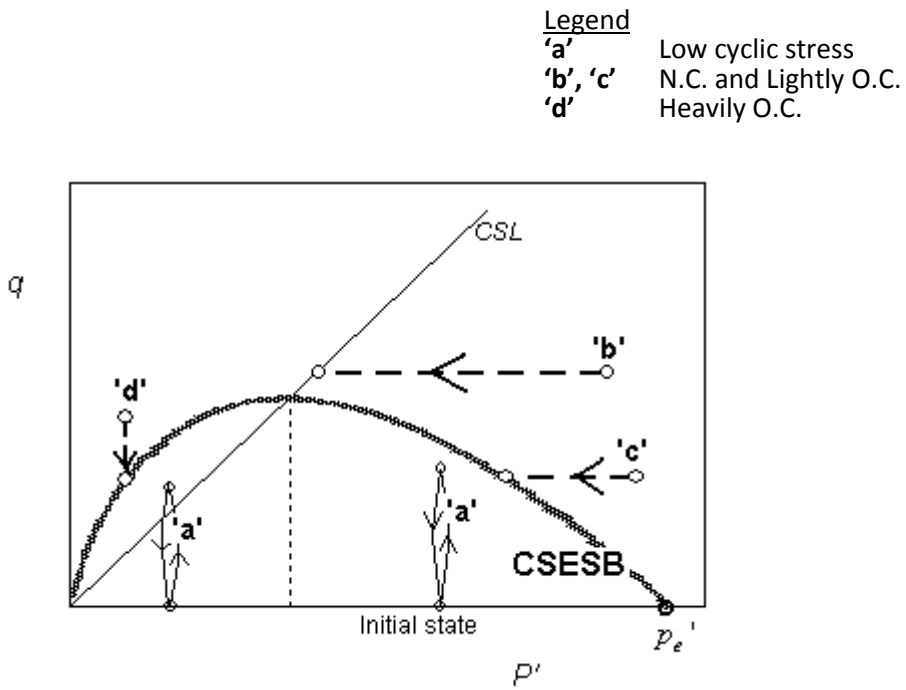

Figure 6-4 Cyclic compression response in terms of the movement of peak stress path in relation to cyclic stress equilibrium state surface (CSESS)

6.3.4 Prediction Model of Cyclic Threshold Stress

Based on observed phenomenon of stress / strain response as illustrated in the above paragraph 6.3.3, where the behavioural patterns of the cyclic stress path (and the peak stress path) in relation to the cyclic stress equilibrium state surface (CSESS) is characteristic of the consolidation state and stress history, theoretical prediction model for estimating the threshold stress of saturated clay under cyclic undrained compression can be derived and established (The details derivation is given in Appendix 1) from Equation (6-8) to Equation (6-10), as shown in the general equations below:

In the case of normally and lightly over-consolidated soil, when

$$\frac{p_i'}{p_o'} \geq e^{\left(\frac{\lambda}{\kappa-\lambda}\right)} \tag{6-13}$$

the threshold stress q_t ,

$$q_t = \frac{M}{e} p_o'^{\left(1-\kappa/\lambda\right)} p_i'^{\left(\kappa/\lambda\right)} \tag{6-14}$$

where p_i' is initial effective mean stress (or initial state) of soil, and

p_o' is the past maximum pre-consolidation pressure

For heavily consolidated clay, when

$$\frac{p_i'}{p_o'} \leq e^{\left(\frac{\lambda}{\kappa-\lambda}\right)} \tag{6-15}$$

the threshold stress (q_t) which can only be the maximum cyclic deviator stress possible within CSESS when $\Delta p' = 0$ (assuming the soil is perfectly isotropic) becomes,

$$q_t = Mp_i' \left(\frac{\kappa - \lambda}{\lambda} \right) \ln \left(\frac{p_i'}{p_o'} \right) \qquad (6\text{-}16)$$

6.3.5 Examination and Validation of Model

The above model for describing the level of threshold stress underscores the fundamental importance of the volumetric compressibility index, λ and κ, in the elasto-plastic behaviour of clay soil in the undrained cyclic compression condition, as it characterizes the level of threshold stress. While there is only one value for λ which describes volumetric compressibility of the isotropic normal-consolidation, the value of κ is normally taken as average of the swelling / rebound compressibility κ_1 and the re-consolidation compressibility κ_2.

Measured data of the threshold stress from series of undrained cyclic compression triaxial tests on reconstituted saturated kaolinite clay, as described in Chapter 4 and 5, is summarily presented in Table 6-1. In computing the predicted threshold stress (as tabulated in Table 6-1), however, the re-consolidation compressibility κ_2 was used in the Equation (6-14) and (6-16). It has been observed that use of re-consolidation compressibility κ_2 better described the elastic volumetric response of clay under undrained compression, as comparison made between the predicted values of threshold stress using Equation (6-14) & (6-16) showed good agreement with observed values (measured data) (see Table 6-1). This may be due to the fact that the in-plane stress (axial stress) of re-consolidation and the axial compressive stress of undrained compression are of the similar vector in terms of its stress direction.

The discrepancy between the predicted and observed threshold stress for the heavily consolidated clay (OCR = 20) was largely attributed to the anisotropic nature of the clay sample prepared using one-dimensional consolidation with top and bottom drainage, when specimen become more compressible in the axial direction that cause

$\Delta p' < 0$. As a result, the peak stress state intercepting CSESS at a slightly lower deviator stress (q).

Table 6-1: Comparison of the model prediction of threshold stress with the observed values from tests conducted. (Kaolin clay)

M = 0.803

λ = 0.176

κ = 0.068

s/no	Stress history	p_i' (kPa)	p_o' (kPa)	q_t (kPa) Predicted	q_t (kPa) Observed
1	Normally-consolidated	300	300	88.6	90
2	OCR=1.5	200	300	75.8	75
3	OCR=4	75	300	51.9	50
4	OCR=20	30	600	44.3	40

6.4 *Summary*

For remoulded saturated clay under cyclic undrained compression, there exists a cyclic stress equilibrium state surface (CSESS) within the stress state boundary surface (SSBS). The theoretical development of the original Cam-clay model

provides the constitutive basis, from which extension models for describing the CSESS and predicting the threshold stress can be derived. This Chapter illustrates the development of extension model based on understanding the volumetric compressibility and the volumetric compatibility within the soil mass, with regards to the plastic and elastic response of a clay soil. The proposed theoretical model is provided as a means to predict the threshold stress of saturated clay of non-sensitive nature under undrained cyclic compression without resort to lengthy testing programme. The model is relatively simple and input parameters can be easily obtained from basic laboratory tests. Measured data from the testing programme on kaolin clay (as described in Chapter 4 and 5) confirmed the authenticity of the model.

Chapter 7 A Rational Approach to Railway Track Foundation Design

7.1 *Introduction*

This chapter presented a rational approach in the design and management of railway track foundation with clay as the subgrade soil. It aimed at rationalizing and formulating the current state of design and management process for railway track substructure. The readily use of critical state theoretical model and design charts for predicting lower-bound threshold stress and its re-assessment offered a key advantage that enables the application of new rational approach over the current practices (Burrow et al. 2007; Heath et al. 1972; Li 1994b; Li and Selig 1996; Li and Selig 1998a; Waters 1968) in the design and management process of railway track foundation.

7.2 *Approach to Substructure Management of Clay Subgrade*

The current analytical approach to the design of rail track foundation with fine-grained soil subgrade has been either strain-focus (Li 1994b; Li and Selig 1996; Li and Selig 1998a) or stress-focus (Heath et al. 1972; Waters 1968). In other words, the design is primarily intended in limiting applied stress to subgrade such that a specific level of axial deformation or a critical level of deviator stress (threshold stress) is allowed near the subgrade surface.

While the strain-focus approach requires the specification of the level of allowable strain and the corresponding magnitude of deformation and it pre-supposed a constant or bi-seasonal soil physical state (soil moisture content and dry density) (Li 1994a), its use certainly requires prior rationalization and justification of what

constitutes allowable strain or deformation for different soil-type and operating condition.

With the passing of train axles / wheels, subgrade soil beneath railway track experiences stress of repeated or cyclic nature that can possibly result in progressive shear failure at a stress level lower than the monotonic strength (Selig and Waters 1994). British researchers (Heath et al. 1972; Waters 1968) have long established the existence of 'threshold stress' in London clay subgrade. When the subgrade of railway track will to be stressed at a level lower than the threshold stress, stabilization of track vertical profile can be achieved. The authenticity of British approach and design method had been validated through a programmed field study and evaluation, despite it being semi-empirical due to its unique tests method and its probabilistic nature that made it applicable only to British ground condition and local traffic characteristics.

Consequently, this study proposed a new approach which favoured the stress-focus approach in adopting the threshold stress criteria, on the premise that strain and deformation would be minimized if the induced stress can be properly controlled at a level below the threshold stress, while additional provision on the track superstructure (sleepers, fastening system to rail) can be made to overcome or alleviate the potential and unforeseen differential settlement of the track.

7.3 *Managing the Current Lower-bound Threshold Stress*

7.3.1 General

Railway track being a fixed rail platform has the sleepers acting like pad footings sitting on subgrade. Provided no localized shear failure with large strain occurs along the rail, with the subgrade soil reasonably homogeneous, differential settlement along the track due to trains loading will not be significant. Any strain / deformation

response below sleeper will generally vary linearly along sleepers, and it will not necessarily causing problem to the track stability and functionality, except where change of foundation stiffness is expected i.e. at the road or culvert crossing, to which a localized design consideration and additional provision should be given.

The characterization of the bearing strength for clay subgrade, on assumption of full saturation and "undrained" condition under cyclic compression represents a "lower-bound" solution. And it should be highlighted that along the entire length of rail track under consideration, it is the "lower-bound threshold stress" of the weakest spot, hence the weakest link that controls and determines the allowable bearing strength (allowable deviator stress) near the subgrade surface for the entire length of track foundation. Otherwise, a localized design and consideration will have to be provided.

However, under repeated loading application, unlike the coarse-grained or well-drained soil that is normally characterized by a single "shakedown" stress ((Indraratna and Salim 2005), clay subgrade which has a current state of stress lightly over-consolidated (i.e. up to over-consolidation ratio of say, 4 for kaolinite clay) can have different and increasing lower-bound threshold stress over time, as excess pore water pressure begin to dissipate. The dissipation of excess pore water pressure causes densification to the subgrade soil with increased strength, albeit increased deformation. All of these factors and considerations have given rise to the notion of designing and managing the rail track foundation with clay subgrade, based on the "current" lower-bound threshold stress.

7.3.2 Concept and Process

The concept on "managing the current lower-bound threshold stress" builds on the understanding that the new clay subgrade though may initially be weaker, will gradually increase its load carrying capacity over time. The key to managing the track foundation with clay subgrade is to limit the induced stress on the subgrade by its 'current' lower-bound threshold stress and help building up the loading capacity of the subgrade progressively. The process entails the followings:

a) Prediction of the initial lower-bound threshold stress for the purpose of design and determination of track bed (granular layer) thickness.

b) Regulating and control of train traffic loading during the "run-in" period.

c) Re-assessment of the threshold stress of subgrade after the initial run-in period.

d) Re-adjustment of the vertical profile of rails above sleepers.

e) Upgrading of the threshold stress and the track loading capacity as appropriate.

f) Ongoing management of b) to e).

7.4 *Application and Procedure*

7.4.1 Predicting Initial Lower-Bound Threshold Stress

When designing and constructing a new rail track, the design objective of the rational approach is to ensure the induced vertical stress (q_{cyc}) (caused by the heaviest axles loading) near the subgrade surface will not exceed the lower-bound threshold stress (q_t) of subgrade soil with the designed initial stress state (consolidated state) (p_i'). The lower-bound threshold stress (q_t) can be predicted using Equation (6-14) or (6-16) as appropriate.

Figure 7-1 is the design chart for the foundation subgrade of general clay soil (developed based on Equation (6-13) to (6-16)), characterized by the ratio of volumetric compressibility (κ/λ). The designed initial stress (p_i') and the lower-

bound threshold stress (q_t) are normalized by the past maximum pre-consolidated pressure p_o', with q_t further normalized by the strength parameter *M*.

To obtain the lower-bound threshold stress (q_t), laboratory tests will be carried out first to ascertain the basic and fundamental properties of the clay specimen collected from ground sampling, and to determine the past maximum consolidation stress (p_o') of the subgrade soil. The values of p_i'/p_o', and κ/λ are then worked out. From the design chart, where the x-coordinate of p_i'/p_o', and the curve of κ/λ intersects, the value of $\left(q_t/p_o'\right)\frac{1}{M}$ can be read out, and the lower-bound threshold stress (q_t) is then calculated.

For example,

Given: $M = 0.803; \lambda = 0.177,\ \kappa = 0.068;$

p_o' = 150 kPa;

Designed consolidated pressure p_i' = 50 kPa.

Then, $p_i'/p_o' = 50/150 = 0.333$

$\kappa/\lambda = 0.068/0.177 = 0.38$

From chart, $\left(q_t/p_o'\right)\frac{1}{M} = 0.241$

Therefore, Lower-bound threshold stress q_t = 0.241 x 0.803 x 150 = 29 kPa

In the case of a compacted subgrade, the past (or new) maximum consolidation stress (p_o') can be estimated using Equation (7-1) as follows:

$$p_o' = \left[\frac{(p_e')^{\lambda}}{(p_i')^{\kappa}} \right]^{\frac{1}{\lambda-\kappa}} \quad \text{kPa} \qquad (7\text{-}1)$$

where, p_e' is the equivalent past maximum pre-consolidation pressure as shown in Equation (7-2).

Alternatively, the lower-bound threshold stress (q_t) can be predicted directly by the process as described in paragraph 7.4.3 later.

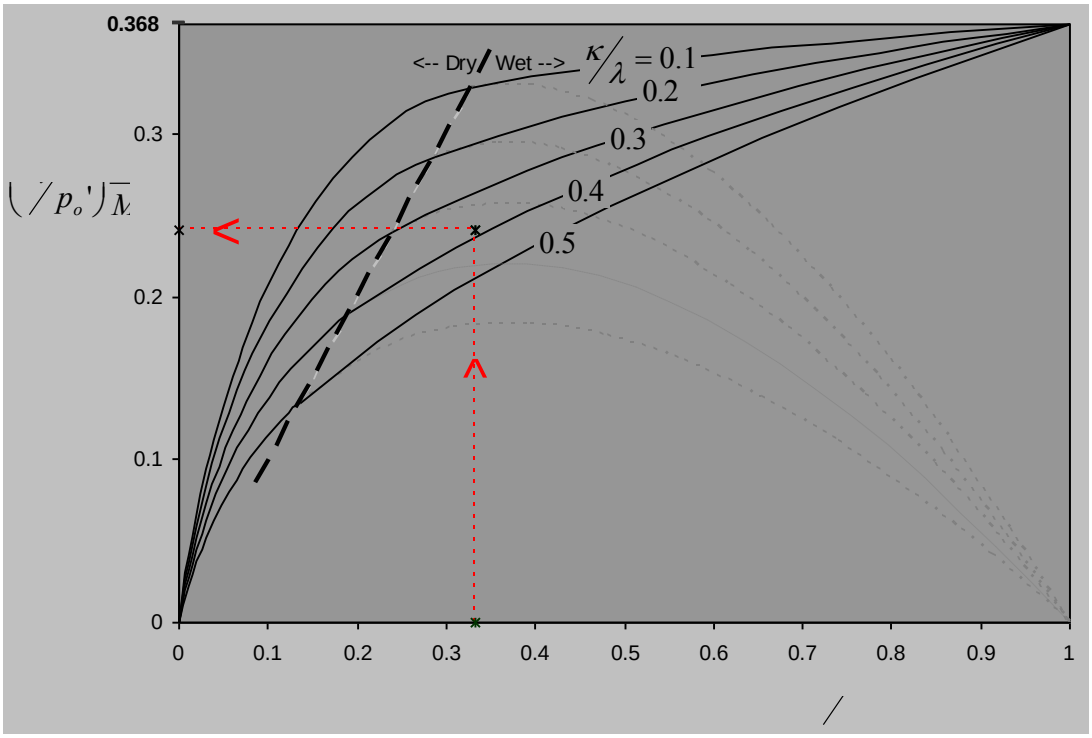

Figure 7-1 Design chart prepared for clay (characterized by the compressibility index λ and κ) for the determination of "lower-bound" threshold stress (Loh and Nikraz 2011)

7.4.2 Regulating and Control of Traffic

Regulating and control of train's traffic will be carried out for the following objective(s):

(1) To prevent overstressing of the subgrade soil caused by overloading by limiting the maximum laden loads of train-carriage.

The lower-bound threshold stress indicates the level of cyclic deviator stress at which subgrade soil will not fail with large strain. However, it is possible that some significant axial strain, say 3 to 4% may still occur if the induced stress close to level of the threshold stress is allowed. To minimize the permanent axial strain / deformation of subgrade, the induced stress may be limited to a percentage of threshold stress such that the amount of strain / deformation is kept within a certain acceptable limit i.e. less than 2 % of which engineering judgement is required. As an illustration, Figure 7-2 showed the characteristic constant-strain contours for the stabilized total axial strain (permanent and recoverable) produced for kaolinite clay. It should be noted that clay with higher over-consolidation ratio, especially heavily over-consolidated clay generates higher total stabilized strain for the same percentage level of threshold stress.

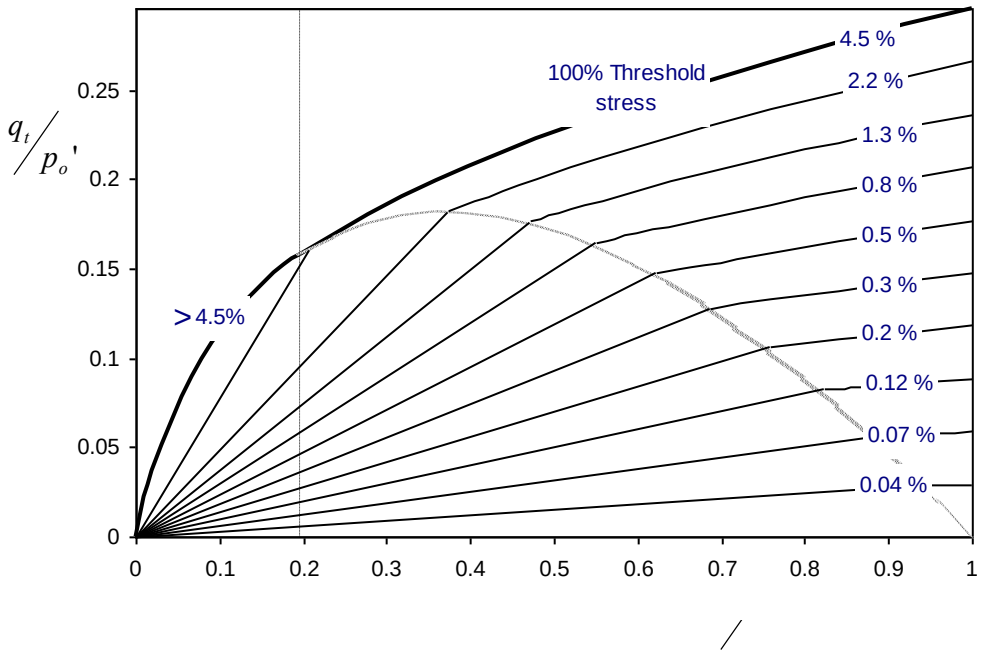

Figure 7-2 Constant strain contours for stabilized total axial strain (from tests conducted on saturated kaolin clay)

(2) To promote better long term soil densification (with consequent higher subgrade bearing strength), by careful scheduling and deliberate running of train loading that will induce stress close to the lower-bound threshold stress.

When shorter run-in period or higher threshold stress is desired, train loading that induces stress at a level close to threshold stress can be scheduled with train travelling at a slower speed i.e. one heavy train passage per day.

(3) To control large accumulation of permanent settlement and localized deformation due to occasional overloading, by maintaining a constant, safe and relatively high travelling speeds (without detrimental to granular layer or generating excessive dynamic loading).

In general, train traffic on railway track with clay subgrade should be running at a constant speed and avoid intermittent stoppage along the rail, during entire run-in period when lower-bound threshold stress of subgrade soil is expected to increase.

7.4.3 Re-assessment and Upgrade of Lower-Bound Threshold Stress

After the initial run-in period, re-assessment of the new lower-bound threshold stress can be carried out. This does not require elaborate and lengthy laboratory testing, but the determination of in-situ dry density γ_{di} (in kN/m^3) of the clay layer near the surface of subgrade. However, it is important that the in-situ testing or the sampling should provide minimum or no disturbance to the ballast / sub-ballast layer immediately underneath the sleepers. To facilitate this, vertical sampling conduits can be installed in advance at some regular interval near the edge of the sleeper. Figure 7-3 showed the proposed layout and cross-sectional view of the sampling conduits.

Having obtained the in-situ dry density subgrade soil, the equivalent past maximum pre-consolidation pressure p_e' can be determined using the following Equation (7-2) (Please refer to Appendix 2) (Loh and Nikraz 2011):

$$p_e' = \exp\left(\frac{N - \frac{9.81 G_s}{\gamma_{di}}}{\lambda}\right) \quad \text{(kPa)} \qquad (7\text{-}2)$$

where the constant N is the specific volume of soil under isotropic consolidation at $p' = 1$ kPa, and G_s is the specific gravity of soil.

The new lower-bound threshold stress can then be ascertained using the design chart as shown in Figure 7-4. Developed from Equation (6-10), the design chart provides a

curve that relates the new lower-bound threshold stress (q_t) to the designed (current) state of subgrade (p_i'), normalized with the equivalent past maximum pre-consolidated pressure (p_e'). With the value of the designed initial stress (p_i') normally remains unchanged; the new lower-bound threshold stress can be obtained. The rail track foundation will now be potentially having higher bearing capacity due to the increased lower-bound threshold stress.

Notwithstanding proper design and regulated traffic control, it is anticipated that small differential settlement between sleepers caused by the densification of subgrade do exist. Fine adjustment of rail vertical profile may be necessary before the loading capacity of railway track can be upgraded to withstand higher train loading. In this regards, provision may be made in the design of rail fasteners and rail bearing plate to enable an easy and moderate adjustment of rail vertical profile, without disturbing the compacted granular layer or having to lift up or disturb the sleepers.

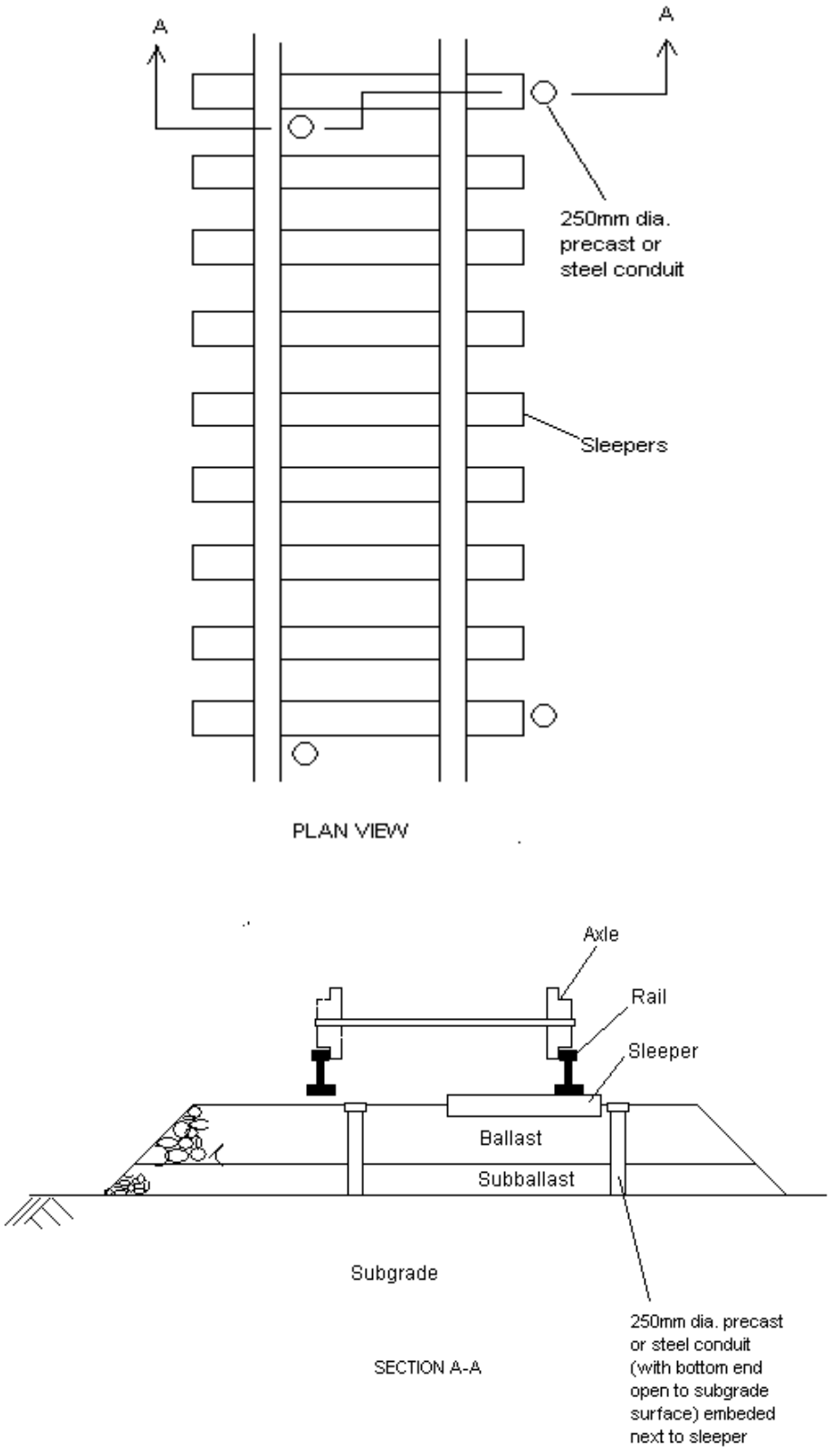

Figure 7-3 Layout and details of pre-installed precast or steel conduits (Loh and Nikraz 2011)

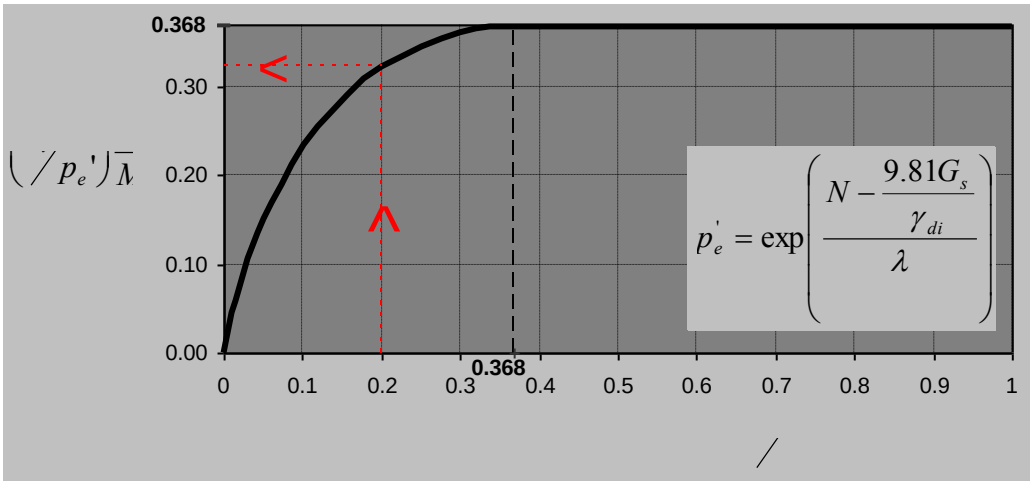

Figure 7-4 Design graph for the re-assessment of lower-bound threshold stress of clay subgrade (Loh and Nikraz 2011)

7.5 *Summary*

This chapter described the rational approach to the design and management of railway track foundation substructure with clay subgrade in potentially high saturation condition. The lower-bound threshold stress is introduced as a parameter for characterizing strength capacity of the clay subgrade soil. The rational approach has build on the premise of potential strengthening and densification for subgrade soil of lightly over-consolidated nature, through progressive and incremental loading of the track foundation.

By managing the "current lower-bound threshold stress" of subgrade soil, strain and deformation is kept under control, while the loading capacity of track foundation can be monitored and progressively upgraded to the maximum capacity.

Based on the developed theoretical critical state model as described in the previous chapter 7, design charts has been proposed for the prediction and re-assessment of lower-bound threshold stress of clay subgrade. It enables the "lower-bound threshold

stress” to be readily obtained with the availability of fundamental soil properties and from the basic soil tests, without resort to lengthy and costly cyclic load testing..

Field evaluation on a trial section of railway track foundation constructed using the new rational approach will be desired before a full scale railway track foundation construction.

Chapter 8 Summary, Conclusions and Recommendations

8.1 *Summary*

The approaches to railway track foundation design with fine-grained soil as subgrade have been one that satisfies either the "threshold stress" criteria or the" strain" criteria, all of which are largely semi-empirical. Fundamentally, it is essential that the behaviour of a clay-type subgrade representing the extreme end of fine-grained soil under cyclic loading be better understood and characterised, for the purpose of improved knowledge and even possible application in any design practice. In this thesis, the behaviour of re-constituted, saturated kaolin clay of different series in both sub- and super-critical region was studied using monotonic and cyclic undrained compression. The monotonic compression test provides a benchmark to which cyclic compression test relates, while the cyclic undrained compression test simulates the subgrade soil response to the induced stress due to passing wheel axles of contemporary train. Focus was placed on stress-strain response peculiar to the railway track foundation design; in particular, the deteriorated strength (i.e. threshold stress) and the deformation characteristic of clay subgrade were investigated in details. The tests were programmed with emphasis on establishing and verifying the influence of the consolidated state and stress history. The effect of cyclic loading rate (frequency) was also investigated. The experimental results were presented and analysed to develop the empirical / analytical and graphical methods which can be used to examine and predict both the threshold stress and deformation characteristics of clay soils. It was subsequently used to substantiate and validate the development of a constitutive relationship (i.e. a critical state model) capable of predicting "lower-bound threshold stress" of general clay-soil under cyclic undrained compression. A new rational approach to railway track foundation substructure design with clay-soil as subgrade was proposed in conjunction with the possible application of the developed theoretical model. The main elements entails in this thesis comprises:

(1) An extensive literature review on the behaviour of clayey soils under cyclic or repeated loading, particularly in the context of railway track foundation subgrade;

(2) A detailed experimental investigation into the behaviour of reconstituted, saturated kaolin clay under undrained cyclic compression;

(3) An examination of the stress response and strain characteristics of clay soil in cyclic undrained compression condition;

(4) A characterisation and development of empirical / analytical and graphical methods for predicting clay-soil (kaolin clay in particular) behaviour under cyclic undrained compression;

(5) A development of a theoretical constitutive model for predicting the strength characteristic (threshold stress);

(6) A proposal on new rational approach to railway track foundation substructure design with clay-soil as subgrade.

8.2 *Conclusions*

8.2.1 Behaviour of Saturated Kaolin Clay in Cyclic Undrained Compression

8.2.1.1 General

- Use of effective stress analysis for clay soil in cyclic undrained compression of fast loading rate, i.e. 1Hz and above, will be valid when the final state of stress equilibrium, rather than transient and interim state, is of prime interest.

- The importance of peak stress path (and peak stress state) on p'–q plot was highlighted as it represents the most vulnerable and critical stress state in the cyclic stress path of undrained cyclic compression.

- The stress-strain of re-constituted clay-soil follows certain behavioural pattern depending on the initial consolidated state and stress history, and the level of cyclic deviator stress. Under cyclic compression, normally-consolidated clay builds up excess pore water pressure and axial strain. For cyclic deviator stress above the "threshold stress", peak stress path (on a $p'-q$ plane) migrates horizontally leftward and reaches the critical state line, while axial strain increases at a constant rate initially follows by sudden and abrupt increase in strain rate, upon which soil fails with large strain. For cyclic deviator stress below threshold stress, peak stress path become stagnant before the critical state line, as excess pore water pressure varies and oscillates within a constant level, signifying the arrival of stress equilibrium state. The axial strain also increases at reducing rate until strain finally stabilized, signifying a state of strain resilience (resilient state). The resilient state exists when both stress equilibrium state arrived and strain is stabilized.

- In heavily over-consolidated clay, there is no excess pore pressure build-up under cyclic undrained compression, except constant-amplitude variation occurs within each loading cycle. State of stress equilibrium is inherent within soil mass under cyclic compression. For cyclic deviator stress below threshold stress, peak stress path appeared as a stagnated peak stress state and it can exist above the critical state line. The resilient state is achieved only when strain become stabilized. For cyclic deviator stress higher than threshold stress, little sign of excess pore water regression can be noticed as soil fails with large strain.

- Lightly over-consolidated clay can exhibit either behavioural pattern similar to the normally-consolidated or the heavily over-consolidated clay (as described above), depending on the level of cyclic deviator stress. Below a specific level of cyclic deviator stress (smaller than the threshold stress), state of stress equilibrium is inherent and the soil has the similar behavioural response to that of the heavily over-consolidated soil which attained the resilient state. For cyclic deviator stress above the same specific level, lightly over-consolidated soil has the similar stress-strain response to that of the normally-consolidated clay.

8.2.1.2 Stress Equilibrium at Resilient State and Deteriorated Strength

- Using critical state soil mechanics framework, the tests results brought to light the intrinsic state of stress equilibrium for over-consolidated clay soil in undrained cyclic loading condition. The state of stress equilibrium is inherent in over-consolidated clay under cyclic undrained compression when the level of deviator stress is within the boundary of the cyclic stress equilibrium state (CSES) in p'- q plane.

- This study described the four characteristic patterns of the line of cyclic stress equilibrium state (LCSES) for kaolinite clay of sub- to super-critical state under

cyclic undrained compression. The LCSES dictates the way threshold stress (or critical level of cyclic stress) can be best identified.

- In the case of normally-consolidated to lightly over-consolidated clay, when the peak of deviator stress is above the boundary of CSES, the arrival of stress equilibrium state implies a state of resiliency in stress and strain response. The level of deviator stress at the intercept of the line of cyclic stress equilibrium state (LCSES) and the critical stress line (CSL) indicates the threshold stress.

- For over-consolidated clay, when the level of deviator stress is within the bound of CSES, a state of resiliency arrives soon after the anisotropic effect due to deviator stress has been realized (with no tendency for volume-change) as total axial strain becomes stabilized.

- In the case of heavily over-consolidated clay, the LCSES goes above the CSL and its terminated end indicates the level of threshold stress. Cyclic deviator stress higher than its threshold stress provides little clue from its effective stress response, but failed ultimately with large strain. Therefore, the detection of threshold stress for heavily over-consolidated soil will be for practical purpose, best identified by trial tests to detect the maximum cyclic deviator stress which produces stabilized strain.

- The level of threshold stress is influenced by both the current state of stress and the stress history of clay. However, heavily over-consolidated clay has a lower cyclic stress ratio for threshold stress.

8.2.1.3 Deformation Characteristic and Resilient Modulus

- It was observed that the relationship of axial strain verse stress obliquity from monotonic compression is indirectly applicable to cyclic compression, with the following postulations:

  a. On the $p'-q$ plot normalized by p_o', the constant strain-contours (straight-lines) which radiate from a point to the left of 'zero' on the p'/p_o'- axis, connects the strain-dot points of the normally-consolidated soil under monotonic compression, to that of an over-consolidated soil (exists near the wet /dry division of critical state line (CSL)), i.e. OC4 series

  b. The constant-strain contours of heavily over-consolidated soil (on the dry side of CSL), radiates from the origin of the normalized plot to join the contours at the wet / dry division of CSL as described above.

- Given the same percentage level of cyclic deviator stress, it was found that clay with higher over consolidation ratio will incur higher total axial strain and resilient strain.

- Soil with higher over-consolidation ratio generally sustains higher stress obliquity at stress equilibrium that associates with lower resilient modulus.

8.2.1.4 Effect of Cyclic Loading Frequency

- Given the same number of loading applications in an undrained condition, higher cyclic loading frequency produces lower build-up of excess pore water pressure and total axial strain in the case of normally-consolidated soil. This resulted in lesser reduction in effective mean stress (p') and lesser permanent axial strain,

as compared to those of the lower cyclic loading frequency. One might interprets that soil appeared stronger under higher cyclic loading frequency.

- It is observed that continuation of loading applications under higher loading frequency, however, produces the same amount of excess pore pressure build-up and total strain accumulation as that under lower loading frequency, at the higher number of loading cycles appropriate to the of cyclic loading frequency.

- The peak stress paths for tests conducted at different cyclic loading frequencies, on soil specimen of same stress history, arrived at the same line of cyclic stress equilibrium state. As such, cyclic loading frequency has no effect on the level of threshold stress for saturated clay in undrained compression.

8.2.2 Constitutive modeling of Deteriorated Strength for Saturated Clay

- Under cyclic undrained compression of saturated clay soil, there exists the cyclic stress equilibrium state surface (CSESS) in which state of stress equilibrium is inherent, within the stress state boundary surface (SSBS). The algebraic equation defining the CSESS on $p'-q$ plane at constant volume can be derived from the original Cam-clay model based on the notion of volume compressibility and volumetric compatibility within soil mass.

- Depend on the initial consolidated state and the stress history of he soil, the state of cyclic stress path relative to the cyclic stress equilibrium state surface (CSESS) determines the specific effective stress response (i.e. the migration / or stagnation of the peak stress path) and strain development, whereby the maximum cyclic deviator stress which will attained stabilized strain indicates the level of threshold stress.

- The theoretical development of the original Cam-clay model provided the constitutive basis, from which extension model for cyclic loading in an undrained compression can be derived. The proposed theoretical model is provided as a means to predict the threshold stress of saturated clay of non-sensitive nature under undrained cyclic compression, without resorting to lengthy testing programme. The model in a form of algebraic equation is relatively easy for application and input parameters can be obtained from standard laboratory tests.

- The modelling of level of "threshold stress" described in this study represents a "lower bound" threshold stress for the design railway tracks foundation sub-structure with clay soil as subgrade in potentially high saturation condition.

8.2.3 Rational Approach to Railway Track Foundation Design

- The new approach rationalized and re-formulated current state of affair in design and management of railway track foundation substructure with clay soil as subgrade; on the premise of potential subgrade soil strengthening and densification through progressive and incremental loading of the track foundation. The lower-bound threshold stress is introduced as a parameter for characterizing strength capacity of clay subgrade.

- Through regulating of traffic-loading and managing the "current lower-bound threshold stress" of subgrade soil, strain and deformation of track foundation substructure will be kept under control, as loading capacity of track foundation subgrade is regularly monitored and can be progressively upgraded to the maximum capacity.

- The developed theoretical model and design charts for predicting and re-assessing lower-bound threshold stress of clay subgrade enables the "lower-

bound threshold stress" to be readily obtained with availability of fundamental soil properties and basic soil tests, without resort to lengthy and costly testing.

8.3 *Recommendations for Future Research*

8.3.1 Experimental Investigation

- The experimental works carried out in this study was on the behaviour of reconstituted kaolin clay subjected to undrained cyclic compression after the initial isotropic consolidation. In order to substantiate the observed behaviour that is likely to be typical of non-structured clay soil in a fair range of consolidation state, other natural clay-soil is recommended for further testing and investigation. Further understanding on the behaviour of railway track clay subgrade can be expanded, by examine the level of threshold stress for clay under cyclic compression with a base-load. The finding from these tests could prove valuable in establishing a more economical solution in track foundation design.

- The proposition that densification occurs and threshold stress will be increased given sufficient time for dissipation of excess pore water pressure could be substantiated by further experimental investigation.

8.3.2 Modelling of the Cyclic Behaviour

- This study attempted only to model a particular aspect of cyclic behaviour, i.e. the cyclic stress equilibrium state and the threshold stress of saturated clay. Further works are possible on modelling the threshold stress of partially-

saturated clay soil, and the strain response in both undrained and a combination of undrained / drained conditions simulating the actual subgrade experience.

8.3.3 Field Evaluation of New Approach

- The new approach to railway track foundation sub-structure design requires site validation. A trial-track overlaying clay subgrade, running "in parallel" with existing network in the lowland can be constructed, monitored and managed using the new approach in order to evaluate its feasibility.

References

Ansal, A. M. (1989). "Undrained behavior of clay under cyclic shear stresses." *Journal of Geotechnical Engineering*, 115(7), 968-983.

AREA. (1973). "Manual of recommended practice." American Railway Engineering Association, Illinois.

Atkinson, J. (1993). *An introduction to the mechanics of soils and foundations*, McGRAW-HALL Book Company Europe.

Blight, G. E. (1963). "The effect of non-uniform pore pressure on laboratory measurements of the shear strength of soils." Symposium on Laboratory Shear Testing of Soils, ASTM Special Technical Publication No.361. American Society for Testing and Materials, Philadelphia, USA, 173-184.

Brown, S. F., Lashine, A. K. F., and Hyde, A. F. L. (1975). "Repeated load triaxial testing of a silty clay." *Geotechnique*, 25(1), 95 -114.

Burrow, M. P. N., Bowness, D., and Ghataora, G. S. (2007). "A comparison of railway track foundation design methods." *Proceedings of the Institution of Mechanical Engineers; Part F; Journal of rail and rapid transit*, 221(1), 1-12.

Carter, J. P., Booker, J. R., and Wroth, C. P. (1982). "A critical state soil model for cyclic loading." Soil Mechanics - Transient and Cyclic Loads, G. N. P. a. O. C. Zienkiewicz, ed., John Wiley & Sons Ltd.

Clarke, C. W. (1957). "Track loading fundamentals." *The Railway Gazette*, Part 1, p.45; Part 2, p. 105; part 3, p. 157; Part 4, p. 220; Part 5, p. 274; Part 6, p. 335; Part 7, p. 479.

Dipilato, M. A., Levergood, A. V., Steinberg, E. I., and Simon, R. M. (1983). "Railroad track substructure - design and performance evaluation practices." *FRA/ORD-83/04.2*, Final Report for USDOT Transportation Systems Center, Cambridge, Massachusetts.

Dobry, R., and Swiger, W. F. (1979). *Threshold strain and cyclic behavior of cohesionless soils*.

Drumm, E. C., Boateng-Poku, Y., and Pierce, T. J. (1990). "Estimation of subgrade resilient modulus from standard tests." *Journal of geotechnical engineering*, 116(5), 774-789.

Egan, J. A., and Sangrey, D. A. "Critical state model for cyclic load pore pressure." *Earthquake engineering and soil dynamics: proceedings of the ASCE Geotechnical Enginnering Division speciality conference*, 410-424.

Head, K. H. (1982). *Manual of soil laboratory testing*, Pentech Press Limited, London.

Head, K. H. (1986). *Manual of soil laboratory testing*, Pentech Press Limited, London.

Heath, D. L., Shenton, M. J., Sparrow, R. W., and Waters, J. M. (1972). "Design of conventional rail track foundations." Proceedings, Institute of Civil Engineers, 251-267.

Heuklelom, W., and Klomp, A. J. G. (1962). "Dynamic testing as a means of controlling pavement during and after construction." Prceedings: First International Conference on Structural Design of Asphalt Pavement, Arbor, MI.

Hicks, R. G., and Monismith, C. L. (1971). "Factors influencing the resilient response of granular materials." *Highway Research Record No.345*(34), 15-31.

Indraratna, B., and Salim, W. (2005). *Mechanics of ballasted rail tracks*, Taylor & Francis, Balkema, Leiden, The Netherlands.

Jeffs, T., and Tew, G. P. (1991). "A review of track design procedures." The Broken Hill Proprietary Company Limited, Melbourne, Australia.

Lambe, T. W. (1951). *Soil testing for engineers*, John Wiley & Sons, New York.

Lambe, T. W., and Whitman, R. V. (1969). *Soil mechanics*, John Wiley & Sons, Inc., New York.

Lefebvre, G. (1986). "Stability threshold for cyclic loading of saturated clay." 3rd Canadian Conference on Marine Geotechnical Engineering., St John's Newfoundl, Cananda, 675-690.

Li, D. (1994a). "Railway track granular layer thickness design based on subgrade performance under repeated loading," University of Massachusetts, Amherst, Mass.

Li, D. (1994b). "Resilient modulus for fine-grained subgrade soils." *Journal of geotechnical engineering*, 120(6), 939-957.

Li, D., and Selig, E. T. (1996). "Cumulative plastic deformation for fine-grained subgrade soils." *Journal of Geotechnical Engineering*, 1006 -1013.

Li, D., and Selig, E. T. (1998a). "Method for railroad track foundation design. I: Development." *Journal of Geotechnical and Geoenvironmental Engineering*, 124(4), 323-329.

Li, D., and Selig, E. T. (1998b). "Method for railroad track foundation design. II: Application." *Journal of geotechnical and geoenvironmental engineering*, 124(4).

Loh, R. B. H., and Nikraz, H. R. (2011). "A rational approach to railway track foundation design with clay subgrade." The 14th Asian Regional Conference on Soil Mechanics and Geotechnical Engineering, Hong Kong Geotechnical Society; Hong Kong Polytechnic University, Hong Kong, China.

Monismith, C. L., Ogawa, N., and Freeme, C. R. (1975). "Permanent deformation characteristics of subgrade soils due to repeated loading." *Transport Research Record No. 537*, Tranportation Research Board, Washington D. C.

Moossazadeh, J., and Witczak, M. W. (1981). "Prediction of subgrade boduli for soil that exhibits nonlinear behaviour."

Navy, U. S. (1962). *Soil mechanics, foundations and earth structures*, US NAVFAC Design Manual DM-7.

Procter, D. C. (1984). "Cyclic triaxial tests on remoulded clays." *Journal of Geotechnical Engineering*, 110(10), 1431-1445.

Puppala, A. J., Mohammad, L. N., and Allen, A. (1999). "Permanent deformation characterization of subgrade soils from RLT test." *Journal of materials in civil engineering*, 11(4), 274-282.

Research, D. o. S. a. I., and Laboratory, R. R. (1961). "Soil mechanics for road engineers." Her Majesty's Stationery Office, London.

Sangrey, D. A. (1969). "Effective stress response of a saturated clay soil to repeated loading." *Canadian Geotechnical Journal*, 6(3), 241-252.

Sangrey, D. A. (1978). "Cyclic loading of sands, silts and clays." Earthquake engineering and soil dynamics: proceedings of the ASCE Geotechnical Engineering Division speciality conference, 836-851.

Schofield, A., and Wroth, P. (1968). *Critical state soil mechanics*, McGRAW - HILL Publishing Company Limited, London.

Seed, H. B., and Martin, G. R. (1966). "Clay strength under earthquake loading conditions." *American Society of Civil Engineers Proceeding, Journal of the Soil Mechanics and Foundations Division*, 92, p53-78.

Selig, E. T. (1981). "Soil failure modes in undrained cyclic loading." *Journal of Geotechnical Engineering Division*, 107(5), 539-551.

Selig, E. T., and Waters, J. M. (1994). *Track geotechnology and substructure management*, Thomas Telford Services Ltd, London.

Smith, I. (2006). *Smith's elements of soil mechanics*, Blackwell Publishing, Edinburgh.

Thompson, M. R., and Robnett, Q. L. (1979). "Resilient properties of subgrade soils." *ASCE, Transportation Engineering Journal*, 105(1), 71-89.

Townsend, F. C., and Chisolm, E. E. (1976). "Plastic and resilient properties of heavy clay under repetive loadings." *Technical Report S-76-16*, Soils and Pavement Lab., U.S. Army Engineer Waterways Experiment Station.

Ullditz, P. (1993). "Mathematical model for pavement performance under moving wheel load." *Transp. Res. Rec. No. 1384*, National Research Council, Transportation Research Board, Washington, D. C.

Uzan, J. (1985). "Characterization of granular materials." *Transportation Research Record 1022, TRB. Washington DC: National Research Council*, p. 52-59.

Waters, J. M. (1968). "Track foundation design." *Railway Gazette*, 124(19), 734-737.

Wood, D. M. (1990). *Soil behaviour and critical state soil mechanics*, Cambridge University Press.

Appendix 1 *Derivation of Equation(s) for Prediction of Threshold Stress*

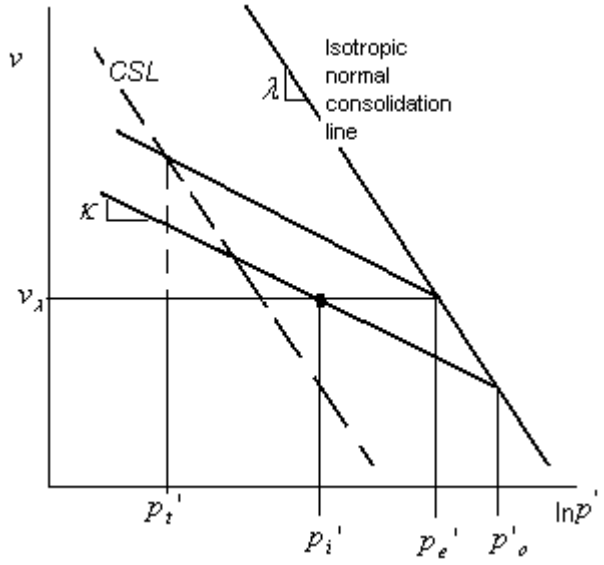

Figure A1–1

For soil of all consolidated state, the equivalent pre-consolidated stress (p_e') can be expressed as follows,

$$p_e' = {p_o'}^{(1-\kappa/\lambda)} \cdot {p_i'}^{\kappa/\lambda} \qquad \text{(A1-1)}$$

For normally-consolidated soil, under cyclic undrained compression ($\Delta v = 0$), the cyclic stress equilibrium state surface (CSESS) has an expression (refer to Equation (6-8) on *p'- q* plane as follows:

$$q = Mp' \ln\left({p_o'}/{p'} \right) \qquad \text{(A1-2)}$$

In general, under cyclic undrained compression ($\Delta v = 0$), the equation (refer to Equation (6-10)) for CSESS is re-stated as,

$$q = Mp' \ln\left({p_e'}/{p'} \right) \qquad \text{(A1-3)}$$

For soil of the sub-critical region (which defined between the normally-consolidated state and the over-consolidated state at wet / dry divisional state ($p'_{w/d}$)), the threshold stress (q_t) will be at the stress state of maximum possible deviator stress where the CSESS intercepts the CSL, at which $p' = p_t'$ and q = threshold stress (q_t), where

$$p_t' = \frac{p_e'}{e} \qquad \text{(A1-4)}$$

And, $$q_t = M \cdot \frac{p_e'}{e} \qquad \text{(A1-5)}$$

Substituting (A1-1) into (A1-4)

$$q_t = \frac{M}{e} p_o'^{\left(1-\kappa/\lambda\right)} \cdot p_i'^{\kappa/\lambda} \qquad \text{(A1-6)}$$

At the wet / dry divisional state, $p'_{w/d} = p_t'$; and $q_t = M \cdot p_t'$. (Assuming perfect isotropic condition),

$$\frac{p'_{w/d}}{p_o'} = e^{\left(\frac{\lambda}{\kappa-\lambda}\right)} \qquad \text{(A1-7)}$$

For soil of the super-critical region (heavily over-consolidated clay), where

$$0 < p_i' < p'_{w/d} \text{ or } 0 < \frac{p_i'}{p_o'} < e^{\left(\frac{\lambda}{\kappa-\lambda}\right)}, \qquad p_i' = p_t'$$

(Assuming perfect isotropic condition). The threshold stress (q_t) will be the deviator stress on the CSESS (at constant volume), where $p' = p_i' = p_t'$. From Equation (A1-1) & (A1-3),

$$q_t = Mp_i'\left(\frac{\kappa-\lambda}{\lambda}\right)\ln\left(p_i'/p_o'\right) \qquad \text{(A1-8)}$$

Appendix 2 Derivation of Equation(s) for Threshold Stress Re-assessment

In the case of normally-consolidated soil, the specific volume (v_λ) can be defined from isotropic normal consolidation line (INCL) (refer to Figure (A1–1)),

$$v_\lambda = N - \lambda \ln p_o' \tag{A2-1}$$

For soil of all consolidated state in general,

$$v_\lambda = N - \lambda \ln p_e' \tag{A2-2}$$

Knowing $$\gamma_d = \frac{G_s \cdot \gamma_w}{1+e} \tag{A2-3}$$

And assuming $\gamma_w = 9.81$ kN/m^3; Equation (A2-3) becomes,

$$v_\lambda = \frac{9.81 G_s}{\gamma_d} \tag{A2-4}$$

From Equation (A2-2),

$$p_e' = \exp\left(\frac{N - v_\lambda}{\lambda}\right) \tag{A2-5}$$

Substitute Equation (A2-4) into (A2-5),

$$p_e' = \exp\left(\frac{N - 9.81 G_s/\gamma_d}{\lambda}\right) \qquad \text{(A2-6)}$$

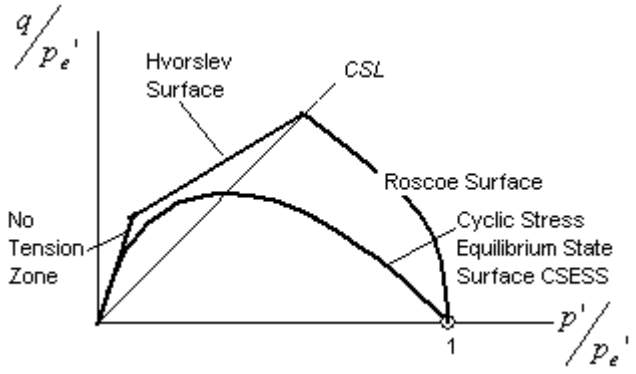

Figure A2–1

The equation defining CSESS (Equation (6-10)) is re-stated here as,

$$q = Mp' \ln\left(p_e' / p'\right) \qquad \text{(A2-7)}$$

Under cyclic undrained compression, the wet / dry divisional state ($p'_{w/d}$) had been observed when $p'_{w/d} = p_t' = p_e' / e$ (same as Equation A1-4) and $q_t = Mp_t'$ (Assuming a perfect isotropic condition). For soil in the sub-critical region (normally-consolidated to over-consolidated clay at wet / dry divisional state ($p'_{w/d}$)), when $1 > p_i' > p_e' / e$, the threshold stress (q_t) occurs when $p' = p_t' = \frac{p_e'}{e}$. Hence, same as Equation (1-15),

$$q_t = \left(M \diagup e\right) \cdot p_e' \qquad \text{(A2-8)}$$

Substitute Equation (A2-6) into (A2-7)

$$q_t = M \cdot \exp\left(\frac{N - 9.81 G_s/\gamma_d}{\lambda} - 1\right) \qquad \text{(A2-9)}$$

For over-consolidated clay, where $0 < p_i' < \frac{p_e'}{e}$ or $0 < \frac{p_i'}{p_e'} < e^{-1}$; $p_t' = p_i'$(Assuming a perfect isotropic condition). From Equation (A2-7), the threshold stress (q_t) become

$$q_t = M p_i' \left[\frac{N - 9.81 G_s/\gamma_d}{\lambda} - \ln p_i'\right] \qquad \text{(A2-10)}$$

Appendix 3 Abstracts of Publications Related to Thesis

A compilation of the published papers (as listed below) which are related to this thesis is made. Due to the large number of pages involved, only the front page containing the abstract and part of the introduction to the paper is reproduced and attached herewith.

A3-1

Effective stress method on threshold stress of clay under high rate cyclic loading (5th Asia-pacific conference on unsaturated soils (AP-UNSAT 2011))

- Loh, R. B. H., and Nikraz, H. R. (2011)

A3-2

Critical state modeling of lower-bound threshold stress for clay subgrade (5th Asia-pacific conference on unsaturated soils (AP-UNSAT 2011))

- Loh, R. B. H., and Nikraz, H. R. (2011)

A3-3

Threshold stress and deformation characteristics of clay subgrade for railway tracks (5th International Symposium on Deformation Characteristics of Geomaterials (IS-Seoul 2011))

- Loh, R. B. H., and Nikraz, H. R. (2011)

A3-4

A rational approach to railway track foundation design with clay subgrade (The 14th Asian Regional Conference on Soil Mechanics and Geotechnical Engineering

(14th ARC 2011))

- Loh, R. B. H., and Nikraz, H. R. (2011)

A3-5

Some observations on the behaviour of soft clay under undrained cyclic loading (Journal of GeoEngineering, Vol.6, No.2)

- Mohamed A. Shahin, Richard B.H. Loh, and Hamid R. Nikraz (2011)

A3-1

Effective Stress Method on Threshold Stress of Clay under High Rate Cyclic Loading

Richard B.H. Loh
Department of Civil Engineering, Curtin University, WA, Australia, beng.loh@postgrad.curtin.edu.au

Hamid R. Nikraz
Department of Civil Engineering, Curtin University, WA, Australia, h.nikraz@curtin.edu.au

ABSTRACT: This paper discussed the undrained triaxial testing of soft clay which may be encountered as subgrade soil in the alignment of railway track or road pavement. Several series of both static and cyclic undrained triaxial test were conducted. The static undrained triaxial test provides a prior indication on the maximum stress level from which the cyclic stress level can be apportioned. The cyclic undrained triaxial test simulates the behaviour of clay subgrade under the passing train axle's loading. The analysis of test results showed the feasible use of "effective stress" analysis in establishing threshold stress for clay under high cyclic loading rate. The study reaffirmed the influence of stress history on the level of threshold stress. In particular, cyclic stress ratio (CSR) of threshold stress was found reducing with higher over-consolidation ratio. The threshold stress so obtained represents the lower-bound bearing strength for unsaturated clay subgrade of railway track.

KEYWORDS: Cyclic Loading; Triaxial; Clay; Threshold Stress; subgrade

1 INTRODUCTION

In planning the railway line, crossing area of soft formation soil for straight line alignment may become necessary either for cost efficiency or shorter travelling time. A better understanding of clay subgrade response under cyclic loading caused by the passing wheels will enable engineers to design for stable track foundation with less frequent track repairs and re-alignment. Traditional railway foundation or substructure consists of a layer of ballast and sub-ballast overlaying a subgrade or natural formation. With the passing of train axles/wheels, subgrade soil beneath railway tracks experiences stress of cyclic nature that can result in progressive shear failure at a stress level lower than its monotonic strength. British researcher (Heath et al. 1972; Waters 1968) has long established the existence of "threshold stress" in clay subgrade. When the track subgrade will to be stressed below the threshold stress level, stabilization of the track vertical alignment can be achieved.

Under undrained cyclic compression, clay specimen with cyclic deviator stress less than its monotonic deviator strength can build up its full excess pore water pressure within hours and led to ultimate failure with large strain. In the real case, clay subgrade though normally exists in unsaturated state can become highly saturated in wet season. The dissipation of the excess pore water pressure built up in the subgrade will likely to be a slow process due to its thickness with longer drainage path. Therefore, an assumption of using an "undrained" testing can be justified. The employment of the undrained triaxial tests on a saturated soil specimen in test simulation and the determination of threshold stress will produce a "lower-bound" solution for subgrade bearing strength in the design of railway track foundation with an unsaturated subgrade.

Previous research and studies have produced various methods of establishing the threshold stress for clay (Frost 2004; Heath et al. 1972; Procter 1984; Sangrey 1969; Sangrey 1978; Shahu 2008; Waters 1968; Yudhbir and Shahu 1995). They are generally being seen as either "total stress" (Heath et al. 1972; Lefebvre 1986; Procter 1984; Shahu 2008; Waters 1968) or "effective stress" (Sangrey 1969; Shahu 2008) method. Use of "effective stress" analysis can provide a more fundamental understanding of the soil behaviour under cyclic loading. But for high rate cyclic loading on clay, "effective stress" analysis was uncommon largely due to concern over the slow process required for equalization of excess pore water pressure within the clay specimen (Sangrey et al. 1978). Notwithstanding this, "effective stress" analysis will be appropriate if the equilibrium state of stress, rather than the transient state of presiding loading cycles, is of prime interest.

A3-2

Critical State Modeling of Lower-bound threshold Stress for Clay Subgrade

Richard B.H. Loh
Department of Civil Engineering, Curtin University, WA, Australia, beng.loh@postgrad.curtin.edu.au

Hamid R. Nikraz
Department of Civil Engineering, Curtin University, WA, Australia, h.nikraz@curtin.edu.au

ABSTRACT: Railway track foundation with fine-grained subgrade, under loading of cyclic nature, can build up excess pore pressure and results in progressive shear failure at a stress level less than its static undrained strength. It is widely accepted a threshold stress level exists, where loading above such level causes large deformation; otherwise stability of vertical track profile will be assured. This paper described the theoretical model that predicts the threshold stress of clay soil. The threshold stress so determined represents the lower-bound solution for bearing strength capacity of clay subgrade which normally exists in an unsaturated state. Developed from the "original Cam-clay" model and validated by series of undrained cyclic triaxial test data on reconstituted kaolin clay, the proposed theoretical model enables the prediction of threshold stress to be made from the fundamental properties of the soil, based on current state of stress and stress history of the subgrade soil. The model reserved its ability to further expand into predicting the threshold stress of soil in its unsaturated state.

KEYWORDS: Cyclic Loading; Constitutive modeling; Clay; Threshold Stress

1 INTRODUCTION

With the passing of train wheels, subgrade soil beneath railway tracks experiences stress of cyclic nature that can result in progressive shear failure at a stress level lower than its monotonic strength. There exists a threshold stress in clay subgrade. When the track subgrade will to be stressed below the threshold stress level, stabilization of the track vertical alignment can be achieved.

Clay subgrade normally exists in unsaturated state can become highly saturated in wet season. The dissipation of the excess pore water pressure built up in the subgrade will be a slow process. Test simulation using undrained triaxial tests on a saturated soil specimen to determine the threshold stress will produce a "lower-bound" solution for subgrade bearing strength in the design of railway track foundation with unsaturated clay subgrade.

Undrained cyclic tests conducted on reconstituted saturated kaolin clay (normal-consolidated at 300 kPa) showed that, under the continuous application of cyclic deviator stress (q) of sinusoidal shape, with cyclic loading frequency of 1Hz simulating the passing axles of a train travelling at a speed of 50 km/hour, excess pore water pressure gradually built up over each cycle of deviator stress application. As cyclic deviator stress oscillates in a sinusoidal way between the maximum and the near zero values, the excess pore water pressure gradually builds up, oscillating in the same phase as the deviator stress. (Fig 1a) shows the maximum excess pore water pressure corresponding to the peak deviator stress of each loading cycle. On the p'- q plot (Figure 1b), cyclic deviator stress smaller than threshold stress produces peak stress path which represents the path of most critical and vulnerable effective stress state of each cycle. The peak stress path migrated leftward and become stagnant before the critical state line (CSL) as the cyclic stress path of each cycle formed hysteresis loop, signifying the arrival of stress equilibrium state (Sangrey 1969). Concurrently, the axial strain developed and subsequently become stabilized. The threshold stress (Ansal 1989; Heath et al. 1972; Lefebvre 1986; Procter 1984; Sangrey 1969; Waters 1968) (or critical level of cyclic stress) will be the maximum possible cyclic deviator stress (q) (at point "Ts") that arrives at the line of stress equilibrium state (LCSES), beyond which, soil yields at large strain.

There have been constant attempts and advances by researchers to model the cyclic behavior of clayey soil (Carter et al. 1982; Egan and Sangrey 1978). This paper began by describing the existence

A3-3

International Symposium on Deformation Characteristics of Geomaterials, September 1~3, 2011, Seoul, Korea

Threshold stress and deformation characteristics of clay subgrade for railway tracks

Loh, Richard B.H.
Department of Civil Engineering, Curtin University, Australia, beng.loh@postgrad.curtin.edu.au

Nikraz, Hamid R.
Professor, Department of Civil Engineering, Curtin University, Australia, h.nikraz@curtin.edu.au

Keywords: Threshold stress, Clay subgrade, Undrained cyclic testing, Critical state model, Railway track subgrade

ABSTRACT: Clay subgrade beneath railway track experiences stress of cyclic nature that can result in progressive shear failure at a stress level lower than the clay monotonic strength. This paper described the effective stress analysis of threshold stress and the deformation characteristics from a series of cyclic undrained triaxial tests carried out on reconstituted kaolin clay, which simulates the behavior of clay subgrade under cyclic loading conditions due to the loading of passing trains/vehicles. Cyclic loading frequency typical to that experienced by railway track foundations near subgrade surface was employed. In addition, a critical state model is proposed for predicting threshold stress of saturated clay under undrained cyclic compression without resorting to lengthy laboratory testing. Validated by observed tests data, the model provides a lower-bound solution of the threshold stress of clay subgrade for rail tracks, from the measured values of fundamental soil properties, based on consolidation history and current state of stress.

1. INTRODUCTION

Railway track foundation consists of a granular media of ballast placed above a naturally deposited subgrade (formation) soil. In planning the railway line, crossing area of soft formation soil for straight line alignment may become necessary either for cost efficiency or shorter travelling time. A better understanding of clay subgrade response under cyclic loading caused by the passing wheels will enable engineers to design for stable track foundation with less frequent track repairs and re-alignment. With the passing of train axles/wheels, subgrade soil beneath railway tracks experiences stress of cyclic nature that can result in progressive shear failure at a stress level lower than its monotonic strength. British researcher (Heath et al. 1972; Waters 1968) has long established the existence of "threshold stress" in clay subgrade. When the track subgrade will to be stressed below the threshold stress level, stabilization of the track vertical alignment can be achieved.

Clay subgrade though normally exists in partial saturation state can become highly saturated in wet season. The dissipation of the excess pore water built up in the subgrade will likely to be a slow process due to its thickness with longer drainage path. The testing of saturated clay under "undrained" condition thus represents the worst possible condition that will produce "lower-bound" solution in threshold stress.

Effective stress response of saturated clay in undrained tests is normally analyzed on very slow cyclic loading rate at which equalization of excess pore pressure takes place and its measurement meaningful (Sangrey 1969). This study employed higher cyclic loading rate of 1 Hz simulating the passing axles of a train traveling at a speed of approximately 50 km/hour. The effective stress analysis for this loading rate will be appropriate and meaningful at the state of stress equilibrium, rather than the transient state of presiding loading cycles (Seed and Martin 1966).

Graphical characteristic strain model describing relationship between strain of cyclic and monotonic compression is presented. In addition, a critical state model for predicting threshold stress of saturated clay under undrained cyclic compression is proposed, as a means to avoid resorting to lengthy laboratory procedure. Developed from original Cam-clay model (Schofield and Wroth 1968) and validated by observed test data, the model enable the threshold stress to be predicted from the

A3-4

A rational approach to railway track foundation design with clay subgrade

Richard B.H. Loh
Department of Civil Engineering, Curtin University, Australia

Hamid R. Nikraz
Professor, Department of Civil Engineering, Curtin University, Australia

ABSTRACT: In planning the railway line, crossing low-lying area of high plasticity clay formation soil for straight line alignment may become necessary either for cost efficiency or shorter travelling time. This paper describes the new approach, which served to rationalize and reformulate the current state of design and management process of rail track substructure involved clay subgrade. It puts forward the concept of "Managing current lower-bound threshold stress" for clay subgrade on the premise that lower-bound threshold stress which represents subgrade capacity of the most vulnerable state, is not necessarily a constant material parameter and can potentially increase two folds which should be taken into consideration for economical design. The readily use of proposed theoretical model and design charts for predicting and re-assessing threshold stress offers a key advantage for the new approach over current practices.

1 INTRODUCTON

Railway track foundation consists of a granular media of ballast placed above a naturally deposited subgrade (formation) soil. In planning the railway line, crossing area of soft formation soil for straight line alignment may become necessary either for cost efficiency or shorter travelling time. The current analytical approach to the design of rail track foundation with fine-grained soil subgrade has been either strain-focus (Li 1994; Li and Selig 1996; Li and Selig 1998a; Li and Selig 1998b) or stress focus (Heath et al. 1972; Waters 1968). In other words, the design is such that a specific level of axial strain/deformation or a critical level of deviator stress (or threshold stress) will be allowed near the subgrade surface.

While the strain-focus approach requires the specification of the level of allowable strain and the corresponding magnitude of deformation, and it pre-supposes a constant or bi-seasonal soil physical state (soil moisture content and dry density), its use certainly requires prior rationalization and justification of what constitutes allowable strain or deformation for different soil-type and operating condition.

With the passing of train axles/wheels, subgrade soil beneath railway tracks experiences stress of cyclic nature that can result in progressive shear failure at a stress level lower than its monotonic strength (Selig and Waters 1994). British researchers has established the existence of "threshold stress" in London clay subgrade (Heath et al. 1972; Waters 1968). When subgrade of railway track will to be stressed at a level lower than threshold stress of the soil, stabilization of the track vertical alignment can be achieved.

Consequently, the new approach favored stress-focus that adopts the threshold stress criteria, on the premise that strain and deformation would be minimized if the induced stress can be properly controlled at a level below the threshold stress, while additional provision on the track superstructure (sleeper, fastening system, rail) can be made to overcome or alleviate unforeseen differential settlement of the track.

2 MANAGING THE CURRENT LOWER-BOUND THRESHOLD STRESS

2.1 *General*

Railway track being a fixed rail platform has the sleepers acting like a pad footing sitting on subgrade. Provided no localized shear failure with large strain occurs along the rail and with the subgrade soil reasonably homogeneous throughout influence depth, any axial strain response / deformation below sleeper should varies linearly along sleepers and there will be minimum or no differential settlement along the track due directly to trains loading.

2.2 *Current lower-bound threshold*

Tests carried out on saturated kaolinite clay showed that, under cyclic undrained compression at a cycle per second with deviator stress slightly higher than its threshold stress, full excess pore water pressure can build up in less than an hour that lead to large strain failure. In the real case,

Journal of GeoEngineering, Vol. 6, No. 2, pp. 109-112, August 2011

Note:

SOME OBSERVATIONS ON THE BEHAVIOR OF SOFT CLAY UNDER UNDRAINED CYCLIC LOADING

Mohamed A. Shahin [1], Richard B. H. Loh [2], and Hamid R. Nikraz [3]

ABSTRACT

This note presents the results of a series of cyclic loading triaxial tests under undrained conditions that examines the effectiveness of consolidation history on reconstituted soft clay. For any particular consolidation history, the experimental results confirm the concept of the critical stress level of repeated deviator stress below which a state of non-failure stress equilibrium exists and above which effective stress failure occurs. However, an interesting finding of this study is that for heavily over-consolidated clay, both the state of stress equilibrium (below the critical stress level) and state of effective stress failure (above the critical stress level) develop at the very first few cycles of loading.

Key words: cyclic loading, triaxial testing, undrained condition, over-consolidation, soft clay.

1. INTRODUCTION

The study of cyclic loading behavior of saturated clay under undrained conditions is of utmost importance to stability of geotechnical engineering structures constructed on low-lying estuarine soils and subjected to cyclic loading such rail track foundations and road pavements. A better understanding of the undrained response of clay subgrade to repeated loading enables a safe design of such structures, with less frequent maintenance and repairs. The undrained behavior of clay under repeated loading has been investigated by many researchers (*e.g.* Heath *et al.* 1972; Larew and Leonards 1962; Lefebvre *et al.* 1989; Mitchell and King 1977; Procter and Khaffef 1984; Sangrey *et al.* 1969; Shahu *et al.* 2008), and the existence of critical stress level (or threshold stress) has been long recognized. The critical stress level is the stress below which the soil does not suffer failure regardless of the number of applied cyclic loading and above which effective stress failure occurs. The present study investigates experimentally the effect of consolidation history on the behavior of soft clay at stress levels below and above the critical stress. Reconstituted soft clay soils of different consolidation history (*i.e.* normally consolidated as well as lightly and heavily over-consolidated) are examined and the results are presented and discussed.

2. EXPERIMENTAL PROGRAM

2.1 Soil Tested

The soil used in this study is kaolinite clay that was reconstituted by one-dimensional consolidation of slurry that is prepared by mixing dried commercial grade kaolinite powder with distilled water. Tube samples of diameter of 35 mm were extracted from the consolidated clay, and the final prepared specimen size was 35 mm in diameter and 70 mm in height. The following properties were found from laboratory tests carried out on the clay samples: Specific gravity G_s = 2.65; plastic limit w_P = 26%; liquid limit w_L = 53%; compression index C_c = 0.42; swelling index C_s = 0.06; and coefficient of consolidation c_v = 1.27 m^2/year.

2.2 Testing Apparatus and Procedures

The testing apparatus used in the current study is capable of conducting static as well as cyclic loadings. The triaxial system used is shown in Fig. 1, which consists of the following components: Triaxial cell, loading frame with computer-control platen that applies cyclic axial load on top of soil specimen, two computer-control flow pumps to control the chamber pressure and back pressure, high performance linear servo control electro actuator for cyclic loading with update rates of 500 times per

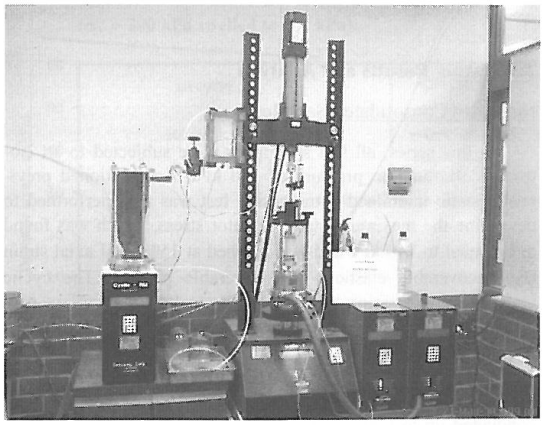

Fig. 1 Static/cyclic loading triaxial system

Manuscript received December 27, 2010; revised March 28, 2011; accepted March 28, 2011.

[1] Senior Lecturer (corresponding author), Department of Civil Engineering, Curtin University, Perth WA 6845, Australia (e-mail: m.shahin@curtin.edu.au).

[2] Ph.D. candidate, Department of Civil Engineering, Curtin University, Perth WA 6845, Australia.

[3] Professor, Department of Civil Engineering, Curtin University, Perth WA 6845, Australia.